

Interplay of TRAIL receptors in PDAC cells: the role of TRAIL-R4

Dissertation in fulfillment of the requirements for the degree “Dr. rer. nat.” of the Faculty of
Mathematics and Natural Sciences at Kiel University

Submitted by

Doaa Tawfik El-Sheikh

Kiel, June 2017

First Referee	Prof. Dr. rer. nat. Anna Trauzold
Second Referee	Prof. Dr. rer. nat. Thomas Roeder
Date of the oral examination	19 June 2017
Dean	Prof. Dr. rer. nat. Natascha Oppelt

TABLE OF CONTENTS

<i>Title</i>	<i>Page</i>
<i>List of Tables</i>	<i>I</i>
<i>List of Figures</i>	<i>II</i>
<i>List of Abbreviations</i>	<i>IV</i>
<i>Summary</i>	<i>VI</i>
<i>Zusammenfassung</i>	<i>VIII</i>
I. <u>Introduction</u>	
<i>PDAC development and heterogeneity</i>	2
<i>PDAC and TNF-related apoptosis-inducing ligand (TRAIL)</i>	4
<i>TRAIL-R4</i>	6
<i>Intracellular TRAIL receptors</i>	8
<i>TRAIL receptors' signaling</i>	9
<i>TRAIL and necroptosis</i>	13
<i>TRAIL and inflammatory cytokines</i>	13
<i>Epithelial-mesenchymal transition (EMT)</i>	15
<i>Cancer and cell adhesion molecules</i>	16
<i>Aim of Work</i>	17
II. <u>Materials & Methods</u>	
1. <u>Materials</u>	
1.1. <i>Chemicals</i>	18
1.2 <i>Western blot antibodies</i>	22
1.3 <i>FACS antibodies</i>	24
1.4 <i>Real Time PCR (RT-PCR) primers</i>	24
1.5 <i>GIPZ lentiviral human shRNA sequences</i>	25
1.6 <i>Buffers and solutions</i>	25
1.7 <i>Apparatuses</i>	28
1.8 <i>Consumables</i>	31
2. <u>Methods</u>	
2.1 <i>Cell Culture</i>	33
2.2 <i>Generating stable TRAIL-R4 over expression cell lines</i>	33
2.3 <i>Generating stable TRAIL-R4 knockdown cell lines</i>	34
2.4 <i>Mycoplasma PCR</i>	35
2.5 <i>Morphology</i>	35
2.6 <i>Effects of endogenous TRAIL</i>	35
2.7. <i>Whole cell lysate</i>	35
2.8. <i>Nuclear/Cytoplasmic fractionation</i>	36
2.9 <i>Immunoblotting/ Western blot</i>	37
2.10 <i>Proliferation assay</i>	37
2.11 <i>Migration Assay/ wound healing assay</i>	38
2.12 <i>Viability testing</i>	39
2.13 <i>RNA isolation</i>	39
2.14 <i>Real Time PCR (RT-PCR)</i>	39
2.15 <i>FACS</i>	40
2.16 <i>ELISA & Multiplex ELISA</i>	40
2.17 <i>Microarray study</i>	41
2.18 <i>nCounter assay</i>	42
2.19 <i>Animal Experiment</i>	43
2.20 <i>Immunohistochemistry</i>	43
2.21 <i>PDAC patients' tissue cohort</i>	44

2.22 Statistical analysis	44
III. Results	
1. Generation of Colo357 cell lines with differentially modified expression of TRAIL receptors	45
1.1. Detection of total protein level of TRAIL receptors	46
1.2. Detection of TRAIL receptors level on the plasma membrane	47
1.3. Determination of the intracellular distribution of TRAIL receptors	49
1.4. Detection of TRAIL receptors expression on mRNA level	50
2. Impact of TRAIL receptors interplay on TRAIL signal transduction pathways	52
2.1. Impact of TRAIL receptors interplay on TRAIL-induced apoptotic signaling	52
2.2. Impact of TRAIL receptors interplay on TRAIL-induced necroptosis	55
3. Microarray analysis of the altered genes due to TRAIL receptor manipulations	
3.1. Gene expression upon TRAIL receptors modulation	57
a. Gene Expression Analysis	57
b. Validating the mRNA levels of TRAIL and TRAIL receptors	58
c. Gene Set Enrichment Analysis (GSEA)	58
d. Validation of the microarray analysis	63
i. Expression of genes coding for cell-cell adhesion molecules	63
j. Expression of genes coding for some inflammatory Cytokines	65
3.2. Expression of the altered stemness markers (Nanostring)	67
4. In vitro functional analyses of the different Colo357 cell lines	71
4.1. Morphological characteristics of Colo357 cell lines	71
4.2. Impact of TRAIL receptor interplay on adhesion	72
4.2.1. Impact of TRAIL receptor interplay on cell-ECM adhesion	73
4.2.2. Impact of endogenous TRAIL on cell-ECM adhesion	74
4.3. Impact of TRAIL receptor interplay on proliferation	74
4.3.1. Impact of TRAIL receptors interplay on proliferation independent of ECM components	74
4.3.2. Impact of TRAIL receptor interplay on adhesion depending on different ECM components	76
4.4. Impact of TRAIL receptor interplay on migration	77
4.5. Impact of TRAIL receptor interplay on EMT	79
5. In vivo experiments	79
5.1. Colo357 cell lines in orthotopic tumor model	79
5.2. Colo357 cell lines in subcutaneous model	84
6. Patient cohort study	86
7. Generation of PancTu1 cell lines with differentially modified expression of TRAIL receptors	90
7.1. Detection of TRAIL receptors level on the plasma membrane	90
7.2. Detection of TRAIL receptors expression on mRNA level	92
7.3. Morphological characteristics of PancTu1 cell lines	93
7.4. Impact of TRAIL receptors interplay on TRAIL-induced cell death	93
7.5. Impact of TRAIL receptors interplay on inflammatory status	96
7.6. In vitro functional analyses of the different PancTu1 cell lines	97
7.6.1. Impact of TRAIL receptors interplay on proliferation	97
7.6.2. Impact of TRAIL receptors interplay on migration	98
IV. Discussion	100
TRAIL receptors interaction models	101
First Scenario TR1(-)TR4(+)	103
Second Scenario TR4(+)	105

<i>Third Scenario TR1(-)</i>	107
<i>Fourth/Fifth Scenario TR2(-) and TR2(-)TR4(+)</i>	108
<i>TRAIL receptors and PDAC heterogeneity</i>	111
<i>Failure of TRAIL-R4 up-regulation in PancTu1 TRAIL-R2 knockdown cell line</i>	113
<i>TRAIL receptors orchestrate PDAC cell death modality</i>	114
<i>Apoptosis</i>	114
<i>Necroptosis</i>	115
<i>TRAIL receptors impact on adhesion in PDAC</i>	116
<i>Orthotopic versus subcutaneous in vivo experiments</i>	117
V. Conclusion	119
VI. Future Perspective and Outlook	120
<i>References</i>	124
<i>Acknowledgement</i>	148
<i>Declaration</i>	149

LIST OF TABLES

<i>Table</i>	<i>Page</i>
Table 2.1 Technical parameters of the microarray analysis	41
Table 2.2 Equation used to calculate the arithmetic fold change	42
Table 3.1 Coding system used for PDAC cell lines	45
Table 3.2 Number of dysregulated genes in the different cell lines	58
Table 3.3 Fold change of mRNA levels of TRAIL and TRAIL receptors	58
Table 3.4 Significantly modified GO Term pathways in the different cell lines (WebGestalt)	60
Table 3.5 Fold change of the mRNA levels of the altered CEACAMs	63
Table 3.6 Fold change of the mRNA levels of the altered inflammatory cytokines	65
Table 3.7 nCounter analysis of TRAIL and TRAIL receptors expression	68
Table 3.8 nCounter analysis of stemness markers expression	68
Table 3.9 StemChecker analysis of stem cell types according to the significantly modified genes	69
Table 3.10 Transcription factor targets of the significantly modified genes	69
Table 3.11 Clinico-pathological patients characteristics of the chosen sub-group	86
Table 3.12 Relation of TRAIL receptor pattern to staging in PDAC tissues	87
Table 3.13 Intracellular distribution of TRAIL receptor in PDAC tissues extracted from the patients	89
Table 3.14 Expression levels of inflammatory cytokines	97

LIST OF FIGURES

<i>Figure</i>	<i>Page</i>
Figure 1.1 Signal transduction pathways activated upon the binding of the TRAIL ligand to its death-inducing receptors	9
Figure 1.2 Inhibitory factors of the mitochondrial pathway in mammals	10
Figure 3.1 Illustration of TRAIL receptors modifications in the different cell lines	46
Figure 3.2 Whole protein expression level of TRAIL receptors	47
Figure 3.3 Plasma membrane levels of TRAIL receptors	48
Figure 3.4 TRAIL receptor expression levels in the cytoplasmic and nuclear compartments	50
Figure 3.5 RT-PCR analysis of the TRAIL receptor on mRNA level	51
Figure 3.6 Viability of the different cell lines under TRAIL-induced apoptosis	52
Figure 3.7 Expression levels of proteins involved in the apoptotic and necroptotic pathways	53
Figure 3.8 Expression levels of proteins involved in cell death	55
Figure 3.9 Viability of the different cell lines under TRAIL-induced necroptosis	56
Figure 3.10 Pathway network analysis of the up-regulated genes in the different groups	61
Figure 3.11 Biological processes network analysis of the up-regulated genes in the different groups	62
Figure 3.12 RT-PCR analysis of CEACAM levels	64
Figure 3.13 Expression level of CEACAMs	65
Figure 3.14 Expression level of some inflammatory cytokines	66
Figure 3.15 RT-PCR analysis of the level of IL6 in Colo357 cells	67
Figure 3.16 Radar charts of the stem cell types and StemChecker data sources	70
Figure 3.17 Radar chart of the highly altered transcription factors	71
Figure 3.18 Light microscopy-based pictures of the different Colo357 cell lines	72
Figure 3.19 Expression levels of proteins involved in cell-ECM adhesion	73
Figure 3.20 Impact of endogenous TRAIL on cell-ECM adhesion molecules	74
Figure 3.21 Impact of TRAIL receptor interplay on proliferation (cell count)	75
Figure 3.22 Impact of TRAIL receptor interplay on proliferation (xCELLigence assay)	76
Figure 3.23 Viability of the different cell lines on different ECM molecules	77
Figure 3.24 Impact of TRAIL receptor interplay on migration	78
Figure 3.25 Expression levels of proteins involved in EMT	79
Figure 3.26 Primary tumor weight and size analyses of the orthotopic tumor model	80
Figure 3.27 Overall analysis of the orthotopic tumor model	81

Figure 3.28 Volumetric analysis of the primary tumors (Ultrasound)	81
Figure 3.29a MRI image of orthotopic tissue model	82
Figure 3.29b MRI image analyses of orthotopic tissue model	83
Figure 3.30 Immunohistochemical staining of the primary tumor tissues	84
Figure 3.31 Overall analysis of the subcutaneous animal experiment	85
Figure 3.32 Survival curves of PDAC patients with differential TRAIL receptor expression tissue patterns	88
Figure 3.33 Survival curves of PDAC patients with tissues expression equivalent to TR1(-) and TR1(-)TR4(+)	88
Figure 3.34 Whole protein expression level of TRAIL receptors in both Colo357 and PancTuI cells	90
Figure 3.35 Plasma membrane levels of TRAIL receptor	91
Figure 3.36 RT-PCR analysis of the TRAIL receptors on mRNA level	92
Figure 3.37 Light microscopy-based pictures of the different PancTuI cell lines	93
Figure 3.38 Viability of the different PancTuI cell lines	94
Figure 3.39 Expression levels of proteins involved in the apoptotic and necroptotic pathways	95
Figure 3.40 Expression levels of proteins involved in cell death	96
Figure 3.41 Expression level of IL-8	97
Figure 3.42 Impact of TRAIL receptor interplay on proliferation	98
Figure 3.43 Impact of TRAIL receptor interplay on migration	99
Figure 4.1 Scenario's illustrations guide	101
Figure 4.2 Basic expression levels of TRAIL receptors and functional properties of the studied PDAC cells	102
Figure 4.3 Illustration of the TR1(-)TR4(+) cell line	104
Figure 4.4 Illustration of the TR4(+) cell line	106
Figure 4.5 Illustration of the TR1(-) cell line	108
Figure 4.6 Illustration of the cell lines with TRAIL-R2 knockdown in Colo357	109
Figure 4.7 Downstream outside-in integrin signaling pathways	117
Figure 6.1 Expression level of TRAIL-R4	120
Figure 6.2 <i>In vitro</i> functional analyses of Colo357 TRAIL-R4 knockdown cell line (TR4-KD)	121
Figure 6.3 Expression levels of some cell-ECM adhesion molecules in MDA-MD-321	122

LIST OF ABBREVIATIONS

Abbreviation	Name
ADM	Acinar-ductal metaplasia
3'UTR	3' untranslated region
BID	BH3 interacting-domain death agonist
CAAC	Centroacinar-acinar compartment
Cas3	Caspase 3
Cas8	Caspase 8
CSCs	Cancer stem cells
CTRL	Control
dATP	Deoxyadenosine triphosphate
DcR1	Decoy receptor 1
DcR2	Decoy receptor 2
DD	Death domain
DISC	Death-inducing signaling complex
DNA	Deoxyribonucleic acid
DR4	Death receptor 4
DR5	Death receptor 5
ECM	Extracellular matrix
FACS	Fluorescence-activated cell sorting
FADD	Fas-Associated protein with death domain
FGF	Fibroblast growth factors
HIF-2α	hypoxia-inducible factor-2 alpha
HtrA2/Omi	High temperature requirement protein A2/Omi
IL6	Interleukin-6
IL8	Interleukin-8
JNK	C-Jun N-terminal kinase
kDa	Kilodaton
FC	Fold change
MAPK	Mitogen-activated protein kinases
MLKL	Mixed lineage kinase domain like protein
mRNA	Messenger ribonucleic acid
MUC	Mucin

NF-κB	Nuclear factor 'kappa-light-chain-enhancer' of activated B-cells
NS	Non silencing
OPG	Osteoprotegerin
PanIN	Pancreatic intra-epithelial neoplasia
PARP	Poly (ADP-ribose) polymerase
PCR	Polymerase chain reaction
PDAC	Pancreatic ductal adenocarcinoma
PDGF	Platelet derived growth factor
RT-PCR	Quantitative PCR
RANK	Receptor activator of NF-κB
RANKL	Receptor activator of NF-κB Ligand
RIPK	Receptor interacting serine/threonine kinase
RNA	Ribonucleic acid
RT-PCR	Real Time PCR
SASP	The senescence-associated secretory phenotype
shRNA	Short hairpin ribonucleic acid
Smac/Diablo	Second mitochondria- derived activator of caspase/direct IAP binding protein with low pI
tBID	Truncated BID
TBST	Tris-buffered saline-tween 20
TGF-β	Transforming Growth Factor-beta
TNF	Tumor necrosis factor
TNFRSF10D	Tumor necrosis factor receptor superfamily 10 D
TRAIL	TNF-related apoptosis inducing ligand
TRAIL-R1	TNF-related apoptosis inducing ligand receptor 1
TRAIL-R2	TNF-related apoptosis inducing ligand receptor 2
TRAIL-R3	TNF-related apoptosis inducing ligand receptor 3
TRAIL-R4	TNF-related apoptosis inducing ligand receptor 4
WB	Western blot
WNT	Wingless-related integration site

SUMMARY

Background: Pancreatic ductal adenocarcinoma (PDAC) is a notorious cancer known for its difficult diagnosis, resistance to treatment and overall bad prognosis. Therefore, a thorough understanding of its pathogenesis is urgently needed. About twenty years ago a group of death-inducing receptors have been identified to be predominantly expressed by cancer cells. These receptors are known as Tumor Necrosis Factor-related apoptosis-inducing ligand (TRAIL) receptors. The discovery of TRAIL receptors and the cognate ligand provided hope for killing cancer cells without harming the normal tissues. The human TRAIL receptor family comprises of two death-inducing receptors (TRAIL-R1 and -R2) and two decoy receptors (TRAIL-R3 and -R4) and also osteoprotegerin. The apoptosis-inducing potential of the TRAIL ligand as well as the impact of the particular death receptor TRAIL-R1 or -R2 has been intensively studied in different cancer cells. Likewise, the anti-apoptotic function of overexpressed TRAIL-R4 was shown in different cellular systems. However, the potential interplay between the different TRAIL receptors has been rarely addressed.

Goal: Create a functional dissection of the TRAIL receptor family, in order to understand the impact of each TRAIL receptor in the context of the others with special emphasis on TRAIL-R4 functions.

Methods: Two PDAC cell lines with differentially modified expression of TRAIL receptors were used in the current study (Colo357 and PancTu1). Several *in vitro* methods have been implemented including Western blotting, FACS, ELISA, RT-PCR, and Bioinformatics together with proliferation, viability and migration assays. As *in vivo* tumor models, SCID-beige mice were inoculated with the Colo357 cell lines as an *in vivo* proof of concept. Finally, a small cohort of patients' tissues has been investigated by immunohistochemistry as well.

Results: The current study showed a tight interconnection between TRAIL-R1, -R2 and -R4. We could show that the combination of TRAIL-R2 knockdown with or without TRAIL-R4 up-regulation were the most aggressive, highly proliferative cells together with a fast migration, and high inflammatory status. However, TRAIL-R4 up-regulation with simultaneous TRAIL-R1 knockdown showed the opposite effects. Additionally, the aggressiveness and the metastatic potential were mirrored with clear dysregulation in

CEACAM5/CEACAM6 levels, where TRAIL-R4 upregulation with the limited expression of TRAIL-R2 boosted their levels while TRAIL-R4 markedly decreased their levels in cells with the limited expression of TRAIL-R1. Furthermore, the cells with TRAIL-R1 knockdown and TRAIL-R4 upregulation exhibited an overall suppressed functions, yet, the cells were growing well when seeded on fibronectin or tenascin-c as extracellular matrix (ECM). While fibronectin is one of the common ECM produced by cells in the normal tissues including pancreas, tenascin-c is an ECM protein found in cancer regions. This observation denotes that this particular cell line – though not very active – is capable of surviving in a physiologically unfavorable environment in comparison to other studied cell lines and this goes in line with the bad survival seen in the patient cohort in those cases. Also, the representation of TRAIL-R2 low expressing cells in the patient tissues were very scarce that denotes that these patients might have been deemed inoperable due to their advanced stage at the moment of diagnosis. Furthermore, the *in vivo* results confirmed the functional properties of the studied cell lines. Regarding TRAIL-R4 effects, TRAIL-R4 upregulation per se showed the fastest tumor growth rate, while TRAIL-R4 up-regulation with TRAIL-R1 knockdown demonstrated the slowest growing tumors. However, TRAIL-R4 over-expression with TRAIL-R2 knockdown showed almost no change in comparison to TRAIL-R2 knockdown cells. These finding shows that TRAIL-R4 has many capacities, where its upregulation in combination with TRAIL-R1 low expression drove the cells to a less aggressive behavior, while with TRAIL-R2 knockdown, this overexpression had minimal impact.

Conclusion: We found that TRAIL receptors act as a highly interdependent system. Cancer cells can use this system to divert/accommodate to physiological unfavorable conditions or proliferate, migrate and send out inflammatory signals in physiologic conditions. In order to understand the molecular impact of these receptors, the levels of all receptors should be analyzed in parallel. Furthermore, the current study suggests a significantly positive post-operative survival state with low expression of TRAIL-R1 denoting the importance of TRAIL receptor profiling to assess the post-operative PDAC patient outcome.

ZUSAMMENFASSUNG

Hintergrund: Das duktales Adenokarzinom des Pankreas ist ein berüchtigter Krebs, bekannt für seine schwierige Diagnose, Resistenz gegen Behandlung und eine insgesamt schlechte Prognose. Daher ist ein gründliches Verständnis der Pathogenese dringend erforderlich. Vor etwa zwanzig Jahren wurde eine Gruppe von Todesrezeptoren identifiziert, welche überwiegend auf Krebszellen exprimiert gefunden wurden. Diese heißen 'Tumor Necrosis Factor-related apoptosis-inducing ligand' (TRAIL)-Rezeptoren. Die Entdeckung der TRAIL-Rezeptoren und des Liganden TRAIL begründete die Hoffnung, Krebszellen zu töten, ohne normale Gewebe zu schädigen. Die humane TRAIL-Rezeptorfamilie besteht aus zwei Zelltod-induzierenden Rezeptoren (TRAIL-R1 und -R2) und zwei 'Decoy'-Rezeptoren (TRAIL-R3 und -R4) sowie Osteoprotegerin. Das Apoptose-induzierende Potential des TRAIL-Liganden sowie die Auswirkungen der jeweiligen Todesrezeptoren TRAIL-R1 oder -R2 wurden intensiv in verschiedenen Krebszellen untersucht. Ebenso wurde die anti-apoptotische Funktion von überexprimiertem TRAIL-R4 in verschiedenen zellulären Systemen gezeigt. Allerdings wurde das mögliche Zusammenspiel der verschiedenen TRAIL-Rezeptoren wenig untersucht.

Ziel: Es sollte eine funktionelle Detailanalyse der TRAIL-Rezeptorfamilie geschaffen werden, um die Auswirkungen der jeweiligen einzelnen TRAIL-Rezeptoren im Kontext der anderen testen zu können – besonders in Hinsicht auf Funktionen von TRAIL-R4.

Methoden: Es wurden zwei PDAC-Zelllinien verwendet (Colo357 und PancTu1). Mehrere *in vitro* Methoden wurden implementiert, einschließlich Western Blotting, FACS, ELISA, Echtzeit-PCR zusammen mit Proliferations-, Vitalitäts- und Migrations-Untersuchungen sowie Bioinformatik. Zusätzlich wurden SCID-beige Mäuse mit den Zelllinien als *in vivo*-Beweis für das Konzept inokuliert. Schließlich wurde auch eine kleine Kohorte von Patientengeweben immunhistochemisch untersucht.

Ergebnisse: Die aktuelle Studie zeigte eine enge Verbindung zwischen TRAIL-R1, -R2 und -R4. Wir konnten zeigen, dass die Kombination von TRAIL-R2-Knockdown mit oder ohne TRAIL-R4-Hoch-Regulation die aggressivsten, stark proliferativen Zellen mit einer schnellen Migrationsfähigkeit und einem hohen Entzündungsstatus waren. Allerdings

zeigte die TRAIL-R4-Hochregulierung mit gleichzeitigem TRAIL-R1-Knockdown die entgegengesetzten Effekte. Darüber hinaus spiegelten sich die Aggressivität und das metastatische Potenzial mit einer deutlichen Dysregulation in den CEACAM5 / CEACAM6-Niveaus wider. Hier verstärkte die TRAIL-R4-Hochregulierung bei begrenzter Expression von TRAIL-R2 ihr Niveau, während bei begrenzter Expression von TRAIL-R1 eine deutliche Reduktion von CEACAM5 / CEACAM6 beobachtet wurde. Darüber hinaus zeigten die Zellen mit TRAIL-R1-Knockdown und TRAIL-R4-Hochregulation eine insgesamt reduzierte Funktion, doch die Zellen wuchsen gut, wenn sie auf Fibronectin oder Tenascin-c als extrazelluläre Matrix (ECM) ausgesät wurden. Während Fibronectin ein ECM Bestandteil ist, der von Zellen in normalen Geweben einschließlich Pankreas produziert wird, ist Tenascin-c ein ECM-Protein, das in Krebsregionen gefunden wird. Diese Beobachtung bedeutet, dass diese besondere Zelllinie - wenn auch nicht sehr aktiv - in der Lage ist, in einer ungünstigen Umgebung im Vergleich zu anderen untersuchten Zelllinien zu überleben, und dies steht in Einklang mit dem schlechten Überleben, das in der Patientenkohorte in den entsprechenden Fällen gesehen wurde. Der Anteil von TRAIL-R2-niedrig-exprimierenden Zellen in den Patientengeweben war sehr gering, was bedeutet, dass diese Patienten möglicherweise aufgrund ihres fortgeschrittenen Status im Augenblick der Diagnose als inoperabel angesehen worden sein könnten. Darüber hinaus bestätigten die *in vivo*-Ergebnisse die funktionellen Eigenschaften der untersuchten Zelllinien. In Bezug auf TRAIL-R4-Effekte zeigte die TRAIL-R4-Hochregulation an sich die schnellste Tumorstadiumsrate, während bei gleichzeitigem TRAIL-R1-Knockdown die am langsamsten wachsenden Tumore beobachtet wurden. Allerdings zeigte eine TRAIL-R4-Überexpression bei TRAIL-R2-Knockdown fast keine Veränderung im Vergleich zu TRAIL-R2-Knockdown-Zellen. Diese Ergebnisse zeigen, dass TRAIL-R4 viele Auswirkungen hat, wobei seine Hochregulierung in Kombination mit einer niedrigen TRAIL-R1 Expression die Zellen zu einem weniger aggressiven Phänotyp führte, während bei TRAIL-R2-Knockdown diese Überexpression nur minimale Auswirkungen hatte.

Fazit: Wir fanden, dass TRAIL-Rezeptoren als ein stark voneinander abhängiges System agieren. Krebszellen können dieses System verwenden, um ungünstigen Bedingungen auszuweichen bzw. sich anzupassen oder sich zu vermehren, zu wandern und entzündliche Signale für günstigere Bedingungen auszusenden. Um die molekularen Auswirkungen dieses Systems zu verstehen, sollten die Expression aller dieser Rezeptoren parallel

analysiert werden. Darüber hinaus deutet die aktuelle Studie auf ein signifikant längeres postoperatives Überleben bei geringer Expression von TRAIL-R1 hin, was die Bedeutung der TRAIL-Rezeptor-Analyse zur Beurteilung des postoperativen Verlaufs der Pankreaskarzinompatienten unterstreicht.

I. INTRODUCTION

The pancreas is an organ of the digestive tract. This organ is composed of two compartments; an endocrine part that is responsible for hormone secretion and an exocrine part –acini, ducts and ductules –that is responsible for the production of digestive enzymes and mucins. Pancreatic ductal adenocarcinoma (PDAC) is an epithelial carcinoma that arises from the pancreatic ducts and ductules (Wong et al., 2016). Unfortunately, the molecular basis of this form of carcinogenesis is still baffling. For that reason, our group is dedicated to a better understanding of PDAC development.

Cancer was and still is a big dilemma in our medical history. Most –if not all– cancer forms carry a bad prognosis and one of the worst is pancreatic cancer. Pancreatic cancer is more prevalent among elderly than younger individuals and it has a 5-years survival rate lower than 5% (Siegel et al., 2017; Torre et al., 2015). The underlying etiology remains unclear, however many factors have been implicated including tobacco smoking, alcohol, coffee intake, use of aspirin (Batty et al., 2009; Genkinger et al., 2009) as well as genetic predispositions (Chu et al., 2010). Withal some genetic syndromes have been shown to increase the risk of developing pancreatic cancer from about 8 to 132 fold, for instance Lynch Syndrome, familial atypical multiple mole melanoma syndrome, hereditary pancreatitis, ataxia-telangiectasia and Peutz-Jeghers Syndrome (Becker et al., 2014). Pancreatic cancer include many sub-types, however, most frequently the patients develop PDAC (~90%) and it has been found that 10% of these PDAC cases have a genetic background (Becker et al., 2014; Hidalgo et al., 2015). Despite of the modern advances in cancer therapy, PDAC remains very challenging, owing to its late and difficult diagnosis on one hand and the old age of the patients and the aggressiveness of the therapy on the other hand (Oberstein and Olive, 2013). Even after the successful resection of the tumor, the 5-year survival rate is only raised to 23.4% (Sahin et al., 2016). Notoriously, PDAC incidence is rather low, and it ranks fourth among the cancer related deaths in United States and Europe (Narayanan and Weekes, 2016; Wong et al., 2016). And although most of cancer related deaths are predicted to be declining by 2020, the death rate from pancreatic cancer is predicted to increase and be the second cause of cancer –related deaths within next decade (Malvezzi et al., 2017; Rahib et al., 2014).

PDAC development and heterogeneity

PDAC occur in the cells most burdened with mutations over the course of many years. Among the early mutations that occur in PDAC is the activation of the K-ras oncogene and that is followed by mutations in TP53, and smad4 on later stages (Shen et al., 2013; Yonezawa et al., 2008). Eventually, many of these mutations build-up and interrupt numerous biological pathways like WNT, hedgehog and DNA repair signaling (Waddell et al., 2015; Witkiewicz et al., 2015). Therefore, it was understood that PDAC develop stepwise; starting from precursor lesions until it is fully developed. PDAC precursor lesions include, pancreatic intra-epithelial neoplasia (PanIN), intra-ductal papillary mucinous neoplasia (IPMN), mucinous cystic neoplasia (MCN), and intra-ductal tubular papillary neoplasia (Guo et al., 2016). PanIN is further categorized according to its degree of atypia into three grades; PanIN1, PanIN2 and PanIN3 (Becker et al., 2014). The above listed precursor lesions are all ductal in origin, yet it has been recently devised that PDAC can also arise from non-ductal cells. It was suggested that either centroacinar-acinar compartment (CAAC) progress to PDAC via acinar-ductal metaplasia (ADM) or the centroacinar cells progress to PDAC through its expansion together with a simultaneous apoptosis of the acinar cells. Recently, a consensus was reached to re-classify the premalignant pancreatic pathology into low-grade and high-grade PanIN or low grade and high grade IPMN/MCN lesions (Basturk et al., 2015).

Several patient-based studies showed the involvement of a vast array of genetic mutations in the development of PDAC. These mutations in turn affected many biological processes and thus denoting the difficult and heterogenic nature of this resistant ailment (Jones et al., 2008; Waddell et al., 2015; Witkiewicz et al., 2015). Furthermore, it has been reported that each case of PDAC entails not only the commonly encountered mutations but also many infrequently seen ones, thus adding up to its complex nature (Bell, 2010). Besides, the presence of cancer stem cells (CSCs) heightens the tumor resistance and heterogeneity. CSCs are sub-class of cancer cells that are undifferentiated and capable of self-renewal (Sahin et al., 2016). This sub-class of cells occupy the highest level on the cellular hierarchy and that makes these cells capable of differentiating into any cell type (Brandi et al., 2017; Tanase et al., 2014). These CSCs are hypothesized to be responsible for tumor aggressiveness and drug resistance, due to their cellular plasticity and self-renewal capabilities. CSCs were reported to strongly activate the sonic hedgehog pathway

genes in comparison to non-stem cancer cells (Sahin et al., 2016). Sonic hedgehog pathway is a growth signaling pathways that promotes angiogenesis, proliferation and survival and is implicated in PDAC development (Bailey et al., 2009, 2008; Marechal et al., 2015; Nolan-Stevaux et al., 2009; Tian et al., 2009; Yauch et al., 2008). Among the approaches to target CSCs was the concomitant inhibition of c-Jun N-terminal kinase (JNK) with TRAIL therapy. It was found that this approach reduced the tumor burden and prompted the killing of CSCs without affecting the untransformed stem cells or the general health in mice (Recio-Boiles et al., 2016).

Another factor that might contribute to PDAC heterogeneity is the production of mucins that will render the tumor milieu very viscous and ill-defined. Even the three pre-malignant lesions; PanIN, IPMN and MCN express mucins (Yonezawa et al., 2008). Mucins are large molecular weight glycosylated proteins produced normally by epithelial cells for protection. There are two types of mucins; transmembrane and secreted forms (Hollingsworth and Swanson, 2004). The normal pancreas expresses transmembrane mucin 1 (MUC1) only on the apical surface of the centroacinar cells, intercalated, intralobular ducts and partially on the interlobular ducts. Yet, MUC1 is not present in the pancreatic ducts, acini or islets. Despite the original physiological protective role of mucins, they have been implicated in the pathophysiological development and aggressiveness of many carcinogenesis. High levels of the secreted MUC2, MUC4 MUC6 and MUC5AC were associated with pancreatic malignancies (Horinouchi et al., 2003; Yokoyama et al., 2016; Yonezawa et al., 2008). Additionally, cancer exploit the capabilities of the membrane-bound mucins –like the aberrant MUC1 expression –to manipulate adhesion, cell-cell and cell-ECM (extra-cellular matrix) interactions and thus promoting proliferation and survival (Jonckheere et al., 2015; Kufe, 2009; Yokoyama et al., 2016). Therefore, MUC1 was reported to be preferentially highly expressed in invasive pancreatic tumors (Lüttges et al., 2002).

The normal exocrine pancreas is comprised mainly of glandular tissues and with the development of chronic pancreatitis the fibrotic tissue formation is increased ranging from mild, moderate to severe fibrosis (Narayanan and Weekes, 2016). In PDAC, there is an additional malignant inflammatory status that mediates the formation of an extensive fibrotic tissue termed “desmoplasia”. It was also reported that this extensive desmoplasia can both predispose to cancer development and augment tumor progression (Pickup et al.,

2014) and in turn adds-up to the tumor heterogeneity. This desmoplastic reaction is formed of different ECM proteins particularly collagens, fibronectin, laminin. These ECM components are excreted in the tumor milieu by the pancreatic stellate cells driven by Transforming Growth Factor- β (TGF- β), platelet derived growth factor (PDGF) and fibroblast growth factors (FGF). Eventually this desmoplasia not only renders the tumor rigid but also represents a barrier for tissue perfusion thus impairing the drug delivery and leading to drug resistance (Feig et al., 2012; Narayanan and Weekes, 2016). It was also revealed that the expression of sonic hedgehog pathway is confined to the stromal compartment and that it plays an important role in PDAC desmoplastic reaction. It was reported that inhibition of the sonic hedgehog signaling facilitates the drug delivery in the tumor tissues (Feig et al., 2012). Hence, some groups are calling-out for a stroma-targeted therapy (Hamada et al., 2013; Li et al., 2012; Xie and Xie, 2015). Most PDAC patients would benefit from such a regimen, since these fibrotic barriers were observed in both the primary pancreatic cancer and metastatic lesion (Whatcott et al., 2015). As a prove of concept, it was found that the hyaluronic acid present in the tumor stroma was responsible for elevating the interstitial fluid pressures thus leading to vascular collapse and in turn rendering the PDAC tissues unreachable. A side note, it was also reported that this interstitial fluid pressures was the highest in PDAC in comparison to other solid tumors (Provenzano et al., 2012).

PDAC and TNF-related apoptosis-inducing ligand

Ultimately, many cancer remedies are focused on terminating the malignant cells via apoptosis. For that sake, radio- and chemotherapeutics are used. Yet, most of the currently available treatment regimens cannot differentiate between the transformed and non-transformed cells and eventually kills both. Hence, new tumor-specific modalities are sought (de Miguel et al., 2016). Among the proposed targeted chemotherapeutics is Tumor necrosis factor-related apoptosis-inducing ligand (TRAIL). TRAIL is a member of the Tumor necrosis factor (TNF) superfamily that is capable of inducing apoptosis. TRAIL is a single-pass type II membrane protein (Mérino et al., 2007). In humans, TRAIL gene resides rather far away from the other TNF family members on chromosome 3q26 (Abdulghani and El-Deir, 2010).

TRAIL and its receptors have been initially identified in the late 1990s. All the TRAIL-receptors are located on chromosome 8 (Marsters et al., 1997; Pan, 1997; Pan et al., 1997; Screaton et al., 1997; Sheridan et al., 1997; Walczak et al., 1997; Wu et al., 1997). Five different TRAIL receptor (TRAIL-R) family members were described; TRAIL-R1/DR4, TRAIL-R2/DR5, TRAIL-R3/DcR1, TRAIL-R4/DcR2 and Osteoprotegerin (OPG). The TRAIL receptors are single-pass, type I transmembrane proteins. These group of proteins have an extracellular N-terminus and an intracellular C-terminus (Mariapia A Degli-Esposti et al., 1997; Pitti et al., 1996; Walczak et al., 1997; Wiley et al., 1995). In the normal pancreas, only a small amount of pancreatic acini have been found to express both TRAIL-R1 and -R4. However, in pancreatitis, it was reported that the exocrine part and some islet cells neo-express TRAIL-R1, -R2 and -R4 (Hasel et al., 2003). Also, TRAIL receptors were reported to be predominantly expressed by cancer cells and are capable of preferentially killing them rather than normal ones (Ashkenazi et al., 1999). Therefore, the discovery of TRAIL ligand and its cognate receptors presented a great hope for a selective cancer therapy (Dai et al., 2015; de Miguel et al., 2016; Lemke et al., 2014; Mérimo et al., 2007; Srivastava, 2001; Wajant, 2015; Wiezorek et al., 2010; Yagita et al., 2004).

Only two TRAIL receptors (TRAIL-R1 and -R2) contain an intracellular death domain (DD) that is capable of inducing cell death, while TRAIL-R3 and -R4 lack this domain either completely or partially, respectively. In case TRAIL binds to the aggregated TRAIL-R1 and/or -R2 homo- or heterodimers, this complex succeeds to recruit Fas-Associated protein with Death Domain (FADD) thus leading to the activation of Caspase-8 that in turn starts the apoptosis cascade leading eventually to cell death. Moreover, that TRAIL induces cell death in a p53-independent manner (Morizot et al., 2011; Neumann et al., 2012). Beside the death receptors TRAIL-R1 and -R2, TRAIL can also bind to three other receptors, TRAIL-R3 and -R4 and the soluble receptor OPG. While TRAIL-R3 is a glycosylphosphatidylinositol anchored receptor completely lacking the cytoplasmic domain, TRAIL-R4 is more homologous to the TRAIL death receptors, yet it lacks a part of the DD (M A Degli-Esposti et al., 1997; Pan, 1997; Pan et al., 1998). In over expression studies, TRAIL-R4 was reported to be able to activate NF- κ B pathway (Mariapia A Degli-Esposti et al., 1997). However, due to its truncated DD, TRAIL-R4 is unable to induce cell death (Mariapia A Degli-Esposti et al., 1997). The last known receptor is OPG that binds

not only to TRAIL but also to RANKL, which upon binding to its receptor RANK, acts as a major inducer of osteoclastogenesis (Emery et al., 1998; Fuller et al., 1998; Lacey et al., 1998). OPG is thought to function by acting as a competitor of TRAIL death receptors for TRAIL-binding, yet the physiological relevance of the OPG-TRAIL interaction is not clear. Moreover, it has been shown that TRAIL-R3 and -R4 can prevent TRAIL-mediated apoptosis (LeBlanc and Ashkenazi, 2003; Meng et al., 2000; Mérimo et al., 2006). These blocking effects have been observed in many human primary cancers; for instance in acute leukemia (Riccioni et al., 2005), in prostatic cancer and breast (A D Sanlioglu et al., 2007; Ahter D. Sanlioglu et al., 2007), PDAC and others (Brost et al., 2014; Celik et al., 2013; Koschny et al., 2015; Liao et al., 2001; Morizot et al., 2011; Sanlioglu et al., 2009). Deeper analyses of the TRAIL receptors biology revealed that the decoy receptors on the plasma membrane either compete with the death receptors for the TRAIL (Sheridan et al., 1997) or interact with TRAIL-R1 or -R2 to hinder cell death signaling pathway (Clancy et al., 2005; Mérimo et al., 2006) and consequently hinder apoptosis (M A Degli-Esposti et al., 1997; Mariapia A Degli-Esposti et al., 1997). Thus, the balance between various TRAIL receptors is essential to induce cellular death or lead to resistance of the cells to TRAIL-induced apoptosis.

TRAIL-R4

The TNFRSF10D gene is located on chromosome 8q21. This gene comprises of 9 exons and codes for TRAIL-R4 protein which is approximately ~41.7 kDa. Despite TRAIL-R4 was previously reported to be physiologically found in many tissues like the pregnant placenta and fetal ovaries (Chen et al., 2004; Krieg et al., 2006; Marsters et al., 1997), yet, there are no reports about the possible physiological functions of TRAIL-R4. Two isoforms have been reported for TRAIL-R4; TRAIL-R4 α (380 base pair) and TRAIL-R4 β (266 base pair). TRAIL-R4 β lacks exon 3 which is corresponding to the first cysteine-rich domain and is involved in the preligand assembly domain, which is essential for TRAIL binding. Therefore, TRAIL-R4 β is incapable of binding to TRAIL (Krieg et al., 2006; López-Gómez et al., 2016). In cancer, a lot of research has been dedicated to understand the function and influence of the death-inducing TRAIL receptors; however, rather few papers are focused on the role and impact of TRAIL-R4.

Interestingly, TRAIL-R1, -R2, -R3 and -R4 are targets of the tumor suppressor protein p53. TRAIL-R4 is capable of not only hindering TRAIL-induced apoptosis but can

also block the p53-driven cell death. TRAIL-R4 was reported to negatively regulate the tumor suppressor gene p53. In 2000, a group reported that both the mRNA and protein levels of TRAIL-R3 and -R4 were augmented upon infecting the cells with p53-expressing adenovirus, denoting a positive feedback from p53 on TRAIL-R4. In the same experiment, it was proved that the high levels of TRAIL-R4 suppressed p53 levels in a negative feedback loop. Additionally, the group performed several C-terminal deletions of TRAIL-R4 and deduced that this p53 inhibitory effect was dependent on the first 43-amino acids of the intracellular domain of TRAIL-R4 protein (Meng et al., 2000).

In 2011, a group of researchers studied the effect of chemotherapy on the TRAIL-R4-mediated resistance to TRAIL-induced apoptosis at the DISC (death-inducing signaling complex) level. In this study, the team combined TRAIL treatment with multiple chemotherapeutics [Cisplatin, etoposide and 5-fluorouracil] in order to sensitize the cells to TRAIL-induced apoptosis through overcoming the TRAIL-R4 blocking effect. This process was achieved via the recruitment and activation of caspase-8 and was independent of the mitochondrial loop (see later). However, this effect was rather short-termed, as TRAIL-R4 managed to re-block the apoptotic process. This re-blockade was driven by the association of TRAIL-R4 with c-FLIP [Cellular FLICE (FADD-like IL-1 β -converting enzyme)-inhibitory protein]. c-FLIP is an inactive caspase-8 homolog, which is capable independently to hinder TRAIL-induced apoptosis. Therefore, the dual effect of both TRAIL-R4 and c-FLIP severely hindered apoptosis in that context (Morizot et al., 2011).

In addition, some studies were dedicated to explore the possibilities of inhibiting TRAIL-R4 and in turn aiding TRAIL-induced apoptotic signaling. In 2005, it was estimated that both interferon gamma and type I interferon alpha intensely suppressed plasma-membrane level of TRAIL-R4. The group also proved the involvement of the proteasome in this process (Wicovsky et al., 2005). Furthermore, it was reported that PARP13 [Poly (ADP-ribose) Polymerase-13] is responsible for the post-translational decomposition of TRAIL-R4 mRNA. It was shown that PARP13 binds to the 3'UTR of the cellular mRNA of TRAIL-R4 and in turn degrading it. To substantiate these results, the cells were depleted from PARP13 and found that TRAIL-R4 mRNA decay was markedly altered. Thus, they presented PARP13 as a pro-apoptotic mediator for TRAIL-induced apoptosis, through overcoming the TRAIL-R4-driven TRAIL resistance (Todorova et al., 2014).

One more action of TRAIL-R4 that could be considered as another get-out-of-death free card for the cancer cells, is cellular senescence (Campisi et al., 2011; Kren et al., 2007; Tacutu et al., 2013). Normally senescent cells are halted in growth and they secrete a rather unique cocktail of mRNA: chemokines, cytokines, growth factors and proteases termed the senescence-associated secretory phenotype (SASP). This SASP alert the immune cells which in turn eliminate these senescent cells via immuno-surveillance. Nevertheless, cellular senescence is a double-edged sword that might have tumorigenic impact as well. Despite senescence may be beneficial by suppressing the tumor initiation process, there are studies that claimed that these senescent cells may promote tumor growth and metastasis in mice (Eggert et al., 2016) and induce epithelial-to-mesenchymal transition (EMT) (Krtolica et al., 2001). Hence, it is believed that SASP induced by the senescent cells might help the tumor cells evade immunity and survive via creating an immunosuppressive immune environment (Eggert et al., 2016). Another theory, with the advancement of age, the body is in a state of genomic instability and ageing that might as well affect the immune cells and DNA repair genes and thus accumulating both tumor cells and senescent cells (Maslov and Vijg, 2009). Since 2005, TRAIL-R4 is regarded as an *in vivo* senescence maker (Collado et al., 2005; Collado and Serrano, 2010; Pare et al., 2013). Therefore, TRAIL-R4 might provide the tumors with another survival mechanism through inducing cellular senescence.

Logically, from the above mentioned information, it could be assumed that TRAIL-R4 should be highly expressed in malignant cells as self-protection mechanism and that is partially true. However, it was reported that TRAIL-R4 gene was highly methylated in many tumors including melanoma, neuroblastoma, pheochromocytoma, breast and lung cancer. Additionally, some indicated that the methylation of the TRAIL-R4 promoter in fact predisposes to tumor formation, relapses and carried an overall poor prognosis (Bonazzi et al., 2011; Kiss et al., 2013; Lau et al., 2012; Ratzinger et al., 2014; Shivapurkar et al., 2004; van Noesel et al., 2002; Yang et al., 2007). Therefore, one can deduce that TRAIL-R4 could bear more functions than what is currently recognized.

Intracellular TRAIL receptors

The membrane-bound TRAIL receptors' functions are intensely studied. However, the role of the intracellular TRAIL receptors is poorly understood. In 2000, a group followed the intracellular distribution of the TRAIL receptors in melanoma upon TRAIL

stimulation. In un-stimulated cells, TRAIL-R3 and -R4 were seen primarily in the nucleus and TRAIL-R1 and -R2 were located on the plasma membrane and in Golgi apparatus. Upon TRAIL stimulation, it was found that the activation of the two death receptors drove the movement of TRAIL-R3 and -R4 to the cytosol and then to the plasma membrane where they compete for TRAIL and act as decoy receptors. However, the functionality of the receptors in the nucleus and Golgi apparatus was not sought (Zhang et al., 2000). More recently, TRAIL-R2 trafficking was investigated in in cervical cancer cell line (HeLa). In this study, it was proven that importin β 1 was responsible for the nuclear localization of TRAIL-R2 in TRAIL-resistant malignant cells upon exposure to TRAIL in HeLa cells (Kojima et al., 2011). Moreover, the presence of the TRAIL receptors intracellularly was investigated and described in a variety of tumor cells of different origin. Additionally, novel pro-tumoral functions for the nuclear TRAIL-R2 were also reported and the high nuclear expression of TRAIL-R4 was found to be correlated with bad prognosis in PDAC patients (Haselmann et al., 2014).

TRAIL receptors' signaling

The binding of TRAIL ligand to cell membrane-bound TRAIL-R1 and/or -R2 triggers the activation of two signaling pathways; the apoptotic and non-apoptotic signaling pathways (Figure 1.1). Since both TRAIL-R1 and -R2 contain an intact DD, they are capable of inducing cell death. Upon their binding with the TRAIL ligand, a multimeric complex is formed and the interaction between the DD facilitates the recruitment of FADD. Accordingly, FADD

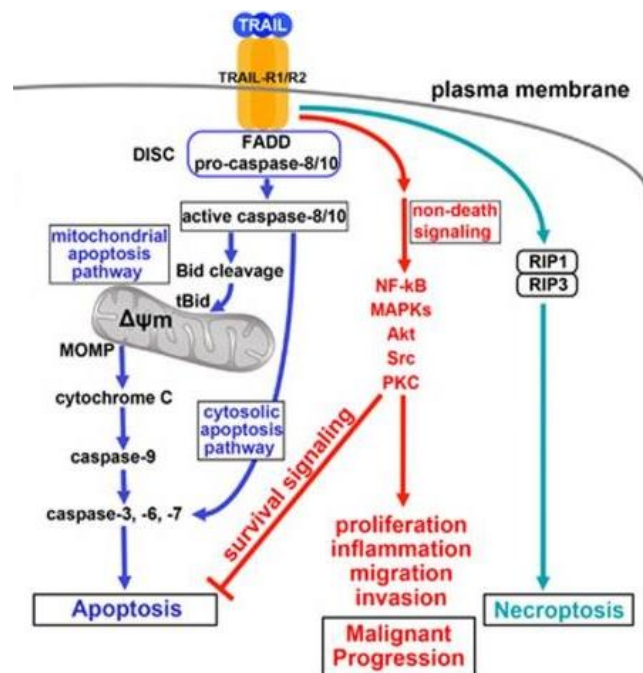


Figure 1.1| Signal transduction pathways activated upon the binding of TRAIL to its death-inducing receptors. [modified (Bertsch et al., 2014)]

closely interacts with the death effector domain (DED) of the initiator pro-caspases-8 and -10, and eventually form the DISC. Upon the formation of the DISC, initiator pro-caspases

are activated via cleavage. The activated initiator caspases are released into the cytoplasm. The cells are then subdivided into two classes according to their response; Type I and Type II (Bertsch et al., 2014; Mérimo et al., 2007).

In type I cells, there is a sufficient amount of activated initiator caspases released into the cytosol, that is capable of activating the effector caspases-3, -6, -7. Whereas, in type II cells, the activated initiator caspases are not enough to trigger cell death, instead a mitochondrial amplification loop is needed to efficiently activate the effector caspases. This amplification loop entails the cleavage of BID (BH3 interacting-domain death agonist) and generation of the active tBID (truncated BID) that in turn activates Bax and Bak that permeabilize the mitochondrial membrane. Once permeabilized the mitochondria release several pro-apoptotic factors into the cytoplasm namely, cytochrome *c*, Smac/Diablo (second mitochondria-derived activator of caspase/direct IAP binding protein with low pI) and HtrA2/Omi (high temperature requirement protein A2/Omi) (Figure 1.2). At this stage

cytochrome *c* together with dATP bind to the cytosolic protein Apaf-1 (apoptotic protease activating factor-1) and form with pro-caspase 9 the so-called apoptosome. In the apoptosome, pro-caspase-9 becomes activated and leads to the activation of the effector caspases and eventually results in eliminating the cells. PDAC cell lines are type II cells (Ashkenazi et al., 1999; Sebastian Hinz et al., 2000).

As much as the TRAIL-induced apoptosis gave the scientific community a great hope of eradicating cancer cells, most of the PDAC cell lines turned out to be resistant to TRAIL-mediated apoptosis. In particular, primary PDAC tumors are either inherently TRAIL-resistant or they acquire this resistance during TRAIL treatment. It is currently known that together with TRAIL-induced apoptotic signaling, TRAIL can induce other

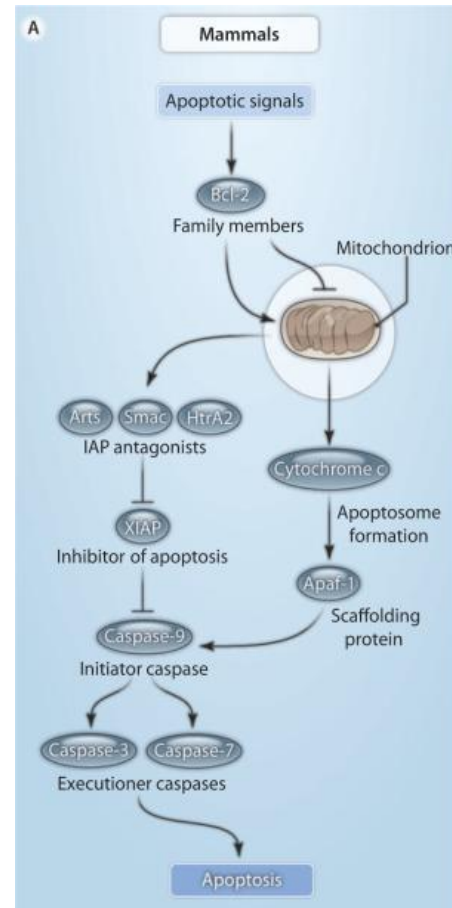


Figure 1.2| Inhibitory factors of the mitochondrial pathway in mammals [modified (Bergmann and Steller, 2010)].

non-apoptotic signaling pathways (Figure 1.1) such as NF- κ B and PKB/AKT (Mariapia A Degli-Esposti et al., 1997; Lalaoui et al., 2011; Trauzold et al., 2001) or MAPK, Src and phosphoinositide 3-kinase (Azijli et al., 2013). The balance between the apoptotic and non-apoptotic TRAIL-induced signaling will eventually determine the cell behavior and fate.

From the aforementioned information, it becomes clear that there is a lot yet to be learnt about TRAIL and its cognate receptors. On one hand, there is an urgent need to know how to sensitize the tumor cells to enhance TRAIL-induced apoptosis and overcome TRAIL resistance. On the other hand, it is crucial to understand the limits of the normal/untransformed cells to these sensitizers. Otherwise, we will lose the benefit of TRAIL being a cancer-specific therapy regimen (Dijk et al., 2013). However, the mechanisms of resistance of both tumor and normal cells were found to be rather similar. This resistance was not only attributed to the effect of the decoy receptors, but also to TRAIL's simultaneous induction of several non-apoptotic proteins. Among the proteins responsible for TRAIL resistance is the expression of the inactive caspase-8 homolog c-FLIP. Another protein was detected at the level of the effector caspase-3 were the activation of caspase-3 is hindered by XIAP (X-linked inhibitor of apoptosis protein) (Figure 1.2). XIAP is potent member of the IAPs (Inhibitors of apoptosis proteins) family that have been previously linked to drug resistance and poor prognosis (Eckelman et al., 2006; Lemke et al., 2014; Salvesen and Duckett, 2002), and XIAP suppression was indicated as a sensitizer to TRAIL-induced apoptosis in pancreatic cancer cell lines (Vogler et al., 2007). Additionally, also BCL-2 (B-cell lymphoma 2) plays an important role in the cells by inhibiting the Bax/Bak activation and thus protecting itself against TRAIL-induced apoptosis (Figure 1.2) (Bergmann and Steller, 2010).

As previously mentioned, it was revealed that TRAIL receptors have pro-malignant functions (Trauzold et al., 2006) and it was shown that the nuclear expression of TRAIL-R2 promoted proliferation of tumor cells through suppression of the maturation of microRNA *let-7* (Haselmann et al., 2014). Furthermore, the expression of TRAIL-R2 and TRAIL-R4 were revealed to be significantly up-regulated in PDAC (Sanlioglu et al., 2009) and in other carcinomas as breast cancer. Also, the high expression of TRAIL-R4 per se was correlated with low survival rate (Ganten et al., 2009). Despite the many strategies that were investigated to sensitize the tumor cells to TRAIL, it remains widely unresolved which markers—in addition to the expression of TRAIL-R1/R2— would identify and allow

the selection of patients that are likely to benefit from a TRAIL-based therapy (Lemke et al., 2014).

Looking at TRAIL-induced apoptosis from a different perspective, a tumorigenic role might be detected namely the “apoptosis-induced compensatory proliferation”. This process occurs in the neighboring cells surrounding the dead cells in order to maintain tissue homeostasis. In normal cells, compensatory proliferation occurs as a part of tissue regeneration in the normal wear-and-tear mechanisms. This compensatory proliferation entails; wound healing and proliferative blastema cells formation in some animals (Fan and Bergmann, 2008; Gurtner et al., 2008). Many studies have been dedicated to the understanding of this process in different animals including mice and also in humans. These studies revealed that apoptosis controlled the proliferative blastemal formation and in turn the compensatory proliferation. Among the pathways implicated in the apoptosis-induced compensatory proliferation were JNK and WNT signaling (Chera et al., 2009; Kondo et al., 2006; Li et al., 2010, 2004; Pellettieri and Alvarado, 2007; Ryoo et al., 2004). In cancer, most of the currently available treatments –and also TRAIL – are based on apoptosis induction. Thus, these regimens might simultaneously induce a compensatory proliferation. Accordingly, it is imperative that we hinder this compensatory proliferation in order to have a successful cancer-specific therapy.

Previous studies focused primarily on the expression levels of specific TRAIL receptors individually and overlooked the overall contribution and the interplay between the whole receptor family members in the progression of carcinogenesis. These studies were aimed to show the actual state of the different TRAIL receptors in the investigated cancer cells. In 2009, a group studied the plasma membrane levels of TRAIL-R1, -R2, -R3 and -R4 in both normal cells and several solid primary tumor cells from Colon, renal, cervical, non-small cell lung cancer and PDAC. They reported that the ratio between TRAIL-R1 expression to TRAIL-R3 and -R4 expression could predict the level of cancer cell resistance to TRAIL-induced apoptosis (Büneker et al., 2009). Likewise, the loss of TRAIL-R1 and upregulation of TRAIL-R2 and -R4 were correlated with hepatocellular carcinoma, and loss of either TRAIL-R1 or -R2 were associated with a deteriorated 5-year survival of hepatocellular carcinoma patients (Koschny et al., 2015; Kriegl et al., 2010).

TRAIL and necroptosis

There is a plethora of information about the apoptotic capabilities of the TRAIL ligand in many types of cancer and many researchers are dedicated to unravel the mechanisms of its resistance. Yet, more recently some groups started to entertain the idea that TRAIL ligand might induce other forms of cell death. Generally, regulated cell death is an important cellular mechanism that maintains the survival of any multicellular organism. The dysregulation of cell death can result in deleterious outcomes like tumor formation (Jin and El-Deiry, 2005; Walsh, 2014). Among the regulated death modalities there is caspase-dependent cell death (e.g. apoptosis), and caspase-independent cell death (e.g. regulated necrosis like necroptosis) (Galluzzi et al., 2012). As previously mentioned, the need to explore alternative pathways to eliminate cancer cells came from the fact that many tumors are resistant to TRAIL-induced apoptosis. Therefore, TRAIL ability to induce necroptosis was recently investigated (Figure 1.1). Undeniably, there are critical differences between apoptotic and necroptotic cell death. Physically both cell death modalities end by the demise of the intended cell, yet apoptosis is a more organized process that generate limited tissue damage and inflammation (Garg et al., 2010). However, necroptosis is a caspase-independent cellular death mode that might represent an alternative anti-cancer treatment regimen (Philipp et al., 2016). This type of regulated necrosis induced by TRAIL (or other death ligands such as TNF) is mediated via the phosphorylation of receptor interacting serine/threonine kinase 1, 3 (RIPK1, RIPK3) and mixed lineage kinase domain like protein (MLKL) (Kaczmarek et al., 2013). Earlier, evidences have been provided that TRAIL-induced necroptosis can be used to eliminate apoptosis-resistant cancer cells (Mocarski et al., 2011; Philipp et al., 2015; Voigt et al., 2014). Additionally, knowing the general signaling pathways and/or molecules that are unique for TRAIL-mediated necroptosis might be helpful in designing a more potent TRAIL-based anti-tumor therapy (Sosna et al., 2016). Hitherto, the effect of the interplay between the TRAIL receptors on the execution of necroptosis was not investigated.

TRAIL and inflammatory cytokines

Another serious problem and a key player in the advancement of many carcinogenesis is chronic inflammation. Therefore, it is currently considered as one of the hallmarks of cancer (Hanahan and Weinberg, 2011). The presence of a chronically inflamed microenvironment predisposes to the development of malignancy which is the

case in many solid tumors like PDAC where chronic persistent pancreatitis makes the tissues more vulnerable to tumor formation (Becker et al., 2014; Dhar et al., 2015; Yeo, 2015). As previously stated, TRAIL – like TNF – induces NF κ B which is known to induce several pro-inflammatory cytokines e.g. TNF itself, interleukin-6 (IL6), interleukin-8 (IL8) and monocyte chemoattractant protein-1 which are known to be involved in cancer progression. In particular, it was reported that there was a mild limitation of proliferation under TNF α treatment, however, the invasion power were boosted in PDAC cells. To confirm these results, these effects of TNF α were investigated *in vivo*, and the experiment revealed an increase in tumor growth and metastasis upon treatment. Also the inhibition of tumor-derived TNF α showed anti-tumoral effects thus denoting the strong impact of such a pro-inflammatory action in PDAC (Egberts et al., 2008).

Moreover, other inflammatory agents might synergize TRAIL's inflammatory potential and thus worsening the patient's prognosis. For instance, IL6 which is one of the known inflammatory cytokines and its high expression has been tightly bound to pancreatic malignancy (Holmer et al., 2014; Wu et al., 2017; Zhang et al., 2013). To emphasize the effect of IL6, it was revealed that PDAC tumor progression was limited via IL6 blockade in mice (Mace et al., 2016). Additionally, it was found that the elevated levels of TRAIL-R2 and -R4 together with an augmented IL6 receptor expression were associated with a higher chance for tumor metastasis upon studying the spindle-shaped stromal cells in breast cancer. In the same study, it was also reported the mere up-regulation of either TRAIL-R4 or IL6 receptor in these cells significantly worsened the patients' disease-free and metastasis-free survival (Labovsky et al., 2016), therefore denoting the interconnection between TRAIL receptors and IL6. Another known inflammatory cytokine is IL8. IL8 has been also associated with malignant transformations (Bassagañas et al., 2015; Waugh and Wilson, 2008). Additionally, IL8 expression has been involved in modulating TRAIL receptor expression in PDAC. In 2016, it was reported that IL8 suppressed the expression of TRAIL-R3 and enhanced the expression of pro-apoptotic receptors (Recio-Boiles et al., 2016). One important aspect of studying these inflammatory cytokines resides in the fact that they can be measured in the patients' sera. The serum level of IL6 was determined to be high in pancreatic cancer patients in many studies (Mitsunaga et al., 2013; Miura et al., 2015; Mroczko et al., 2010; Okada et al., 1998; Zhang et al.,

2013). Likewise, the serum level of IL8 was correlated with bad prognosis in pancreatic cancer (Chen et al., 2012; Ebrahimi et al., 2004).

Epithelial-mesenchymal transition (EMT)

EMT is a process where the epithelial cells replace its well-differentiated form to acquire a more mesenchymal form. This process is regarded as an essential step for cancer cells to be able to disseminate and metastasize (Tanase et al., 2014). Several pathways and markers among which are NOTCH signaling and E-cadherin, vimentin, NANOG, ZEB1, TWIST, SLUG and Snai1, have been implicated in the process of EMT in cancer cells. For instance, the level of the epithelial marker E-cadherin is decreased whereas the mesenchymal markers as vimentin, Snai1, N-cadherin levels are increased during the EMT process. E-cadherin is a plasma membrane protein found mainly on epithelial cells, whereas vimentin has been reported to be linked with the mesenchymal phenotype (Lu et al., 2014; Wang et al., 2014). It was previously stated that the cells during this transformation switch from cell-cell communication to cell-ECM denoting also the important role of the ECM in the EMT process (Park and Schwarzbauer, 2014). Moreover, different members of NOTCH signaling pathway has been associated with EMT (Gu et al., 2016; Ito et al., 2016; Orzechowska et al., 2016) together with many proteins that have been also associated with EMT, for instance, NANOG (Qin et al., 2016), and also ZEB1, TWIST, SLUG, Snai1 that were reported as EMT markers in colorectal, breast cancer and hemangiomas (Mego et al., 2015; Yamada et al., 2016; Zhai et al., 2016).

Some studies were dedicated to estimate the correlation between the EMT process and the death-inducing TRAIL receptors. For instance, some studies revealed that the resistance of breast and urothelial cancer cell lines to TRAIL-induced apoptosis was associated with EMT and that mediated the metastatic process (McConkey et al., 2009; Wang et al., 2014). Another study showed that knockdown or suppression of E-cadherin was partially responsible of TRAIL-induced resistance and thus suppressing apoptosis. This suppression of apoptosis denotes that E-Cadherin is involved in TRAIL-R1 and -R2 clustering and is capable of aiding in the formation of DISC and thus enhancing the apoptotic cell death (Lu et al., 2014).

Cancer and cell adhesion molecules

Cellular migration is a complex process that leads a major role in embryogenesis as well as in cancer dissemination (Zhao and Guan, 2011). In cancer, cellular migration either involves the ECM, cell adhesion proteins and the polymerization of actin stress filaments or it may also be an adhesion free process (Tozluoğlu et al., 2013). Cellular adhesion is mediated by either the interaction between the integrins and the ECM proteins (cell-ECM adhesion) or by interaction between the cells with each other (cell-cell adhesion). Cell-ECM interaction starts a cascade of focal adhesion protein phosphorylation, changes in cellular pH and calcium level and activation of MAPK pathway (Turner, 2000). However, until now, the correlation between other TRAIL receptors and cellular adhesion is yet to be elucidated.

Recently, the importance of the tumor microenvironment gained a lot of popularity. Many groups are studying the important impact of the ECM and the peri-tumoral environment on tumor progression and therapy (Feig et al., 2012; Provenzano et al., 2012; Rucki et al., 2016; Sun et al., 2016). Among these studies, the effects of the different integrin molecules on a variety of tumors were investigated. In 2007, it was elucidated that the deletion of integrin $\beta 1$ from the pancreatic β -cell tumors inhibited the ability of the cells to metastasize or proliferate and drove the cells to senescence (Kren et al., 2007). Later on, the expression of integrin $\alpha V\beta 6$ was also reported to be elevated in many epithelial tumors but not in normal tissues (Koopman Van Aarsen et al., 2008). Another study on colon cancer cell lines showed that EMT may cause an enhanced expression of integrin $\alpha V\beta 6$ and thus can be regarded as a marker for bad prognosis (Bates et al., 2005). Additionally, another group aimed to block $\alpha V\beta 6$ receptor and realized that this blockage hindered the inflammatory process and tumor dissemination in pharyngeal carcinoma via the localized inhibition of TGF- β pathway (Koopman Van Aarsen et al., 2008) and thus indicating the essential role of adhesion in cancer.

Tenascin-c is one the large glycoproteins that are expressed in embryonic tissues and is a rarity in adult tissues. However, tenascin-c was found to be up-regulated in many solid tumors including breast cancer and lymphoma (Brellier et al., 2012; Mackie et al., 1987; Orend and Chiquet-Ehrismann, 2006; Schliemann et al., 2009). Likewise, tenascin-c has been implicated in PDAC carcinogenesis (Esposito et al., 2006). In PDAC, tenascin-c is highly expressed in undifferentiated tumors and its presence facilitates tumor

progression, invasion and metastasis (Paron et al., 2011) and hence providing more evidence on the important and essential role of cell-ECM communication in solid tumors.

In addition to cell-ECM adhesion molecules, cell-cell adhesion molecules play an important role in cell survival and tumor formation. Carcinoembryonic antigen-related cell adhesion molecule (CEACAMs) are cell-cell adhesion molecules expressed in many cells – including epithelial cells – all over the human body and are needed in many physiological processes; adhesion, proliferation and differentiation. Beside their important roles in normal cells, CEACAMs have been correlated with malignant transformation and cellular survival in epithelial tumors as well (Beauchemin and Arabzadeh, 2013; Tchoupa et al., 2014). In PDAC, dysregulation of CEACAM member 5, 6 and 1 were reported as biomarkers for tumor dissemination and patient prognosis (Gebauer et al., 2014; Kuhlmann et al., 2016). Overall, it is obvious that cellular adhesion – whether cell-ECM or cell-cell – and the tumor microenvironment have an important impact on tumor proliferation and progression.

AIM OF THE STUDY

The aim of this study was to characterize the impact of the particular TRAIL receptors' configuration in creating the malignant phenotype in PDAC and to investigate the possible functions of TRAIL-R4 with consideration to its interplay with TRAIL-R1 or TRAIL-R2 in two PDAC cell lines; Colo357 and PancTuI. Additionally, the current study intended to show the behavior of the cell lines in response to TRAIL-induced death apoptosis and necroptosis. Furthermore, the aim was to scope the interactions between the TRAIL receptors from the *in vitro*, *in silico*, and *in vivo* points of view. And as a proof of concept, an adaptation of the results was sought to correlate the immunohistochemical staining of the TRAIL receptors in the tissues of a small *ex vivo* patient cohort with the patients' survival.

II. MATERIALS & METHODS

1. Materials

1.1. Chemicals

chemical / reagent	Company
2-Propanol, 70%	Otto Fischar, Saarbrücken, Germany
Accutase (DPBS, 0.5 mM EDTA), with Phenol red	PAN Biotech, Aidenbach, Germany
Acetic acid, 100%	Merck Milipore, Darmstadt, Germany
Anexate (Flumazenil, 0.1mg/ml)	Roche, Grenzach-Wyhen, Germany
Antisedan (Atipamezol, 5 mg/ml)	Pfizer, Karlsruhe, Germany
Universal-Agarose, peqGOLD	PEQLAB - Life Science, Germany
Bovine serum albumin fraction V	Biomol GmbH, Hamburg; Germany
Bromphenol blue	Sigma Aldrich, Steinheim, Germany
Complete ultra-tablets protease inhibitor cocktail (EDTA free)	Roche, Mannheim, Germany
Cristal violet	Merck Milipore, Darmstadt, Germany
DC Protein Assay	Bio-Rad Laboratories, Munich, Germany
Developer, G153 A/B	AGFA, Mortsel, Belgium
DharmaFECT [®] 1	Thermo Fisher Scientific
DharmaFECT [®] DUO	Thermo Fisher Scientific
Dimethyl sulfoxide (DMSO)	Sigma Aldrich, Stennheim, Germany
Dithiothreitol $\geq 99\%$ p.a.	Roth, Karlsruhe, Germany
DNA Zap [™] (solution 1, 2)	Invitrogen, Thermo Fisher Scientific
Dormitor (Medetomidin, 1mg/ml)	Pfizer, Karlsruhe, Germany

DPBS	Gibco, Life Technologies, Darmstadt, Germany
EDTA dihydrate	Merck Millipore, Darmstadt, Germany
Eosin 0.5% solution	Geyer Th. GmbH & Co. KG, Germany
Ethanol, $\geq 99.8\%$ p.a.	Roth, Karlsruhe, Germany
Fentanyl (0,05 mg/ml)	Janssen-Cilag, Neuss, Germany
Fetal Bovine Serum	PAN Biotech, Aidenbach, Germany
Fibronectin	EMD Millipore, Temecula, USA
GelRed Nucleic Acid Gel Stain 10,000 in Water	Biotium, Hayward, USA
Geneticin disulfate (G418)	Carl Roth GmbH+ Co. KG, Cellpure [®] , Karlsruhe, Germany
Glucose 5%	Delta select, Germany
GlutaMax	Gibco, Life Technologies, Darmstadt, Germany
Glycerol	Sigma Aldrich, Steinheim, Germany
Glycine $\geq 99\%$ p.a.	Roth, Karlsruhe, Germany
Hematoxylin solution	Geyer Th. GmbH & Co. KG, Germany
Homoharringtonine (HHT), sc-202652A	Santa Cruz, USA
Hydrochloric acid, 25%	J.T. Baker, Griesheim, Germany
HEPES Buffer (1M)	Sigma Aldrich, Steinheim, Germany
Human TRAIL antibodies- MAB375	R&D systems, USA
Igepal CA 630 (Nonidet P40/N-P40)	Sigma Aldrich, Steinheim, Germany
Potassium chloride	Merck Milipore, Darmstadt, Germany

Lipofectamine [®]	Invitrogen, Thermo Fisher Scientific
Magnesium chloride	Merck Milipore, Darmstadt, Germany
Matrigel [®] basement membrane matrix	Corning, USA
Methanol, $\geq 99,9\%$ p.a.	Roth, Karlsruhe, Germany
Midazolam (1mg/ml)	Roche, Grenzach-Wyhen, Germany
Mitomycin C	Sigma-Aldrich, catalog number M0503
Mounting medium	Dianova, Hamburg, Germany
Naloxon (0.4 mg/ml)	CuraMed, Karlsruhe, Germany
Non-fat dried milk powder, blotting grade	Roth, Karlsruhe, Germany
OptiMEM [®] I (1x): HEPES, 2.4g/L sodium bicarbonate, L-Glutamine)	Gibco Life Technologies
PhosphoStop phosphatase inhibitor	Roche, Mannheim, Germany
PhosStop EASYpack phosphatase inhibitor cocktail	Roche, Mannheim, Germany
Pierce BCA Protein Assay	Fisher Scientific, Schwerte, Germany
Pierce ECL Plus	Fisher Scientific, Schwerte, Germany
Pierce [®] ECL Western blot substrate	Thermo Fisher Scientific
Ponceau-S-solution (0,1% in 5% HAC)	Sigma Aldrich, Steinheim, Germany
Protein G-Sepharose 4 Fast Flow	GE Healthcare, Freiburg, Germany
Puromycin dihydrochloride (P8833)	Sigma Aldrich, Steinheim, Germany
Rapid fixer, G354	AGFA, Mortsels, Belgium
Rely+on Virkon - Virkon disinfectant	Antec, Du Pont, England
Recombinant human TRAIL (TRAIL)	PeprTech EC., London, UK
RPMI 1640	Gibco, Life Technologies, Darmstadt,

	Germany
SDS (10%)	Applichem, Darmstadt, Germany
Sodium azide	Sigma Aldrich, Steinheim, Germany
Sodium chloride	J.T. Baker, Griesheim, Germany
Sodium deoxycholate	Applichem, Darmstadt, Germany
Sodium Pyruvate	Gibco, Life Technologies, Darmstadt, Germany
Spectra Multicolour Broad Range Protein ladder	Fisher Scientific, Schwerte, Germany
Tenascin-C	Merck Milipore, Darmstadt, Germany
Tris BASE	CalBiochem, Merck Millipore, Darmstadt, Germany
Tris HCl, $\geq 99\%$ p.a.	Roth, Karlsruhe, Germany
Triton X 100	Sigma Aldrich, Steinheim, Germany
Trypan blue-solution, 0,4%	Gibco, Life Technologies, Darmstadt, Germany
Trypsin EDTA (0.5%/0,2% in PBS), 10x, W/O Ca ⁺⁺	Millipore, Biochrom, GM, Germany
Tween-20	Merck Milipore, Darmstadt, Germany

1.2. Western blot antibodies

Specificity	Source	Clone	Diluted in*	Company	Catalog number	Diluted in*
α Tubulin	Rabbit	Monoclonal	0.5% M	Epitomics	1878-1	0.5% M
BID	Rabbit	Polyclonal	0.5% M	R&D Systems	AF846	0.5% M
Caspase-3	Mouse	IgG1 (3G2)	5% M	Cell Signaling Technology	9668S	5% M
Caspase-8	Mouse	IgG1 (1C12)	5% M	Cell Signaling Technology	9746S	5% M
CEACAM5	Mouse	T84.66 cell line	5% M	Home-made (conc. 450 μ g/mL)	----	5% M
CEACAM6	mouse	IgG1 (9A6)	5% M	Acris	AM02001 PU-N	5% M
E-cadherin	Mouse	IgG2a, κ	5% M	BD transduction laboratories	610181	5% M
HMGA2	Rabbit	Polyclonal	0.5% M	Cell Signaling Technology	5269S	0.5 % M
Integrin α V	Goat	Polyclonal	5% M	Santa Cruz	sc-6617	5% M
Integrin β 1	Goat	Polyclonal	5% M	Santa Cruz	sc-9936	5% M
Integrin β 6	Goat	Polyclonal	5% M	Santa Cruz	sc-6632	5% M
Lamin A/C	Rabbit	Polyclonal	0.5 % M	Cell Signaling	2032	0.5 % M

				Technology		
PARP	Rabbit	Polyclonal	5% M	Cell Signaling Technology	9542S	5% M
p-MLKL	Rabbit	monoclonal	TBST	Abcam	ab187091	5% M
RIPK1	Mouse	Polyclonal	5% M	BD Biosciences	610459	5% M
SLUG	Goat	polyclonal	5% M	Santa Cruz	sc-10436x	5% M
Snai1	Goat	Polyclonal	5% M	Santa Cruz	sc-10432x	5% M
TRAIL-R1	Rabbit	Polyclonal	5% M	Millipore	ab16955	5% M
TRAIL-R2	Rabbit	polyclonal IgG	5% M	ProSci	2019	5% M
TRAIL-R4	Mouse	(B-P30)	0.5% M	Santa Cruz	sc-65310	0.5% M
β -actin	Mouse	IgG1 (AC-15)	0.5% M	Sigma-Aldrich	A5441	0.5% M

* M = non-fat dried milk powder in tris-buffered saline-tween 20 (TBST),

Blocking of membrane was done by incubation in 5% Milk (M) in TBST for 1 hour at RT.

1.3. FACS antibodies

Clone	Target	End-conc.	Background	Company
11711	Isotype control	25 µg/16µl	Mouse monoclonal IgG1	R&D systems
133303	Isotype control	25 µg/16µl	Mouse monoclonal IgG2B	
69036	human TRAIL-R1	25 µg/16µl	Mouse monoclonal IgG1	
71908	human TRAIL-R2	25 µg/16µl	Mouse monoclonal IgG2B	
104918	human TRAIL-R4	25 µg/16µl	Mouse monoclonal IgG1	

Antibodies and solutions were diluted in 0.5% BSA/PBS.

1.4. Real time PCR (RT-PCR) primers

Target		Sequence
TRAIL-R1 (SYBR)	Forward	5'-AGA GAG AAG TCC CTG CAC CA -3'
	Reverse	5'-GTC ACT CCA GGG CGT ACA AT -3'
CEACAM5 (SYBR)	Forward	5'-CTTTATCGCCAAAATCACGC -3'
	Reverse	5'-CCAGCTGAGAGACCAGGAGA -3'
CEACAM6 (SYBR)	Forward	5'-GCATGTCCCCTGGAAGGA -3'
	Reverse	5'-CGCCTTTGTACCAGCTGTAA -3'
RPL22 (SYBR)	Forward	5'-TCGCTCACCTCCCTTTCTAA -3'
	Reverse	5'-TCACGGTGATCTTGCTCTTG -3'

1.5. GIPZ lentiviral human shRNA sequences

Target	Cell line ID	Sequence
TRAIL-R1	383714	Antisense: TGATCATGAAGTTTGATGG
TRAIL-R2	16711	Antisense: GCATTAAAGCAGCGTATC
TRAIL-R4	16774	Antisense: TCTGATATAAATTTCTCCC
TRAIL-R4	34449	Antisense: AAGAAATGAATTTCTTCCG

1.6. Buffers and solutions

Solution	composition
Culture medium	500 ml RPMI medium 1640 (1x) 10% Fetal bovine serum 1% sodium pyruvate 1% GlutaMax
EMSA I	10mM HEPES 10mM KCl 0.4mM NaCl 0.2mM EDTA 0.6% Triton 1mM DTT pH 7.9 Protease inhibitor Phosphatase inhibitor
Lämmli buffer 4 x	250 mM Tris-HCl (pH = 6.8) 12.5% SDS

	40 % glycerol 3 % DTT Bromphenol blue
LB-medium	10 g tryptone 5 g yeast extract 10 g NaCl ad 1 L dH ₂ O autoclave and cool down to 55 °C 25µg/mL Zeocin 100µg/mL Ampicillin
PBS	137 mM NaCl 2.7 mM KCl 10 mM Na ₂ HPO ₄ 2 mM KH ₂ PO ₄ ad 800 ml dH ₂ O adjust with HCl to pH=7.4 ad 1000 ml dH ₂ O
Polysome I	10 mM HEPES 150 mM KCl 5mM MgCl ₂ Protease inhibitor Phosphatase inhibitor
Polysome II	10mM HEPES 150mM KCl 5mM MgCl ₂ 10% NP40

	Protease inhibitor Phosphatase inhibitor
RIPA Lysis buffer	50 mM Tris HCl (pH=7.5) 150 mM NaCl 1 % NP40 0.5 % Sodium deoxycholate 0.2 % SDS
RIPA Lysis buffer ⁺⁺	10 ml RIPA Protease inhibitor (1 mini-tablet Complete) Phosphatase inhibitor (1 tablet PhosphoStop)
SDS-running buffer 1 x (1 L)	100 ml of 10 x SDS-running buffer 900 ml dH ₂ O
SDS-running buffer (RB) 10 x (10 L)	302.9 g Tris Base 1440.9 g glycine 1 L SDS-solution, 10 % Adjust to 10 L dH ₂ O
Cell stocking medium	90 ml FCS 10 ml DMSO
TBS 10 x (1 L)	24.3 g Tris Base 80 g NaCl 800 ml dH ₂ O adjust with HCl to pH = 7.6 Adjust to 1 L dH ₂ O
TBST 1 x (1 L)	100 ml 10 x TBST 900 ml dH ₂ O

TBST 10 x (1 L)	24,3 g Tris Base 80 g NaCl 800 ml dH ₂ O adjust with HCl to pH = 7.6 10 % Tween-20 (v/v) Adjust to 1 L dH ₂ O
Transfer buffer 1 x (1 L)	200 ml MeOH ≥ 99% 100 ml Transfer buffer 10 x 700 ml dH ₂ O
Transfer buffer 10 x (10 L)	1211,4 g Tris Base 1426 g Glycin 8 L dH ₂ O adjust with HCl to a pH = 8.3 adjust to 10 L dH ₂ O
Tris buffer saline (TBS) 1 x (1 L)	100 ml TBS 10 x 900 ml dH ₂ O

1.7. Apparatuses

Name	Manufacturer
-80°C Freezer	Forma Scientific
8-channel-pipette 300µl	Eppendorf, Hamburg, Germany
Analytical balance BP3100	Satorius, Göttingen, Germany
Analytical balance BP310S	Satorius, Göttingen, Germany
Autoclave CS-Labor 91782	Webeco, Selmsdorf, Germany

Benchtop centrifuge mini Spin plus, rotor: F-45-12-11	Eppendorf, Hamburg, Germany
Cell counter Cellometer Auto T4	Nexcelom Bioscience, Lawrence, USA
Centrifuge Rotina 48R, Rotor: 4394	Hettich Zentrifugen, Tuttlingen, Germany
CO ₂ Incubator Heraeus Function line	Heraeus, Hanau, Germany
Fotometer Sunrise Remote Touch screen	Tecan, Männedorf, Germany
Gibco BRL ST305 Electrophoresis Power Supply	Life Technologies, Darmstadt, Germany
Heatable water bath	GFL GmbH, Burgwedel, Germany
HeraSafe HS12 Sterile Hood	Heraeus instruments, Hanau, Germany
Hydraulic pump suctioning machine	KNF, Freiburg, Germany
Hypercassette RPN 11642	GE Healthcare, Freiburg, Germany
Icemaker AF 200	Scotsman, Milan, Italy
Incubator (60°C) type B6	Heraeus instruments, Hanau, Germany
Laminar flow Hera Safe HS 09/2	Heraeus instruments, Hanau, Germany
Magnetic stirrer MR3001	Heidolph, Schwabach, Germany
Microscope ID03	Zeiss, Oberkochen, Germany
MILLI-Q Reagent water system	Merck Millipore, Darmstadt, Germany
Mini Trans-Blot Cell	Bio-Rad Laboratories, Munich, Germany
Nanodrop UV-Vis Spectrophotometer	Thermo Scientific, Wilmington, USA
pH-meter inolab pH-Level1	WTW GmbH, Weilheim, Germany

Pipetboy pipetus	Hirschmann Laborgeräte, Eberstadt, Germany
Pipettes Eppendorf research 2.5/ 10/ 20/ 100/ 200/ 1000 µl	Eppendorf, Hamburg, Germany
Refrigerated centrifuge 5415R, rotor: F-45-24-11	Eppendorf, Hamburg, Germany
RM5 Assistant	Assistent, Sondheim/Rhön, Germany
Roller mixer SRT6	Stuart, Staffordshire, UK
Roller mixer SRT9	Stuart, Staffordshire, UK
Rotator/ centrifuge	Kisker Biotech, Steinfurt, Germany
Shaker-Duomax 1030	Heidolph Instruments, Schwabach, Germany
Shaker-Incubator TH30	Edmund Bühler, Germany
Sonicator	MSE Scientific Instruments, London, UK
Standard Power Pack P25 power supply	Biometra, Göttingen, Germany
StepOne Plus real time PCR system	Applied Biosystems
Stepper Multipette plus	Eppendorf, Hamburg, Germany
Thermomixer 5436	Eppendorf, Hamburg, Germany
Ultracentrifuge TL-100 Ultra, Rotor: TLA100	Beckmann Coulter, Krefeld, Germany
Vortex mixer Vortex Genie 2	Scientific Industries, New York, USA
Water bath	Gesellschaft für labortechnikmbh

	Burgwedel, Germany
Water-jacketed Incubator	Forma Scientific
XCell SureLock	Life Technologies, Darmstadt, Germany
X-ray film processor Curix 60	AGFA, Mortsel, Belgium

1.8. Consumables

Name	manufacturer
Cell counting chamber SD100	Nexcelom Bioscience, Lawrence, USA
Cell culture multi-well plates, 6-, 12-, 24-, 48-, 96-Well	Greiner Bio-One, Frickenhausen, Germany
Cell scraper, 16/ 25 cm	Sarstedt, Nümbrecht, Germany
CryoPure tube 1.8 ml white	Sarstedt, Nümbrecht, Germany
30 μ -Dish 35mm, high, Culture-Insert 2 Well	Ibidi® Germany
EZ4U Cell Proliferation Assay	BI-5000, Biomedica Medizin produkte GmbH & Co. KG, Wien
Hyperfilm ECL	GE Healthcare, Freiburg, Germany
Kombitip, 2.5/ 5/ 10 ml	Eppendorf, Hamburg, Germany
LEGENDplex™	BioLegend, Germany
Microloader pipette tip	Eppendorf, Hamburg, Germany
Microtest plate 96-Well	Sarstedt, Nümbrecht, Germany
nCounter® stem cell	Nanostring technologies, USA

Needles, Microlance 3 (26G)	Becton Dickinson, Heidelberg, Germany
Nitril-gloves, Nitratex micro-touch	Ansell, Munich, Germany
Parafilm M	Brand, Wertheim, Germany
Pasteur pipette, 230 mm	Hecht-Assistant, Sondheim, Germany
Precision 2X RT-PCR Mastermix with Rox	Primerdesign, M01255
Pipette tips, 20/ 200/ 1000 µl	Sarstedt, Nümbrecht, Germany
PVDF-Membran, Immobilon-P 0.45 µm	Merck Milipore, Darmstadt, Germany
RNeasy mini kit	Qiagen, Germany
Reaction tube, 0.5/ 1.5/ 2 ml	Sarstedt, Nümbrecht, Germany
Serological pipette 5/ 10/ 25 ml	Sarstedt, Nümbrecht, Germany
Sterile filter Filtropur 0.2 µm	Sarstedt, Nümbrecht, Germany
Syringe, 1/ 50 ml	Becton Dickinson, Heidelberg, Germany
Tissue culture dish, 150 x 20 mm	Sarstedt, Nümbrecht, Germany
Tube 15/ 50 ml	Sarstedt, Nümbrecht, Germany
Tissue culture flask 25/75/175 cm ²	Sarstedt, Nümbrecht, Germany
Whatman paper 3 mm	GE Healthcare, Freiburg, Germany

2. Methods

1.1. Cell Culture, the current study was focused mainly on two human PDAC cell line, Colo357 and PancTuI. The cells were kept frozen as highly standardized stock cultures for *in vitro* studies. Both cell lines were cultured in RPMI Medium 1640 with 1% Glutamine, 1% Sodium Pyruvate 100M and 10% Fetal calf serum (FCS). The cells were maintained at 37°C in a humid atmosphere with 5% CO₂ (Forma Scientific). The cells were cultured when the cells reached ~80% confluence, twice or three times per week in T25, T75 or T175 culture flasks under sterile conditions. All solutions and media were warmed to 37°C in a water bath. Upon cell culturing, the cells were carefully washed using PBS after removal of the old medium. Trypsin or Accutase were used detach the cells from the culture flasks. Accutase is milder than trypsin, hence it was used to detach cells before flow cytometry and animal experiments. Cells were incubated with Trypsin or Accutase for about 10- 30 minutes depending on the adhesion power of the cells. Upon detachment, trypsin and Accutase were stopped by adding regular culture media, where the enzymatic reaction was neutralized by the FCS content. The cell suspension was centrifuged at 1440 rpm for 4 minutes at room temperature. The supernatant was discarded and the cells were re-suspended in fresh regular media. The culture supernatant was regularly tested to avoid mycoplasma contamination (see later).

2.2 Generating stable TRAIL-R4 over expression cell lines, Cells were seeded in a 6-well plate at a density of 2.0 and 2.5x10⁵ for PancTuI and Colo357, respectively. After 24 hour incubation, the cells were transfected with either expression vector for TRAIL-R4 (kindly provided by Prof. Micheau Olivier, UMR86, INSERM, Dijon, France) or pCR3.1 control plasmid. The transfection was done using DharmaFECT DUO (Thermo Scientific) and OptiMEM (serum-free medium, Gibco Life Technologies). The plasmid end-concentration used was 0.5 µM. DharmaFECT Duo was diluted in OptiMEM (1:50). The transfection mix was prepared by adding equal amount DharmaFECT DUO/OptiMEM mix to the plasmid solution and the mix was incubated for 20 minutes at room temperature. Later, the old culture medium was discarded and an amount of 400µL transfection mix was added pro-well together with 800µL fresh medium. The cells were then

incubated under regular cell culture conditions. After 48 hours, positive cells were selected by the addition of G418 antibiotic with a concentration of 250µg/ml or 600µg/ml for PancTuI or Colo357, respectively. Western blotting and RT-PCR were used to confirm the successfulness of the procedure.

1.3. Generating stable TRAIL-R4 knockdown cell lines, the stable knockdown of TRAIL-R1 short hairpin RNA (shRNA clone 383714, see section 1.5 of Materials for more information) and TRAIL-R2 shRNA (shRNA clone 16711) was previously established in Prof. Anna Trauzold laboratory. The stable TRAIL-R4 knockdown cells were established via the viral transduction of TRAIL-R4 shRNA (shRNA, clone 16774). All the transduction procedure was performed under S2 laboratory guidelines. To assemble the lentiviral particles, HEK293T cells were used. HEK293T cells were grown in DMEM high glucose, 10% FCS, 1% sodium pyruvate. On the first day, the cells were seeded at 1.2×10^6 (6-well format) and were incubated at 37°C with 5% CO₂ for 24 hours. On the second day, a transduction mixture was made in polystyrene tube using, 6µg lentiviral vector, 4.3µl trans-Lentiviral packaging mix and 15µl calcium chloride then 150µL of 2x HBSS was added dropwise. The transduction mix was triturated and incubated at room temperature for 3 minutes. A total of 300µL was added dropwise to each well and the cells were incubated for 10-16 hours under normal culture conditions. Later, the medium was replaced with 2mL reduced-serum media comprising of high glucose DMEM, 5% FCS, 2mµ L-glutamine and 1% Penicillin/Streptomycin and the cells were again incubated for 48 hours. Later, the medium (now containing the viral particles) was harvested and centrifuged at 1600 ×g, 4°C for 10 minutes to pellet cell debris. Then, the supernatant was slowly transferred to a fresh tube, triturated and filtered via a sterile, 0.22-0.45 µM low protein binding filter. This filtered lentiviral stock was then used to transduce both Colo357 and PancTuI cells and the rest was aliquoted and frozen at -80°C freezer.

For the cell line's lentiviral transduction, the cells were seeded at a concentration of 2×10^5 pro well (6-well format) and incubated for 24 hours in regular cell culture medium. On the second day, the cells were 40-50% confluent, the old medium was discarded and replaced with 1mL serum-free media with different concentration of the lentivirus/multiplicity of infection (MOI). Two

different MOI were used (MOI 5, MOI 10) and the amount of virus was calculated via the following formula, amount of virus (μl) = $\frac{\text{amount of cells per well} * \text{MOI}}{\text{viral titer } (1 \times 10^6)}$. After 4-6 hours incubation, 1mL regular medium was added (also containing 1% penicillin/streptomycin) and the cells were incubated again for 48 hours. Later, the antibiotic selection was started using puromycin at 1 $\mu\text{g/ml}$ or 2 $\mu\text{g/ml}$ concentration for PancTuI or Colo357, respectively. The cells were then propagated until appropriate number of cells was reached and the efficacy of transduction was tested via Western blotting and RT-PCR.

1.4. Mycoplasma PCR, Venor® GeM classic mycoplasma detection kit (Minerva Biolabs GmbH, Germany) was used to ensure that the cells were not contaminated with Mycoplasma. An amount of 500 μl of a 3-days cell culture supernatant was boiled at 95°C for 10 minutes and centrifuged at 16,100 xg for 5 seconds and then 2 μl of the supernatant was used in the reaction mix together with positive and negative controls to perform the PCR according to the manufacturer's protocol.

1.5. Morphology, the cells were seeded at 4x 10⁵ in 6-well format. After 24 hours, a series of photos were taken using light microscopy (NIB-100 Inverted Biological Microscope from Müller Germany) equipped with a MA88-300 Premiere® Camera Eyepiece. The digital photos and scaling were done using TSVIEW version 7.1.1.2 software (Tucsen Image Technology Co., Ltd.).

1.6. Effects of endogenous TRAIL, In order to block the effects of endogenous TRAIL, neutralizing antibodies against TRAIL (anti-TRAIL, MAB375, R&D systems, 0.5 $\mu\text{g/mL}$) were used. The antibodies were added directly during the cell seeding and the mixture was incubated for 24 hours under regular cell culture conditions. Later a whole cell lysate was performed (see later).

1.7. Whole cell lysate, Cells were grown in 6-well for 24 hours under regular cell culture conditions, then the cells were washed carefully using cold PBS and an appropriate amount of RIPA⁺⁺ buffer was added per well (150 μl for ~ 80% confluent cells). The cells were then incubated on ice for 10 minutes and frozen by

-80°C for ~20 minutes, then defrosted on ice and the lysate were scrapped and sonicated (Ultrasonic Homogenizer, MSE at 12 microns amplitude) three times 8 seconds each. The lysate were then centrifuged at 16,100 xg for 15 minutes at 4°C and the supernatant was stored by -20°C. The protein concentration was determined via Pierce™ BCA protein assay (Thermo Scientific) according to the manufacturer's protocol. Lysates from the same experiment were then adjusted to the same protein concentration using RIPA⁺⁺ buffer and supplemented with 4X Lämmli buffer then boiled at 95°C for 5 minutes.

2.8. Nuclear/Cytoplasmic fractionation, Cells from five wells (6-well format) were used to extract the nuclear/ cytoplasmic fraction and one well was used to perform a whole cell lysate using RIPA buffer (see before). To extract the nuclear and cytoplasmic fractions EMSA I and polysome buffers were used. Cells were seeded at 4×10^5 pro well and incubated for 48 hours under regular cell culture conditions. Then, the cells were washed twice with cold PBS and EMSA I buffer was added (~150µl for 80% confluent cells). The low salt content of EMSA I allows the cell membrane to burst without affecting the nuclear membrane and thus allowing the separation of the cytoplasmic fraction. The lysate was then centrifuged at 16,100 xg for 8 minutes and the supernatant (cytoplasmic fraction) was stored at -20°C. The pellet was then washed with 500µl EMSA I buffer four times to remove any cytoplasmic residues. The nuclear fraction was then extracted by suspending the pellet in polysome buffer and disrupting the nuclear membrane via running the extract through a 28G syringe 10-15 times. Finally, the mix was centrifuged at 16,100 xg for 30 minutes. The supernatant (now containing the nuclear fraction) was collected and frozen at -20°C for further use. Protein estimation was done using DC-assay according to the manufacturer's protocol. All the lysates involved in the same experiment were then adjusted to the same protein concentration using EMSA I or polysome buffer for cytoplasmic and nuclear fractions, respectively. The salt concentrations of the cytoplasmic buffer was then equilibrated to the salt content of polysome buffer using potassium chloride in order to be able to load both fractions in the same gel. Later, the lysates were supplemented with 4X Lämmli buffer and boiled at 95°C for 5 minutes.

2.9. Immunoblotting/Western blot, Equal amounts of protein lysates were separated by gel-electrophoresis using SDS-polyacrylamid (PAGE) using Novex® 4-20% tris-glycine gels 1.0ml. The gel-electrophoresis was performed at 125 volts for 2 hours. The proteins were then transferred to PVDF Immobilon membranes (Millipore) via blotting. Blotting was performed at 400 mA for circa 90 minutes. Non-specific binding was blocked with 5% milk in TBST for 1 hour at room temperature and later incubated overnight at 4°C with a primary antibody (see section 1.2 of Materials). On the next day, the membrane was washed 3 times using copious amounts of TBST on a shaking platform. Then, the membrane was incubated with an appropriate concentration of the HRP-conjugated secondary antibody for 1 hour at room temperature and later the washing step was repeated (3X in TBST). The blots were developed using ECL (Amercham, GE Healthcare, UK) according to the manufacturer's protocol. The membranes were developed on X-ray films in a dark room.

1.10. Proliferation assay, Cellular proliferation was assessed by cell counting using *Cellometer*® automated cell counters (Nexcelom) or xCelligence assay (ACEA Biosciences). For cell counting, the cells were seeded at 1×10^5 cells (6-well format) and incubated in regular medium under regular conditions for 24 hours. Later, first cell counting was done out of 2 wells. To count the cells, the old medium was discarded and the wells were carefully washed twice with warm PBS. The cells were then detached using trypsin and later the enzymatic reaction was stopped using regular media. Fifteen ml Falcons were weighed and used for collecting the cell suspensions. The cell suspension was then centrifuged at 1440 rpm for 4 minutes at room temperature. The cell pellet was then re-suspended in 500µl regular media. The falcons were weighed again to determine the weight of the cell suspension. Cellometer was used to count the cells (3 counts per well) and the mean value of all counts was calculated. 96 hours later, the rest of the cells were counted using the same procedure. The 24 hours' values were further used as a baseline control for the 96 hours counts. Absolute cell counts were calculated by multiplying the average cell suspension weight times the average cell count.

The xCELLigence technology was also used to determine the cell proliferation. xCELLigence is a real life cell analysis system, where the cells are

dynamically monitored over the course of the experiment. xCELLigence measures the cell index which represents cell count, changes in cellular morphology and adhesion. This cell index is the impedance measured through gold electrodes present at the bottom of each well that detects all signals coming from the cells. The cells were seeded at 1×10^4 cells per well and mounted on the xCELLigence machine for 90 hours. The proliferation was then determined via the provided software.

Additionally, Alamar Blue was also used to detect cellular proliferation/viability. Alamar blue is cell proliferation/viability assay that measures the metabolic status of the cells and does not entail vigorous washing steps. Alamar blue is reduced by the living cells and hence leading to a change in the color. The wells (96-well format) were coated with fibronectin ($2 \mu\text{g}/\text{cm}^2$), tenascin-c ($1 \mu\text{g}/\text{cm}^2$), or were washed with PBS as control. The plates were incubated overnight in 37°C CO_2 humid atmosphere overnight. Extra fluid was careful removed from the plates and the cells were seeded at a density of 1×10^4 per well and incubated for 96 hours. Alamar Blue was added and incubated under regular cell culture condition until Alamar Blue was reduced (pink color). Finally, fluorescence was read on TECAN SpectraFluor Plus (Tecan group LTD, Switzerland) at excitation wavelength of 550nm and emission wavelength of 595nm and Gain 60 manual.

1.11. Migration assay/ Wound healing assay, Migration was assessed by scratch assay technique using Ibidi culture inserts. Ibidi wells were marked on the bottom side with several fine scratches to allow taking the pictures at the same spot later on. The cells were seeded at a density of 8×10^4 cells in $70 \mu\text{l}$ medium per well. After the formation of a full monolayer (~ 24 hour), cells were treated with Mitomycin C (Sigma-Aldrich) for 2-3 hours in 5% CO_2 Incubator at 37°C . Mitomycin was used to stop the cellular proliferation via its action as a DNA crosslinking agent that leads to inhibition of DNA synthesis. The inserts were then carefully removed leaving a fixed $\sim 500 \mu\text{m}$ cell-free gap. Several photographs were taken immediately (0 hour) and then in intervals depending on the speed of migration of each cell line. The images were analyzed using ImageJ software with the help of its wound healing macros tool.

1.12. Viability assay, Effects of TRAIL-induced apoptosis and necroptosis were tested using EZ4U Cell Proliferation Assay (Biomedica Medizinprodukte GmbH & Co. KG, Vienna) and Western blotting. EZ4U Kit entails minimal manipulations and no washing steps. Cells were seeded at a density of 1.5×10^4 [(96-well), 8 wells pro treatment] and incubated for 24 hours at 37°C 5% humid atmosphere. For necroptosis testing, the wells were pretreated with 2 mM zVAD-fmk and 0.5 mM HHT. One hour later, the cells were treated with 50ng/mL (Colo357) or 100ng/mL (PancTuI) TRAIL (Peprotech) and incubated again for 24 hours under the same conditions. For apoptosis testing, the cells were either treated with TRAIL or left untreated for 24 hours. EZ4U substrate was added and incubated at 37°C 5% CO₂ humid atmosphere. The optical density was read every hour on Sunrise™- Tecan reader at absorbance of 450nm and reference 620nm after shaking the plate for 5 seconds. All apoptosis and necroptosis experiments were done in parallel.

For Western blotting, a whole cell lysate was performed (see before). However, 24 hours after seeding the cells were either treated with TRAIL or zVAD+HHT then TRAIL or left untreated (same procedure as EZ4U) and incubated again for 24 hours. The protein lysates were then prepared as previously explained.

1.13. RNA isolation, Cells were seeded at 4×10^5 and incubated for 24 hours. The cells were then rinsed twice with cold PBS and whole mRNA was isolated using Qiagen RNeasy mini kit (Qiagen, Germany) according to the manufacturer's protocol. The amount and purity of RNA was measured by Nanodrop uv-spectrophotometer (Thermo Scientific). First strand cDNA synthesis was done using Maxima first strand cDNA synthesis kit according to the manufacturer's protocol.

1.14. Real Time PCR (RT-PCR), Two quantitative RT-PCR systems were used; SYBR green Maxima and Taqman (Applied Biosystems). Refer to section 2.3 in Materials for primer sequences. Taqman best converge RT-PCR assays were used to detect the mRNA expression of TRAIL-R2 (Hs00366278_m1), TRAIL-R4 (Hs00388742_m1). TATA-binding protein [TBP, Hs00427620_m1] was used as a reference gene for detecting TRAIL receptors using Taqman technique. Maxima

SYBR Green/ROX RT-PCR Master Mix (Maxima) was used to detect the mRNA levels of CEACAM5, CEACAM6, interleukin-6 and interleukin-8 with RPL22 and RPL27 as reference genes. RT-PCR was performed using StepOne Plus Real Time PCR System (Applied Biosystems). Both Taqman and SYBR green techniques were performed according to the manufacturer's protocol. Delta-delta CT method was used to evaluate the results (Livak and Schmittgen, 2001).

1.15. FACS (Fluorescence-activated cell sorting), or flow cytometry was used to detect the plasma membrane levels of the TRAIL receptors. Cells were seeded in T25 flask. Next day, cells were rinsed with warm PBS and detached from the flask using Accutase. The enzymatic reaction was stopped using regular media and centrifuged at 1440 rpm at room temperature for 4 minutes. The cells were then counted and a number of 1×10^6 cells were washed again using 0.05% sodium azide in PBS and centrifuged at 300 xg for 5 minutes at 4°C. Then, the cells were incubated for 30 minutes in a dark environment with corresponding APC-associated TRAIL receptor (see section 1.3 of Materials) or the suitable IgG isotype control. Later, the cells were rinsed again using 0.05% sodium azide in PBS and centrifuged at 300 xg for 5 minutes at 4°C. Finally, the cells were fixed in 2% PFA in PBS and the plasma membrane levels were detected via FACS machine (courtesy of Immunology department, UKSH, Kiel).

1.16. ELISA and Multiplex ELISA (Enzyme Linked-Immuno-Sorbent Assay), ELISA assay was performed using DuoSet Anticillary reagent kit (R&D systems). Cells were seeded at 4×10^5 cells (6-well format) and incubated for 48 hours. The supernatant was collected and centrifuged at 16.100 xg for 15 minutes at 4°C. Meanwhile, ELISA plate (96-well format) was coated with specific capture antibody and was incubated overnight at room temperature. Later, the samples were incubated for 2 hours at room temperature. After incubation, the wells were rinsed twice with a copious amount of washing buffer. A detection antibody was then added and incubated for an additional 2 hours. A washing step was repeated after the second incubation. Finally, the plates were incubated with streptavidin – HRP at room temperature in a dark environment for 20 minutes and another washing step was performed then the substrate solution was added. The plate was

read on the Sunrise™- Tecan reader at 450nm. Additionally, a multiplex ELISA using LEGENDplex™ assay (BioLegend) was performed in collaboration with Dr. Ole Helm according to the manufacturer's protocol.

1.17. Microarray study, An automated genome wide gene expression study was done using the Agilent Sureprint G3 Human GE 8×60K (Agilent, Santa Clara, CA, USA) microarray. The analysis was performed using mRNA extracts from the different Colo357 cells. The cells were seeded at 5×10^5 cells and RNA was isolated 24 hours later using Qiagen RNeasy mini kit according to manufacturer's protocol. In order to ensure a good quality control, the optical density 260/280 ratio of the extracted mRNAs was measured by Nanodrop where the values of all the samples were >2.0 and that was further validated using the Agilent 2100 bioanalyser system. The RNA samples were sent to imaGenes (Agilent Expression Profiling service, Berlin) on dry ice and the microarray was performed by Source Bioscience (Source BioScience GmbH, Berlin, Germany). The microarray tested a number of ~ 42,532 oligo-dT that represented ~35,970 altered genes in the 6 cell lines (Table 2.1). Initially, the normalization method performed by company was the quantile method. To eliminate low signals, all the values lower than the 0% quantile were set to the 0% quantile levels.

Table 2.1| Technical parameters of the microarray analysis

	TR4(+) vs CTRL	TR1(-) vs CTRL	TR1(-))TR4(+) vs CTRL	TR2(-) vs CTRL	TR2(-))TR4(+) vs CTRL
Number of Oligos	42532	42532	42532	42532	42532
Number of Genes after Normalization	35970	35970	35970	35970	35970
Number of Oligos after filtering	42527	42530	42530	42532	42532
Number of Genes after filtering	35968	35969	35969	35970	35970
Quantile used for cut-off (0%)	2.520636	2.57174	2.73782	2.58185	2.55262
Inter quartile range used for filtering	0.0	0.0	0.0	0.0	0.0

Analysis of the data was done using Microsoft® Access 2010. The gene enrichment analysis was done using the online freely-available bioinformatics tool; WebGestalt (Wang et al., 2013; Zhang et al., 2005). Furthermore, the multiple gene list feature enrichment analyzer for the dissection of biological

systems “Toppcluster” was used to compare the different groups in terms of biological processes, molecular functions and pathways (Kaimal et al., 2010). Additionally, StemChecker online tool was used to predict the possible stem cell signature modified in the investigated cells (Pinto et al., 2015).

To complete the statistical analysis, the dysregulated genes were initially filtered by *p-value* <0.05 (done by T-Test with Unequal variance, unpaired). Then, the *p-value* was corrected using Benjamini-Hochberg (BH; False Discovery Rate) method, also a < 0.05 cut-off was set. Additionally, the data were filtered by means of arithmetic fold change (≥ 4 or ≤ -4) (Table 2.2). The arithmetic fold change was calculated using Microsoft® office Excel 2010.

Table 2.2| Equation used to calculate the arithmetic fold change

Arithmetic Fold change	=IF(Average(Treatment range)/Average(Control range)>1;(average(treatment range)/average(Control range));(average(control range)/average(treatment range))*-1)
------------------------	---

1.18. nCounter® stem cell assay, (Nanostring Technologies®, Seattle, USA), Colo357 cell lines were assessed for stem-cell markers via the Nanostring technology. The assay was done in cooperation with Dr. Monika Szczepanowski from hemato-pathology institute, UKSH, Kiel. Nanostring is a new ultrasensitive technology that tests the gene expression via its nCounter assays. nCounter assay is designed to detect molecular barcodes of the genes of interest that is directly counted with high accuracy. The reaction includes a reporter tag, capture tag, target-specific probes (stem cell markers), and target molecules that hybridize to one another. The reporter tag carries a signal and the capture tag contains biotin that interacts accordingly with streptavidin. This reaction does not entail any amplification; it directly counts the already present mRNA copies. RNA from the respective cell lines was isolated via Qiagen RNeasy kit. RNA was set to the concentration of 100ng of purified total RNA in 30 µL reaction volume. nCounter analysis used 8 negative controls were the mean –in addition to the value of (2) as a standard deviation – were subtracted from samples. The samples are also normalized to the geometric mean of 6 positive controls in addition to 3 different housekeeping genes. The nSolver™ 2.6 software was used for analysis, where all cell lines were compared to the CTRL cell line. Since precision of the analysis increases with

expression level (counts), all the genes with an mRNA level below 30 counts were excluded from further analysis and a fold change cut-off of ≥ 2 or ≤ -2 was also implemented.

1.19. Animal Experiment, two *in vivo* studies were performed using immune deficient SCID-beige mice models. The animal experiments were done together with Dr. Jan-Paul Gundlach, Dr. Charlotte Hauser, Prof. Jan Egberts (Klinik für Allgemeine, Viszeral-, Thorax-, Transplantations- und Kinderchirurgie, UKSH, Kiel), Karen Legler and Prof. Susanne Sebens (Institute for Experimental Cancer Research, UKSH, Kiel). In the orthotopic model, 2 weeks old female SCID-beige mice were injected orthotopically in the pancreas with 1×10^6 cells in 25 μ l Matrigel. The cells were on the fifth passage. Mycoplasma was tested prior to the mice inoculations to avoid contamination. A number of 8 mice were used per group. Initially, the mice were weighed at the start point, narcotized using a mixture of [Dormicum (0.5 mg/kg), Fentanyl (0.05mg/kg) and Midazolam (5mg/kg)]. The operation was performed under sterile conditions. After the operation the mice were given antagonistic mixture [Anexate (Flumazenil, 0.5 mg/kg), Naloxon (1,2 mg/kg) and Antisedan (Atipamezol, 2.5 mg/kg)] and glucose and warmed up using a UV-lamp. For the subcutaneous inoculation experiment, the same procedure for cell preparation was implemented; however the cells were re-suspended in saline solution. Here, a number of 5 mice per group were used, where each mice was injected twice (once in each flank). In both experiments, the mice were regularly checked, weighed and cared for. In the orthotopic model, molecular imaging methods (sonography and MRI) were done to monitor tumor growth and metastases. In the MRI, the volume was measured by multiplying the number of voxel (three dimensional pixel, MRI volume unit) times the resolution of a single voxel.

1.20. Immunohistochemical staining, the tissues recovered from the animal experiment were imbedded in Paraffin and the sections were stained by hematoxylin and eosin. The sections were fixed in ice-cold acetone at -20°C for 7 minutes. The slides were allowed to dry and then the slides were incubated with hematoxylin for 5 minutes. After washing with distilled water, the sections were

stained with 1% eosin in ethanol for 1-1.5 minutes. The sections were then passed through different concentrations of alcohol (70%, 80% then 100%). The sections were then covered with cover-slips using mounting media and stored in room temperature.

1.21. PDAC patients' tissue staining, a re-evaluation of a previously analyzed *ex-vivo* study (Haselmann et al., 2014) involving the Immunohistochemical staining of TRAIL receptors was performed. The current analysis evaluated the impact of the interplay between TRAIL-R1, -R2 and -R4 on the patients' survival.

1.22. Statistical analysis, statistical analyses were done using one-way ANOVA. Significance was determined when *p-value* <0.05 (*= significant, ns =non-significant). Experiments were done in duplicates or triplicates. In the animal experiment, a nonparametric method was used to calculate the significance: Kruskal Wallis and adjusted with Holm FWER method. In the patient cohort, the significance between the patient's survival duration was measured using Log-Rank test.

N.B. The research team used the smallest possible number of laboratory animals and the ethical guidelines of the local authorities were strictly followed. The Molecular Oncology Laboratory has a long-standing expertise in animal experiments increasingly using multi-modal molecular imaging methods as read-out for tumor growth and progression.

III. RESULTS

In an attempt to unravel the complexity of the TRAIL receptor system, we have established a double transfection model in PDAC cell lines with different TRAIL receptors' expression levels. In this study, we focused on TRAIL-R4 impact in context of the two death receptors (TRAIL-R1 and -R2).

1. Generation of Colo357 cell lines with differentially modified expression of TRAIL receptors

In order to better understand the functions of the different TRAIL receptor members, a functional dissection of these receptors was needed. And considering the fact that the main focus of the current study was TRAIL-R4, we wanted to further analyze its functions in the constitutive and/or limited expression of TRAIL-R1 and TRAIL-R2. To that end, the levels of either TRAIL-R1 or TRAIL-R2 were artificially down regulated in Colo357 cell line. Colo357 cell line was chosen as it is a well-studied cell line in our group. After establishing the stable clone pools with TRAIL receptors knockdown, pCR3.1 plasmids carrying a TRAIL-R4 coding sequence or the corresponding empty vector were introduced in each cell line pool. This way a group of stably transfected Colo357 cells was constructed with differential TRAIL receptor levels (Figure 3.1, 3.2). This multiple TRAIL receptor modifications allowed the analysis of TRAIL-R4 with special regard to its interaction with TRAIL-R2, in the limited expression of TRAIL-R1 [Colo357 TR1(-)TR4(+)], as well as its interaction with TRAIL-R1, with the knockdown of TRAIL-R2 [Colo357 TR2(-)TR4(+)].

Given the complicated nature and the long cell line nomenclature, a simple coding system was improvised for easier recalling of the cell lines (Table 3.1).

Table 3.1| Coding system used for PDAC cell lines

CTRL = non-silencing shRNA/pCR3.1	TR1(-)TR4(+) = TRAIL-R1 shRNA/TRAIL-R4
TR4(+) = non-silencing shRNA /TRAIL-R4	TR2(-) = TRAIL-R2 shRNA/pCR3.1
TR1(-) = TRAIL-R1 shRNA /pCR3.1	TR2(-)TR4(+) = TRAIL-R2 shRNA /TRAIL-R4

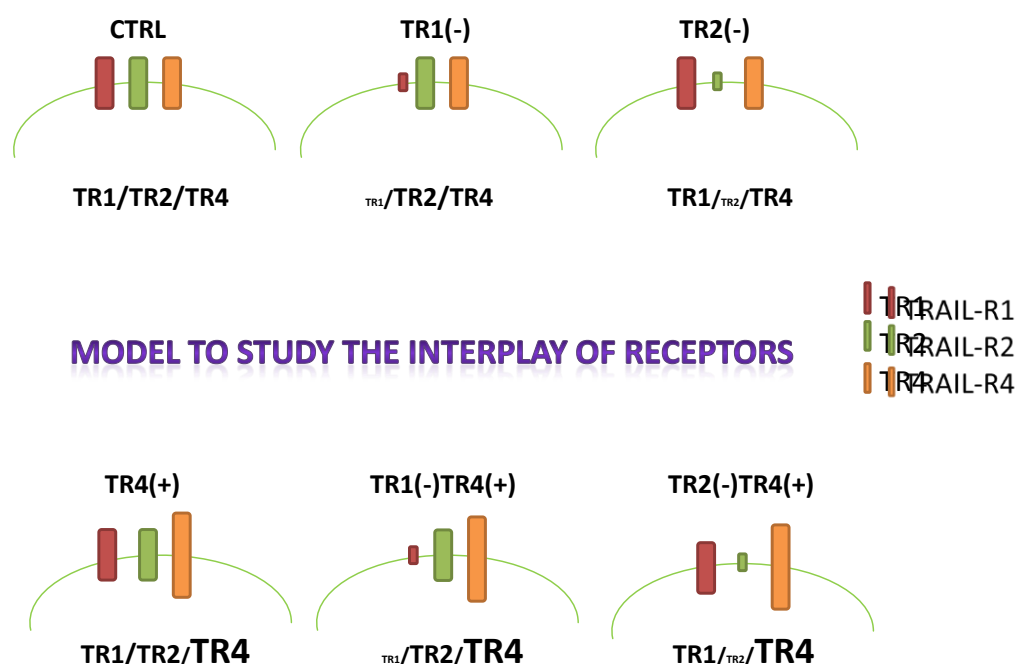


Figure 3.1| Illustration of TRAIL receptors modifications in the different cell lines. The diagram shows 6 illustrations corresponding to the constructed six cell line in Colo357 cells. In each cell illustration, one can see the represented receptors where receptor knockdown shown as small rectangle and written in small letters and receptor up-regulation shown as larger rectangles and written in bigger letters.

1.1. Detection of the total protein level of TRAIL receptors

To validate the successful transfection and transduction of Colo357 cells, the expression of TRAIL receptors was initially evaluated at the protein level via Western blotting (Figure 3.2). As depicted from the blots, there is a successful decrease in the TRAIL-R1 as seen in both TR1(-) and TR1(-)TR4(+) cell lines. Also there is a clear down-regulation of the short ~40kDa and long ~48kDa protein forms of TRAIL-R2 in both TR2(-) and TR2(-)TR4(+) cells.

Regarding TRAIL-R4, an obvious up-regulation of the ~47 kDa band could be detected in TR4(+), TR1(-)TR4(+) and TR2(-)TR4(+) cells. Additionally, the blots showed a clear increase of TRAIL-R4 in TRAIL-R1 knockdown cells that revealed always a relatively higher TRAIL-R4 levels in comparison to the other TRAIL-R4 up-regulated cells [TR4(+) and TR2(-)TR4(+)].

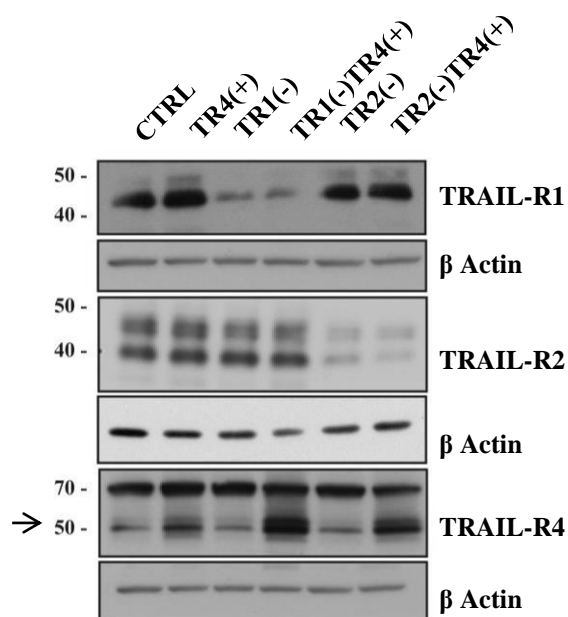


Figure 3.2| Whole protein expression level of TRAIL receptors. Colo357 cells with differentially expressed TRAIL receptors were seeded (4×10^5 cells, 6-well format) and incubated for 24 hours. Then the protein level of TRAIL receptors was analyzed in the whole cell lysate via immunoblotting. The Western blots show the successful TRAIL receptor alterations. Arrow pointing TRAIL-R4 band. Beta actin was used as loading control. This experiment is a representative of three performed.

1.2. Detection of TRAIL receptors level on the plasma membrane

In order to further validate the TRAIL receptors' level in the established clone pools, the plasma membrane levels of the TRAIL receptors were investigated via flow cytometry (Figure 3.3). From the FACS analysis, Colo357 CTRL cells express the three tested TRAIL receptors in detectable amounts (Figure 3.3 B). The TRAIL-R1 plasma membrane level was down regulated to about ~68% in both TR1(-) and TR1(-)TR4(+). Additionally, the successful knockdown of TRAIL-R2 followed by ~58% in both TR2(-) and TR2(-)TR4(+). Regarding the up-regulation of TRAIL-R4, it was boosted to about almost 6 folds in TR1(-)TR4(+). Also, TR4(+) demonstrated a ~3.5 folds up-regulation of TRAIL-R4. Moreover, the TRAIL-R4 plasma membrane level was the least augmented with a circa 1.45 folds in TR2(-)TR4(+). TRAIL-R4 knock-in was most successful with TRAIL-R1 knockdown as was seen in the Western blots.

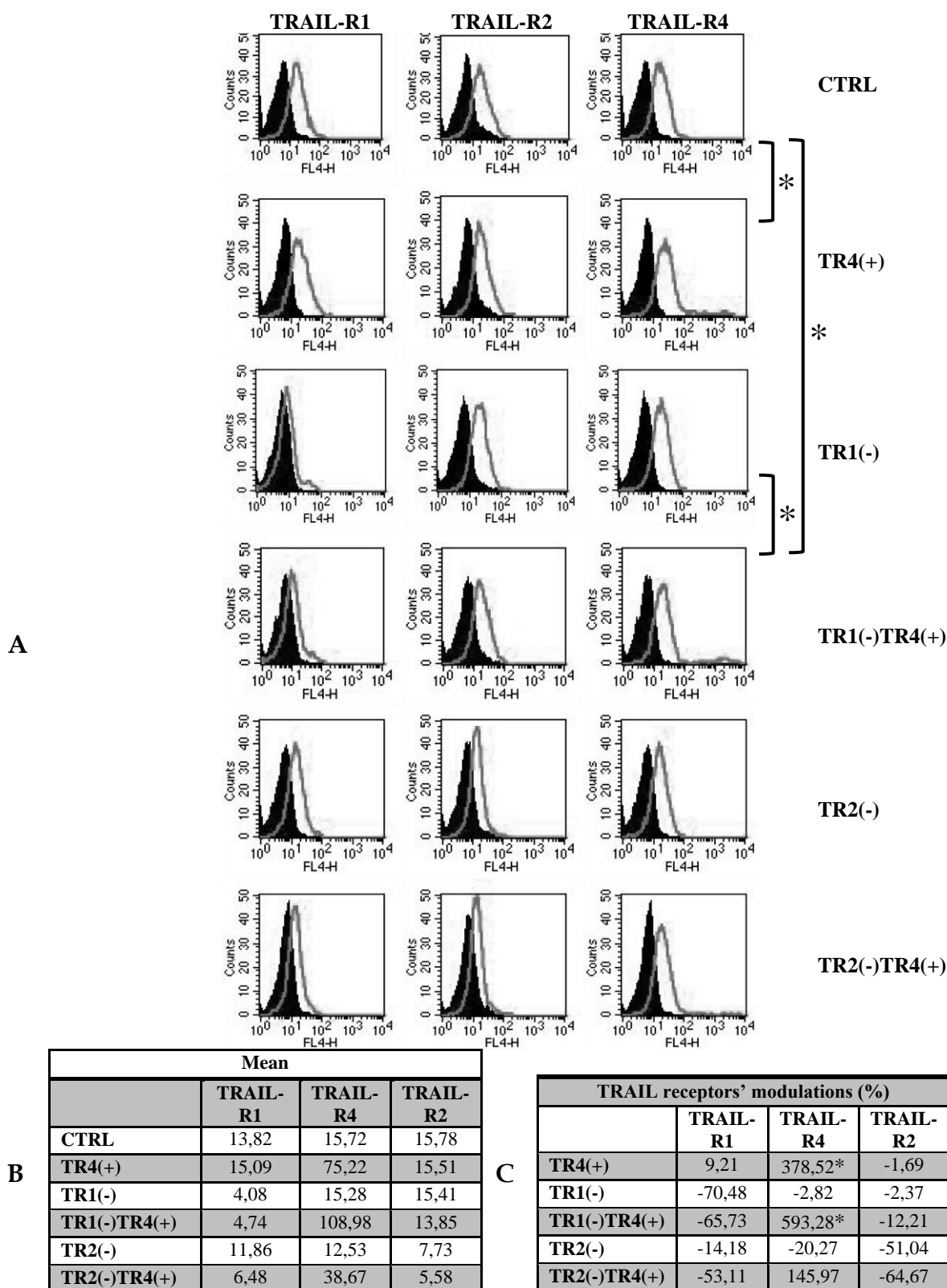


Figure 3.3| Plasma membrane levels of TRAIL receptors. Colo357 cells with differentially expressed TRAIL receptors were seeded in T25 flask and incubated for 24 hours. Then a flow cytometric analysis was done. **A**, plasma membrane expression of TRAIL receptors in non-permeabilized Colo357 cell lines. Black area represents the corresponding IgG control and the hollow curve represents the intended TRAIL receptor. Shown is one experiment of three experiments performed. **B**, mean of TRAIL receptor expression from 3 experiments **C**, percentage of expression compared to CTRL. ANOVA was used to determine the significance (*; n=3, *p*-value < 0.05).

By cross-evaluating the FACS analysis, it can be noted that the plasma membrane levels of TRAIL-R1 was also inhibited in TR2(-)TR4(+) cells. Moreover, TRAIL-R4 level in TRAIL-R2 knockdown cells was about 20% suppressed. However, TRAIL-R1 inhibition did not show the same effect on the TRAIL-R4 expression.

1.3. Determination of the intracellular distribution of TRAIL receptors

TRAIL receptors can be localized in different cellular compartments as plasma membrane, cytoplasm and nucleus. Therefore, a nuclear/cytoplasmic fractionation was performed, in order to further characterize Colo357 cell lines (Figure 3.4). At the first glance, one can deduce that the three TRAIL receptors (TRAIL-R1, -R2, and -R4) are present in both the nuclear and cytoplasmic compartments. Regarding TRAIL-R1, both cytoplasm and nuclear extracts demonstrated the same form where it was strongly present in the nucleus than cytoplasm. Additionally, TRAIL-R2 showed a similar distribution, where it was mainly present in the nucleus as well. Additionally, the knockdown of TRAIL-R1 was successful in both compartments; however, the knockdown of TRAIL-R2 was mainly detected in the nucleus.

Looking at the TRAIL-R4 expression and intra cellular distribution, figures show again a notable up-regulation of TRAIL-R4 in both compartments with a rather stronger presence in the nucleus especially in TR4(+) cells. Also, the over expression of TRAIL-R4 enhanced the level of the nuclear fraction of TRAIL-R2 in TR4(+) cell line. TRAIL-R4 forms were distinguishable between the cytoplasmic and nuclear forms. Both compartments displayed a clear increment in TRAIL-R4 main protein band at 47 kDa (TRAIL-R4 α). In the nucleus, TRAIL-R4 showed a double band circa 35 kDa (TRAIL-R4 β).

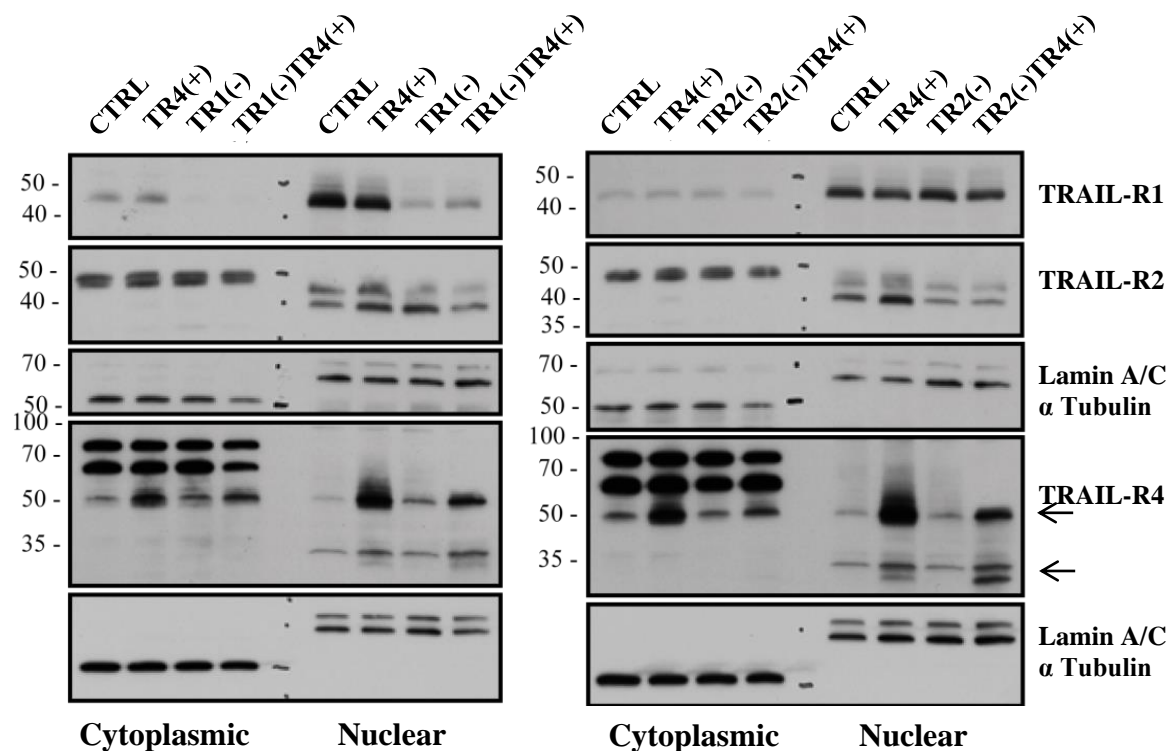


Figure 3.4| TRAIL receptor expression levels in the cytoplasmic and nuclear compartments. Colo357 cells with differentially expressed TRAIL receptors were seeded (3×10^5 cells in 6-well format) and incubated for 48 hours. Then the protein levels of TRAIL receptors in the intracellular compartments were detected via immunoblotting. Left panel shows the cytoplasmic and nuclear distribution of the TRAIL receptors in the two TRAIL-R1 knockdown cell lines together with CTRL and TR4(+) cells. On the right side, the panel shows the distribution in the two TRAIL-R2 down regulated cell lines, again together with the CTRL and TR4(+). The Western blots demonstrated the successful modifications of the studied TRAIL receptors in both compartments and the level of each receptor in both compartments. Arrows show TRAIL-R4 bands. Lamin A/C and alpha Tubulin were used to ensure the nuclear/cytoplasmic separation success and also served as a protein loading control.

1.4. Detection of TRAIL receptors expression on mRNA level

After validating the TRAIL receptor modulations on the protein level, the changes on the messenger RNA (mRNA) level was estimated via RT-PCR as well. The RT-PCR analyses were performed to determine the successfulness of the manipulations of the TRAIL receptors in the established clone pools for Colo357 (Figure 3.5).

From the graphs, it could be shown that the mRNA levels of TRAIL-R1 has showed a significant knockdown of ~50% in both TR1(-) and TR1(-)TR4(+). Also, TRAIL-R2 mRNA levels were down regulated by about 60% in both TR2(-) and TR2(-)TR4(+) cell lines. Additionally, TRAIL-R4 mRNA level was boosted by an average of four folds in TR4(+) and TR1(-)TR4(+) and TR2(-)TR4(+) denoting the successfulness of the transfection. Overall, the TRAIL-R1 and -R2 levels were not affected by the

upregulation of TRAIL-R4 in TR4(+) in comparison to CTRL cells or in TR1(-)TR4(+) in comparison to TR1(-) cells or TR2(-)TR4(+) in comparison to TR2(-) cells.

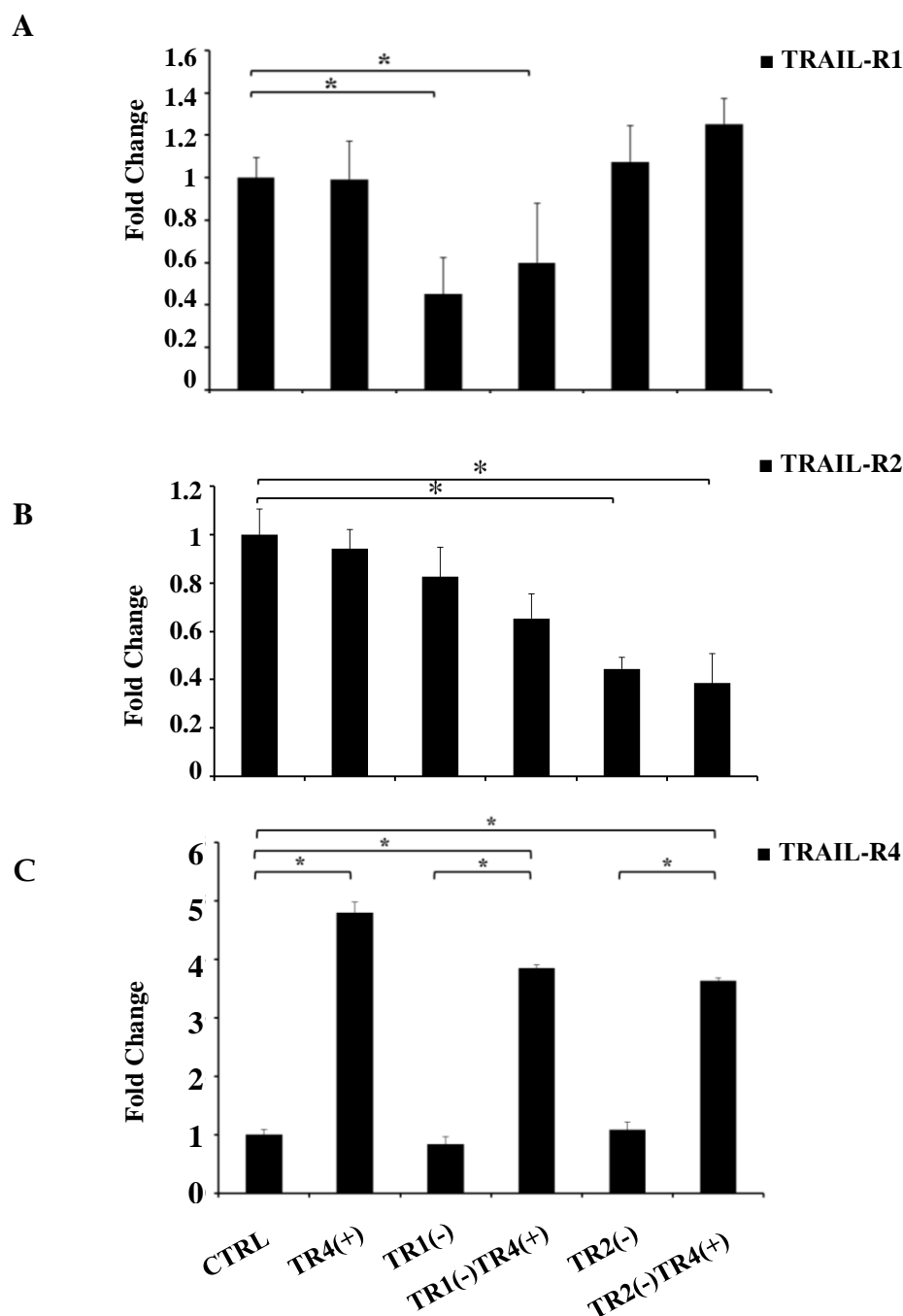


Figure 3.5| RT-PCR analysis of the TRAIL receptors on mRNA level. Colo357 cells with differentially expressed TRAIL receptors were seeded (4×10^5 cells, 6-well format) and incubated for 24 hours. Then the mRNA expression level of TRAIL receptors was investigated via RT-PCR. CTRL cells were set as control. The mRNA of the three receptors demonstrated the successful modification of the intended receptors. **A**, fold change of TRAIL-R1, **B**, fold change of TRAIL-R2, **C**, fold change of TRAIL-R4, shown is the mean of three independently performed experiments (biological replicates). ANOVA was used to determine the significance (*, $n=3$, p -value < 0.05).

2. Impact of TRAIL receptors interplay on TRAIL-induced cell death

Since our TRAIL receptor modifications involved not only the death-inducing TRAIL receptors (TRAIL-R1 and -R2) but also one of the decoy receptors, TRAIL-R4, it was rather intriguing to see in which context TRAIL-R4 will protect against cell death. Together with apoptosis, we decided to investigate yet another cell death modality namely necroptosis, to test whether TRAIL-R4 protects the cells against cellular death in general, or is it a rather selective process.

2.1. Impact of TRAIL receptors interplay on TRAIL-induced apoptotic signaling

To substantiate the different behaviors of the established cell lines under TRAIL-induced cell death, the viability of the different cell lines was measured via EZ4U assay. EZ4U is a nonradioactive cell proliferation and cytotoxicity assay that depends on the presence of functional mitochondria. In this assay, the cells were either treated with TRAIL or left untreated as control. In concept, the TRAIL-induced apoptosis, in other words, the cell survival of the different cells under TRAIL treatment were detected via the measurement of metabolic status of the surviving cells (Figure 3.6).

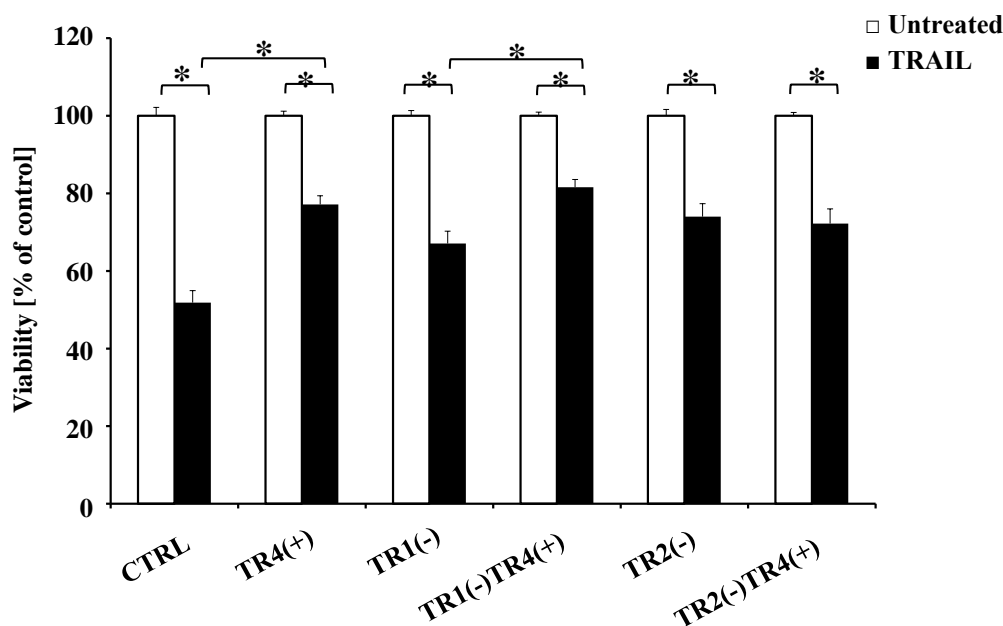


Figure 3.6] Viability of the different cell lines in response to TRAIL-induced apoptosis. The cellular viability of Colo357 cell lines under TRAIL treatment was detected via EZ4U analysis. Colo357 cells with differentially expressed TRAIL receptors were seeded (1.5×10^4 cells, 96-well format) and incubated for 24 hours. Then the cells were treated with 50ng TRAIL and re-incubated for 24 hours. Later, EZ4U substrate was added and the absorbance was read on Tecan sunrise microplate reader every hour. Shown is the mean of two independently performed experiments (biological replicates). ANOVA was used to determine the significance (*, $n=2$, p -value < 0.05).

Form the assay results, the protective effect of TRAIL-R4 upon TRAIL treatment was verified in both TR4(+) and TR1(-)TR4(+) cells. However, this anti-apoptotic effect of TRAIL-R4 was abolished in TR2(-)TR4(+) cells. Additionally, the knockdown of TRAIL-R1 and -R2 both showed a protective effect on Colo357 cells.

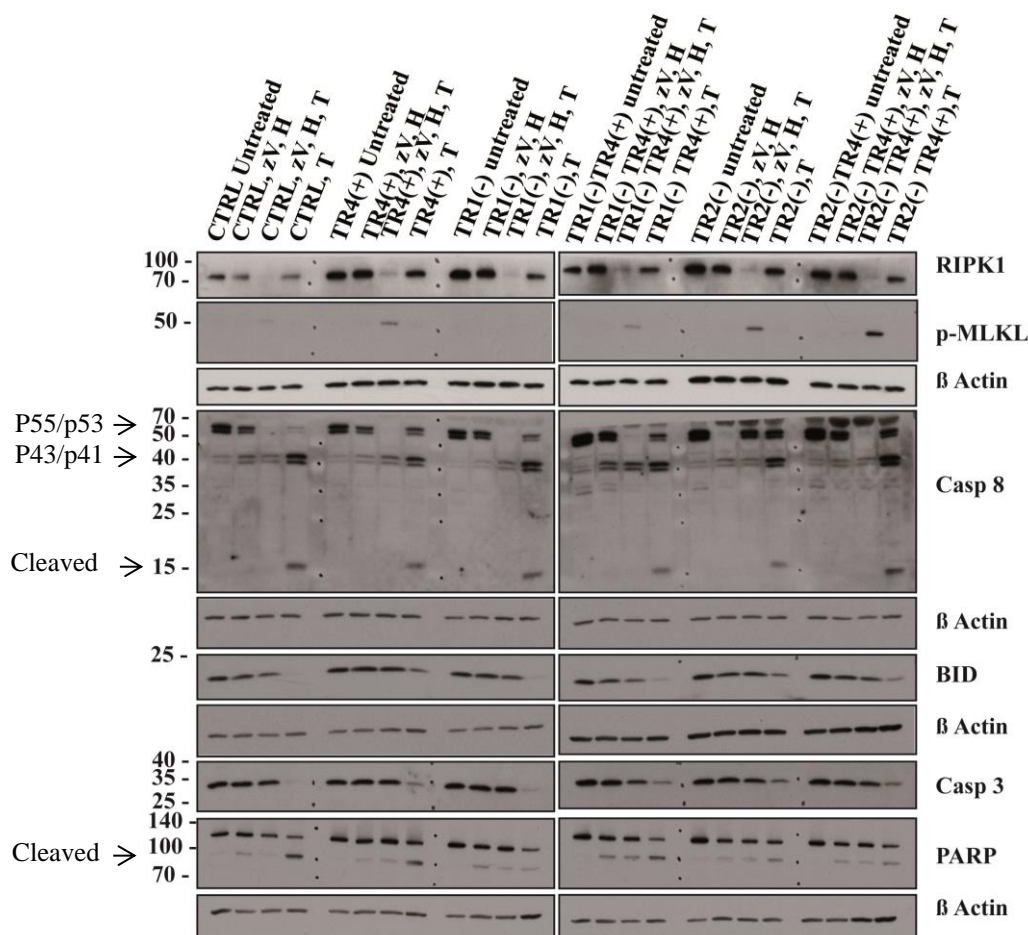


Figure 3.7| Expression levels of proteins involved in the apoptotic and necroptotic pathways. Colo357 cells with differentially expressed TRAIL receptors were seeded (3.5×10^5 cells, 6-well format) and incubated for 24 hours then the cells were either untreated or treated with 50ng TRAIL (T) to induced apoptosis. For necroptosis, cells were either pretreated with 2mM zVAD (Z) and 0.5mM HHT (H), or treated with zVAD+HHT+TRAIL to induce TRAIL-induced necroptosis. The levels of RIPK1, p-MLKL (for necroptosis) and casp. 8, BID, casp 3, PARP (for apoptosis) were investigated in whole cell lysates by means of Western blotting. The Western blots demonstrate the alterations in the proteins involved in both the apoptotic and necroptotic signaling pathways. The detection of beta actin is shown as loading control. Shown is one experiment out of two performed that show a similar trend.

In order to further evaluate the response of our proposed cell lines to TRAIL treatment, the levels of some proteins that are critically involved in apoptosis were investigated via Western blotting (Figure 3.7, 3.8 a). Among which is the activation of the initiator caspase, caspase-8. Since, Colo357 are type II cells, the activation of BH3 Interacting Domain Death Agonist (BID) was also investigated to show if the

mitochondrial loop was stimulated. BID is a member of the BCL-2 pro-apoptotic protein family which is activated by truncation (truncated BID; tBID) (Delbridge and Strasser, 2015). Moreover, the cleavage/activation of other downstream caspases including the executor caspase, caspase-3 was also investigated (Srivastava 2001). Additionally, PARP [Poly (ADP-ribose) polymerase-1] level was assessed, PARP is a 116-kDa protein involved in DNA repairing after environmental stress (Shall and de Murcia, 2000). Since, PARP inactivation is needed for the apoptotic process to continue, it is inactivated via cleavage by caspase-3 during the apoptotic process (Soldani and Scovassi, 2002).

As depicted from the blots (Figure 3.7), the level of activation of both caspase-8, BID and caspase 3 were decreased in TR4(+) and TR1(-)TR4(+) cells in comparison to CTRL and TR1(-) cells, respectively. Also, the inactivated band of PARP (140 kDa) was more prominent in TR4(+) and TR1(-)TR4(+) cells than CTRL and TR1(-) cells, respectively. From the evaluation of these proteins, one can confirm the protective effect of the TRAIL-R4 protein up-regulation against apoptosis. However, we could also report the dependency of the protective effect exerted by TRAIL-R4 up-regulation on the presence of TRAIL-R2 [in TR4(+) as well as TR1(-)TR4(+)] and that the absence of TRAIL-R2 [TR2(-)TR4(+)] completely abolished this anti-apoptotic effect. In fact, it seems from the protein level analysis in both TR2(-) and TR2(-)TR4(+) cells, that TRAIL-R4 up-regulation displayed a slight pro-apoptotic effect in this context. Here, the activated caspase-8 band shows a slight increase and the inactivated PARP band was decreased in TR2(-)TR4(+) cells denoting the activation of the apoptotic transduction pathway. However, this pro-apoptotic effect of TRAIL-R4 was not seen in EZ4U analysis. Collectively, TRAIL-R4 acts as an anti-apoptotic protein only in collaboration with TRAIL-R2. Yet, TRAIL-R4 interaction with TRAIL-R1 after TRAIL-R2 knockdown [TR2(-)TR4(+)] abolished this anti-apoptotic effect.

In order to verify the changes between the different apoptotic transduction pathway proteins, all the TRAIL-treated samples were re-assessed on the same immunoblotting experiment (Figure 3.8 a). The levels of the tested proteins confirmed the changes between the different cell lines. The cleavage of BID, Caspase 3, and Caspase 8 are more prominent in CTRL and TRAIL-R1 knockdown cells. Alternatively, the lowest level of activation was seen in TR4(+) and both cell lines with TRAIL-R2 knockdown. Plainly, this confirms our

deduction that TRAIL-R4 inhibits TRAIL-induced apoptosis only in collaboration with TRAIL-R2 and that TRAIL-R1 drives the TRAIL-induced apoptosis in Colo357 cell line.

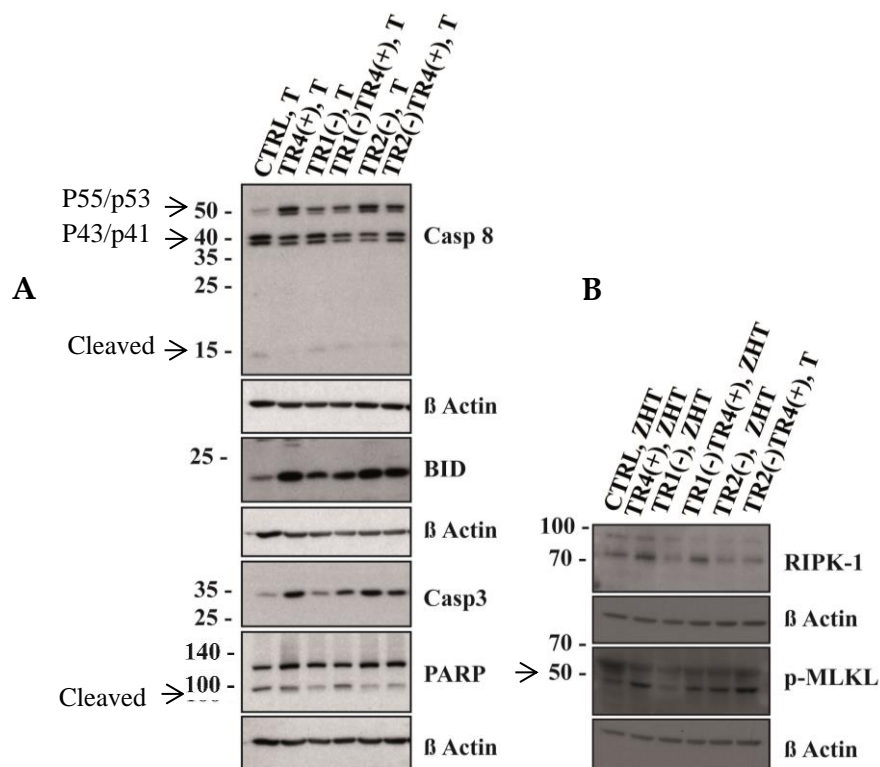


Figure 3.8| Expression levels of proteins involved in cell death. Colo357 cells with differentially expressed TRAIL receptors were seeded (3.5×10^5 cells, 6-well format) and incubated for 24 hours. Then treated with either **A**, treated 50ng TRAIL (T), to detect the protein levels of caspase 8, tBID, caspase-3 and PARP in (T) treated samples only in whole cell lysate via Western blotting or **B**, treated with 2mM zVAD(Z)+ 0.5mM HHT(H)+ 50ng TRAIL(T) to detect the protein levels of RIPK-1 and p-MLKL in Z+H+T treated probes in whole cell lysate via Western blot. These experiments were performed to observe the fluctuations of the studied proteins in comparison to each other. The detection of beta actin is shown as loading control. Shown is one experiment out of two performed that show a similar trend.

2.1. Impact of TRAIL receptors interplay on necroptosis

Hitherto, only the basic role of TRAIL receptors in apoptosis is known, however, their effect on necroptosis is yet to be elaborated. In the present study, we analyzed the effects of the differentially expressed TRAIL receptors on necroptotic cell death mode as well (Figure 3.7, 3.8 b, 3.9). In order to hinder the apoptotic pathway, a broad spectrum caspase inhibitor zVAD-fmk that was previously used successfully by other groups (Voigt et al. 2014, Thon et al. 2006, Holler et al. 2000) was utilized. Nevertheless, after inhibition of TRAIL-induced apoptosis via zVAD-fmk, necroptosis did not run automatically. In order to accelerate necroptosis, HHT (Homoharringtonine; also known as omacetaxinemepesuccinate) was used as a sensitizer for TRAIL-induced necroptosis.

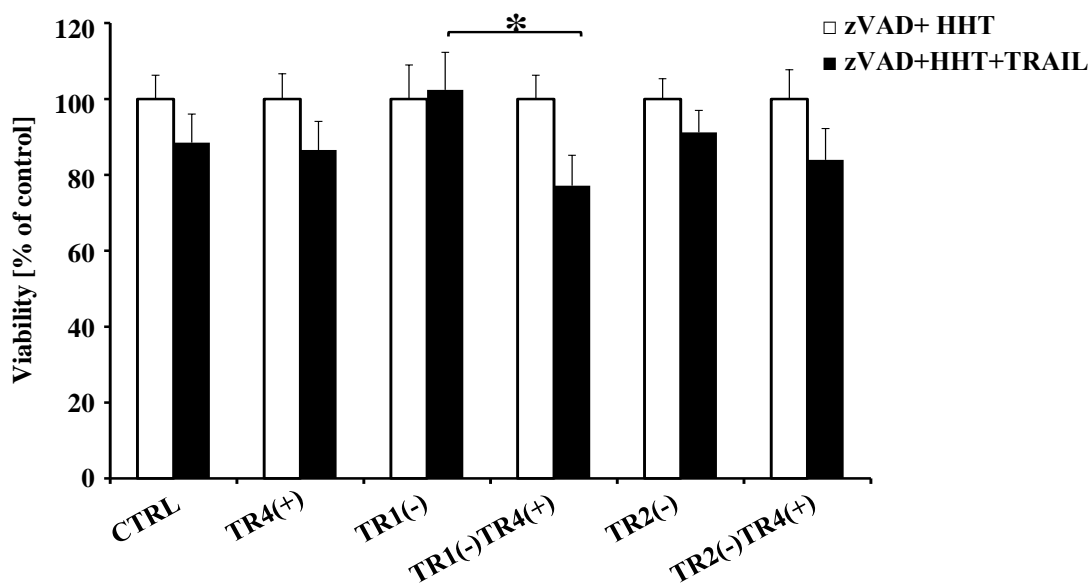


Figure 3.9| Viability of the different cell lines in response to TRAIL-induced necroptosis. Cellular viability was tested via EZ4U assay. Colo357 cells with differential expression of TRAIL receptors were seeded (1.5×10^4 , 96-well format) and incubated for 24 hours. The cells were then pretreated with 0.5mM HHT and 2mM zVAD. One hour later, the cells were either treated with 50ng TRAIL or left untreated. 24 hours later, EZ4U substrate was added and the absorbance was read on Tecan microplate reader ever hour. Shown is the mean of two independent experiments (biological replicates). ANOVA was used to determine the significance (*, $n=2$, p -value < 0.05).

Again, the cellular viability of the different cells was estimated via EZ4U assay to determine the effect of TRAIL-induced necroptosis (Figure 3.9). From the results, it could be generally deduced that Colo357 cell lines die more readily via apoptosis (~50% death in CTRL, Figure 3.6) than necroptosis (~10% in CTRL, Figure 3.9). The overall effect of necroptosis on the Colo357 cell lines was rather a novel finding. The analysis showed that the overall killing capacity induced by TRAIL was significantly sensitized by TRAIL-R4 in TR1(-)TR4(+) cells in comparison to TR1(-). Furthermore, the protective effect of TRAIL-R1 inhibition was also detected in necroptosis as it was seen in apoptosis.

Likewise, we checked the modulation of some crucial components of the necroptotic pathway in the different cell lines via Western blotting (Figure 3.7, 3.8 b). We analyzed the level of RIPK1 in all cell lines. Furthermore, we assessed the MLKL protein, which is a critical downstream target of RIPK3 (Murphy et al., 2013; Sun et al., 2012). MLKL activation during necroptosis occurs via phosphorylation (Sun et al., 2012). Thus, an antibody detecting exclusively the phosphorylated form of MLKL (p-MLKL, 50 kDa) was used. Western blot results consistently showed that p-MLKL fragment protein was only detected in the necroptotic samples. Conversely, p-MLKL was not detectable in any of the samples treated only with TRAIL, denoting the successful dissociation of the two

cell death transduction pathways. As depicted from the Western blots (Figure 3.7, 3.8 b), we detected that TRAIL-R4 up-regulation had no protective effect on necroptosis but rather TRAIL-R4 – in fact – sensitized the cells to TRAIL-induced necroptosis. The level of p-MLKL displayed obvious fluctuations in its amount between the different cell lines and thus confirming that TRAIL-R4 clearly induced necroptosis in both TR4(+) and TR1(-)TR4(+) cells. Yet again, this TRAIL-R4 sensitization of TRAIL-induced necroptosis was boosted by the inhibition of TRAIL-R1. Alternatively, knockdown of TRAIL-R2 with TRAIL-R4 induction showed no sensitization of TRAIL-induced necroptotic potential.

3. Microarray analysis of the altered genes due to TRAIL receptor manipulations

3.1. Gene expression alterations upon modulated TRAIL receptor expression

a. Gene expression analysis

A whole genome microarray screening analysis was performed using mRNA extracts from the different Colo357 cells. This screening was done to see the overall impact of the interplay between TRAIL-R1, -R2 and -R4 in Colo357. The results received were in the form of comparisons; each cell line against the CTRL group (Table 3.2). The overall picture showed that TR2(-) had the most dysregulated genes; 132 in comparison to CTRL; of which 102 were up- and only 30 down regulated. That was followed by TR1(-) that expressed a number of 128 dysregulated genes, this group showed the most down regulated genes of 48 in comparison to CTRL and 80 genes were up regulated. Next was TR2(-)TR4(+) of about 110 genes (90 up- and 20 down regulated). The last two comparisons revealed a relatively small range of gene modifications, where only 53 and 32 genes were dysregulated in TR4(+) and TR1(-)TR4(+) groups, respectively. In other words, one can deduce that TR1(-)TR4(+) cell line is the least biologically active cells since the overall altered genes are only 32 in comparison to the CTRL that had 53 altered genes. However, the knockdown of TRAIL-R1 alone and the down regulation of TRAIL-R2 with or without TRAIL-R4 up-regulation showed the highest biological activity.

Table 3.2| Number of dysregulated genes in the different cell lines

	TR4(+) vs CTRL	TR1(-) vs CTRL	TR1(-)TR4(+) vs CTRL	TR2(-) vs CTRL	TR2(-)TR4(+) vs CTRL
Up regulated genes	43	80	14	102	90
Down regulated genes	10	48	18	30	20
Total number of dysregulated genes	53	128	32	132	110

b. Validating the mRNA levels of TRAIL and TRAIL receptors

The microarray analysis confirmed the mRNA expression levels of TRAIL-R1 and -R2 (Table 3.3). There was a clear knockdown of TRAIL-R1 level by (- 4.95) and (-3.36) fold change as seen in TR1(-) and TR1(-)TR4(+) cells, respectively. Likewise, the down-regulation of TRAIL-R2 was observed in both TR2(-) by - 4.10 fold change and TR2(-)TR4(+) by -5.29 fold change. On one hand, we could show that the up-regulation of TRAIL-R4 increased the levels of TRAIL-R1 in TRAIL-R1 knockdown cell lines. On the other hand, this effect was reversed in case of TRAIL-R2 expression level that was further suppressed by TRAIL-R4 over expression as was depicted from the Western blots. Worth noting, the up-regulation of TRAIL-R4 itself was not detectable since the sequence used for TRAIL-R4 detection in the Agilent assay did not identify the artificially up-regulated TRAIL-R4 used in this study. Besides, TRAIL ligand level showed the lowest level in TR1(-)TR4(+) where it is slightly decreased in comparison to its corresponding control.

Table 3.3| Fold change of mRNA levels of TRAIL and TRAIL receptors as detected in the microarray analysis

	TR4(+) vs CTRL	TR1(-) vs Ctrl	TR1(-)TR4(+) vs CTRL	TR2(-) vs Ctrl	TR2(-)TR4(+) vs CTRL
TRAIL	1,35	1,83	- 1,33	1,34	1,31
TRAIL-R1	1,02	- 4,95	- 3,36	- 1,03	- 1,01
TRAIL-R2	1,11	1,01	- 1,00	- 4,10	- 5.29
TRAIL-R3	1,03	1,53	- 1,06	1,21	1,30
TRAIL-R4	- 1,02	1,09	1,31	1,01	1,06
Osteoprotegerin	1,13	-1,58	1,02	- 1,53	- 1,83

c. Gene Set Enrichment Analysis (GSEA)

A database was established using Microsoft® Access 2010 for a more integrative and inter-comparative assessment. In order to detect the difference in the major molecular functions and pathways, an *in silico* GSEA was performed with the help of Toppcluster and WebGestalt online bioinformatics tool (Kaimal et al., 2010; Wang et al., 2013; Zhang et al., 2005). WebGestalt (WEB-based Gene SeT AnaLysis Toolket) predicted the number

of the dysregulated genes in the different categories of gene ontology (GO); whether in biological process, cellular components or molecular processes (Table 3.4).

From the WebGestalt analysis, the highest changes in the molecular functions were found to be involved in protein binding in all cell lines. Also, a large number of the dysregulated genes were involved in ion binding and transferase activity in TR1(-) cells. Ion, nucleic acid and nucleotide binding were highly modified in TR1(-), TR2(-) and TR2(-)TR4(+) cells. Moreover, both cell lines with suppressed TRAIL-R2 expression showed changes in antioxidant activity. Regarding alterations in the cellular components, the altered genes in the different cell lines were predicted to alter a large number of membrane, extracellular space, vesicle, nuclear and cytosol components. Additionally, there were fluctuations in extracellular matrix and cytoskeletal components as well, denoting a possible change in the adhesive capacity (see later). Moreover, the alterations in cytoskeleton and cell projections might indicate modifications in cellular motility and migration. Cell projections entail cellular protrusion for instance pseudopodia, filopodia or lamellipodia. Regarding the biological processes, there were major changes predicted in biological regulation, response to stimuli, cell communication together with metabolic and developmental processes.

Additionally, another bioinformatics tool; Toppcluster was used to confirm the range of alterations between the different cell lines. Toppcluster is a freely-available multi-gene list enrichment analyzer (Figure 3.10). According to Toppcluster comparative analysis the up-regulated genes in TR4(+), TR2(-) and TR2(-)TR4(+) were allocated to alter major networks including cytokine, chemokine, inflammation, NOD-like, toll-like, senescence, integrin and ECM-adhesion. However, the up-regulated genes in TR1(-) and TR1(-)TR4(+) cells were not correlated to the alterations of any pathway except for the insulin-like growth factor signaling. Therefore, the knock down of TRAIL-R1 per se might be associated with blood sugar and metabolic diseases. Additionally, the down regulated genes in all the cell lines did not share in any pathway adjustments.

Table 3.4| Significantly modulated GO Term pathways in the different groups (WebGestalt)

Pathway Name	TR4(+) vs CTRL		TR1(-) vs CTRL		TR1(-)TR4(+) vs CTRL		TR2(-) vs CTRL		TR2(-)TR4(+) vs CTRL	
	up	down	up	down	Up	down	up	down	up	Down
Biological Processes										
Biological Regulation	27	7	56	26	10	12	69	17	60	13
Response to stimulus	25	6	54	19	8	9	61	11	54	10
Cell communication	23	5	47	14	6	7	50	10	45	8
Metabolic process	22	5	48	22	9	12	62	14	58	13
Localization	22	6	32	17	7	7	46	11	41	7
Multicellular organismal process	22	9	45	22	7	8	53	19	49	11
Developmental process	19	8	42	18	7	7	46	18	41	9
Cell proliferation	14	1	21	5	3	2	23	3	21	1
Cellular component organization	13	4	34	6	7	5	32	8	30	5
Multi-organism process	13	1	14	5	1	1	27	2	23	3
Growth	5	1	7	1	1		15	2	11	
Reproduction	3	1	11	2	1		10		11	1
Molecular Functions										
Protein binding	30	6	55	22	10	11	67	16	61	7
Transferase activity	4	1	8	2		1	7	2	7	3
Hydrolase activity	4	3	12	3	2	2	12	6	14	3
Nucleotide binding	3		7	3		2	9	1	6	
Nucleic acid binding	3		5	8	1	3	7	6	7	1
Structural molecule activity	3	1	2	1	1		3	1	3	
Transporter activity	3		3	7	1	2	7	1	3	
Lipid binding	3	1	2	2	2	1	6	1	6	1
Ion binding	3	2	16	10	2	4	18	8	24	4
Enzyme regulator activity	2		3	1	1		5		5	2
Molecular transducer activity	2	2	10	4	1	3	7	4	8	2
Chromatin binding	1		2	1			2	1	4	
Electron carrier activity	1		1	2		1	1		1	
Carbohydrate binding		1	1					1	1	
Molecular adaptor activity			1				1			
Antioxidant activity							2		1	
Cellular Components										
Membrane	23	6	49	22	9	7	59	13	53	12
Extracellular space	15	4	21	2	5	3	33	6	30	3
Vesicle	14	1	27	6	6	5	38	4	35	6
Macromolecular complex	9	1	14	6	2	7	21	6	12	2
Nucleus	6		16	11		4	18	8	15	4
Cytosol	6		15	2	1	1	18	3	13	3
Endomembrane system	5	5	20	6	5	2	19	6	18	5
Vacuole	3		4	1	1		4		5	1
Cytoskeleton	3	1	9	5	1	1	11	4	10	1
Extracellular matrix	2	1	8	3	2	4	3	2	6	1
Chromosome	1		3				1	2	2	
Mitochondrion	1		2	3		1	2	1	1	1
Endosome	1		4	1			5	1	6	
Endoplasmic reticulum	1	1	9	3		1	4	1	5	3
Membrane-enclosed lumen	1		9	8	1	2	9	3	7	3
Envelop	1		2	2		1	3		1	
Golgi apparatus		4	6	2	3	1	3	3	5	2
Cell projection		1	10	6	2	5	5	4	5	3
Microbody			1							

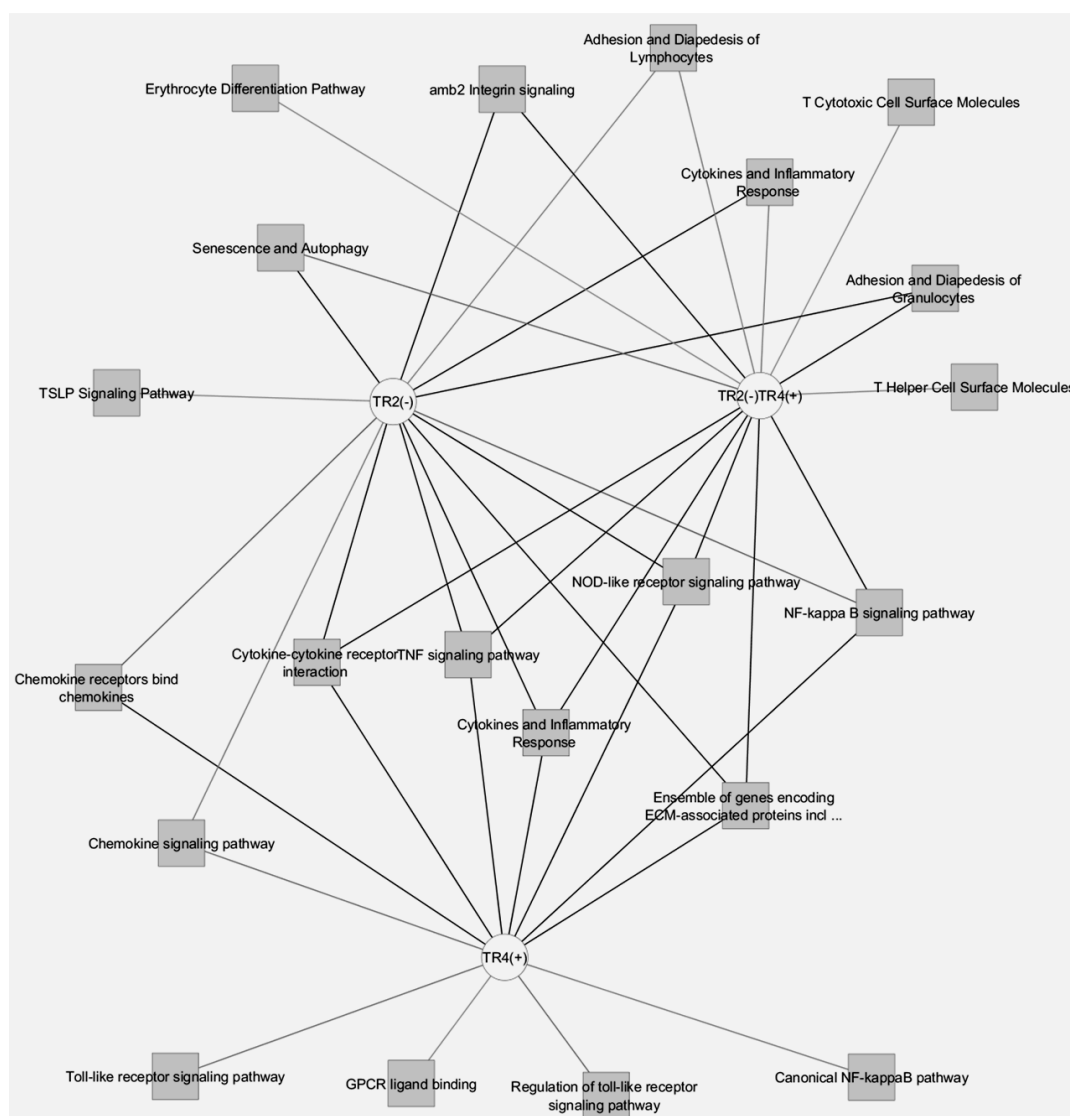


Figure 3.10| Pathway network analysis of the up-regulated genes in the different groups. The final dysregulated gene lists obtained from the comparisons between Colo357 cells with the differentially expressed TRAIL receptors were further analyzed *in silico* to determine the networks and pathways altered in the different cell lines. The pathway analysis was done using the freely-available multiple list enrichment analyzer, Topocluster.

Topocluster also compared the impact of the significantly modified genes in the different cell lines regarding the biological processes. Again, there were many biological processes altered in the different cell lines (Figure 3.11). Among the altered biological process, the genes dysregulated in TR1(-) and TR1(-)TR4(+) were responsible for the changes in regeneration and the negative regulation of both signal transduction and the developmental processes. Also, the genes altered by TRAIL-R4 up-regulation had the highest impact on altering I-kappa B kinase/NF-kappa B signaling. Some processes like myeloid differentiation, angiogenesis, and protein localization to the nucleus were correlated with the altered genes in both TR4(+) and TR2(-)TR4(+), that mean that the

collaboration between TRAIL-R1 and -R4 eventually affect these important biological processes. Additionally, cell-cell adhesion, and cell-cell signaling were predicted to be affected by the alterations in the dysregulated genes in all cell lines except TR1(-)TR4(+). Also, there was a predicted impact on the inflammatory response and cytokine production and cytokine mediated signaling in the same cells. Moreover, the response to nitrogen and reactive oxygen species as well as senescence, autophagy and activating Toll-like signaling were correlated with the genes regulated by TRAIL-R2 knock down mainly in TR2(-)TR4(+). The activation of the immune response was reported in TR4(+), TR2(-) and TR2(-)TR4(+) cells denoting that this function might be ruled by the genes dysregulated by TRAIL-R1.

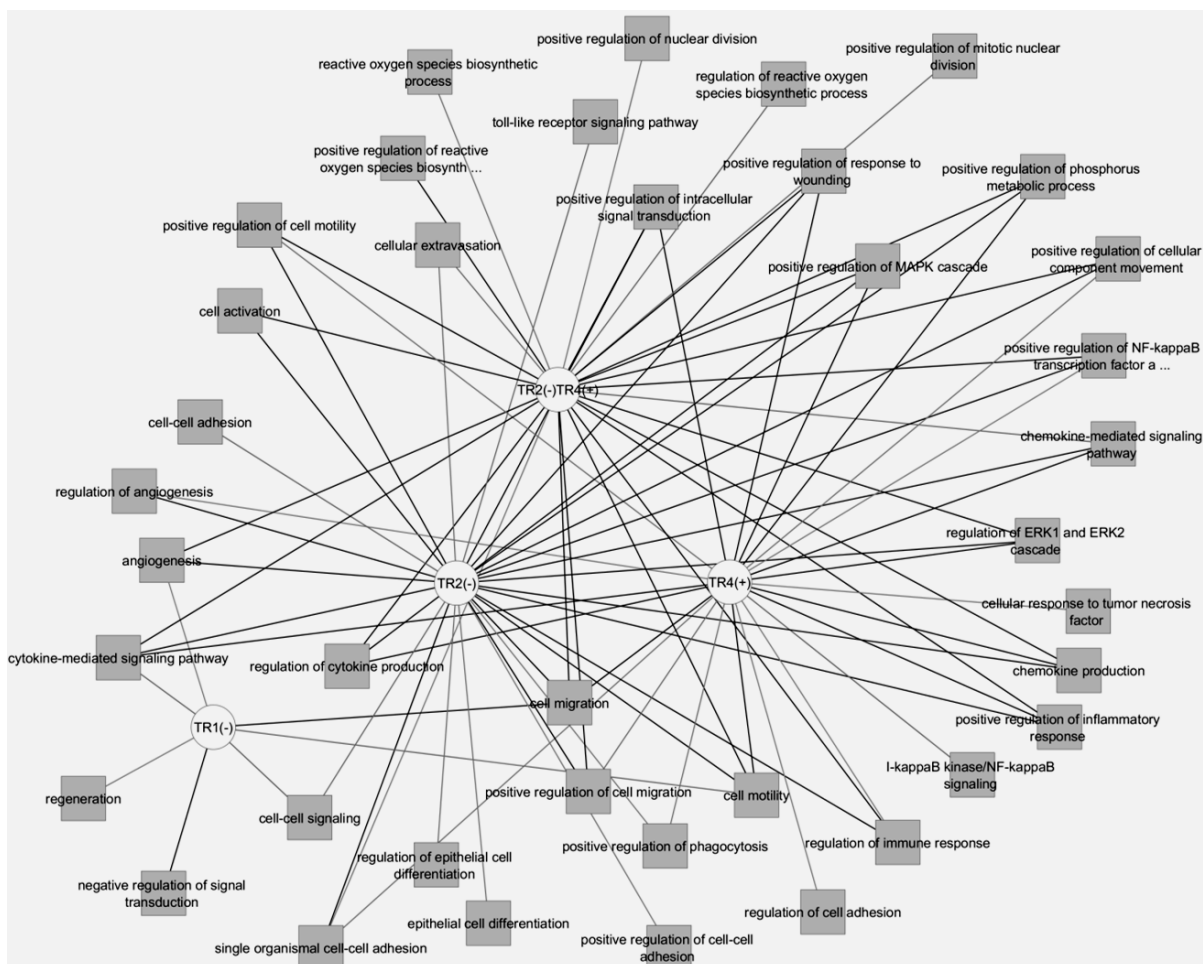


Figure 3.11| Biological processes network analysis of the up-regulated genes in the different groups. The final dysregulated gene lists obtained from the comparisons between Colo357 cells with the differentially expressed TRAIL receptors were further analyzed *in silico* to determine the networks and pathways altered in the different cell lines. The pathway analysis was done using the freely-available multiple list enrichment analyzer, Topcluster.

d. Validation of the microarray analysis

In order to validate the results predicted by the GSEA done based on the performed microarray study, some of the dysregulated molecules were detected using other methods. From the analysis, the genes altered in TR1(-), TR4(+), TR2(-),TR2(-)TR4(+) cells were predicted to positively regulate the inflammatory cytokines production and response also cell-cell adhesion molecules and cell-cell signaling were altered as well.

i. Expression of genes coding for cell-cell adhesion molecules

Carcinoembryonic antigen-related cell adhesion molecules (CEACAMs)

Since the cell-cell adhesion, cell-cell communication and signaling were predicted to be altered by the significantly dysregulated genes in most of the groups, a confirmation of the carcinoembryonic antigen-related cell adhesion molecules levels were sought. The fold change of the significantly dysregulated CEACAMs is listed in Table 3.5 as analyzed in the microarray. It was found that the levels of CEACAM5, CEACAM6, CEACAM3, CEACAM7 and CEACAM1 were among the highly modulated molecules as seen in the gene expression analysis. Evaluation of the data revealed that TR2(-)TR4(+) showed the highest levels of CEACAM molecules, followed by TR2(-), TR4(+), TR1(-) and finally the lowest levels in most CEACAMs were detected in TR1(-)TR4(+) cells.

Table 3.5| Fold change of the mRNA levels of the altered CEACAMs as detected by the microarray analysis

	TR4 vs CTRL	TR1(-) vs CTRL	TR1(-)TR4 vs CTRL	TR2(-) vs CTRL	TR2(-)TR4 vs CTRL
CEACAM5	9,602	---	---	7,217	8,591
CEACAM6	9,515	3,040	1,440	9,881	---
CEACAM3	8,865	2,986	1,416	7,553	---
CEACAM7	---	3,393	1,577	9,658	10,922
CEACAM1	5,420	2,549	2,833	6,944	---

To further validate the CEACAM alterations, we authenticated the microarray results by measuring both the mRNA and protein levels of CEACAM5 and CEACAM6 via RT-PCR and Western blots, respectively (Figure 3.12, 3.13). Indeed, the RT-PCR confirmed the high levels of CEACAM5 and CEACAM6 in the cell lines with knockdown of TRAIL-R2 and the lowest level was seen in TR1(-) TR4(+) cell line.

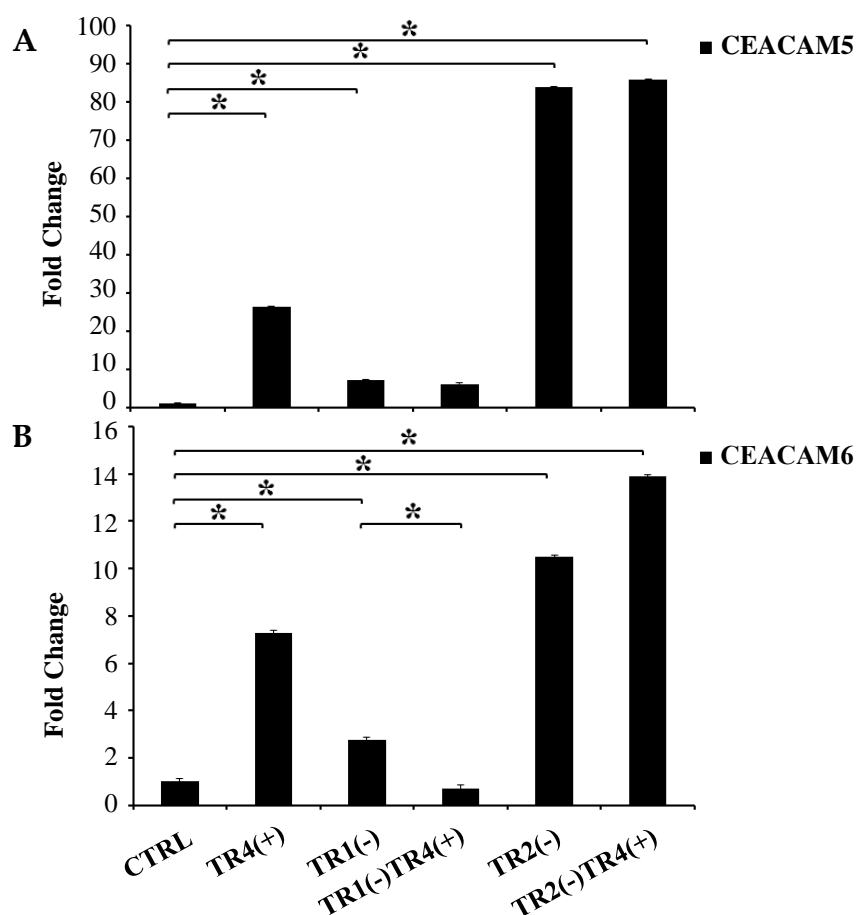


Figure 3.12| RT-PCR analysis of the CEACAM levels. Colo357 cells with differentially expressed TRAIL receptors were seeded (4×10^5 cells, 6-well format) and incubated for 24 hours. Then the mRNA levels of CEACAM5 and CEACAM6 in Colo357 different clones were analyzed by RT-PCR. CTRL cells were set as control. The mRNA levels confirmed the fluctuations of CEACAM5 and CEACAM6 demonstrated in the microarray. **A**, fold change of CEACAM5, **B**, fold change of CEACAM6. ANOVA was used to determine the significance (*, $n=2$, p -value < 0.05). Shown is the mean of two independent experiments (biological replicates) performed.

Additionally, the levels of the CEACAM proteins were also visualized via Western blotting (Figure 3.13). The two intercellular proteins, CEACAM5 and CEACAM6 were investigated. As expected, both Western blots and the RT-PCR showed a remarkable increase in the levels of both CEACAM5 and -6 orchestrated by TRAIL-R4 over expression [TR4(+)] as well as by TRAIL-R2 knockdown. Additionally, TRAIL-R1 suppression obliterated CEACAM5 augmentation but augmented the level of CEACAM6. In TR1(-)TR4(+) cells, the levels of both CEACAM5 and CEACAM6 were the lowest among the studied cells. Additionally, the up-regulation of TRAIL-R4 in the limited expression of TRAIL-R2 had no impact on both CEACAM molecules.

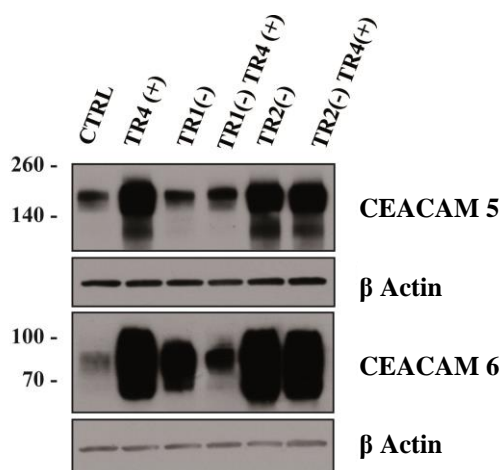


Figure 3.13| Expression levels of CEACAMs. Colo357 cells with differentially expressed TRAIL receptors were seeded (4×10^5 cells, 6-well format) and incubated for 24 hours. Then the protein levels of CEACAM5 and CEACAM6 in the whole cell lysate were detected via Western blotting. The detection of beta actin is shown as loading control. Shown is one experiment out of three performed that show a similar trend.

ii. Expression of genes coding for some inflammatory cytokines

There were significant alterations in the genes coding for some inflammatory cytokines in the microarray analysis. The highest differentially regulated inflammatory cytokines were Interleukin-6 (IL6), Interleukin-8 (IL8), Interleukin-1 beta (IL1 β) and Tumor Necrosis Factor α (TNF α) (Table 3.6). Moreover, Serum Amyloid A1 (SAA1) and its paralog SAA2 changes were also highly modulated in the different cells. According to Entrez and UniProtKB/Swiss-Prot, both SAA1 and SAA2 are annotated as major acute phase proteins that are expected to be up-regulated in inflammatory environment.

Table 3.6| Fold change of the mRNA levels of the altered inflammatory cytokines

	TR4(+) vs CTRL	TR1(-) vs CTRL	TR1(-)TR4(+) vs CTRL	TR2(-) vs CTRL	TR2(-)TR4(+) vs CTRL
IL6	22,078	---	---	12,953	7,230
IL1β	24,507	6,522	---	26,327	43,493
IL8	---	---	---	9,224	---
TNFα	22,175	---	---	24,352	26,476
SAA1	---	13,148	---	45,945	---
SAA2	36,341	23,447	---	91,442	149,793

From the microarray results (Table 3.6), it was demonstrated that almost shown cytokines were highly up-regulated in TR4(+) and TR2(-)TR4(+) cells whereas all cytokines were undetected in TR1(-)TR4(+). Also, TR1(-) showed no expression of IL6, IL8, TNF α and a rather low IL1 β .

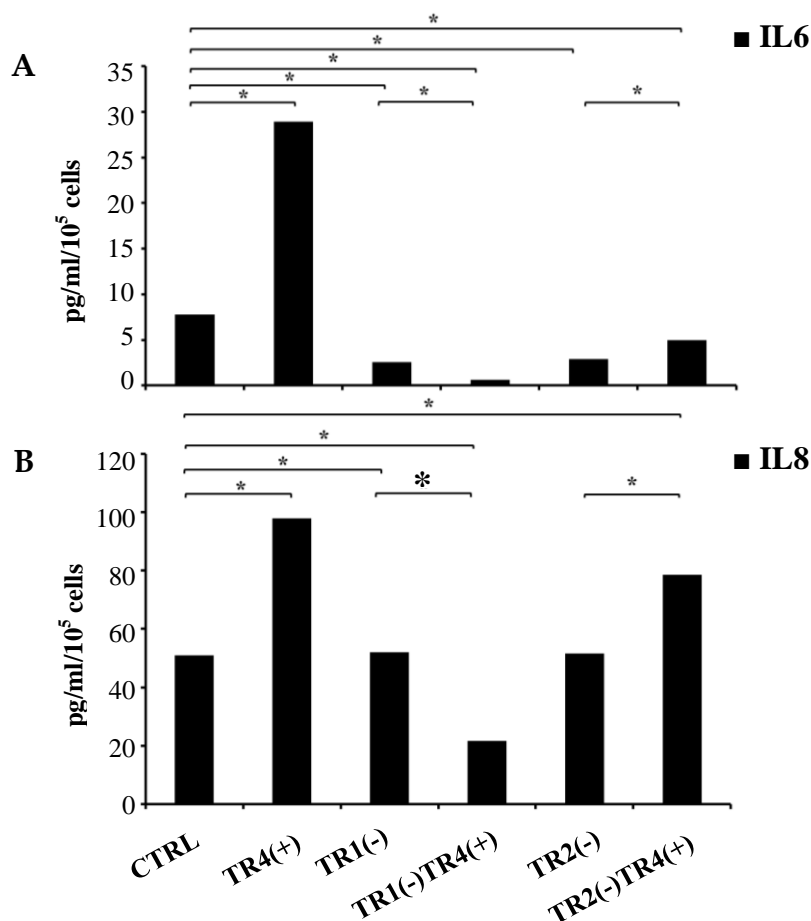


Figure 3.14| Expression level of some inflammatory cytokines. Colo357 cells with differentially expressed TRAIL receptors were seeded (3.5×10^5 in 6-well format) and incubated for 48 hours. Then the protein level of IL6 (A) and IL8 (B) were detected in the cell culture supernatant via ELISA. In parallel the cells in the wells were counted and the values of the detected cytokines were calculated per 10^5 cells. ANOVA was used to determine the significance (*, $n=3$, p -value < 0.05). Shown is the mean of three experiments (biological replicates) performed.

To confirm the microarray results, ELISAs were performed to test the levels of IL6 and IL8 in the cell culture supernatant (Figure 3.14). The ELISA analyses indicated a high levels of IL6 and IL8 levels in the supernatant of the cells with up regulated expression of TRAIL-R4 [TR4(+)] and also in TR2(-)TR4(+) cells. Regarding IL8, also TR2(-) demonstrated a high level of IL8 in the supernatant. On the contrary, the expression of both IL6 and IL8 were markedly reduced in cells with the down regulated expression of TRAIL-R1 and more intensively with TRAIL-R4 up-regulation [TR1(-)TR4(+)]. Evidently, TRAIL-R4 augmented the expression of the genes coding for IL6 and IL8 but the presence of TRAIL-R1 is essential for this process.

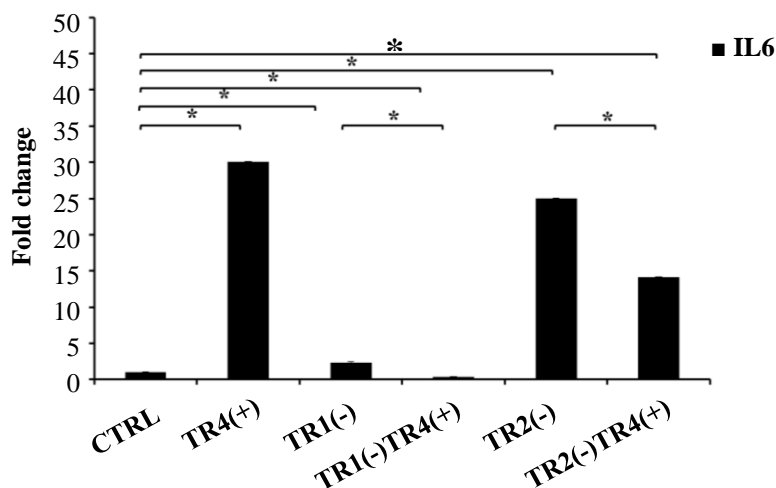


Figure 3.15| RT-PCR analysis of the level of IL6 in Colo357 cells. Colo357 cells with differentially expressed TRAIL receptors were seeded (4×10^5 in 6-well format) and incubated for 24 hours and the mRNA level of IL6 was determined by RT-PCR. Illustrated is the fold change of IL6. ANOVA was used to determine the significance (*, $n=2$, p -value < 0.05). Shown is the mean of three experiments (biological replicates) performed.

Additionally, RT-PCR analysis was performed to detect mRNA level of IL6 levels in Colo357 cells (Figure 3.15). The PCR results showed a marked increase in the levels of IL6 in both cell lines with TRAIL-R2 knockdown, although that was not evident from ELISA. These results coincide with the microarray results. For the abovementioned experiments, one can deduce that TRAIL-R4 up-regulation either alone or concomitantly with TRAIL-R2 down regulation [TR2(-)TR4(+)] showed the highest inflammatory status in all Colo357 cells. However, the cells with TRAIL-R2 knockdown showed high levels of IL6 on the mRNA level as seen in the RT-PCR results in comparison to a rather low level in the supernatant as depicted via ELISA. Thus, only TR4(+) cell line is capable of up-regulating IL6 on both the mRNA and protein levels.

3.2. Changes in the expression of stemness markers (Nanostring)

Another transcriptional analysis was performed using the Colo357 cells by means of the Nanostring technology. Nanostring is a new ultrasensitive technology that tests the gene expression via its nCounter assays. The nCounter analysis confirmed again the levels of the TRAIL receptors (Table 3.7). The level of TRAIL-R1 was suppressed more than three folds in TR1(-) cell line and more than 2 folds in TR1(-)TR4(+) cells. Besides, the knockdown of TRAIL-R2 was detected to be (-1.69) and (-2.27) in TR2(-) and TR2(-)TR4(+), respectively. Furthermore, the level of TRAIL ligand showed some alterations between the cell lines, where TRAIL recorded an augmentation of the mRNA in TR4(+)

and TR1(-) cell lines than the other cell lines, 1.67 and 1.83, respectively. Yet again, the nCounter did not detect our artificially over expressed TRAIL-R4. Therefore, it was not possible to confirm the up-regulation of TRAIL-R4 using this technology.

Table 3.7| nCounter analysis of TRAIL and TRAIL receptors

	TR4 vs CTRL	TR1(-) vs CTRL	TR1(-)TR4 vs CTRL	TR2(-) vs CTRL	TR2(-)TR4 vs CTRL
TRAIL	1,67	1,83	1,13	1,27	1,34
TRAIL-R1	1,13	-3,35	-2,57	1,17	1,53
TRAIL-R2	1,03	1,01	1,02	-1,62	-2,27
TRAIL-R3	-1,35	-1,34	-2,21	-1,69	1,03
TRAIL-R4	1,21	1,49	-1,14	1,12	1,3

Using nCounter, we analyzed specifically the expression of 199 stemness-related genes. The first filtering criteria was setting up a cutoff of ≥ 30 gene counts, thus a list of only 137 genes were further analyzed. The second filtering criterion was a fold change cutoff of ≥ 2 or ≤ -2 . It is shown that TR1(-), TR2(-) and TR2(-)TR4(+) cell lines displayed the highest alterations on the stemness markers among the six investigated cell lines (Table 3.8). In TR1(-)TR4(+) cell line, there was a subtle balance between the stemness markers. Additionally, TR4(+) cell line showed a rather balanced state with three stemness markers up-regulated (>2) in comparison to two down regulated (> -2), however, evidently was the strong down regulation of WNT3A. Moreover, TR1(-) showed a clear up-regulation of both WNT2B and CDH2 (N-Cadherin) followed by DLL1, PLAU, PRKCQ and WNT7A to a lesser extent. Finally, TRAIL-R2 knock down cell lines expressed a high level of CDH2 or WNT2B in TR2(-)TR4(+) and TR2(-), respectively. Therefore, the overall nCounter analysis demonstrated that TRAIL receptors play a role WNT signaling and also cadherins.

Table 3.8| nCounter analysis of the differentially regulated stemness markers

Gene Name	TR4(+) vs CTRL	TR1(-) vs CTRL	TR1(-)TR4(+) vs CTRL	TR2(-) vs CTRL	TR2(-)TR4(+) vs CTRL
BMP2	1,98	-2,37	-1,30	1,7	1,9
CDH2	-2,97	34,21	0,46	4,33	12,45
DLL1	1,3	2,72	1,54	1,43	1,39
GLI3	-1,91	-1,6	-0,83	-2,69	-2,67
PLAU	2,02	3,2	2,13	2,92	6,25
PRKCQ	1,79	2,36	-1,06	1,84	2,43
SMO	-1,35	-1,23	-0,47	-2,01	-1,42
WNT2B	7,84	26,86	3,78	21,71	6,74
WNT3A	-14,87	-7,11	-0,65	-13,21	-2,63
WNT7A	3,05	3,81	2,03	2,72	4,44

Furthermore, the list of the altered stemness markers was loaded into StemChecker bioinformatics tool for additional *in silico* GSEA (Table 3.9, 3.10). The StemChecker analyses derive its conclusion from previous expression profile, transcription factor gene profile data and also from literature (Pinto et al., 2015). Additionally, this bioinformatics tool provides a list of transcription factors that are targeted by the transcriptionally dysregulated genes (Figure 3.16, 3.17). From the StemChecker analysis, it can be deduced that SUZ12, SOX2, OCT4 and NANOG are among the significantly correlated transcription factors that can be manipulated via the altered gene list. Not to mention that four out of the ten dysregulated genes were correlated with embryonic stem cell characteristics thus denoting the state of un-differentiation in the studied cell lines. Other genes predicted to be implicated in hematopoietic, mammary stem cells and embryonal carcinoma. The overall analysis indicated that TRAIL receptors play a role in cell differentiation as well as stemness potential.

Table 3.9| Stem cell Types affected by the significantly altered genes

Cell Type	Overlapping Genes	<i>p-value</i>	Adjusted <i>p-value</i>
Embryonic Stem cells	4	0.062	0.556
Hematopoietic Stem cells	1	0.409	1
Mammary Stem cells	1	0.151	1
Embryonal carcinoma	1	0.297	1

Table 3.10| Transcription factor targets of the significantly dysregulated genes

Set Name	Overlapping Genes	<i>p-value</i>	Adjusted <i>p-value</i>
SUZ12	5	5.79E-4	0.006
SOX2	4	0.002	0.022
OCT4	2	0.034	0.344
NANOG	3	0.04	0.4
SMAD2	1	0.066	0.657
SMAD3	1	0.066	0.657
SMAD4	3	0.121	1

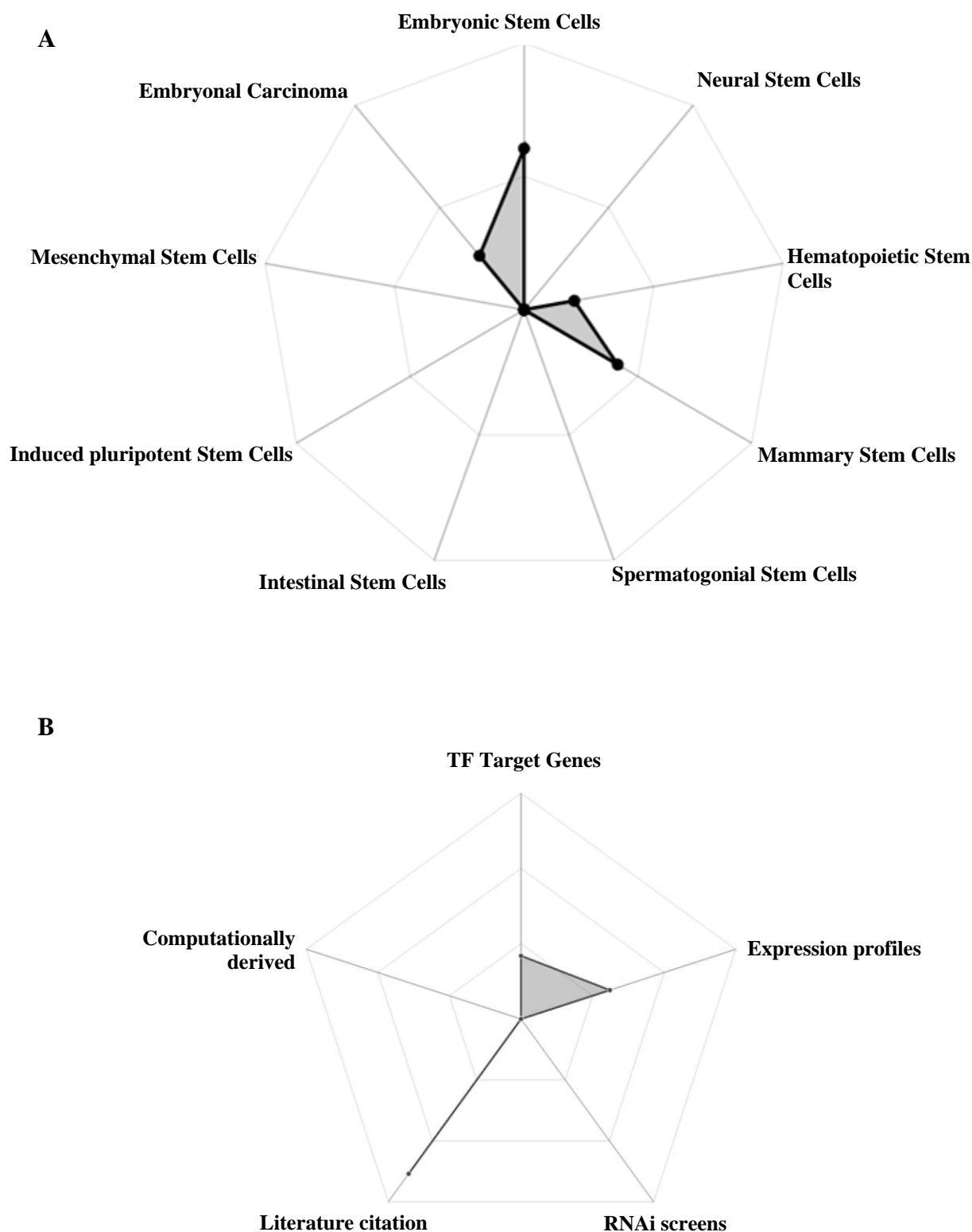


Figure 3.16| Radar charts of the stem cell types and StemChecker data sources. The final dysregulated stemness genes that were significantly altered in the different Colo357 cells with the differentially expressed TRAIL receptors were further analyzed by means of StemChecker bioinformatics tool. **A**, radar chart representing the involvement of the altered genes in the different stem cell types as generated by StemChecker, **B**, radar chart of the stemness signature data sources used by StemChecker, which are derived from expression profiling, Transcription factor (TF) target genes and literature citations.

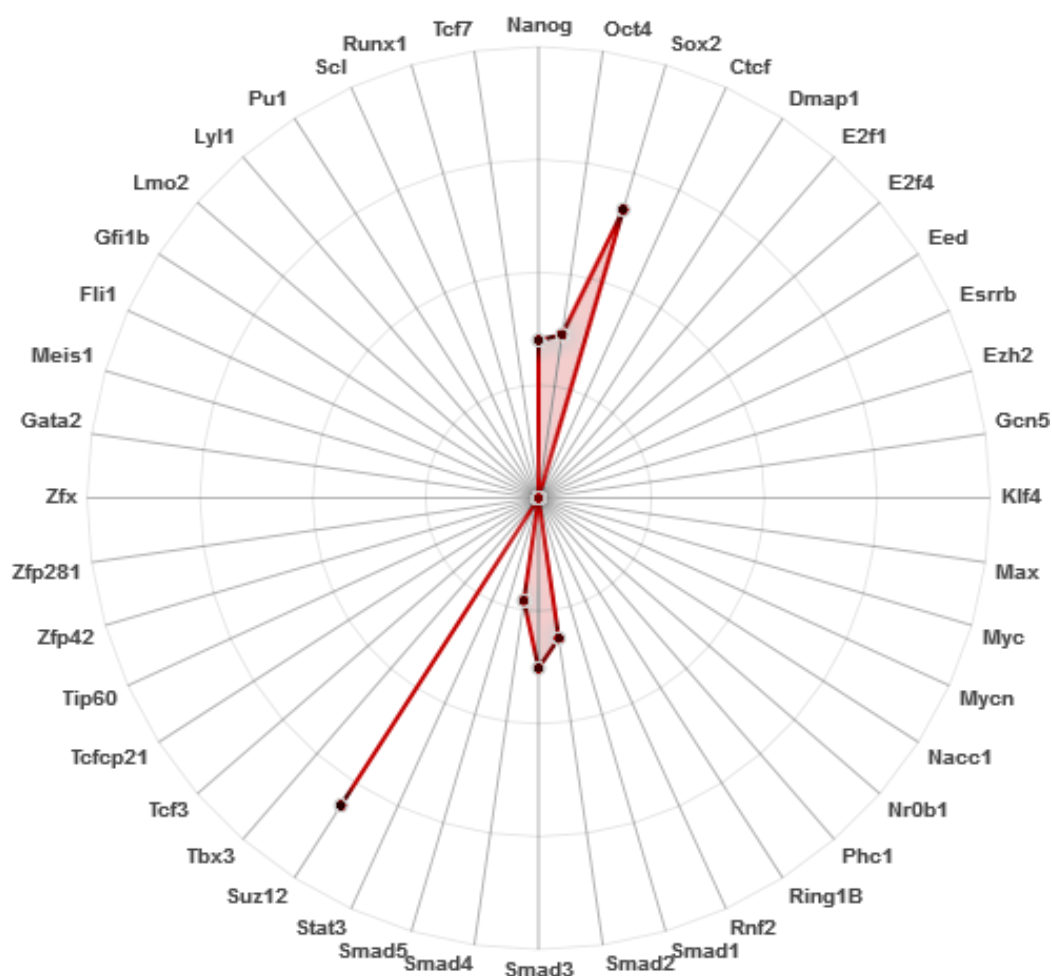


Figure 3.17| Radar chart of the highly altered transcription factors. The final dysregulated stemness genes that were significantly altered in the different Colo357 cells with the differentially expressed TRAIL receptors were further analyzed by means of StemChecker bioinformatics tool. The chart points towards possible transcription factors that can be possibly involved in the stemness process according to the transcriptionally modulated gene list.

4. *In vitro* functional analyses of the different Colo357 cell lines

Multiple functional analyses were performed to determine whether TRAIL receptors dysregulation would affect the aggressiveness of Colo357 cells. Hereby, the consequences of the interplay between the three studied receptors were tested from the morphological point of view and on the level of adhesion, proliferation, migration, and EMT.

4.1. Morphological characteristics of Colo357 cell lines

Since Colo357 cell line originated from differentiated metastatic epithelial cells, we tested if the manipulations of the TRAIL receptor gene expression would change the original behavior of the cells. The morphological characteristics of the six cell lines were assessed under light microscopy (Figure 3.18). From this aspect, the cell lines appeared

rather similar and the cells looked relatively cubical in shape. Nevertheless, it was observed that all the cell lines of Colo357 grow at first as compact colonies and if allowed to grow, they formed a complete monolayer with exception of TR1(-)TR4(+) cells.

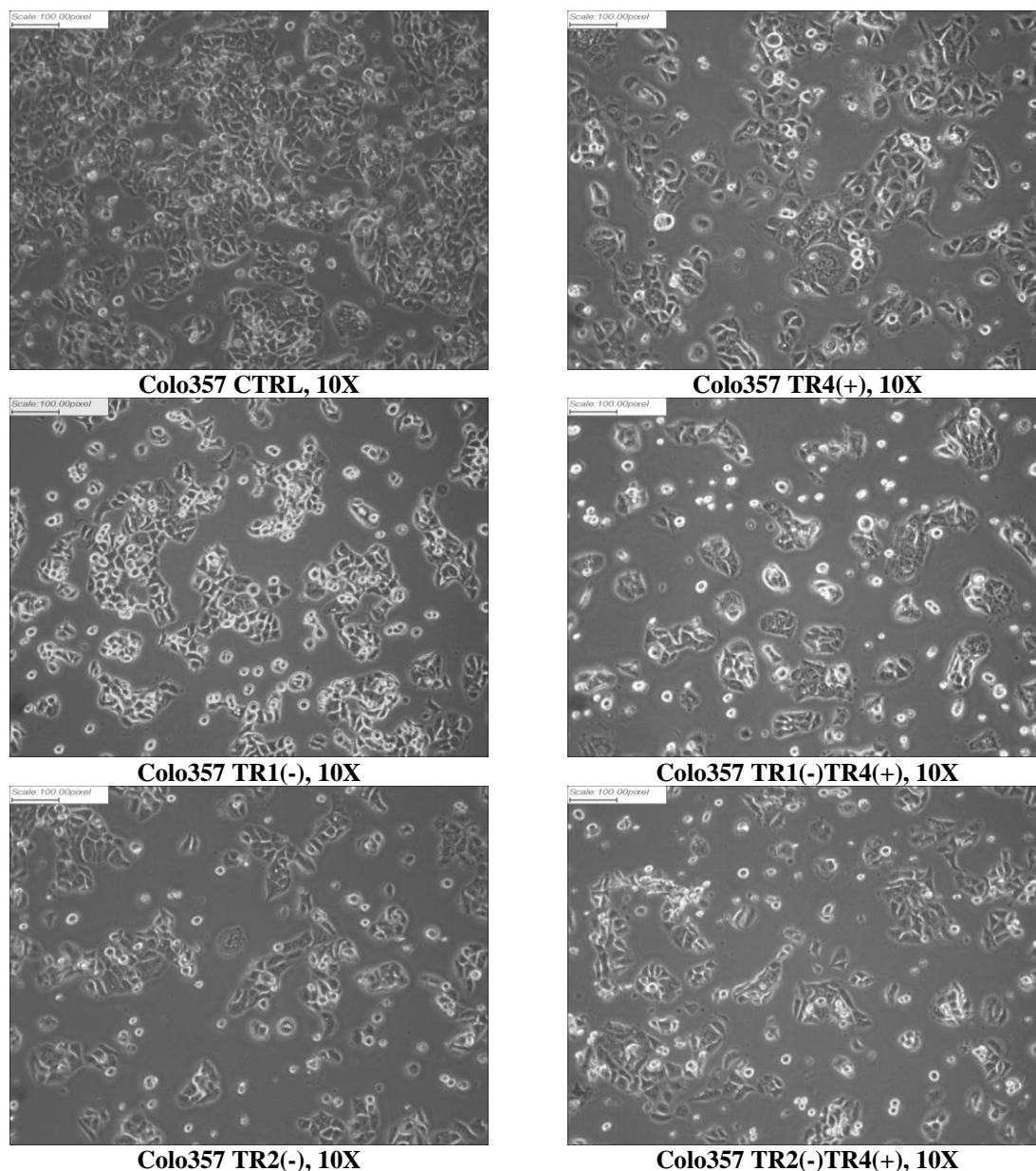


Figure 3.18| Light microscopy-based pictures of the different Colo357 cell lines. Colo357 cells with differentially regulated TRAIL receptors were seeded (4×10^5 cells, 6-well format) and were incubated for 24 hours. Light microscopic pictures were taken with 10x magnification lens (scale 128 μ m).

4.2. Impact of TRAIL receptors interplay on other adhesion molecules

Upon the characterization of the behavior of the different cell lines in culture, it was noticed that the adhesion of the different Colo357 cell lines vary considerably. TR1(-)TR4(+) cell line failed not only to form a monolayer, as previously mentioned, but also it

took shorter time to detach after incubation with trypsin than the other cell lines. The detachment duration in Colo357 cell lines ranged from circa 10 minutes in TR1(-)TR4(+) to ~30 minutes for TR4(+) and both cell lines with TRAIL-R2 knockdown. This conclusion was also supported by the *in silico* predictions. Therefore, some ECM-cell adhesion molecules were tested together with determining the viability of the cells when seeded on different extracellular matrix protein.

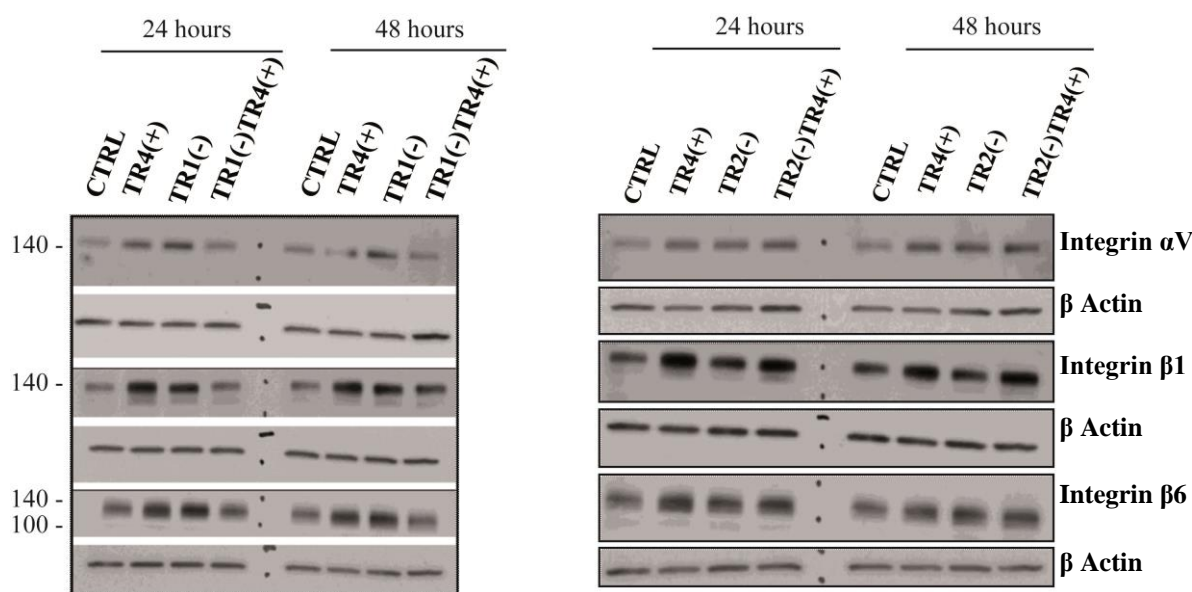


Figure 3.19| Expression levels of proteins involved in cell-ECM adhesion. Colo357 cells with differentially expressed TRAIL receptors were seeded and incubated for 24 (4×10^5 cells, 6-well format) and (2.5 $\times 10^5$ cells, 6-well format) 48 hours. Then the protein levels of integrin α V, β 1 and β 6 were determined in whole cell lysate via Western blotting. On the left panel, CTRL, TR4(+), TR1(-) and TR1(-)TR4(+). On the right side, CTRL, TR4(+), TR2(-) and TR2(-)TR4(+). The detection of beta actin is shown as loading control. The shown experiment is a representative of three performed exhibiting a similar trend.

4.2.1. Impact of TRAIL receptors interplay on cell-ECM adhesion

To examine the difference in cell adhesion capabilities, the protein levels of integrin alpha V, beta 1 and beta 6 were measured in all Colo357 cell lines by Western blotting (Figure 3.19). The levels of the integrins measured were in line with the cell culture observations. The Western blots showed again that TRAIL-R4 over expression exhibited refractory effects. Clearly, TRAIL-R4 [TR4(+)] appears to augment the tested integrin levels, however this effect is reversed upon TRAIL-R1 suppression [TR1(-)TR4(+)] and mostly abolished via TRAIL-R2 knock down [TR2(-)TR4(+)]. Also, the integrin levels were enhanced in TR1(-) and both TR2(-) and TR2(-)TR4(+) cells.

4.2.2. Impact of endogenous TRAIL on cell-ECM adhesion

To address whether the production of the endogenously expressed TRAIL manipulate the detected adhesion discrepancies, the changes in integrin levels were tested under treatment with a neutralizing antibody against human TRAIL (anti-TRAIL) by means of Western blotting (Figure 3.20). Consequently, we found that the integrin protein level changes were completely independent of the endogenously produced TRAIL. Again, the levels of Integrin α V, β 1 and β 6 were enhanced in TR1(-), TR2(-) and TR2(-)TR4(+) cell lines. Also the array of TRAIL-R4 knock-in effects on the integrin levels were also not altered by neutralizing the endogenous TRAIL.

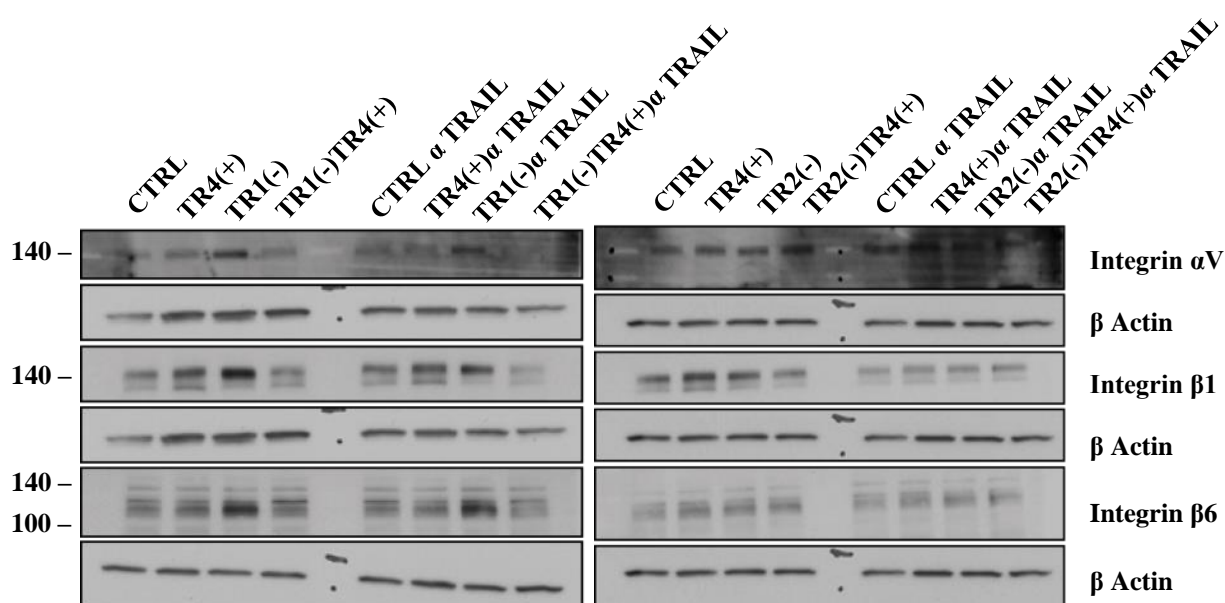


Figure 3.20| Impact of endogenous TRAIL on cell-ECM adhesion molecules. Colo357 cells with differentially expressed TRAIL receptors were seeded (4×10^5 cells, 6-well format) with and without adding a neutralizing antibody against TRAIL and incubated for 24 hours. The protein levels of integrin α V, β 1 and β 6 in the whole cell lysate were visualized via Western blotting. Left panel show CTRL, TR4(+) and two TRAIL-R1 knockdown samples. This experiment was done to determine whether the endogenous TRAIL ligand drive the integrin changes demonstrated in the studied cells. Right panel shows CTRL, TR4(+) and the two TRAIL-R2 samples. The detection of beta actin is shown as loading control. The shown experiment is a representative of three performed exhibiting a similar trends.

4.3. Impact of TRAIL receptors interplay on proliferation

4.3.1. Impact of TRAIL receptors interplay on proliferation independent of ECM components

To study the possible impact of the TRAIL receptors' modification on cell proliferation, the cell counting technique was applied. From the results (Figure 3.21), one can interpret that Colo357 cells with TRAIL-R2 down regulation have the highest proliferative capacity regardless of the TRAIL-R4 status. On the second level came TR1(-)

), TR4(+), CTRL and slowest was TR1(-)TR4(+) cell line. Accordingly, it can be deduced that TRAIL-R4 abundance accelerated Colo357 proliferation capacity. Yet, TRAIL-R1 knockdown reverses this TRAIL-R4-driven induction of cell proliferation, meanwhile, TRAIL-R2 knockdown abolishes TRAIL-R4 effects. Altogether, the concomitant expression of TRAIL-R2 and up-regulation of TRAIL-R4 decelerated the cellular growth only with TRAIL-R1 suppressed expression. However, the simultaneous expression of both TRAIL-R1 and -R2 with up-regulated TRAIL-R4 induces proliferation in Colo357 cells.

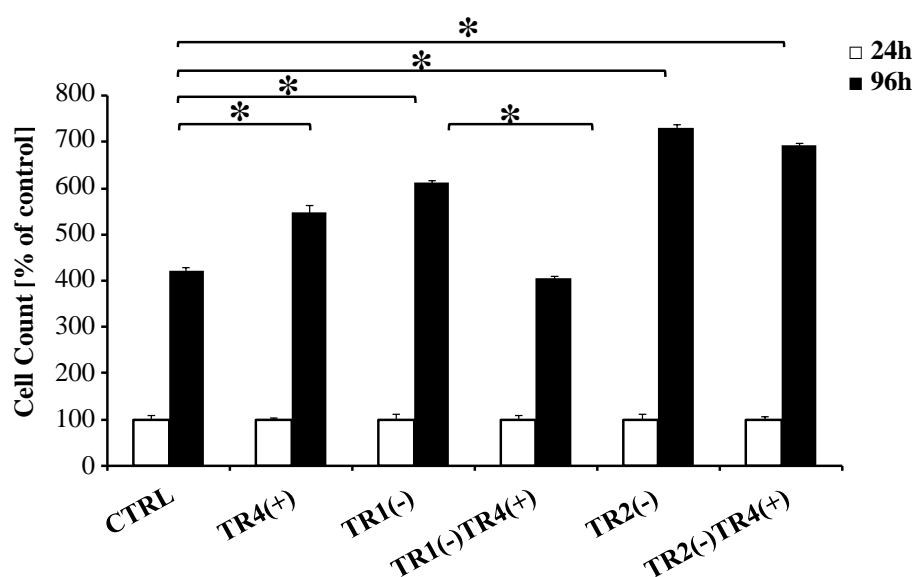


Figure 3.21| Impact of TRAIL receptors interplay on proliferation (cell count). Colo357 cells with differentially expressed TRAIL receptors were seeded (1.5×10^5 cells, 6-well format) and incubated. Later, the cells were counted using Cellometer[®] at two time points; 24 and 96 hours. The first reading was set as 100% (seen in white) and the 96 hours reading (seen black) was calculated accordingly. Shown is the mean of three independent experiments (biological replicates). ANOVA was used to determine the significance (*, $n=3$, p -value < 0.05).

Additionally, the proliferative capacity of Colo357 cell lines was analyzed via xCELLigence assay. According to the xCELLigence results (Figure 3.22), it was found that TR2(-)TR4(+) had the highest proliferation rate followed by TR1(-), TR4(+), TR2(-) and still the slowest are the CTRL and TR1(-)TR4(+) cell lines. The xCELLigence results were consistent with the cell counting, as it also shows that TRAIL-R4 up-regulation in Colo357 – whether alone or in context of TRAIL-R2 knockdown – induces cellular proliferation unlike its effect with TRAIL-R1 knockdown.

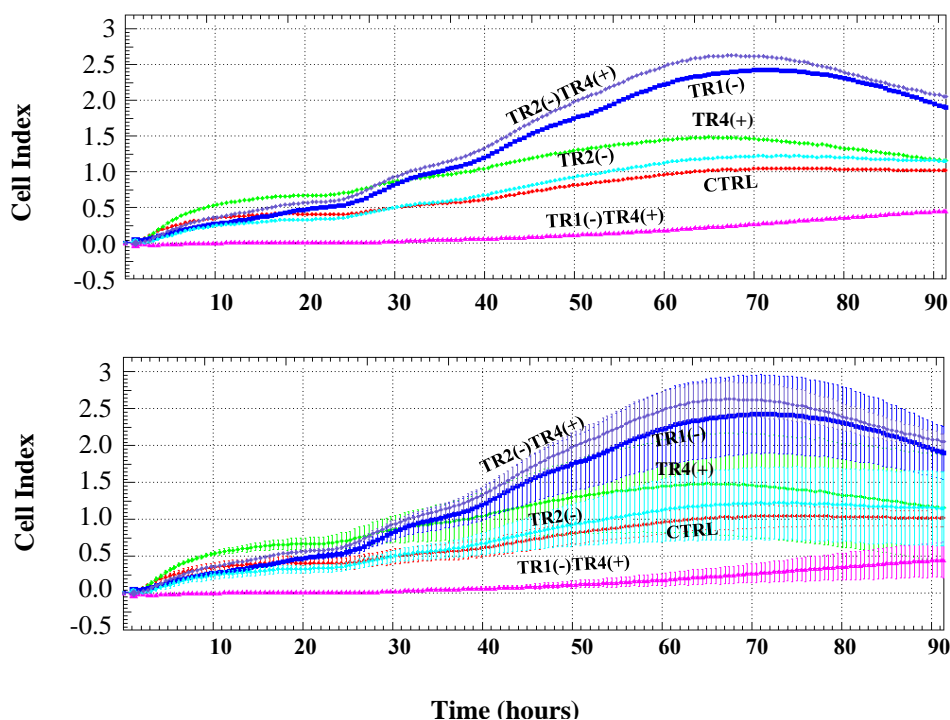


Figure 3.22| Impact of TRAIL receptors interplay on proliferation (xCELLigence assay). Colo357 cells with differentially expressed TRAIL receptors were seeded (0.6×10^4 in $100 \mu\text{l}$) in xCELLigence plates and incubated 90 hours. The upper panel shows the cell index as measured over the course of time, where the lower panel shows additionally the standard deviation. Shown is a representative experiment (technical replicates) of three performed exhibiting a similar trend.

4.3.2. Impact of TRAIL receptor interplay on cell proliferation on different ECM components

The capability of the different cells to proliferate on both fibronectin- and tenascin-c plated wells was tested using Alamar blue-based analysis (Figure 3.23). The aim was to test the proliferation of the cells once seeded on either one of the benign normally present ECM protein namely fibronectin (Bentzinger et al., 2013) or one of the malignant ECM component, tenascin-c, which is mainly found in cancer microenvironment (Esposito et al., 2006). Thus, comparing which cells will be able to proliferate on tenascin-c. Accordingly, it was observed that the cell proliferation on both PBS and fibronectin-plated wells were insignificant in all the groups (Figure 3.21). Vainly, the two cell lines with TRAIL-R2 down regulation could not even detach after more than one hour incubation with Accutase, when seeded on fibronectin. However, the impact of tenascin-c showed significant alterations in the proliferation between the different cell lines. Apparently, most of the cell lines were limitedly proliferating in the presence of tenascin-c, only two cell lines could. There was circa 20% decrease in the proliferation in CTRL, TR4(+), TR1(-) and TR2(-) cell lines. Yet, TR1(-)TR4(+) and TR2(-)TR4(+) cell lines did not show any significant

change in their proliferation potential when seeded on tenascin-c compared to CTRL, TR4(+), TR1(-) and TR2(-) cells. Obviously, these two cell lines can multiply more readily when seeded on tenascin-c unlike the rest of the cell lines that showed a significant suppression in cell growth. Thus, the studied cell lines showed evident proliferation preferentiality to certain ECMs in the surrounding environment.

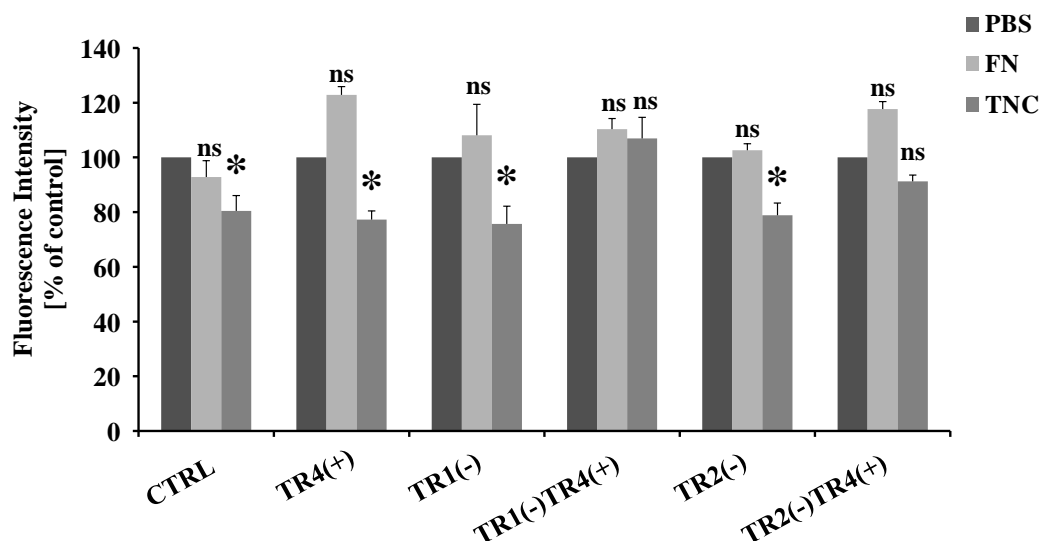


Figure 3.23| Proliferation of the different cell lines on different ECM molecules. The fluorescence intensity of Alamar Blue was detected via Tecan sunrise fluorometer. The plates (96-well format) were plated with tenascin-c ($0.1\mu\text{g}/\text{cm}^2$), fibronectin ($0.1\mu\text{g}/\text{cm}^2$) or on PBS- washed wells. Then, Colo357 cell lines with differentially expressed TRAIL receptors were seeded (1.5×10^4 cells) and were incubated for 72 hours then Alamar blue was added and the fluorescence was measured after the substrate reduction. ANOVA was used to determine the significance (*, $n=2$, $p\text{-value} < 0.05$), ns=non-significant. Shown is the mean of two independent experiments (biological replicates) performed.

4.4. Impact of TRAIL receptors interplay on migration

The migration capacity of the studied cell lines was also investigated to explore another aspect of the involvement of TRAIL receptors in the malignant behavior. Migration was assessed via scratch assay/wound healing technique and the duration taken by each cell line to close the $\sim 500\mu\text{m}$ cell-free gap was measured at time-intervals. In the migration assays performed, Mitomycin-C was used to halt cellular proliferation. Therefore, the observed results can only demonstrate cellular migration (Figure 3.24). As demonstrated, the migratory speed of Colo357 cell lines were identified and the fastest rate was observed in TR1(-) followed by TR2(-) together with TR2(-)TR4(+) then TR4(+) then CTRL and the slowest rate was encountered with TR1(-)TR4(+) cells. Thus, the scratch assay results showed that the migration of the cells was accelerated by TRAIL-R4 up-regulation but the concomitant knockdown of TRAIL-R1 [in TR1(-)TR4(+)] reverses this capacity. Moreover, no effect was seen upon TRAIL-R4 up-regulation in TR2(-)TR4(+) cells.

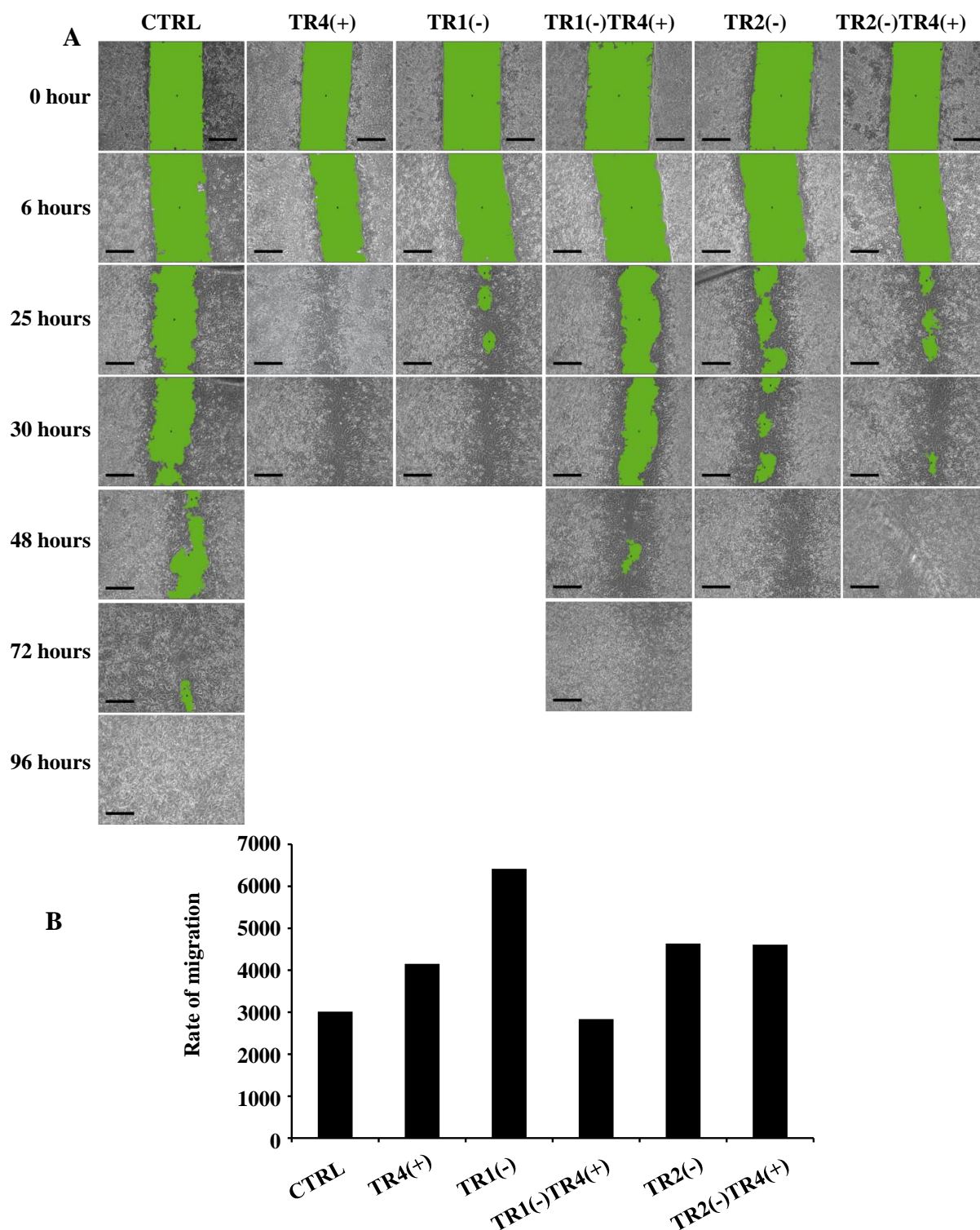


Figure 3.24| Impact of TRAIL receptors interplay on migration. Colo357 cells with differentially expressed TRAIL receptors were seeded (8×10^4 cells) on both sides of the Ibidi® culture inserts. 24 hours later, the inserts were removed leaving a 500µm gap. The cells were treated with Mitomycin C for 3 hours to inhibit proliferation. The cells were allowed to close the gap and pictures were taken at different time points to follow up the speed. **A**, Sequential pictures taken during the scratch assay at different time points. **B**, graph showing the rate by which each cell line closed the cell free area (dividing difference in cell free area by the difference of time). Shown is the mean of two independent experiments (biological replicates) performed (scale bar =166µm).

4.5. Impact of TRAIL receptors interplay on EMT

As described before, it was observed that TR1(-)TR4(+) cell line could not form a monolayer and was the fastest cell line to detach with trypsin incubation. Thus, this cell line might be considered – theoretically – to be showing more mesenchymal characteristics. Consequently, some EMT markers were evaluated in the different cell lines. However, we could not validate this hypothesis, in fact there were no changes seen in E-Cadherin, TWIST, Snai1, or SLUG protein levels (Figure 3.25).

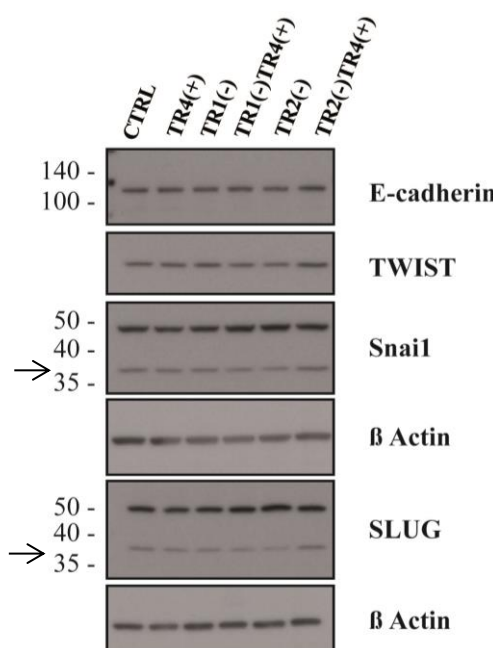


Figure 3.25| Expression levels of proteins involved in EMT. Colo357 cells with differentially expressed TRAIL receptors were seeded (4×10^5 cells, 6-well format) and incubated for 24 hours. The protein levels of E-Cadherin, TWIST, Snai1 and SLUG in the whole cell lysate were visualized via Western blotting. The detection of beta actin is shown as loading control. The blots revealed no difference between the different cell lines.

5. *In vivo* experiments

5.1. Colo357 cell lines in orthotopic tumor model in mice

As previously elaborated, TRAIL-induced signaling is both the devil and divine, due to the concomitant activation of the non-apoptotic inflammatory pathway that is feared to worsen the patients' condition. Additionally, in the current study, we could show that the inflammatory cytokines IL6 and IL8 were also altered upon TRAIL receptor manipulations. Thus, that is what we expected and eventually observed upon performing the animal experiments. We have performed two animal experiments using SCID-beige mice in order to validate the *in vitro* data obtained from Colo357 cell lines. The first

experiment entailed 8 mice per group and spanned over a period of twenty eight days (Figure 3.26, 3.27). At the end point, the mice developed rather small tumors; nevertheless the experiment had to be ended because the animals had developed large cysts. Overall, the tumor weights and sizes did not show significant differences between the different groups. Mice with knockdown of TRAIL-R1 presented with relatively the heaviest tumors. Also, the tumor sizes were rather similar with the largest being recorded in TR1(-)TR4(+) group, where the mice demonstrated the largest pancreatic cysts.

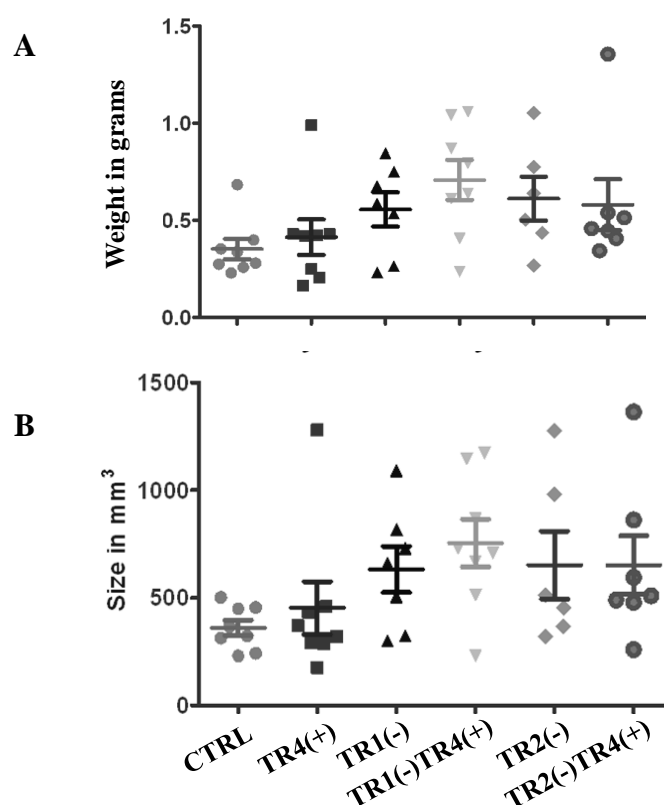


Figure 3.26 | Primary tumor weight and size analyses of the orthotopic tumor model. SCID-beige mice were orthotopically injected with Colo357 cells with differentially expressed TRAIL receptors in the pancreas. At the end point, the tumors were extracted and the size and weight were determined. **A**, the end-weight of the tumors including cysts, **B**, end-size of the tumors including cysts in all mice (n=8) in the different groups. Significance was calculated via adjusted Kruskal Wallis method (*, *p*-value < 0.05).

The number of grossly observed hypo-pigmented spots was counted as probable metastases at organ harvesting (Figure 3.27). There were no hypo-pigmented spots on the surfaces of either the spleens or the livers of TR1(-) group. Likewise, there were no liver or spleen surface hypo-pigmentation in TR4(+) and TR2(-) groups, respectively. Both TR2(-) and TR2(-)TR4(+) groups showed the most number of mice with hypopigmentation on the liver's surface, especially in TR2(-)TR4(+) group.

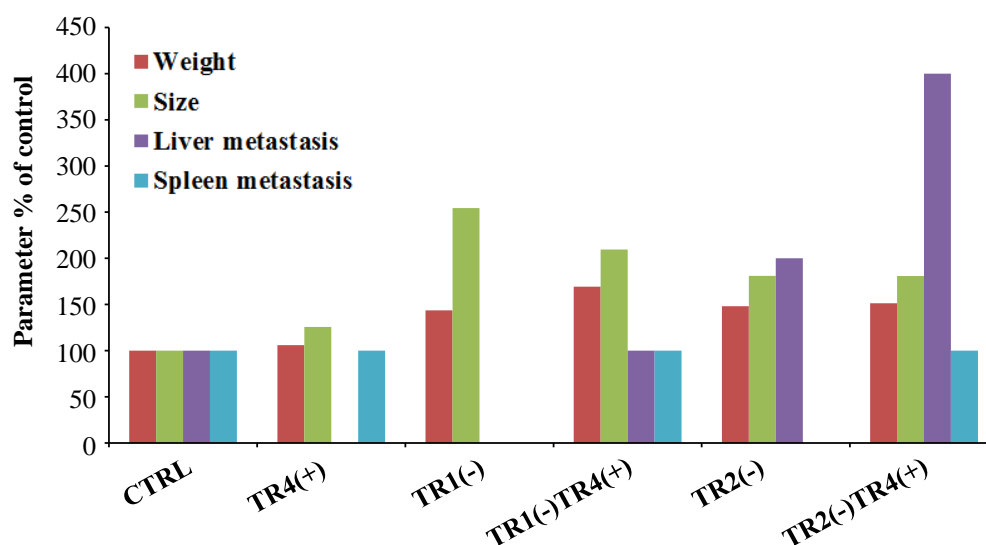


Figure 3.27| Overall analysis of the orthotopic animal experiment. SCID-beige mice were orthotopically injected with Colo357 cells with differentially expressed TRAIL receptors in the pancreas. Tumors from all the mice from each group (n=8) were examined at the experiment's end-point. The graph shows the percent of the end-tumor weight and size together with the liver and spleen metastasis.

Additionally, the tumors were monitored via sonography (Figure 3.28) that was performed twice and one MRI was done at the end point (Figure 3.29 a,b). Ultrasonography allowed us to measure the tumor volumes and the cyst size. Technically, it was difficult to detect any metastasis in the ultrasound images. Indeed, the tumor volumes depicted from the sonography data goes in line with our grossly estimated calculations at the experiment end point.

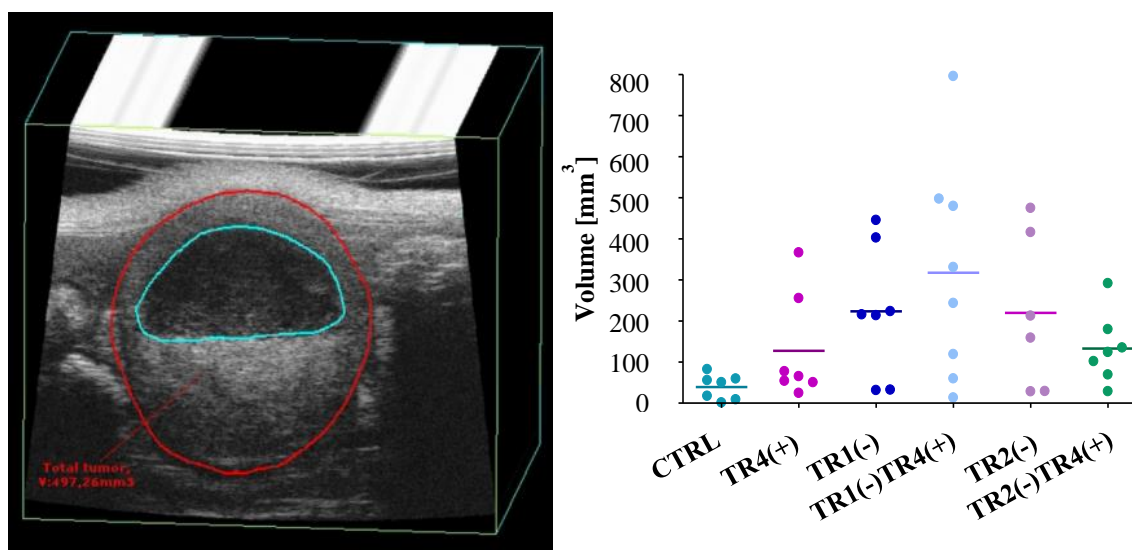


Figure 3.28| Volumetric analysis of the primary tumor (ultrasound). SCID-beige mice were orthotopically injected with Colo357 cells with differentially expressed TRAIL receptors in the pancreas. Primary tumors were followed-up via ultrasound twice through the course of the experiment (n=8 per group). **A**; 3D image reconstruction of the ultrasound pictures, primary tumor lined with red color and the cyst inside (seen in turquoise), shown is a mouse from TR4(+) group **B**; primary tumor volumes as depicted from sonography data. Significance was calculated via adjusted Kruskal Wallis method (*, p -value < 0.05).

From the MRI (Figure 3.29 a, b), the tumor sizes were measured, as well as the cysts and the possible metastases. From this imaging modality, the primary tumor volumes calculated confirmed the gross and ultrasonic measurements. Again, the two mice groups with TRAIL-R1 knockdown produced larger tumors than the other groups. Despite the apparent discrepancy between TR1(-) and TR1(-)TR4(+) groups and the others still these changes were not significant. Furthermore, the MRI was the only modality that allowed the counting of all possible liver and abdominal wall metastasis. Interestingly, although the TR1(-)TR4(+) group developed relatively the largest tumors, there was no metastasis observed in these mice. Additionally, mice in the group injected with TR4(+) cells did not show gross metastasis as well. The CTRL group showed the most metastasis followed by TRAIL-R2 knockdown groups with or without TRAIL-R4 up-regulation and TR1(-) group. Worth mentioning that TR1(-) developed more abdominal wall metastasis than liver metastasis (=21), conversely, the TRAIL-R2 knockdown groups formed less abdominal wall than liver metastasis (=12).

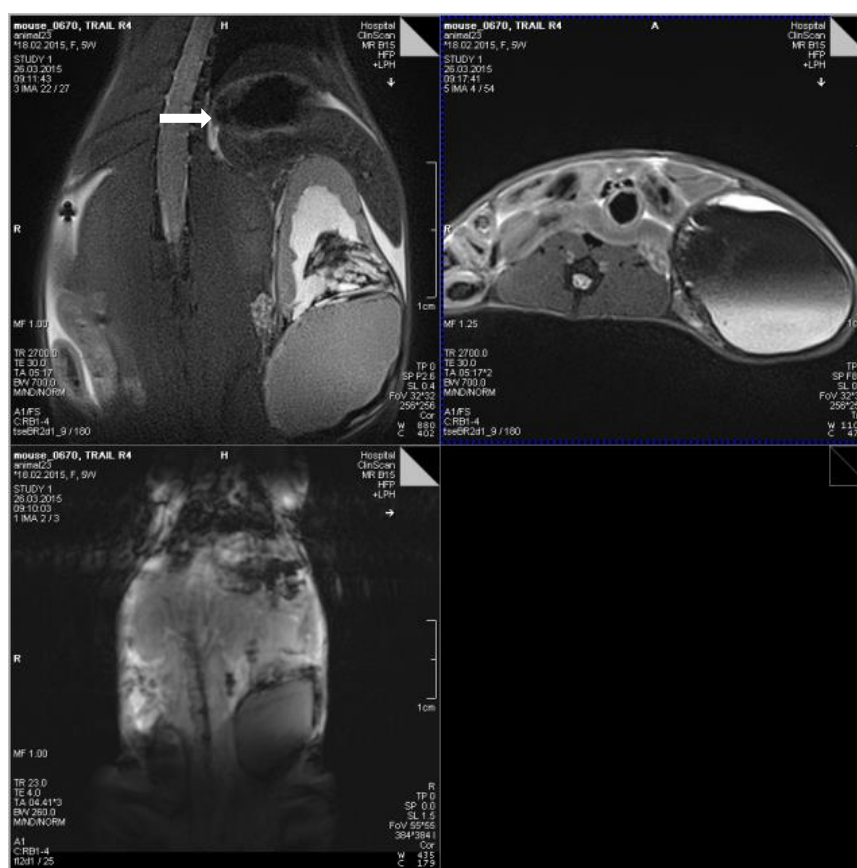


Figure 3.29a| MRI image of the orthotopic tumor model. SCID-beige mice were orthotopically injected with Colo357 cells with differentially expressed TRAIL receptors in the pancreas. MRI scanning was done at the end-point of the *in vivo* experiment (n=8 mice per group). An example of an MRI images showing the sagittal (upper left), coronal (lower left) and axial (right) views of a mouse [an example from TR1(-) group]. The arrow is pointing to the tumor site.

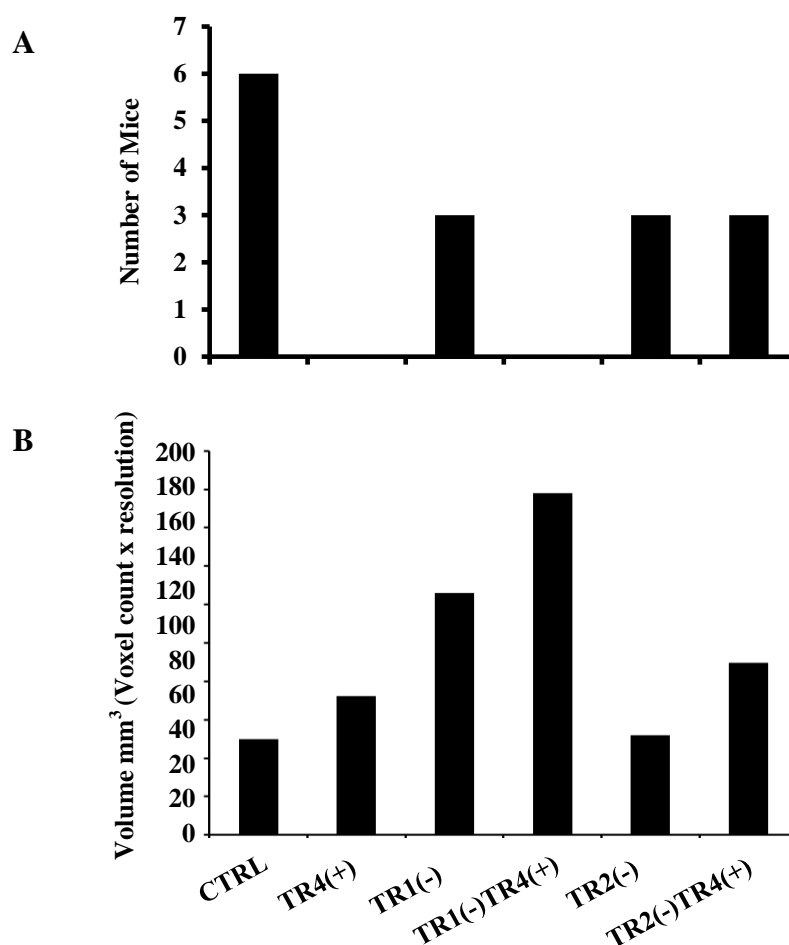
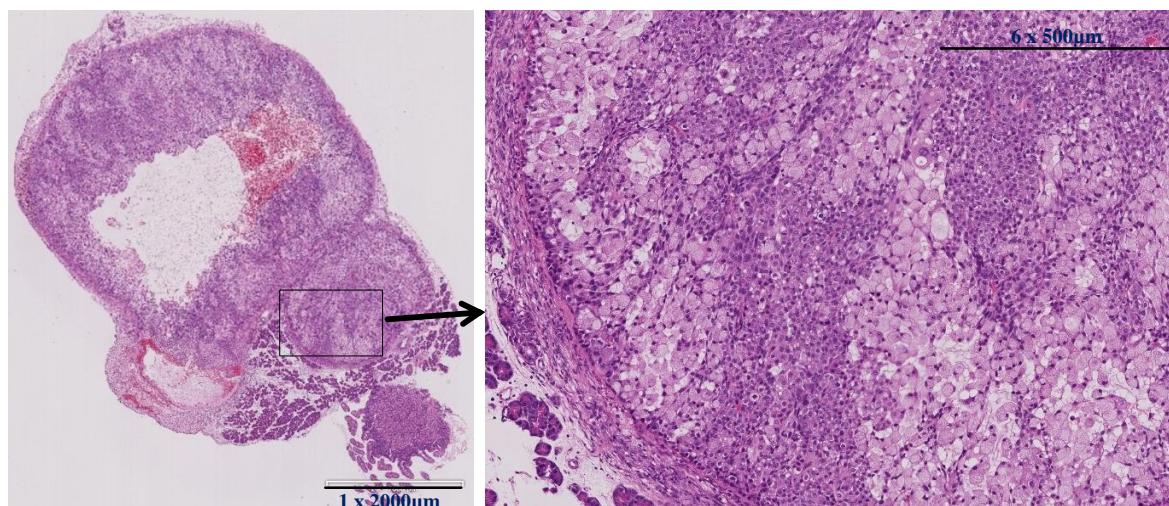


Figure 3.29b| MRI image analyses of the orthotopic tumor model. SCID-beige mice were orthotopically injected with Colo357 cells with differentially expressed TRAIL receptors in the pancreas. **A**, Total number of Mice showing metastasis (both liver and abdominal wall) as detected from the MRI image scans in each group (n=8 mice per group). **B**; Mean tumor volume as measured by MRI. Significance was calculated via adjusted Kruskal Wallis method (*, *p*-value < 0.05).

Moreover, the immunohistochemical staining of paraffin-sections from the tissues obtained from these experimental tumors showed an extensive slimy structure with small scattered islands of tumor cell collection in the primary tumor site (Figure 3.30). The tumor was largely comprised of signet-ring like cells. This unusual pathology made the analyses of our staining very difficult.



Mouse #48 PT_Colo357, TR2(-)TR4(+)

Figure 3.30| Immunohistochemical staining of the primary tumor tissues. SCID-beige mice were orthotopically injected with Colo357 cells with differentially expressed TRAIL receptors in the pancreas. The tumor tissues extracted from the mice were partially blocked in paraffin and prepared for Immunohistochemical staining. **A;** Hematoxylin and Eosin staining of the orthotopic tumor tissue sections, an example from TR2(-)TR4(+) primary tumor (PT) tissues (scale bar = 2000µm). **B,** enlarged image (scale bar = 3000µm). The animals developed anomalous tumors showing scattered tumor cell islands with intervening lakes of fluid and/or clear signet-ring like cells.

5.2. Colo357 cell lines in subcutaneous model in mice

Owing to the difficulties faced with the orthotopic model of Colo357 cell lines, another animal experiment was done. In this experiment, the cells were injected subcutaneously in SCID-beige mice (Figure 3.31). One million cells were injected subcutaneously in the flanks with 5 mice per group. Notably, the subcutaneously grown tumors exhibited more solid nature and this model also allowed for the follow-up of tumor volume development over the course of the experiment (Figure 3.31 a, b). Generally, the trend of the tumor development followed the *in vitro* proliferation results. The largest primary tumor volumes were detected in TRAIL-R4 over expression cell lines followed by TR1(-), TR2(-) and TR2(-)TR4(+) groups. And as expected from the *in vitro* analyses, TR1(-)TR4(+) formed the smallest tumors with the slowest rate of growth. Similarly, tumor weighing followed the same tendency (Figure 3.31 c).

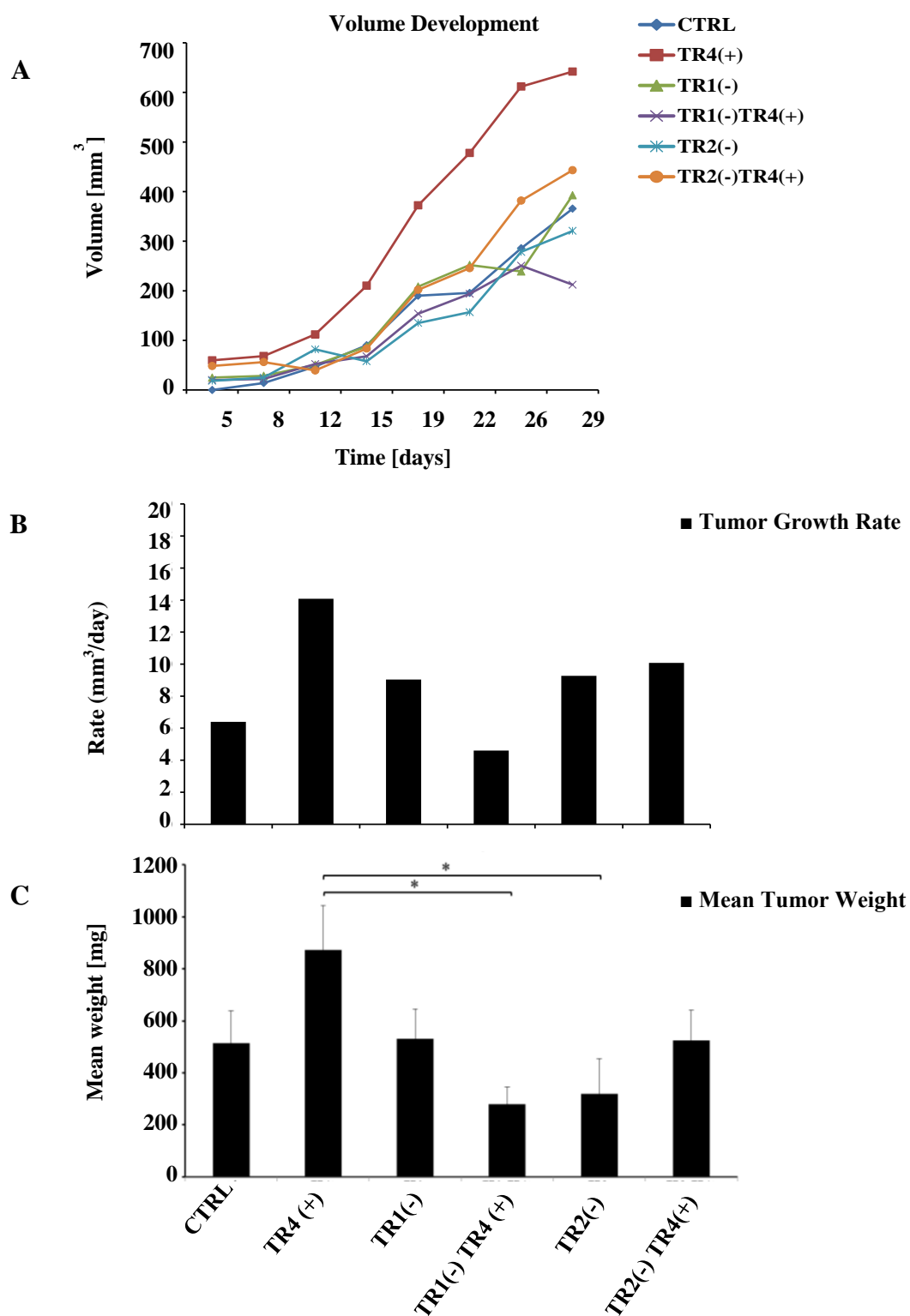


Figure 3.31| Overall analysis of the subcutaneous animal experiment analysis. SCID-beige mice were subcutaneously injected with Colo357 cells with differentially expressed TRAIL receptors in the flanks. **A**; primary tumor volume development over the course of the experiment, **B**; primary tumor volume growth rate, measured by dividing the difference in tumor volume by time difference (days). **C**; primary tumor mean weight in the different groups, Significance was measured by Kruskal Wallis and adjusted with Holm FWER method (*, *p*-value < 0.05).

6. Patient cohort study

With the successful characterization of Colo357 cell lines and similarities between the *in vitro* and subcutaneous *in vivo* study results, it was rather intriguing to know whether these conclusions could be adapted to the patient as well. Therefore, a cohort of 106 PDAC patients' tissues was studied. The tissue samples were collected postoperatively from the patients, this cohort was previously analyzed in Prof. Anna Trauzold group (Haselmann et al., 2014). The former study was done to emphasize on the importance of the nuclear expression of the TRAIL receptors. This PDAC patients' panel was then adapted with our proposed system and the data were reanalyzed accordingly. The original data included a number of 51 female (48.1%) to 55 male (51.9 %) patients. The patient age ranged from 47 to 85 years old at the operation day. The tumor differentiation grading ranged from G1 (10,4%), G2 (55,7 %), G3 (33%) to G4 (0.9%).

The patients' tissue-sections were immunohistochemically stained for TRAIL-R1, -R2 and -R4. In order to conform to the groups investigated in the current study, the levels of the TRAIL receptors were re-evaluated and from the total of 106 patients only 35 patients (33.02%) fitted with our groups (Table 3.11). Keeping in consideration the small number of patients in each group, the analysis revealed that the largest patient sub-group (n=15) was equivalent to TR1(-)TR4(+) cells followed by 12 patients in TR4(+), five patients in TR1(-). Finally, the lowest represented cases were patients with TRAIL-R2 knockdown groups (n= 3) pattern with zero percent survival, despite the low tumor grading (G1-2) (see later).

Table 3.11| Clinico-pathological patients' characteristics of the chosen sub-group

	Nº of Patients (%)	Gender* (%)	Grade (Nº)	Grade (%)
Equivalent to TR4(+)	12 (11.32)	1= 4 (33.3) 2= 8 (66.7)	G2 (6) G3 (6)	G2 (50) G3 (50)
Equivalent to TR1(-)	5 (4.72)	1= 2(40) 2= 3(60)	G1 (1) G2 (3) G3 (1)	G1 (20) G2 (60) G3 (20)
Equivalent to TR1(-)TR4(+)	15 (14.15)	1= 8 (53.3) 2= 7 (46.7)	G1 (2) G2 (7) G3 (6)	G1 (13.33) G2 (46.66) G3 (40)
Equivalent to TR2(-)	1 (0.94)	2= 1(100)	G1	G1 (100)
Equivalent to TR2(-)TR4(+)	2 (1.89)	1= 1 (50) 2= 1 (50)	G1 (1) G2 (1)	G1 (50) G2 (50)

*Gender 1=male, 2=female

Table 3.12| Relation of TRAIL receptor pattern to staging in PDAC tissues

Staging	TR4(+) (%)	TR1(-) (%)	TR1(-)TR4(+) (%)	TR2(-) (%)	TR2(-)TR4(+) (%)
Tumor (T)					
Tis	--	--	--	--	--
T1	--	--	--	--	--
T2	--	--	--	--	--
T3	10 (83.3)	4 (80)	13 (86.7)	1 (100)	1 (50)
T4	2 (16.7)	--	1 (6.7)	--	1 (50)
Nodal metastasis (N)					
N0	3 (25)	--	1 (6.7)	1 (100)	--
N1	9 (75)	4 (80)	13 (86.7)	--	1 (50)
Distal metastasis (M)					
M0	1(8.3)	3 (60)	2 (13.3)	--	1 (50)
M1	1(8.3)	--	1 (6.7)	--	--
Mx	3(13.6)	--	3 (20)	1 (100)	1 (50)
Residual tumor (R)					
R0	7 (58.3)	3 (60)	9 (60)	1 (100)	1 (50)
R1	4 (33.3)	2 (40)	3 (20)	--	1 (50)
R2	--	--	1 (6.7)	--	--
Rx	1 (8.3)	--	1 (6.7)	--	--

Tis; Tumor *In situ*, **T1**; confined to pancreas <2cm, **T2**; confined to Pancreas >2cm, **T3**; extended outside the pancreas but did not invade the coeliac or superior mesenteric arteries, **T4**; extended outside the pancreas and invaded the coeliac or superior mesenteric arteries, **N0**; no local lymph node metastasis, **N1**; lymph node metastasis, **M0**; no distant metastasis, **M1**; distant metastasis, **Mx**; undetermined distal metastasis, **R0**; no residual tumor, **R1**; microscopic residual tumor, **R2**; macroscopic residual tumor, **Rx**; undetermined residual tumor.

Additionally, the tumor staging was also re-evaluated in the chosen patient subgroup using the TNM staging system (Table 3.12). Some staging information was not included in the database, for instance, only 4 (80%) out of 5 patients were staged as T3 in TR1(-) and one patient was not documented. Also, in TR1(-)TR4(+) adapted group there were only 14 out of 15 patients with documented tumor stage.

Furthermore, the re-evaluation of the patients' survival rate showed overall a bad prognosis except for patients with TRAIL-R1 low expressing tumors [TR1(-)] showed better survival duration (Figure 3.32).

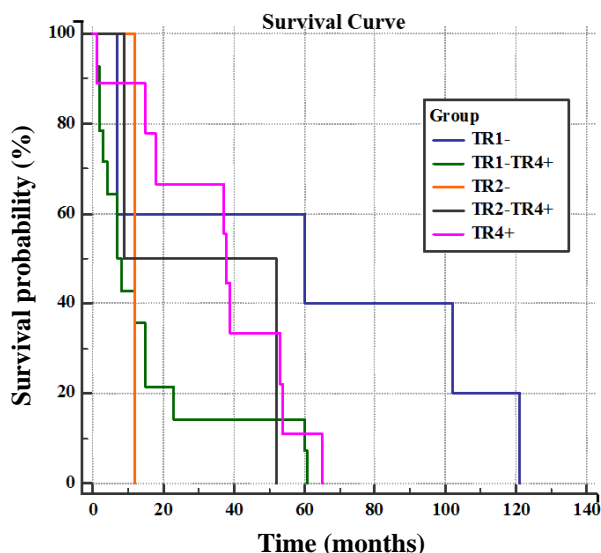


Figure 3.32| Survival curves of PDAC patients tissues with differential TRAIL receptor expression patterns. A cohort of 35 PDAC patients' tissue profiles were adapted to the studied TRAIL receptors' modifications investigated in the current study. The post-operative survival of the patients was calculated via Kaplan-Meier curves where the survival probability percent is plotted against time in month.

These patients with low tissue expression of TRAIL-R1 had a significantly longer survival duration in comparison to TR1(-)TR4(+) patients (Figure 3.33) denoting, on one hand, the obvious impact of the collaborative TRAIL-R2 and - R4 in deteriorating these patients' survival chances. On the other hand, this demonstrated the essential role of TRAIL-R1 in driving the tumor aggressiveness.

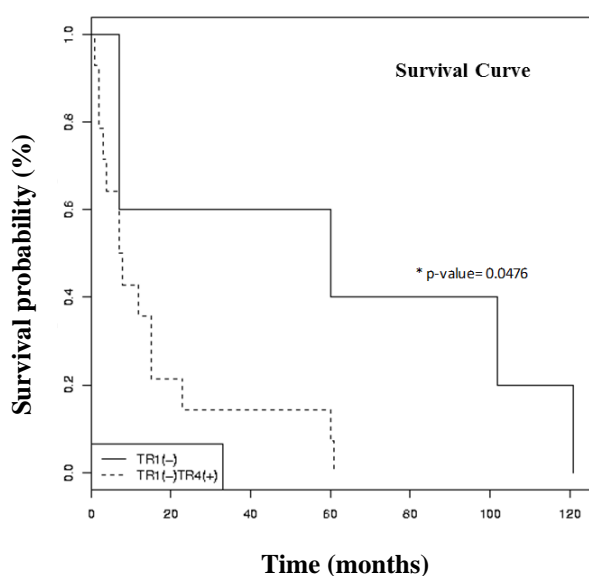


Figure 3.33| Survival curves of PDAC patients with tissue expression equivalent to TR1(-) and TR1(-)TR4(+). A cohort of 35 PDAC patients' tissue profiles were adapted to the studied TRAIL receptors' modifications investigated in the current study. The post-operative survival of the patients was calculated via Kaplan-Meier curves where the survival probability percent of TR1(-) and Tr1(-)TR4(+) is plotted against time in month p -value was determined by using Log-Rank test (Chisq= 3.9 on 1 degrees of freedom, $p=0.0476$).

Additionally the intracellular distribution of TRAIL receptors were investigated (Table 3.13). The cases representing TRAIL-R1 or TRAIL-R2 knockdown expressed low levels of the intended protein in both the cytoplasmic and nuclear compartments. Regarding TRAIL-R4 up-regulation, the groups expressed the protein in high levels in the cytoplasm in 100% of cases and to a lesser extent in the nuclei. There was a concomitant high expression of TRAIL-R2 with the up-regulation of TRAIL-R4 in 100% of the cases in TR4(+) and 80% of the cases in TR1(-)TR4(+).

Table 3.13| Intracellular distribution of TRAIL receptors in PDAC tissues extracted from PDAC patients

		TR4(+)		TR1(-)		TR1(-)TR4(+)		TR2(-)		TR2(-)TR4(+)	
		Cytoplasm	Nuclear	Cytoplasm	Nuclear	Cytoplasm	Nuclear	Cytoplasm	Nuclear	Cytoplasm	Nuclear
		№ (%)									
TRAIL-R1	Low	0 (0)	10 (83,33)	5 (100)	5 (100)	15 (100)	15 (100)	0 (0)	0 (0)	0 (0)	2 (100)
	Medium	12 (100)	1 (8,33)	0 (0)	0 (0)	0 (0)	0 (0)	1 (100)	1 (100)	1 (50)	0 (0)
	High	0 (0)	1 (8,33)	0 (0)	0 (0)	0 (0)	0 (0)	0 (0)	0 (0)	1 (50)	0 (0)
TRAIL-R2	Low	0 (0)	11 (91,67)	0 (0)	5 (100)	0 (0)	9 (60)	1 (100)	1 (100)	2 (100)	2 (100)
	Medium	0 (0)	0 (0)	3 (60)	0 (0)	3 (20)	5 (33,33)	0 (0)	0 (0)	0 (0)	0 (0)
	High	12 (100)	1 (8,33)	2 (40)	0 (0)	12 (80)	1 (6,67)	0 (0)	0 (0)	0 (0)	0 (0)
TRAIL-R4	Low	0 (0)	9 (75)	2 (40)	5 (100)	0 (0)	9 (60)	0 (0)	1 (100)	0 (0)	0 (0)
	Medium	0 (0)	0 (0)	3 (60)	0 (0)	0 (0)	1 (6,67)	1 (100)	0 (0)	0 (0)	0 (0)
	High	12 (100)	3 (25)	0 (0)	0 (0)	15 (100)	5 (33,33)	0 (0)	0 (0)	2 (100)	2 (100)

7. Generation of PancTuI cell lines with differentially modified expression of TRAIL receptors

In order to further validate the results of Colo357 cell lines, the same system was intended to be mirrored in the PancTuI cell line. The construction of the TR4(+) and TR1(-)TR4(+) were successful. However, the generation of a TRAIL-R4 overexpressing cell lines was not possible in PancTuI TRAIL-R2 knockdown [TR2(-)] cells thus far. Consequently, PancTuI group lacks these two cell lines (Figure 3.34). As depicted from the whole cell protein analyses, PancTuI cell line produced higher levels of both TRAIL-R4 and -R2 than Colo357 cells. However, the level of TRAIL-R1 was comparable in both cell lines. Additionally, the levels of TRAIL-R1 was successfully inhibited in both TR1(-) and TR1(-)TR4(+) cells and TRAIL-R4 levels were boosted in both TR4(+) and TR1(-)TR4(+) cell lines.

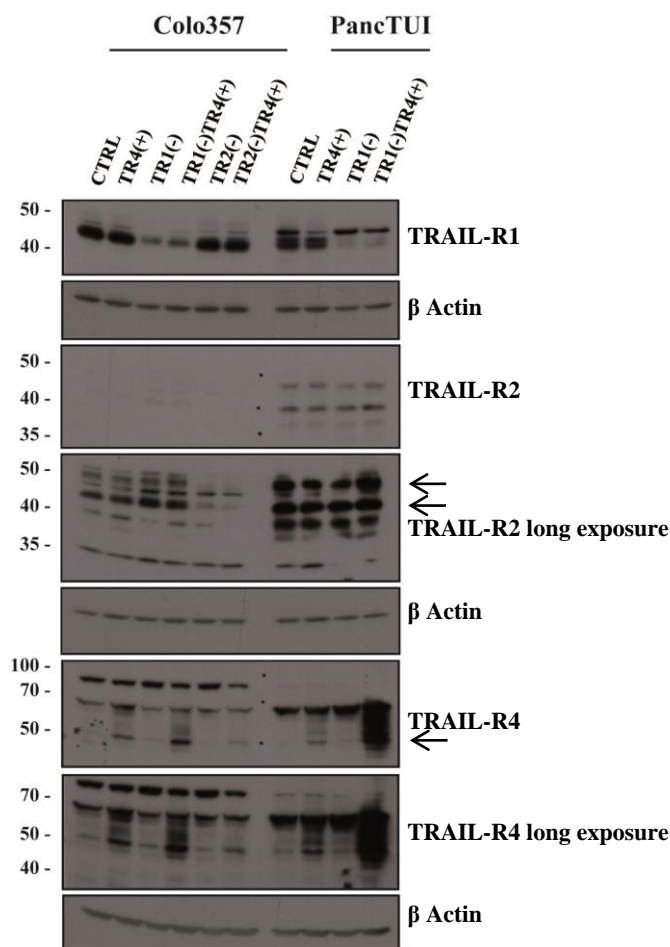


Figure 3.34 Whole protein expression level of TRAIL receptors in both Colo357 and PancTuI cells. The cells with differentially expressed TRAIL receptors were seeded ($\sim 4 \times 10^5$, 6-well format) and incubated for 24 hours. Later, the protein level of TRAIL receptors were analyzed in the whole cell lysate of both Colo357 and PancTuI cell lines via immunoblotting. The protein levels of the TRAIL receptors shows the successful alterations together with the basal level of each receptor in both studied cell lines. The detection of beta actin is shown as loading control. This experiment is a representative of three performed.

7.1. Detection of TRAIL receptors level on the plasma membrane

The cell surface presentation of the TRAIL receptors in PancTuI cell lines was also investigated (Figure 3.35). The levels of the differentially modulated TRAIL receptors could be validated on the plasma membrane of PancTuI cells. Here, the knockdown of

TRAIL-R1 was - 57.15% and - 78.46% in TR1(-) and TR1(-)TR4(+), respectively. A successful TRAIL-R4 up-regulation were also observed in PancTuI cells. It was clear that the knockdown of TRAIL-R1 facilitated TRAIL-R4 up-regulation (~ 400%). However, the direct enforced expression of TRAIL-R4 was successful in the CTRL cell line by about 90% increase in TR4(+). Additionally, both TRAIL-R1 and -R2 were slightly suppressed in TR4(+) cell line. Through the FACS analysis of the PancTuI cells, it was observed that the TRAIL-R4 and -R2 demonstrated readily more detectable levels as was previously seen on the protein level in comparison to Colo357 cells.

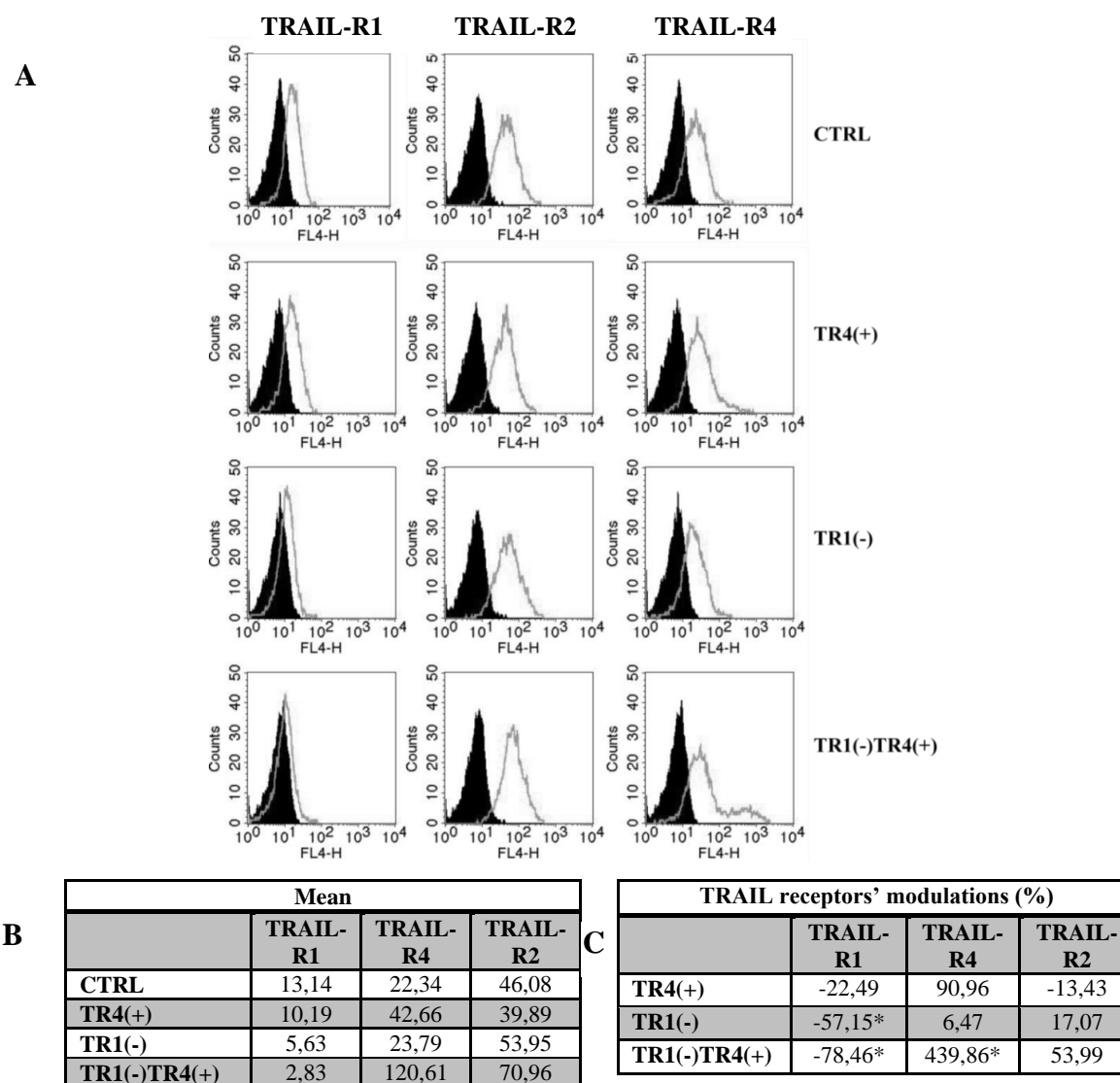


Figure 3.35| Plasma membrane levels of the TRAIL receptors in PancTuI cell lines; PancTuI cells with differentially expressed TRAIL receptors were seeded in T25 flask and incubated for 24 hours. Then a flow cytometric analysis was done. **A**, plasma membrane expression of TRAIL receptors in non-permeabilized PancTuI cell lines. Black area represents the corresponding IgG control and the hollow curve represents the intended TRAIL receptor. Shown is one experiment of three experiments performed. **B**, mean of TRAIL receptor expression from 3 experiments **C**, percentage of expression compared to CTRL. ANOVA was used to determine the significance (*; n=3, *p*-value < 0.05).

7.2. Detection of TRAIL receptors expression on mRNA level

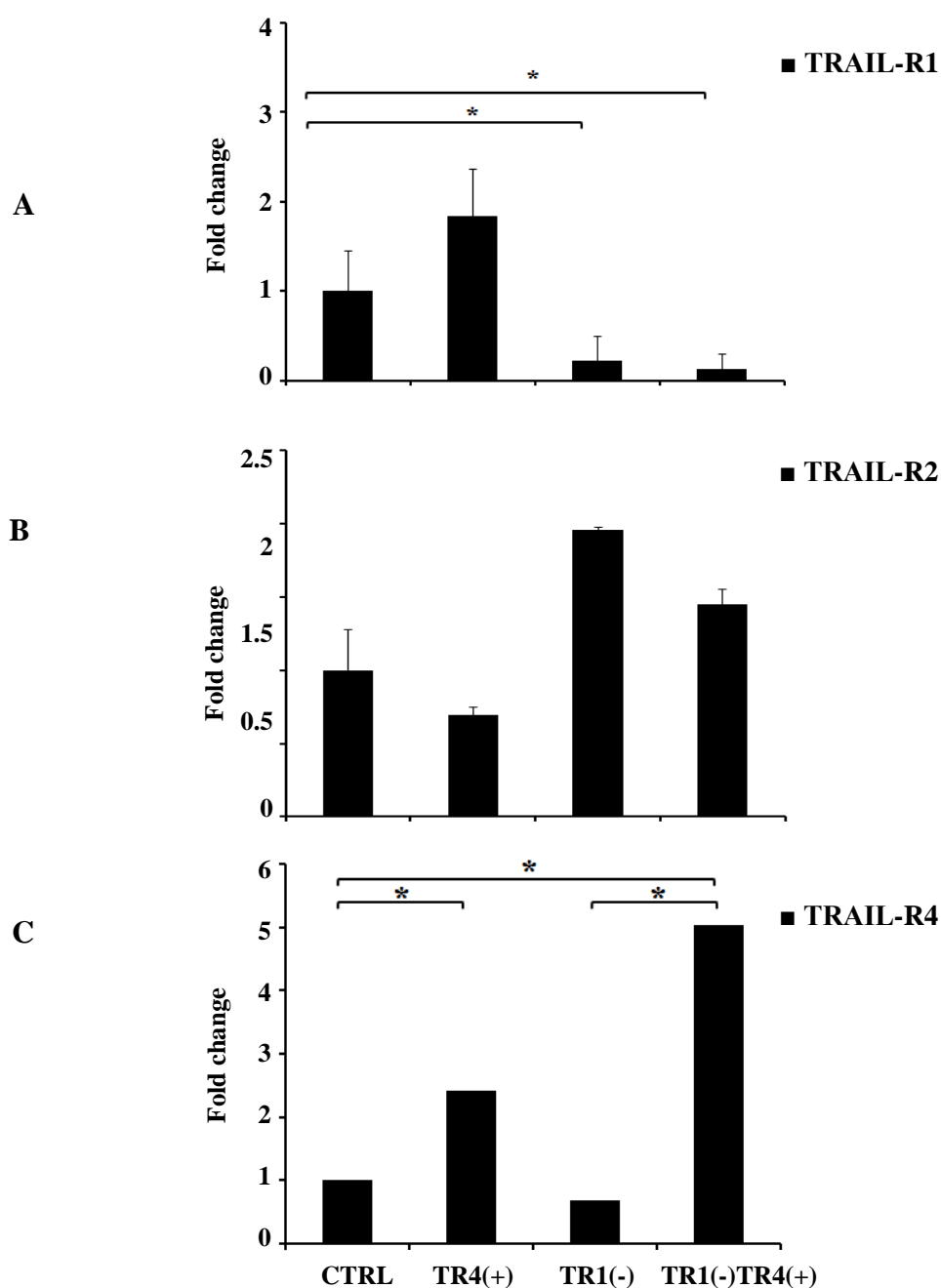


Figure 3.36| RT-PCR analysis of TRAIL receptors on mRNA level, PancTuI cells with differentially expressed TRAIL receptors were seeded (4×10^5 cells, 6-well format) and incubated for 24 hours. Then the mRNA expression level of TRAIL receptors was investigated via RT-PCR. CTRL cells were set as control. The mRNA of the three receptors demonstrated the successful modification of the intended receptors. **A**, fold change of TRAIL-R1, **B**, fold change of TRAIL-R2, **C**, fold change of TRAIL-R4, shown is the mean of three independently performed experiments (biological replicates). ANOVA was used to determine the significance (*, $n=3$, p -value < 0.05).

Consistent with the protein levels, TRAIL-R4 mRNA levels showed a successful up-regulation in PancTuI (Figure 3.36), where TRAIL-R4 demonstrated a significantly higher levels in TR1(-)TR4(+) cell line followed by TR4(+) in comparison to their corresponding controls: TR1(-) and CTRL, respectively. Similarly, the down regulation of

TRAIL-R1 was significantly achieved in PancTuI cell lines as well and thus validating the overall protein expression levels of the established cell lines. Furthermore, the level of TRAIL-R2 was slightly boosted in the concomitant knock-in of TRAIL-R4 and restriction of TRAIL-R1 and also in TR1(-) cells.

7.3. Morphological characteristics of PancTuI cell lines

The morphology of the PancTuI cell lines was also examined and it showed no apparent differences between the different cell lines (Figure 3.37). Generally, PancTuI were smaller in size and more spindle-shaped unlike Colo357. From the colony forming point view, the four cell lines tend to grow in a less compact pattern in comparison to Colo357 cell lines. All PancTuI cell lines could form a full mono-layer if allowed to grow.

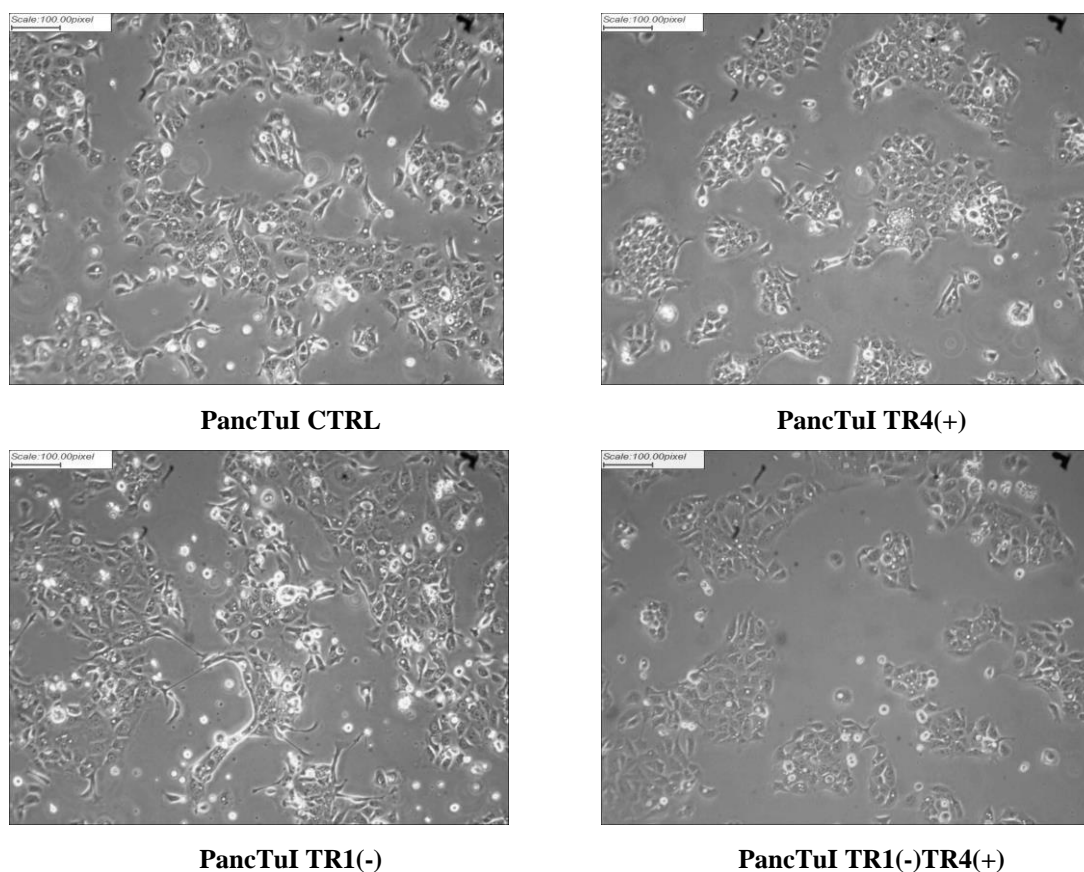


Figure 3.37| Light microscopy-based pictures of the different PancTuI cell lines. PancTuI cells with differentially expressed TRAIL receptors were seeded at 4×10^5 cells per well (6-well format) and were incubated for 24 hours. Light microscopic pictures were taken with 10x magnification lens (scale bar 128 μ m).

7.4. Impact of TRAIL receptor interplay on TRAIL-induced cell death

In order to evaluate the apoptotic and necroptotic response in PancTuI cell lines, the viability of PancTuI cells was also measured after the cells being treated with TRAIL or a

combination of zVAD, HHT and TRAIL for twenty four hours. Again, the viability of the four PancTuI cell lines was evaluated via EZ4U assay (Figure 3.38). From this experiment, the impact of TRAIL-R4 over expression on the cellular response to apoptosis and necroptosis was detected. TRAIL-R4 played a protective role of about 15% on both cell death modalities; yet, this protective effect was either decreased in case of apoptosis or completely lost in necroptosis when TRAIL-R1 was knockdown. Again, TRAIL-R1 knockdown showed a protective role against both apoptosis and necroptosis. Moreover, the sensitizing effect of TRAIL-R4 on TRAIL-induced necroptosis was not observed in PancTuI cells.

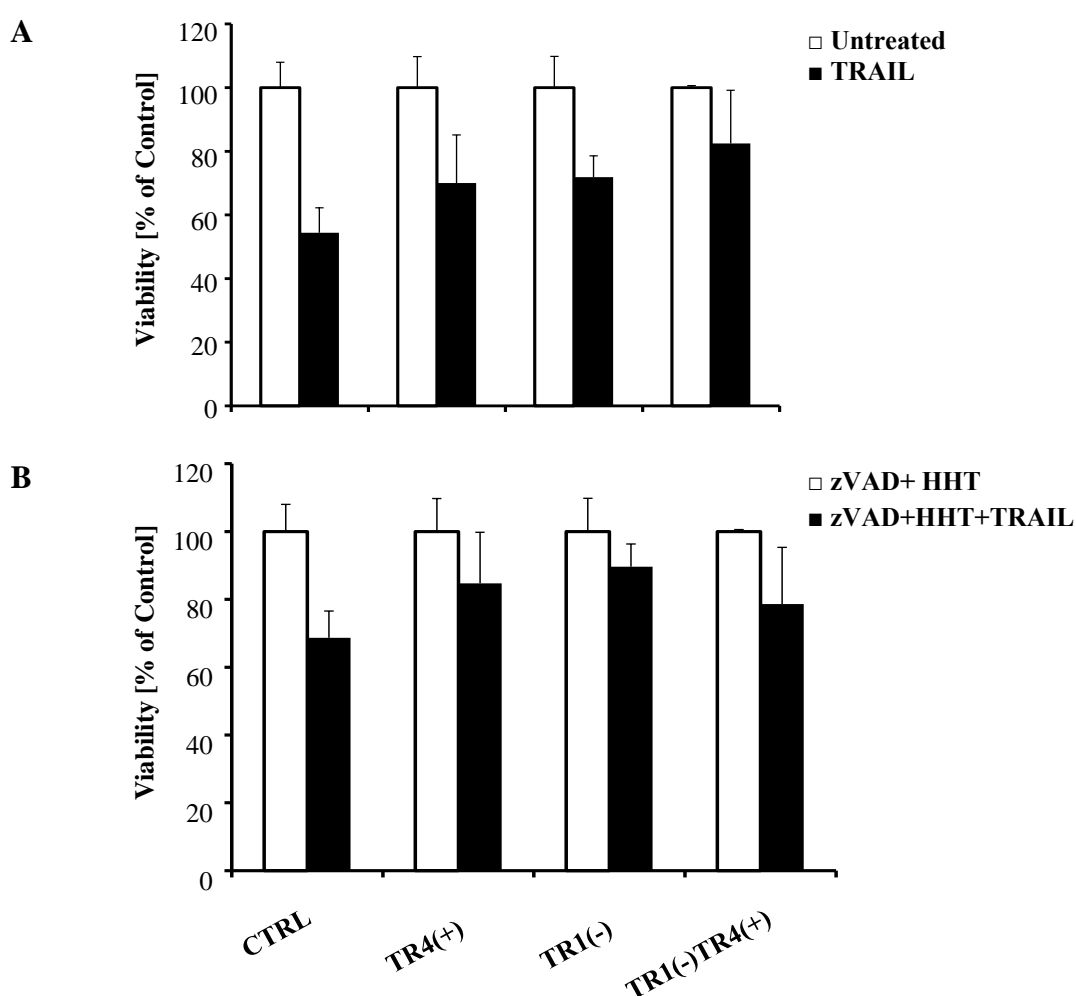


Figure 3.38| Viability of the different cell lines in response to TRAIL-induced cell death. Cellular viability was tested via EZ4U assay. PancTuI cells with differential expression of TRAIL receptors were seeded (1.5×10^4 , 96-well format) and incubated for 24 hours. For apoptosis testing, the cells were either treated with 100ng TRAIL or left untreated. For necroptosis, the cells were pretreated with 0.5mM HHT and 2mM zVAD. One hour later, the cells were either treated with 100ng TRAIL or left untreated. 24 hours later, EZ4U substrate was added and the absorbance was read on Tecan microplate reader ever hour. Shown is the mean of two independent experiments (biological replicates). ANOVA was used to determine the significance (*, $n=2$, p -value < 0.05).

Additionally, some of the apoptotic and necroptotic signaling proteins were analyzed in PancTuI cells by means of Western blotting. Similar to Colo357, the result of the PancTuI Western blot analysis revealed that the up-regulation of TRAIL-R4 levels showed an anti-apoptotic protective effect (Figure 3.39). Meanwhile, this protective tendency was lost upon TRAIL-R1 knockdown. Therefore, it seems that TRAIL-R1 might be playing a role in TRAIL-R4 driven anti-apoptotic effects. Additionally, it was observed that TRAIL-R1 is required for optimal cell death in PancTuI. Both Caspase-3 and -8 were less cleaved in TR1(-) and TR1(-)TR4(+) in comparison to CTRL and TR4(+) cell lines. Therefore, PancTuI CTRL cell line showed the highest TRAIL-induced cell death.

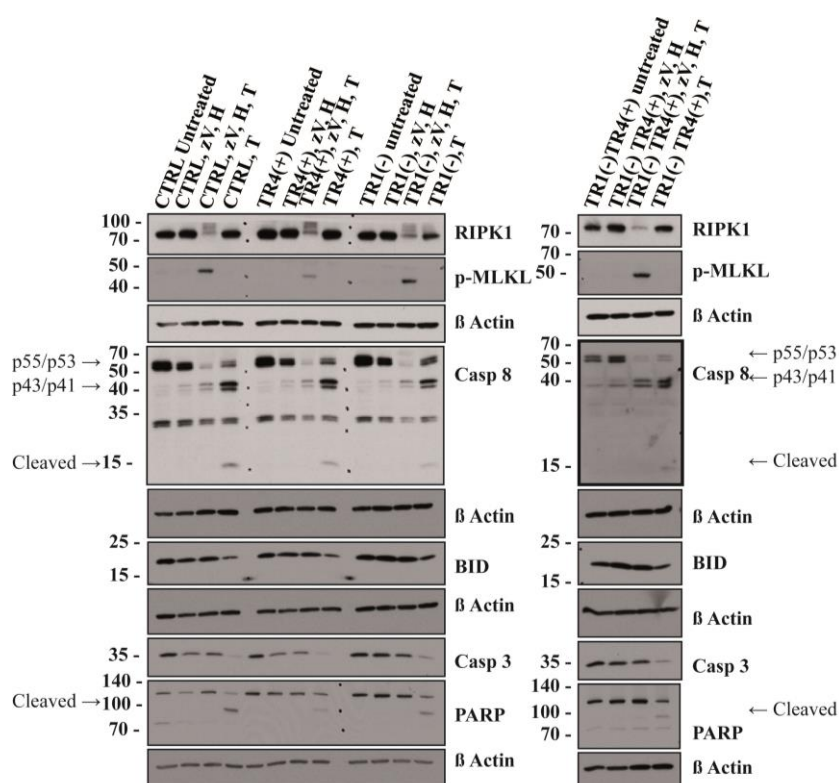


Figure 3.39| Expression levels of proteins involved in the apoptotic and necroptotic pathways. PancTuI cells with differentially expressed TRAIL receptors were seeded (3.5×10^5 cells, 6-well format) and incubated for 24 hours then the cells were either untreated or treated with 100ng TRAIL (T) to induced apoptosis. For necroptosis, cells were either pretreated with 2mM zVAD (Z) and 0.5mM HHT (H), or treated with zVAD+HHT+TRAIL to induce TRAIL-induced necroptosis. The levels of RIPK1, p-MLKL (for necroptosis) and casp. 8, BID, casp 3, PARP (for apoptosis) were investigated in whole cell lysates by means of Western blotting. The Western blots demonstrate the alterations in the proteins involved in both the apoptotic and necroptotic signaling pathways. The detection of beta actin is shown as loading control. Shown is one experiment out of two performed that show a similar trend.

PancTuI differed distinctly from Colo357 in the terms of necroptosis. First of all, one can see a clear separation of the two death modes via p-MLKL and RIPK1 on one hand and BID, PARP and the caspases on the other hand in PancTuI Western blots (Figure

3.39). Additionally, it was noted that PancTuI showed a more readily detectable levels of p-MLKL and RIPK1 than Colo357. However, the distinguished roles of the individual TRAIL receptor members were not as clear in PancTuI necroptosis probes as it was in Colo357 (Figure 3.40). Here, TRAIL-R4 protects slightly against TRAIL-induced apoptosis as seen from the decrease PARP cleavage, as well as necroptosis as seen from the decreased p-MLKL level. Yet, TRAIL-R4 protection was lost with TRAIL-R1 down regulation. Evidently, TRAIL-R4 protective effect worked in collaboration with TRAIL-R1 in both cell death modalities in PancTuI cells. Altogether, the knockdown of TRAIL-R1 together with TRAIL-R4 up-regulation in PancTuI demonstrated similar effects on both TRAIL-induced apoptosis and necroptosis.

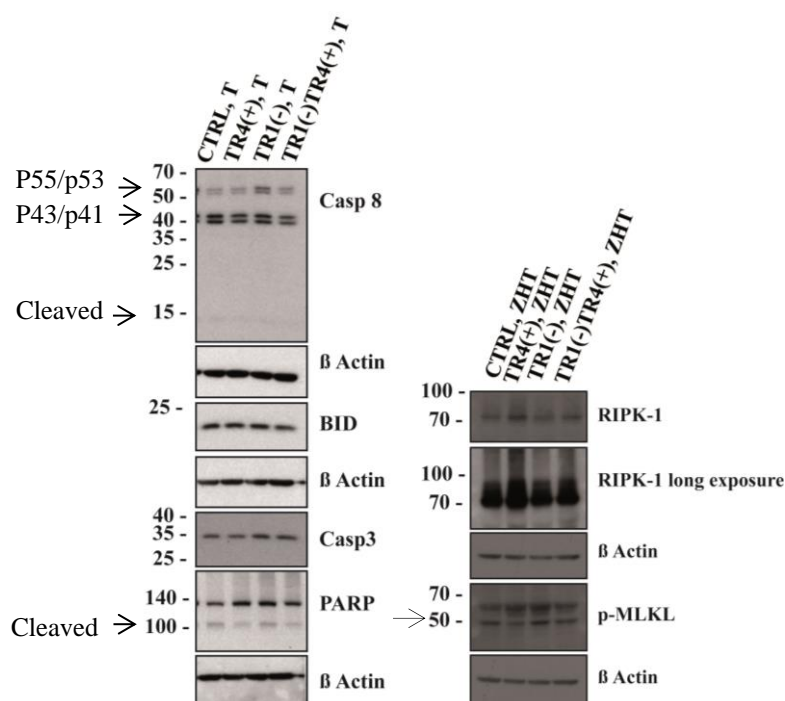


Figure 3.40| Expression levels of proteins involved in cell death. PancTuI cells with differentially expressed TRAIL receptors were seeded (3.5×10^5 cells, 6-well format) and incubated for 24 hours. Then treated with either **A**, treated 100ng TRAIL (T), to detect the protein levels of caspase 8, tBID, caspase-3 and PARP in (T) treated samples only in whole cell lysate via Western blotting or **B**, treated with 2mM zVAD(Z)+ 0.5mM HHT(H)+ 100ng TRAIL(T) to detect the protein levels of RIPK-1 and p-MLKL in Z+H+T treated probes in whole cell lysate via Western blot. These experiments were performed to observe the fluctuations of the studied proteins in comparison to each other. The detection of beta actin is shown as loading control. Shown is one experiment out of two performed that show a similar trend.

7.5. Impact of TRAIL receptor interplay on inflammatory status

Regarding the inflammatory cytokines, the expression levels of a panel of 13 different inflammatory cytokines were investigated by means of ELISA technology. Out of this panel only IL-8 was significantly altered in PancTuI cells (Table, 3.13 and Figure

3.41). Like Colo357, TR1(-) cell line showed a reduction in IL-8 level. Unexpectedly, the level of IL-8 was significantly boosted with the up-regulation of TRAIL-R4 in TRAIL-R1 knockdown cell lines. Overall PancTuI exhibited a relatively minimal changes regarding the inflammatory cytokines in comparison to Colo357. Additionally, the role of TRAIL-R4 in PancTuI cell lines demonstrated an opposite behavior, regarding inflammation, to Colo357 cell lines.

Table 3.14| Expression levels of inflammatory cytokines

Sample ID	IL-1b	IFN-a	IFN-g	TNF-a	MCP-1	IL-6	IL-8	IL-10	IL-12p70	IL-17A	IL-18	IL-23	IL-33
	pg/ml												
CTRL	<1.44	<0.86	<2.93	<1.42	<2.18	2,29	128,59	<1.03	0,66	<2.59	<0.92	<2.62	<5.73
TR4(+)	<1.44	<0.86	<2.93	<1.42	<2.18	2,29	198,79	<1.03	0,66	<2.59	<0.92	<2.62	<5.73
TR1(-)	<1.44	<0.86	<2.93	<1.42	<2.18	4,91	92,67	<1.03	0,66	<2.59	<0.92	<2.62	<5.73
TR1(-) TR4(+)	<1.44	<0.86	<2.93	<1.42	<2.18	15,38	410,89	<1.03	0,66	<2.59	<0.92	<2.62	<5.73

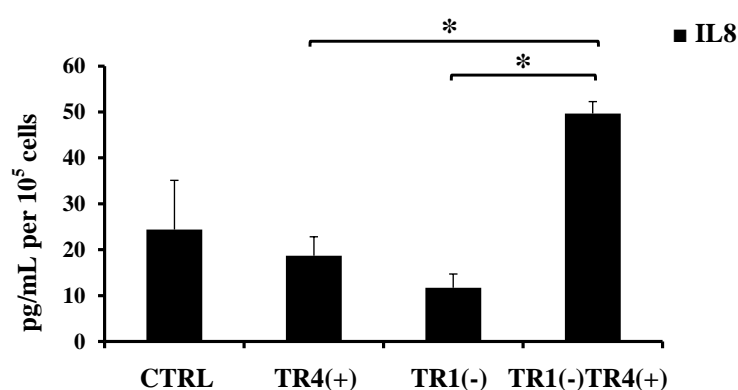


Figure 3.41| Expression level of IL8. PancTuI cells with differentially expressed TRAIL receptors were seeded (3.5×10^5 in 6-well format) and incubated for 48 hours. Then the protein level of IL8 was detected in the cell culture supernatant via ELISA. In parallel the cells in the wells were counted and the values of IL8 cytokine were calculated per 10^5 cells. ANOVA was used to determine the significance (*, $n=3$, p -value < 0.05). Shown is the mean of three experiments (biological replicates) performed.

7.6. *In vitro* functional analyses of the different PancTuI cell lines

7.6.1. Impact of TRAIL receptor interplay on proliferation

Using cell counting technique, the proliferation capacity of the PancTuI cells was investigated (Figure 3.42). Here, PancTuI proliferation seemed rather different from the Colo357 profile. In PancTuI, the effect of TRAIL-R4 up-regulation was significantly slowing the cellular growth in comparison to the CTRL cell line. Furthermore, the differences between the various cells were not significant except for the decelerated potential exerted by TRAIL-R4 up-regulation. Moreover, TR1(-)TR4(+) cell line showed

no effect on PancTuI proliferation when compared with TR1(-) cells. To recapitulate, TRAIL-R4 had a reciprocal effect of growth limiting in PancTuI and growth enhancement in Colo357 cell lines.

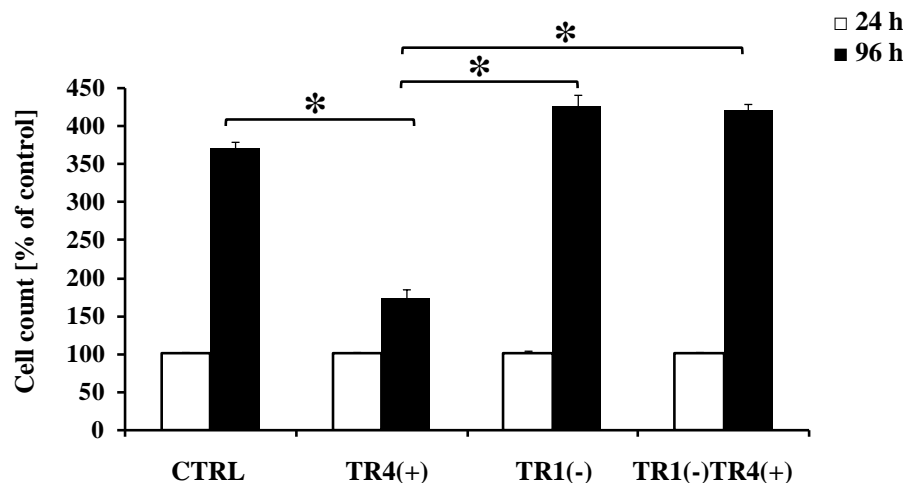


Figure 3.42| Impact of TRAIL receptors interplay on proliferation. PancTuI cells with differentially expressed TRAIL receptors were seeded (1.5×10^5 cells, 6-well format) and incubated. Later, the cells were counted using Cellometer[®] at two time points; 24 and 96 hours. The first reading was set as 100% (seen in white) and the 96 hours reading (seen black) was calculated accordingly. Shown is the mean of two independent experiments (biological replicates). ANOVA was used to determine the significance (*, $n=3$, p -value < 0.05).

7.6.1. Impact of TRAIL receptor interplay on migration

The discrepancy seen between Colo357 and PancTuI was also observed on the migration level (Figure 3.43). From the first glance, it can be observed that the differences in migration rate between the four studied PancTuI cells were rather smaller when compared to Colo357 cells. Also, it is obvious that generally PancTuI (all gaps closed within 36 hours) cell lines are much faster than Colo357 (gaps closed over 96 hours). In PancTuI, we have observed that TR1(-)TR4(+) was the fastest to close the gap, the followed by TR1(-), and at last were CTRL then TR4(+) cell line. In other words, the over expression of TRAIL-R4 decelerated the movement of PancTuI cells and TRAIL-R1 knockdown abolished this effect.

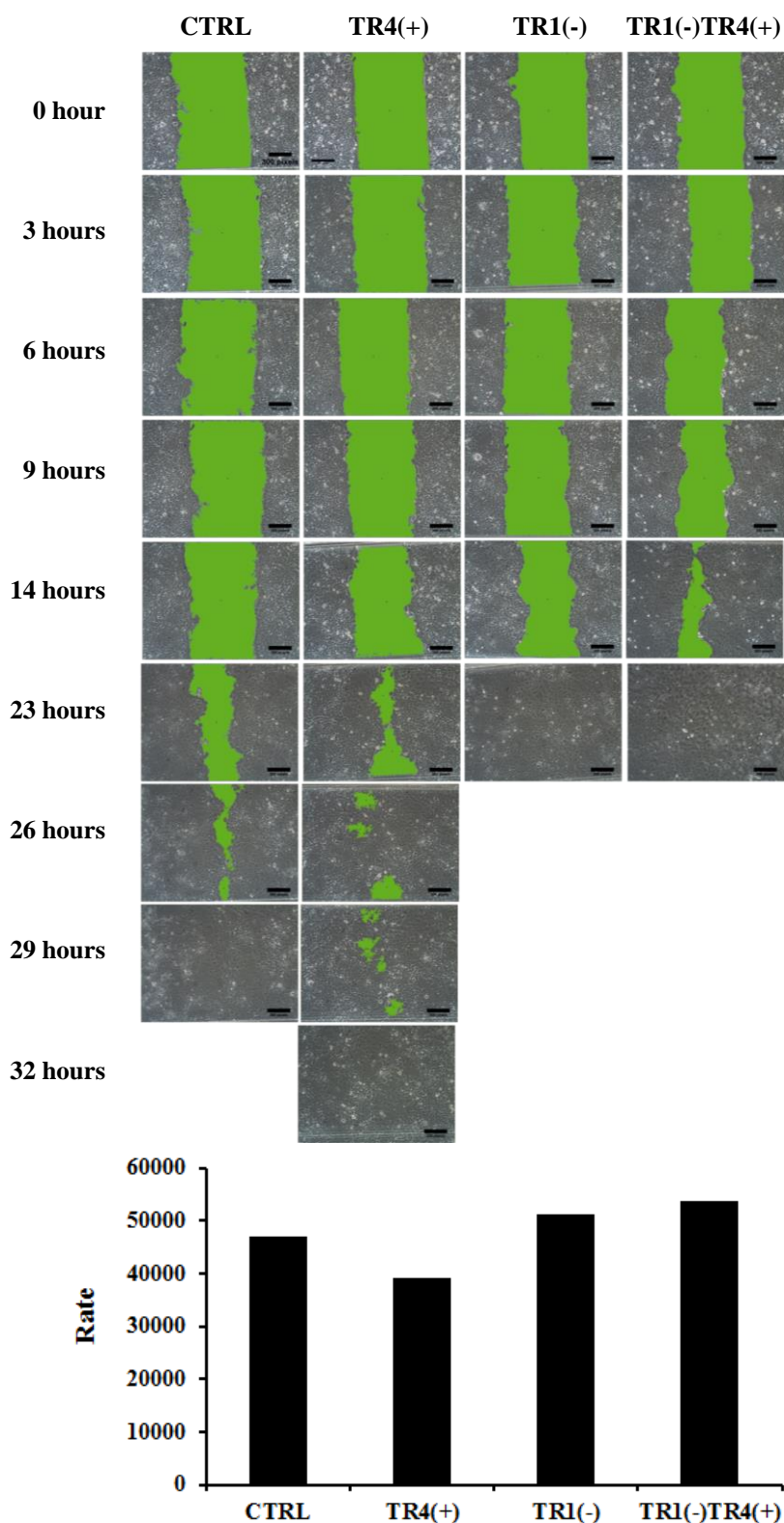


Figure 3.43| Impact of TRAIL receptors interplay on migration. PancTu1 cells with differentially expressed TRAIL receptors were seeded (8×10^4 cells) on both sides of the Ibidi® culture inserts. 24 hours later, the inserts were removed leaving a $\sim 500 \mu\text{m}$ gap. The cells were treated with Mitomycin C for 3 hours to inhibit proliferation. The cells were allowed to close the gap and pictures were taken at different time points to follow up the speed. **A**, Sequential pictures taken during the scratch assay at different time points. **B**, graph showing the rate by which each cell line closed the cell free area (dividing difference in cell free area by the difference of time). Shown is the mean of two independent experiments (biological replicates) performed (scale bar $166 \mu\text{m}$).

IV. DISCUSSION

Aiming towards the understanding of the interwoven interactions between the different members of the TRAIL receptors, a complex TRAIL receptor system was established. Particularly, this study was intended to thoroughly comprehend TRAIL-R4 role in this system and test whether or not, it is just a decoy receptor or will perform differently in different contexts. As known from literature, the TRAIL receptor proteins are mainly expressed by malignant cells. On one hand, it has been reported that TRAIL-R1 and -R2 activation via TRAIL binding initiate the apoptosis cascade. Thus, they provide a good possibility to drive cancer cells to their own demise (Dimberg et al., 2013; Micheau et al., 2013; Wiezorek et al., 2010). On the other hand, the presence of the decoy receptors; TRAIL-R3 and -R4 hinders this process (Bisgin et al., 2010; LeBlanc and Ashkenazi, 2003; Riccioni et al., 2005; Sanlioglu et al., 2005). In most of the currently available studies, the levels of the TRAIL receptors are screened in different cancer entities to detect their status-quo. However, there are no studies that investigated the role of multiple manipulations of the TRAIL receptors on the different cancer forms yet.

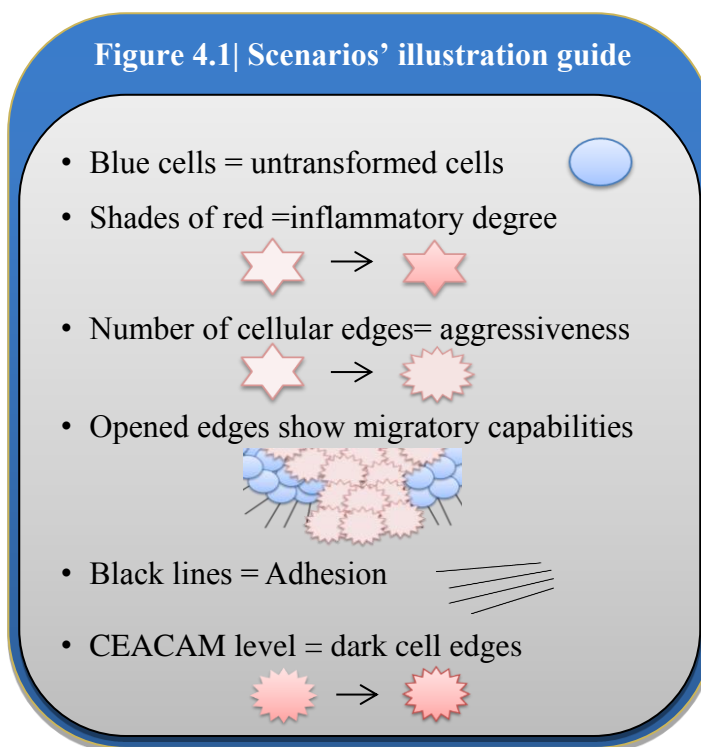
In 2009, Sanlioglu and his team stained TRAIL ligand and the four TRAIL receptors immunohistochemically in 34 PDAC patients' tissues together with 31 tissues from patients without PDAC as control subjects. In addition, they used immunofluorescence to stain Annexin V as a marker for apoptosis. The tumors ranged from T1 to T4 on the TNM scale, from well to poorly differentiated and with/without nodal metastasis, yet all patients were collectively analyzed as one group. They have found that PDAC patients' tissues demonstrated high levels of TRAIL-R1 and -R4 receptors in comparison to non-malignant tissues (Sanlioglu et al., 2009). This observation could represent our proposed group TR2(-)TR4(+) which could not only denote the presence of PDAC but also point out an aggressive form of it as was demonstrated in the current study.

In 2013, another group investigated the four TRAIL receptors in 84 PDAC patients. They performed a microarray analysis and then stained the patients' tissues. The group concluded that the surface staining of TRAIL-R1 and -R2 decreased in PDAC in comparison to the surrounding tumor-free zones. Moreover, they correlated the loss of the surface expression of TRAIL-R2 to poorer outcome in patients with nodal spread. However, they have found no prognostic relevance for TRAIL-R3 and -R4 (Gallmeier et

al., 2013). Likewise, other studies mainly stained the TRAIL receptors and correlated their surface expression with other diseases i.e. hepatitis C, inflammatory bowel diseases, varicocele-induced testicular dysfunction and meningioma (Brost et al., 2014, 2010; Celik et al., 2013; Koschny et al., 2015). Also, TRAIL receptors have been implicated in bad prognosis in some malignancies, for instance, the decrease in the plasma membrane levels of TRAIL-R1 and -R2 in hepatocellular carcinoma cells was correlated with decreased survival. In the same study, it was also found that TRAIL-R2 was lost in the hepatocellular carcinoma cells in comparison to the peri-tumoral tissues (Kriegl et al., 2010). Additionally, nuclear localization of TRAIL-R2 was correlated with bad prognosis (Haselmann et al., 2014). However investigating the actual interplay between the TRAIL-R1, -R2 and -R4 was not previously addressed. Therefore, the current research focused on this complex interdependence of the TRAIL receptors in order to see the wide array of actions induced by these receptors.

TRAIL receptors interplay models

This study aimed to provide the impact of the different TRAIL receptors' modulation on PDAC cell behavior. However, we faced an obstacle that the reaction of the two studied cell lines did not coincide. Nevertheless, different scenarios can be foreseen that can help in anticipating the tumor aggressiveness and possible prognosis to benefit the patients (see Figure 4.1 for a simple guide for the scenarios' illustrations).



At the first glance, PancTuI appears to have a more aggressive nature. That was proven rather correct in terms of migration speed, where all PancTuI cell lines closed the gap in maximally 36 hours, unlike Colo357 cells that closed the gap in 96 hours (Figure 4.2). However, the overall picture revealed that CTRL cells in both cell lines have rather the same proliferative capacity (96 hours counts were ~350 % of the 24 hours counts).

Despite IL8 cytokine expression levels implied that PancTuI have a reversed inflammatory status as Colo357, the situation is much more complicated than the mere IL8 level analysis. Regarding PancTuI, the cells showed no detectable levels of any other inflammatory cytokine, again unlike Colo357 where the cells – with the least levels of the inflammatory cytokines – still had detectable levels of IL6 and IL8. Hence, the overall inflammatory status in PancTuI is actually very low when compared to Colo357. From literature, PancTuI is a known TRAIL resistant cell line (Trauzold et al., 2003). In other words, PancTuI cells – that originally express higher basic levels of TRAIL-R2 and TRAIL-R4 – are resistant to apoptosis and exhibit a low inflammatory state. These high basic levels of TRAIL-R2 and -R4 might explain the apparently opposing reaction regarding the IL8 cytokine level in both Colo357 and PancTuI. One should also bear in consideration that the highest level of IL8 detected in PancTuI cell lines corresponds to the level detected in Colo357 CTRL cell line. However, in Colo357 cells it was clear that TRAIL-R1 was responsible for the high inflammatory cytokines status and that was reversed by TRAIL-R1 inhibition.

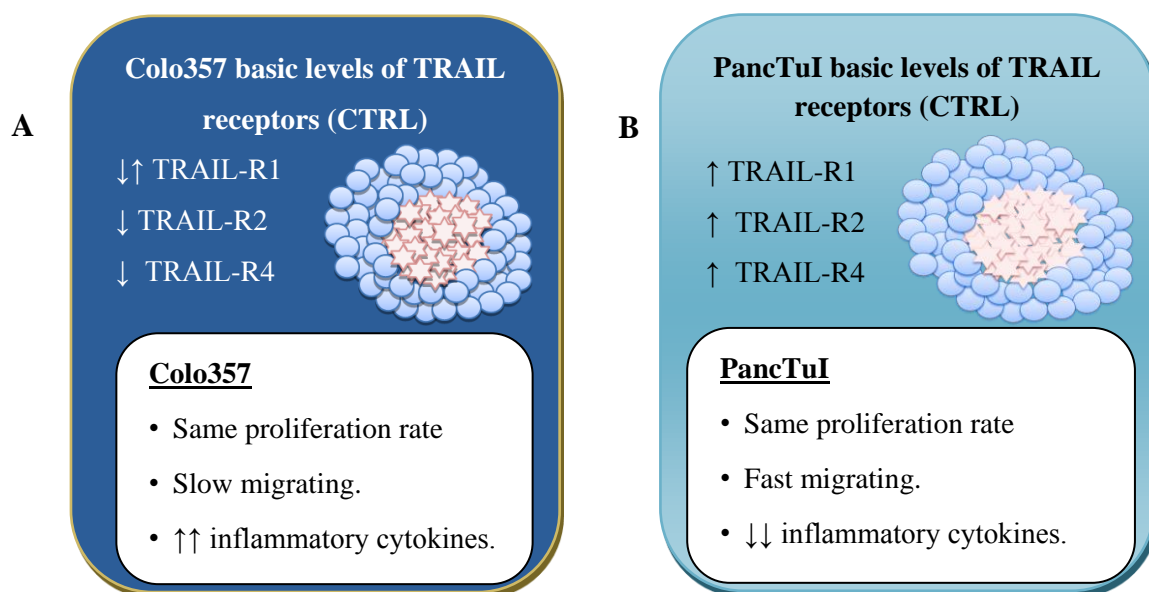


Figure 4.2| Basic levels of TRAIL receptors and functional properties of the studied PDAC cells. A comparative state of TRAIL receptors in the CTRL cell lines of both Colo357 (A) and PancTuI (B). Additionally, a summary of the functional properties of these cell lines are featured in the illustration and in the white card.

Colo357 cells originally expressed low amount of TRAIL-R2 and relatively low levels of TRAIL-R4. Regarding TRAIL-R1 expression, Colo357 expressed a comparable constitutive level as PancTuI cells. These receptors' expression pattern correlates with

Colo357 high sensitivity to TRAIL-induced apoptosis. Moreover, the response of Colo357 cell lines to necroptosis was quite complex. From the above mentioned reasons, different scenarios can be deduced from the overall analyses.

First scenario TR1(-)TR4(+)

Three of the proposed scenarios involved a high level of TRAIL-R4 in Colo357, these three settings showed that this receptor has multiple faces. In this first scenario, the TRAIL receptors expression pattern was as follows: high TRAIL-R4, low TRAIL-R1 and non-manipulated, constitutive levels of TRAIL-R2 [TR1(-)TR4(+)] (Figure 4.3). Plainly, here the scenario entails the interaction between TRAIL-R2 and TRAIL-R4 with minimal interference from TRAIL-R1. This cell line was resistant to TRAIL-induced apoptosis in Colo357 but not in PancTuI cells. In Colo357, this cell line was the least aggressive cell line with restricted proliferative, migratory and inflammatory capabilities and it showed a significant sensitivity to TRAIL-induced necroptosis. To emphasize, the bioinformatics *in silico* analyses also demonstrated that this cell line showed also suppressed biological processes. In addition, the stemness markers identified via the Nanostring analysis were also mainly unchanged or down regulated, in comparison to the CTRL cell line, except for 3 genes that were apparently elevated. However, these three genes are actually down regulated in comparison to the corresponding control [TR1(-) cells]. These *in vitro* results can be supported by the subcutaneous *in vivo* tissue model analyses. Colo357 TR1(-)TR4(+) cells produced no metastasis and produced the smallest primary tumor size *in vivo* as well. Furthermore, Colo357 TR1(-)TR4(+) cells were significantly more resistant to TRAIL-induced apoptosis than TR4(+), yet, had an increased potential for TRAIL-induced necroptosis. In this scenario, PancTuI demonstrated a limited increase in proliferative and migratory activities and one inflammatory cytokine (out of 13) was significantly elevated.

In our patient cohort, this group was encountered in 14.1% of the studied cases. In this group, TRAIL-R1 was present at a low level in both the cytoplasm and nuclei of corresponding tissues of the patient cohort. TRAIL-R2 was moderate to highly expressed in the cytoplasm in 100% of cases and minimally expressed in the nuclei (60%). However, TRAIL-R4 was highly expressed in the cytoplasm (100% of cases) and was detected in 100% of the cases in the nucleus. Here, we have both the combined action of TRAIL-R2 and -R4 in mainly in the cytoplasm and to a lesser extent in the nucleus. Bearing in mind the isoform distribution of TRAIL-R4, one can assume that in the cytoplasm, this effect

could be driven by TRAIL-R2 and TRAIL-R4 α . Yet, in the nucleus, the function might be performed via TRAIL-R2 together with either TRAIL-R4 α or β . The distinction between the nuclear and cytoplasmic functions of these two receptors might clarify the significant deterioration of survival between the patients from this scenario and TR1(-) patients (see later), despite the promising *in vitro* results. Furthermore, this cell line showed the lowest levels of CEACAM5 and CEACAM6 in comparison to all cell lines in Colo357, denoting the less aggressive nature of these cells. Moreover, the deterioration in the patients' survival could be explained by the fact that PancTuI TR1(-)TR4(+) cells showed the highest IL8 levels among all other PancTuI cell lines, that might be driven by the nuclear role of TRAIL-R2 and -R4. Thus, the level of IL8 should be estimated in these patients prior to assessing the whole patient's prognosis. Furthermore, the patient cohort studied was rather small and the metastatic tissues were not available for staining. Additionally, PancTuI is grade 3 primary cell line isolated from the pancreas of a PDAC patient, while Colo357 is a grade 2 metastatic cell line derived from lymph node metastasis. Therefore, the primary tumors from the patient cohort might reflect the effect of primary tumor tissues represented by PancTuI and not Colo357. Hence, the correlation of the patient cohort and Colo357 might be hampered, because both cell lines were originally extracted from different sites and tumor developmental stages.

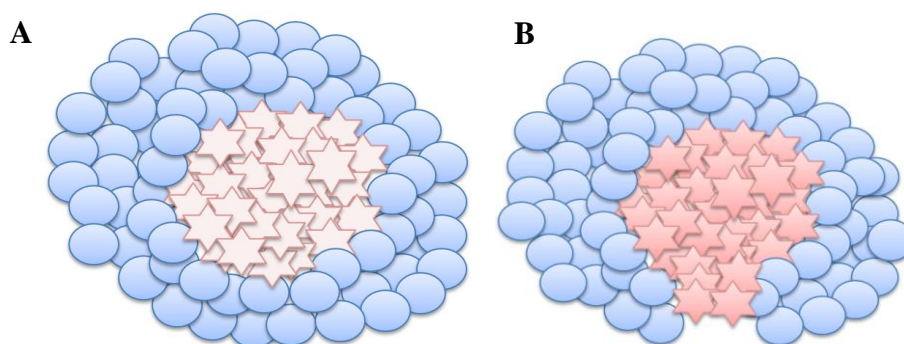


Figure 4.3| Illustration of the TR1(-)TR4(+) cell line. **A**, Colo357, showing a rather low inflammatory status with suppressed aggressiveness and **B**, PancTuI, showing a relatively higher inflammatory and migratory status with relatively moderate aggressiveness.

Moreover, this TRAIL receptor combination in TR1(-)TR4(+) cells was capable of proliferating on both commonly encountered ECM (Fibronectin) as well as on un-physiologic malignancy-related tenascin-c. Theoretically, this cell line might represent an intermediary step that is needed by the tumor to maintain its existence in new environments –hence the protective function against TRAIL-induced apoptosis– rather

than heightening the tumor progression. One can also deduce that this cell line might represent a slightly senescent form of PDAC, and that the cells undergone this slow functionality to overcome the surrounding physiologically unfavorable environment. On top of that, cells with such TRAIL-receptor constellation provide the tumor with an escape mechanism, because many of the currently available cytotoxic drugs aim to kill highly active cells only. However, further investigations are needed to prove this hypothesis. Moreover, this TRAIL receptor alterations demonstrated a significant decrease in cell viability under TRAIL-induced necroptosis. Accordingly, this model will correlate with a patient profile that would benefit the most from TRAIL-induced necroptosis.

Second scenario TR4(+)

The second setting is TRAIL-R4 up-regulation with non-modified TRAIL-R1 or -R2 levels [TR4(+) cells]. As expected, this model confirmed the well-known TRAIL-R4 protection against TRAIL-induced apoptosis. Otherwise, the two cell lines showed almost completely different behaviors. On one hand, Colo357 showed not only an increased proliferative power as was previously demonstrated in cervical adenocarcinoma (Lalaoui et al., 2011) but also migratory and inflammatory status (Figure 4.4). Besides, most of the stemness markers were unchanged. However, the expression of two WNT signaling pathway members were highly dysregulated, WNT2B (7.84 folds) and WNT3A (-14.8 folds). Despite both genes are members of the WNT signaling pathway, WNT2B was rarely correlated with carcinogenesis (Katoh, 2001). However, WNT3A has been repetitively associated with carcinogenesis and EMT (Bao et al., 2012; He et al., 2015; Qi et al., 2015, 2014). Therefore, the fourteen fold down-regulation of WNT3A would denote a suppressed WNT signaling, and a decrease in malignancy and stemness potential in these cells. Regarding the *in vivo* experimentation, the tumor volumes were the largest between all the cell lines in the subcutaneous inoculation which goes in line with the *in vitro* functional analyses.

On the other hand, this cell line in PancTuI was the least aggressive one due to the inhibition in proliferation and speed of migration together with an even more suppressed inflammatory status. The modification of the TRAIL-receptor expression in these cells produced two distinctly different phenotypes in the two studied cell lines. This might give a hint that the TRAIL receptors' alterations could produce radically different cell phenotypes according to the various cancer stages. In other words, boosting TRAIL-R4

expression led to a minimally aggressive phenotype in primary tumor cells (PancTuI) yet to one of the most aggressive ones in the metastatic Colo357 cell line. Moreover, our results are supported by the facts that PancTuI is known to be resistant to TRAIL-induced apoptosis (Trauzold et al., 2001). Formerly, it was also found that cells resistant to TRAIL are prone to TRAIL-induced proliferation instead of apoptosis in a TRAIL resistant derivative of Jurkat cells (Ehrhardt et al., 2003).

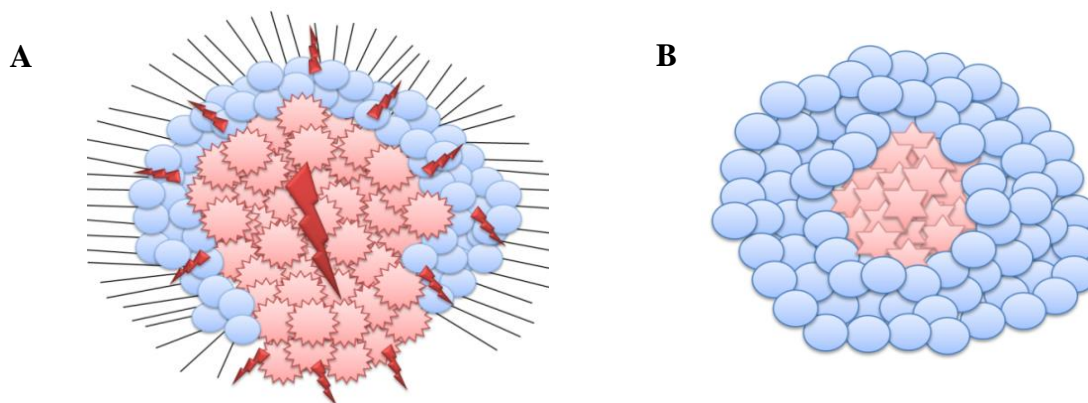



Figure 4.4| Illustration of the TR4(+) cell line. **A**, Colo357 and **B**, PancTuI. The shades of red show the inflammatory degree and this sign  denotes a high inflammatory status. Also, the dark edges of the red/cancer cells represent the high level of CEACAM5 and CEACAM6 and the black strikes represent the adhesive strength of each cell line.

Colo357 TR4(+) cells expressed high levels of CEACAM5 and CEACAM6. CEACAM5 and CEACAM6 were previously described as tumor markers (Arabzadeh et al., 2013; Gebauer et al., 2014; Gold and Freedman, 1965; Schölzel et al., 2000). CEACAMs are cell-cell adhesion molecules that can manipulate a wide variety of pathways in untransformed and malignant cells. Normally, CEACAM5 is known to bind to itself via its N-terminal IgV-like domain or bind to other CEACAM molecules (CEACAM1 and CEACAM6) and thus binding cells to each other and helping in maintaining normal architecture and aiding in cellular adhesion and migration. Moreover, over expression of CEACAM5 and CEACAM6 were found to inhibit anoikis and causing disruption in the structure of the normal tissues that would in turn contribute to the malignant transformation process (Ordoñez et al., 2000). Furthermore, CEACAM5 and CEACAM6 over expression was found to regulate the integrin signaling via promoting the binding of integrin $\alpha 5 \beta 1$ to fibronectin (Duxbury et al., 2004; Hong et al., 2015; Ordonez et al., 2007; Singer et al., 2010). Also, the high levels of CEACAM5 were correlated with nodal metastasis and over expression of CEACAM6 was correlated with distant metastasis

in PDAC patients (Gebauer et al., 2014). Therefore, this obvious boosting of the CEACAM5 and CEACAM6 levels in these cells is a clear sign of malignant transformation and denotes the definite modulation of cellular aggressiveness, adhesion and metastasis.

Finally, Colo357 TR4(+) cells showed an enhanced expression of integrin $\beta 1$ and $\beta 6$ which have been formerly correlated with tumor aggressiveness (Keller and Brown, 2004; Kren et al., 2007; McCabe et al., 2007; Shibue and Weinberg, 2009). The differences in stemness behavior, CEACAM5/CEACAM6 and integrins would explain the discrepancies between Colo357 and PancTuI in this particular cell line. Also, this would explain the rather low survival rate seen in the small patient cohort investigated, where these primary tumors (representing PancTuI cells' behavior) might be less aggressive however, these patients' might have suffered from aggressive metastasis (representing Colo357 cells' behavior). In our cohort, there was a concomitant up-regulation of TRAIL-R2 with the high TRAIL-R4 expression levels in the cytoplasm (100% of the cases) and high simultaneous expression levels in the nucleus (25%), denoting that most probably this is a combined effect of TRAIL-R2 and -R4 in both the cytoplasm and to a lesser extent in the nucleus. Thus, hypothetically, this patient profile might represent a minimally active primary tumor with highly aggressive metastasis. Thus, the patient's prognosis will vary according to the TRAIL receptor modulation in both the primary tumor and metastatic tumor tissues.

Third scenario TR1(-)

Another setup was the mere inhibition of TRAIL-R1 level with non-modulated constitutive TRAIL-R2 or -R4 levels (Figure 4.5). This particular TRAIL receptors' constellation was rather interesting because it characterized cells with a relatively aggressive phenotype in terms of high proliferation (in line with the *in vivo* data) and migration speed (principally Colo357) yet these cells demonstrated a rather low inflammatory status, unlike all the other cell lines where aggressiveness seemed to be directly proportional to the inflammatory behavior. However, both cell lines showed the lowest inflammatory status together with a predicted negative regulation of signal transduction and developmental processes. Obviously, TRAIL-R1 could be responsible for the activation of the inflammatory pathway in PDAC as was previously reported (Lemke et al., 2010). Moreover, this particular TRAIL receptor modification status showed the

highest stemness characteristics, TR1(-) cell line expressed both CDH2 and WNT2B in very high levels. Also from the *in silico* analyses, these data might suggest that PDAC patients with such TRAIL receptor constellation might suffer from an imbalanced blood sugar level due to the altered insulin like growth factor signaling. Additionally, the CEACAM5 and CEACAM6 levels were rather low.

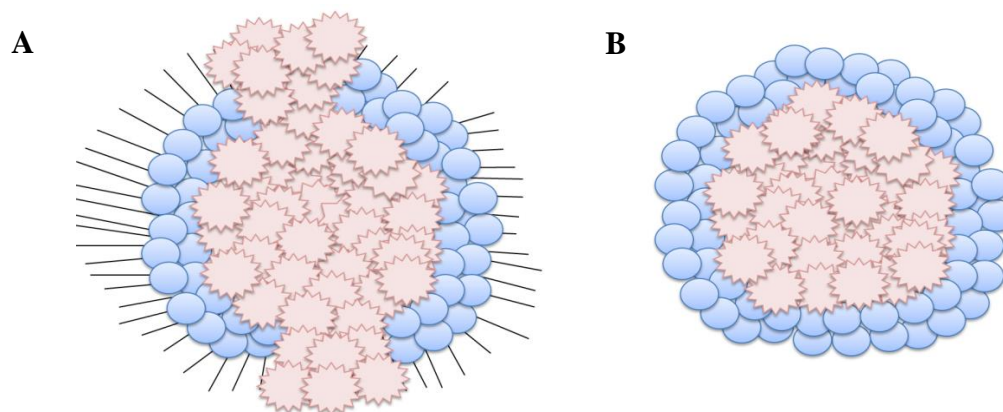


Figure 4.5| Illustration of the TR1(-) cell line. A, Colo357 and B, PancTuI. The shades of red show the inflammatory degree. Also, the number of edges/ corners of the cells are equivalent of how aggressive the cell lines are. Also, the dark edges of the red/cancer cells represent the high level of CEACAM5 and CEACAM6 in Colo357 cells.

In the patient cohort, patients with such TRAIL receptor expression pattern were moderately represented in the whole cohort and were diagnosed with a rather low nodal and distal dissemination and had a high chance of total primary tumor removal. These patients had low TRAIL-R1 level in the cytoplasm together with no detectable levels of both TRAIL-R1, -R2 or -R4 in the nucleus. In the cytoplasm, TRAIL-R4 was low to moderately expressed together with moderate to high TRAIL-R2 protein expression. Therefore, this scenario is mostly orchestrated by the cytoplasmic role of TRAIL-R2 and -R4. Evidently, this scenario refers to a patient with rather aggressive primary tumor with limited metastasis. Yet, this scenario demonstrated a high resistance to TRAIL-induced apoptosis, as was also previously reported that using a blocking antibody against TRAIL-R1 increased cell viability (Lemke et al., 2010).

Fourth/fifth scenario TR2(-) and TR2(-)TR4(+)

Through PancTuI we managed to duplicate the TRAIL receptor modifications presented in the previous scenarios, however, TRAIL-R2 knockdown scenarios were difficult to substantiate due to the persistent failure of TRAIL-R4 up-regulation in TRAIL-R2 knockdown cells. Thus, the last two models were only present in Colo357 and were the

most aggressive cell lines. In these two models, TRAIL receptors expression was modified as follows; non-manipulated TRAIL-R1 level and suppressed TRAIL-R2 with or without TRAIL-R4 augmented expression [TR2(-)TR4(+) and TR2(-)cell lines], respectively. The up-regulation of TRAIL-R4 in this case [TR2(-)TR4(+)] did not show major differences in comparison to [TR2(-)] cells per se (Figure 4.6). Both cell lines showed a high proliferation (again in line with the *in vivo* data), migration speed and inflammation rates. However, TRAIL-R4 up-regulation gave three signature differences, the first being the loss of the anti-apoptotic potential of TRAIL-R4. Secondly, there was a clear abolishment of the sensitization effect of TRAIL-R4 on TRAIL-mediated necroptosis that was seen in TR1(-)TR4(+) cell line, denoting that this function is governed by TRAIL-R4 in collaboration with TRAIL-R2. Another key difference between these two cell lines is the up-regulation of WNT2B and CDH2 (N-cadherin) in TR2(-) and TR2(-)TR4(+), respectively. This difference denotes that both cell lines may enhance the tumor aggressiveness and stemness via two different pathways. It was formerly reported that CDH2 – highly expressed in TR2(-) – together with FGF-2 boost metastasis via MAPK-ERK pathway in breast cancer cells (Suyama et al., 2002). While TR2(-)TR4(+) cell line stemness behavior was attributed to the alterations in WNT signaling. Additionally, both cell lines demonstrated very high levels of both CEACAM5 and CEACAM6 denoting the severity of tumor aggressiveness.

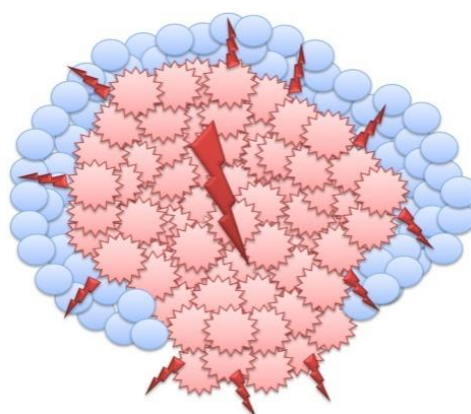



Figure 4.6| Illustration of the cell lines with TRAIL-R2 knockdown in Colo357. A diagram illustrating TR2(-) and TR2(-)TR4(+) cell lines. The shades of red show the inflammatory degree and this sign  denotes a high inflammatory status. Also, the number of edges/ corners of the cells are equivalent of how aggressive the cell lines are. Also, the dark edges of the red/cancer cells represent the high level of CEACAM5 and CEACAM6.

One distinct observation – which was rather intriguing in these two cell lines – was the observed discrepancies between the mRNA and protein levels of IL6 as detected by RT-PCR/microarray and ELISA, respectively. In these two cell lines, it was clearly demonstrated that the mRNA level was elevated however the protein level was not. In this case, there might be some activation of the miRNA responsible for IL6 degradation, and hence not allowing the protein to be translated. In case of IL6, the responsible miRNA is *let-7* that can manipulate the level of IL6 and in turn influence the inflammatory status only in malignant cells (Iliopoulos et al., 2009). This result is in line with a previous study where nuclear TRAIL-R2 was reported to inhibit the maturation of *Let7* miRNA and in turn its knockdown elevated the level of mature *Let7* (Haselmann et al., 2014) and that will eventually decrease IL6 protein expression.

In our patient cohort, TRAIL-R2 knockdown cases were the lowest represented cases that might be owed to the deteriorated status at the point of diagnosis that would deem the patients inoperable at the first evaluation. This explanation is supported by the fact that all the patients in the cohort with these two TRAIL receptors expression patterns died rather early. This would also fit with our *in vivo*, *in silico* and *in vitro* data. Both groups in the patient study expressed low to none TRAIL-R2 protein levels in both cytoplasm and nuclei. TRAIL-R1 was mainly present in moderate to high levels in the cytoplasm. For the patients with TR2(-) profile they presented with a moderate level of TRAIL-R4 in the cytoplasm and a low level in nucleus. However, in TR2(-)TR4(+) scenario TRAIL-R4 were high in both the cytoplasm and nucleus. Thus, this scenario is result of TRAIL-R1 and -R4 collaboration in the cytoplasm or the soul function of TRAIL-R4 in the nucleus.

In the light of these results, there is a big challenge to catch these cases on time, where the tumor is still in an operable status. From the prognostic point of view, the tumors in both scenarios will be very aggressive and could be slightly eliminated under TRAIL-induced apoptosis. However, these two scenarios should be better addressed with other cytotoxic treatment modality, as the cells here are very active. Otherwise, using TRAIL treatment will worsen the prognosis due to the additional activation of the NFκB pathway that will add to the patients' burden of an already highly inflamed status.

TRAIL receptors and PDAC heterogeneity

One of the hurdles that is still faced in pancreatic carcinogenesis is its complexity and heterogeneity that eventually lead to the difficulty of its early diagnosis (Narayanan and Weekes, 2016; Vaz et al., 2015). This heterogeneity became also obvious upon manipulating the TRAIL receptors in our two PDAC cell lines. As previously mentioned, we have observed differential responses from Colo357 and PancTuI in some aspects, starting from the capability of transducing TRAIL-R4 plasmid into the different cell lines to the discrepancies in their functional responses. A couple of theories could be foreseen that might explain the discrepancies between Colo357 and PancTuI responses and render PancTuI more resistant. Undeniably, the basal protein expression levels of the TRAIL receptors and the abundance of certain receptor forms over another might play a role in the reciprocal behavior of the two PDAC cell lines. As known from literature, the abundance of TRAIL-R4 expression was correlated with TRAIL resistance (Lalaoui et al., 2011), thus the high basal level of TRAIL-R4 in PancTuI than in Colo357 might play a role and might also explain the discrepancies in terms of aggressiveness.

Another theory: Looking at the results from a different perspective, TRAIL receptors could be tools for cancer to maintain its existence in the body. TRAIL receptors can manipulate the cellular behavior and thus allowing the cancer to control its development by sacrificing weaker cells that cannot metastasize or invade the surrounding tissues in return for the cells that can. In accordance, TRAIL receptors could drive the cancer cells to send off inflammatory signals to manipulate and prime the surrounding both transformed and untransformed cells around it. Consequently, if TRAIL receptors could orchestrate the cancer cell behavior, it could be expected that the roles of the individual receptors would be modified in different cellular phenotypes that might clarify the refractory responses between Colo357 and PancTuI. In fact that the two cell lines represent a very different phenotype, PancTuI is a primary tumor [pancreatic microenvironment] and Colo357 is metastatic [lymph node microenvironment] cell line which might also explain why the TRAIL receptors might have different roles in different cell phenotypes and different tumor development stages.

Additionally, many differences were previously reported between PancTuI and Colo357 in the expression of some important apoptosis related molecules. As PancTuI has shown higher levels of anti-apoptotic proteins like, BCL-XL, Smac/DIABLO, BID and c-

IAP2 together with lower levels of pro-apoptotic proteins like FADD in comparison to Colo357 cells that caused PancTuI to be more TRAIL resistant (Trauzold et al., 2003). Moreover, it has been also reported that Colo357 cells secrete trypsin, elastase and chymotrypsin which are normally secreted by the exocrine pancreas (Morgan et al., 1980). Also, Colo357 cells contain mutation KRAS2 genes (Gysin et al., 2005), an atypical mutation in p53 (A. Trauzold, unpublished observation), whereas PancTuI contains mutations in KRAS and p53 only together with methylated p16 gene (Moore et al., 2001). Therefore, these fundamental differences would also contribute to the aberrant responses of both cell lines. That was formerly demonstrated by the different behavior of Colo357 and PancTuI upon the inhibition of caspases using zVAD-fmk. Although this broad spectrum caspase inhibitor drove PancTuI to a heightened pro-inflammatory response, it inhibited this response in Colo357 cells (Siegmond et al., 2016). Thus, it could be deduced that TRAIL receptors trigger different responses in the different cells within the same ailment.

Finally, it has been repeatedly observed that TRAIL receptors were expressed in patients' sera (Jablonska et al., 2008; Mielczarek-Palacz et al., 2015; Oztas et al., 2016; Ratzinger et al., 2014; Sánchez-Lázaro et al., 2012; Yagyu et al., 2008; Yildiz et al., 2010). However, the current study only focused on the TRAIL receptors expressed inside the cells and the total expressed TRAIL receptor mRNA and protein levels that will include the mRNAs for the soluble forms as well. Not to mention that the TRAIL receptors comprised of 5 different receptors (Mert and Sanlioglu, 2016). Therefore, there could be a possible role for TRAIL-R3 and/or OPG in this mix, yet, here the focus is only on TRAIL-R1, -R2 and -R4. However, as was seen from the microarray and the nCounter results, TRAIL-R3 and OPG were not fundamentally modified in the different cell lines.

In light of our results, the TRAIL receptors interplay provided the cells with different capabilities. Consequently, the tumor heterogeneity might not only imply the discrepancies between the different patients, but also the heterogeneity in the same tumor. In other words, the cells near a blood supply in the same tumor could modulate the TRAIL receptors' level differently than the cells in the hypoxic center or at the tumor edge. On one hand, it has been demonstrated that silencing hypoxia-inducible factor-2 alpha (HIF-2 α) down regulated TRAIL-R2 on both the mRNA and protein levels in renal, lung and prostatic cancer cells. This regulatory potential of HIF-2 α was reported in both TRAIL sensitive and TRAIL resistant renal cancer cell lines as well and was reversed by treating

the cells with PS-341. PS-341 is a protease inhibitor that increases the levels of HIF-2 α and c-Myc where both apparently have a positive regulatory effect of TRAIL-R2 (Mahajan et al., 2008). On the other hand, in hypoxic conditions, hypoxia-inducible factor-1 alpha (HIF-1 α) induced the level of TRAIL-R4 in colon cancer cells (Pei et al., 2010). Therefore, one can deduce that TRAIL receptors are manipulated in response to hypoxic and normoxic conditions.

In the current study, the heterogeneity of PDAC was very obvious, however, this problem extends beyond the 2 studied cell lines. As previously discussed, not only that each PDAC patient is unique but also in the same patient the primary and secondary tumors might behave differently and may be these discrepancies could be seen also within the primary tumor tissues itself. Furthermore, it is also important to keep in mind that TRAIL might render each tumor environment different than one another because it plays an important role in immune surveillance. Interferon gamma is capable of sensitizing natural killer cells and monocytes to produce TRAIL and in turn help eliminating cancer cells (Griffith et al., 1999; Takeda K et al., 2001). Therefore, the immune system will play an additional role rendering each situation different. Hence, it is crucial to understand tumor heterogeneity in each context in order to understand why some PDAC patients will react differently to the same therapy than other patients suffering from the same illness.

Failure of TRAIL-R4 up-regulation in PancTuI TRAIL-R2 knockdown cell line

During the preparatory phase of the current study, another limitation was observed. In Colo357 cell line, it was possible to up-regulate TRAIL-R4 in TRAIL-R2 knockdown cells, however, there was a persistent failure in PancTuI TRAIL-R2 knockdown cells. Again one can deduce some theories here to interpret why that was not possible. Theory one: it is established that TRAIL-R4 interacts closely with TRAIL-R2 on the plasma membrane level (Clancy et al., 2005; Lalaoui et al., 2011; Mérimo et al., 2006). In the current study, the results showed that PancTuI expressed higher basal levels of both TRAIL-R2 and -R4. Also, TRAIL-R4 up-regulation in Colo357 TRAIL-R2 knockdown cell line was – despite being significant – the most limited on the plasma membrane level among the three TRAIL-R4 up-regulated cell lines. Consequently, it can be deduced that TRAIL-R2 and -R4 interaction could be essential for the survival of PancTuI that might in turn explain the repeated failure i.e. death of the cell lines upon TRAIL-R4 up-regulation in the limited expression of TRAIL-R2. So, that will further denote the distinct interplay

between the TRAIL-R2 and -R4 receptors in the different sites and tumor developmental phases, where it is vital for primary tumors and to a lesser extent in metastatic tumor cells. To confirm this theory, one can try to knockdown TRAIL-R2 after TRAIL-R4 over expression. Thereby, we can point out which of these two receptors manipulate the other.

Second theory: Although, it was previously reported that TRAIL-R4 has a dominant negative influence on TRAIL-R1 (Neumann et al., 2014), it could be deduced from the current results that TRAIL-R1 might in fact compete with TRAIL-R4 expression/function especially in PancTuI. This hypothesis can be supported by the failure of TRAIL-R4 over expression in TRAIL-R2 knockdown cell lines, where TRAIL-R1 would be unopposed. This could be corroborated by the enhanced TRAIL-R4 knock-in when TRAIL-R1 is restricted.

Once more, this can be a “pseudo” failure of TRAIL-R4 over expression as there is still the possibility that TRAIL-R4 was indeed up-regulated, yet only in the soluble form. However, this could be negated by the fact that we have measured the TRAIL receptors’ level on the mRNA level as well.

TRAIL receptors orchestrate PDAC cell death modality

Apoptosis

Another aspect of this study was done to clarify the influence of TRAIL receptors on two major cell death modalities: apoptosis and necroptosis. Our proposed mixed knockdown and over expression system allowed us to observe and analyze the individual role of these receptors in these contexts. Worth mentioning, all the apoptosis and necroptosis experiments were done in parallel for a clear distinction of the individual roles in both cell death modes. Regarding apoptosis, we have clearly demonstrated that TRAIL-R2 guided the TRAIL-R4-mediated anti-apoptotic effect pointing out the close interaction between both receptors as was reported previously by other groups (Clancy et al., 2005; Mérimo et al., 2006). Similarly, it was previously indicated that PDAC tissues showed significantly higher levels of TRAIL-R1 and -R4 in comparison to normal pancreas in a cohort of PDAC (Sanlioglu et al. 2009). As previously stated, PancTuI is originally more resistant to TRAIL-induced apoptosis than Colo357 cell line (S Hinz et al., 2000; Trauzold et al., 2003). Together with basal resistance level, there is an extra protection provided by TRAIL-R4 over expression against TRAIL-induced apoptosis. Earlier, it was shown that the lower the balance between the pro-apoptotic receptors (TRAIL-R1 and -R2) and – the

known to be – decoy receptors (TRAIL-R3 and -R4), the better the chance the cells are killed (Büneker et al., 2009). Likewise, it was reported also in PDAC patients that TRAIL-R3 and -R4 did not have any impact on patient prognosis, only the low levels of TRAIL-R1 and -R2 was correlated with pancreatic malignancy (Gallmeier et al. 2013). Nevertheless, the current research demonstrated that TRAIL receptors interplay is much more complicated and it could be used in PDAC as markers for TRAIL sensitivity. To conclude, TRAIL-R4 protection can be clearly seen only in collaboration with TRAIL-R2. Therefore, by inhibiting TRAIL-R2, this protection was completely lost. Furthermore, the analyses showed that TRAIL-R1 knockdown was as well resistant to the TRAIL-mediated apoptosis in both cell lines, thus, proposing TRAIL-R1 as a major player in apoptosis induction in PDAC cells as was previously shown (Lemke et al., 2010).

Necroptosis

Some cancer treatment is based on drugs inducing apoptosis like cisplatin, 5-fluorouracil, and gemcitabine. Yet, drug resistance is a commonly encountered problem due to an imbalance between the apoptotic and pro-inflammatory pathways tipping the scale towards the pro-survival mode in tumor cells (Su et al. 2016). So, owing to the tumor resistance to TRAIL-induced apoptosis, other alternative cell death modalities are sought to overcome this problem. One of these methods is necroptosis; there are a number of new researches that are focused on this topic (Huang et al. 2013, Jouan-Lanhouet et al. 2012, Meurette et al. 2007, Moriwaki et al. 2015, Oliver Metzger et al. 2015, Philipp et al. 2015, Takemura et al. 2015, Xie et al. 2015). The capability of TRAIL to induce necroptosis was previously investigated, however the effect of TRAIL receptors interplay on TRAIL-induced necroptosis was not addressed (Jouan-Lanhouet et al. 2012, Philipp et al. 2015). Accordingly, we intended to measure the impact of the particular TRAIL receptor interactions on necroptosis and test whether or not these receptors will have a similar effect on necroptosis as with apoptosis. Two evident differences can be demonstrated between the two cell death modalities. On one hand, apoptosis signaling must be inhibited via a wide-range caspase inhibitor, zVAD-fmk, in order to assure that cell death occur solely via necroptosis. On the other hand, necroptosis cannot be efficiently induced by TRAIL alone, however a sensitizer like HHT is essential (Philipp et al., 2015). HHT has recently been approved by the U.S. Food and Drug Administration for treating patients with chronic or accelerated phase chronic myeloid leukemia with resistance and/or intolerance to two or

more tyrosine kinase inhibitors [reviewed in (Heiblig et al., 2014)]. Furthermore, HHT was previously presented as a potential non-toxic sensitizer for TRAIL-induced apoptosis (Beranova et al. 2013) and necroptosis (Philipp et al. 2015). Despite the complicated approach needed for efficiently triggering necroptosis, necroptosis could still carry new hope for cancer patients. As continually inferred from literature, TRAIL-R4 plays a protective role against TRAIL-induced apoptosis (Duru et al. 2015, Todorova, Bock, and Chang 2014, O'Leary et al. 2016) and it could be expected that TRAIL-R4 might play a similar role in necroptosis. Surprisingly, we demonstrated a novel function of TRAIL-R4 where it significantly enhanced the cellular killing via TRAIL-induced necroptosis in Colo357 TR1(-)TR4(+) cells. Thereby, we demonstrated a new potential role for TRAIL-R4 as a sensitizer for TRAIL-induced necroptosis in combination with TRAIL-R2 rather than a mere inhibitor of TRAIL-induced apoptosis as represented in both WB and EZ4U analyses. Probably, it could be again owed to the higher affinity of TRAIL-R4 to TRAIL-R2.

TRAIL receptors impact on adhesion in PDAC

Upon comparing the ECM-cell adherence with proliferative and migratory potentials shown in this study, one can conclude that, the stronger the ECM-cell adhesion, the faster the proliferation and the more metastatic the cells are. Our proposed TRAIL receptor alterations showed evident –yet different – effects on the integrin expression levels. The up-regulation of TRAIL-R4 augmented the expression of the tested integrins, however, this effect was reversed via TRAIL-R1 knockdown. Moreover, the effect of TRAIL-R4 on integrins was completely lost upon TRAIL-R2 knockdown. Consequently, if TRAIL receptors are capable of manipulating the integrin levels, it would be expected that the cellular behavior can be altered as well. On one hand, integrin-ECM interaction can manipulate the cell fate via the integrin's inside-in pathway, where integrins can activate AKT and MAPK pathways (Figure 4.7) (Legate et al., 2009). On the other hand, it was previously reported that TRAIL receptors can as well manipulate AKT and MAPK pathways (de Miguel et al., 2016) and in turn increase tumor proliferation, migration and cell survival. In cervix cancer cells, it was demonstrated that TRAIL-R4 enhance proliferation of the cells via activation of AKT (Lalaoui et al., 2011). Also, TRAIL-R1 and -R2 signaling was found to activate both AKT and ERK(1/2) in ovarian cancer (Yang et al., 2016). Therefore, here we report that TRAIL receptors might activate these pathways via

the integrin outside-in signaling and thus be able to manipulate cell fate. Herewith, the ECM-cell adhesion can indeed be correlated to cellular proliferation and migration.

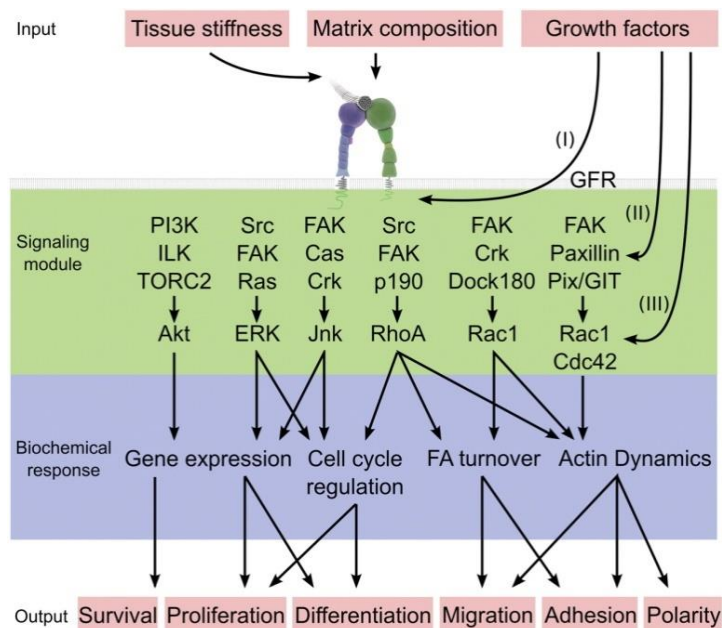


Figure 4.7| Downstream outside-in integrin pathways. Integrin interaction with ECM starts a lot of signaling pathways leading eventually to cell cycle regulation, changes in gene expression, actin dynamics and other (Legate et al., 2009)

Moreover, we could report discrepancies in the response of the studied cell lines to the presence of tenascin-c. Tenascin-c plays a major role during embryonic development; however, in adult tissues it is rarely encountered. Furthermore, tenascin-c has been repeatedly detected in high levels in malignant tissues including PDAC (Esposito et al., 2006; Faissner et al., 2016; Paron et al., 2011; Stamenkovic et al., 2016). By creating an artificial and rather malignant environment, it was possible to test the capability of the different cell lines to adapt to this condition. Apparently, tenascin-c could be considered as a welcoming microenvironment for cells that are rich in TRAIL-R4 with -R1 [TR2(-)TR4(+)] and more prominently TRAIL-R4 with -R2 [TR1(-)TR4(+)]. In other words, these cell lines will easily grow in physiologically unfavorable microenvironments and these potential patients with high levels of TRAIL-R4 with either TRAIL-R1 or -R2 might have a more readily metastasizing cancer.

Orthotopic versus subcutaneous *in vivo* experiments

In the current research, we have performed two *in vivo* experiments using Colo357 cells in SCID-beige mice. The interpretation of the Colo357 orthotopic model was largely hampered by the formation of large slimy tumors. Worth noting, that MUC2, MUC6 and

MUC5AC secreted mucins were previously reported to be highly expressed in pancreatic malignant and pre-malignant lesions (Horinouchi et al., 2003; Lüttges et al., 2002; Yonezawa et al., 2008). Additionally, Colo357 was originally described as mucinous tumor isolated from the lymph node metastasis (Morgan et al., 1980). Accordingly, this finding points that the context of the tumor microenvironment greatly matters; whether it is inoculated in the murine pancreatic tissues or subcutaneously. Therefore, more intensive studies on the impact of interplay of the different TRAIL receptors on survival potential are urgently needed. Additionally, the role of mucin production in PDAC needs more elucidation.

Since the results of this orthotopic model were not easily interpretable, a subcutaneous model was performed. The gross analyses of the data in the subcutaneous model were in line with our *in vitro* and *in silico* analyses. We could show that the mice with the smallest tumors were seen in TR1(-)TR4(+) as depicted from the suppressed functional behavior of the cells *in vitro*. Additionally, the least metastasis were detected in TRAIL-R1 knockdown group which goes in line with the low levels of CEACAM5 and CEACAM6. Finally, the largest tumors were seen in TRAIL-R2 knockdown groups which as well coincide with our *in vitro* and *in silico* predictions.

V. CONCLUSION

Through the present work, the data could show that TRAIL-R1, -R2 and -R4 indeed tightly interplay and thus leading the PDAC cells to different fates. Not only the abundance/absence of the receptor expression is important, but also the phenotype of the cells plays a role in the overall response together with the intracellular distribution of the different receptors and the surrounding environment. Hence, we could now aim to better understand why some patients would carry a bad or a good prognosis, however, studying a larger cohort of patients is necessary. Subsequently, we will be able to understand every patient's response according to his/her individual profile. Additionally, TRAIL-R4 was regarded as a decoy receptor that competes with TRAIL-R1 and -R2 for TRAIL to prevent apoptosis and it might also bind to them and inhibits their ligand-dependent functions. Through this study, the data elaborated a different potential for this receptor. Therefore, this simplistic interpretation of TRAIL-R4 being only addressed as a decoy receptor in tumors and correlating it with a poor prognosis needs to be extended. The results have shown that TRAIL-R4 could be an active member of the TRAIL receptor family – depending on the context – and not merely a decoy receptor. Our investigations showed TRAIL-R4 –together with TRAIL-R1 or -R2 – as an active player in many functional processes. Through our proposed system, we were able to show the different faces of TRAIL-R4 in enhancing necroptosis or limiting apoptosis. On one hand, the known inhibition of the apoptosis via TRAIL-R4/-R2 interaction could be confirmed. On the other hand, TRAIL-R4/-R2 was reported to activate the necroptotic potential driven by TRAIL in Colo357. Although these findings will require further validation in primary cancer cells and patient models, this new and promising approach could provide a valuable input to the understanding of the role of TRAIL receptors in PDAC progression and pancreatic cancer therapy. Finally, TRAIL ligand has been proposed as a potential therapeutic modality in cancer (Mérino et al., 2007). However, our results gave more insight that some of the TRAIL receptors' actions in Colo357 were independent of the TRAIL ligand, this might give a hint about the complicated nature of this system. Therefore, deeper understanding of TRAIL and TRAIL receptors' capabilities in the different tumor stages is required before TRAIL can be proposed as a legitimate cancer treatment modality.

VI. FUTURE PERSPECTIVE AND OUTLOOK

The current study clarifies the genuine interdependence of TRAIL receptors and the variety of fates they could drive the PDAC cells to undergo. Besides, I reported the flexible functions of the known-to-be a decoy receptor: TRAIL-R4. However, since the whole concept of the current work was based on up-regulation of TRAIL-R4, here I present some preliminary data of TRAIL-R4 successful down-regulation. TRAIL-R4 was knocked down using shRNA technology in both Colo357 and PancTuI cell lines. The same shRNA technology that was previously used for TRAIL-R1 and TRAIL-R2 down regulation was implemented to facilitate all future comparisons. The protein and mRNA expression levels of TRAIL-R4 were analyzed using Western blotting and RT-PCR, to ensure the successful suppression of the TRAIL-R4 on both levels (Figure 6.1).

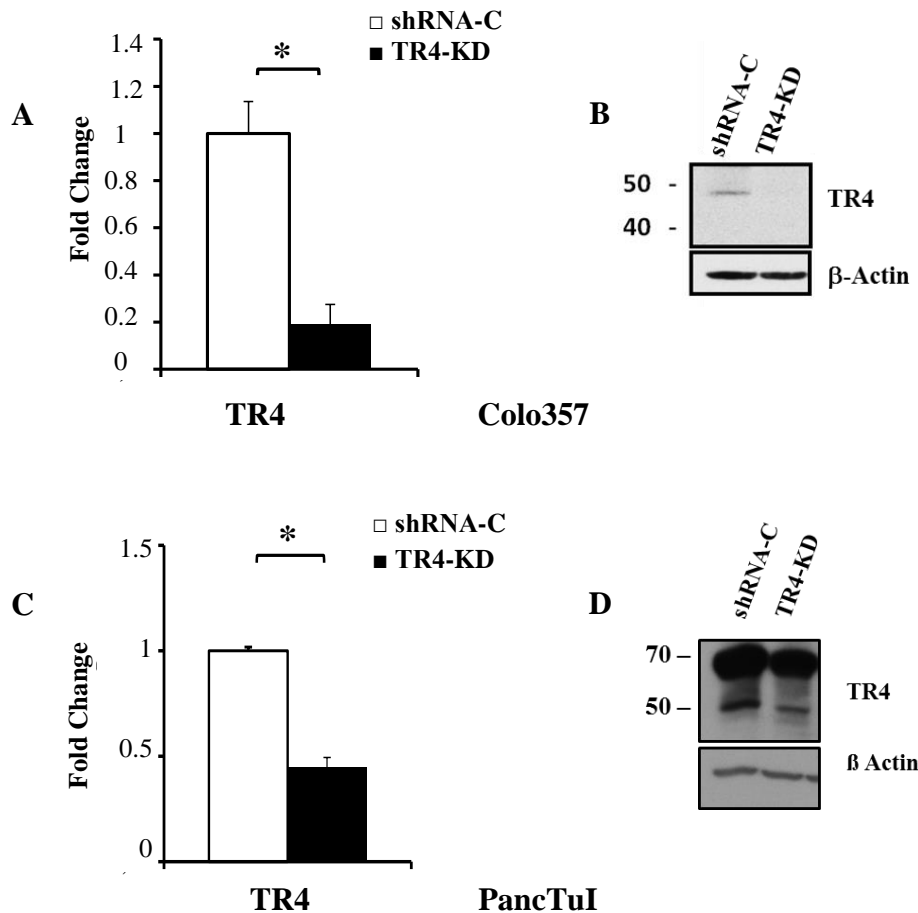


Figure 6.1| Expression level of TRAIL-R4. The panel shows the successful knockdown of TRAIL-R4 (TR4-KD) together with the corresponding non-silencing control (shRNA-C) in two PDAC cell lines. **A;** RT-PCR of TR4-KD in Colo357. **B,** Western Blot denoting the successful down regulation of TRAIL-R4 in Colo357 on the protein level. **C;** RT-PCR of TR4-KD in PancTuI. **D,** Western Blot denoting the successful down regulation of TRAIL-R4 in PancTuI on the protein level.

Some functional analyses were performed to test our newly established cell lines. As expected, the suppression of TRAIL-R4 in Colo357 limited both the proliferative and the migratory capabilities of the cells and rendered the cells more susceptible to TRAIL-induced apoptosis (Figure 6.2). Currently, our group is further validating the impact of TRAIL-R4 down regulation in both cell lines.

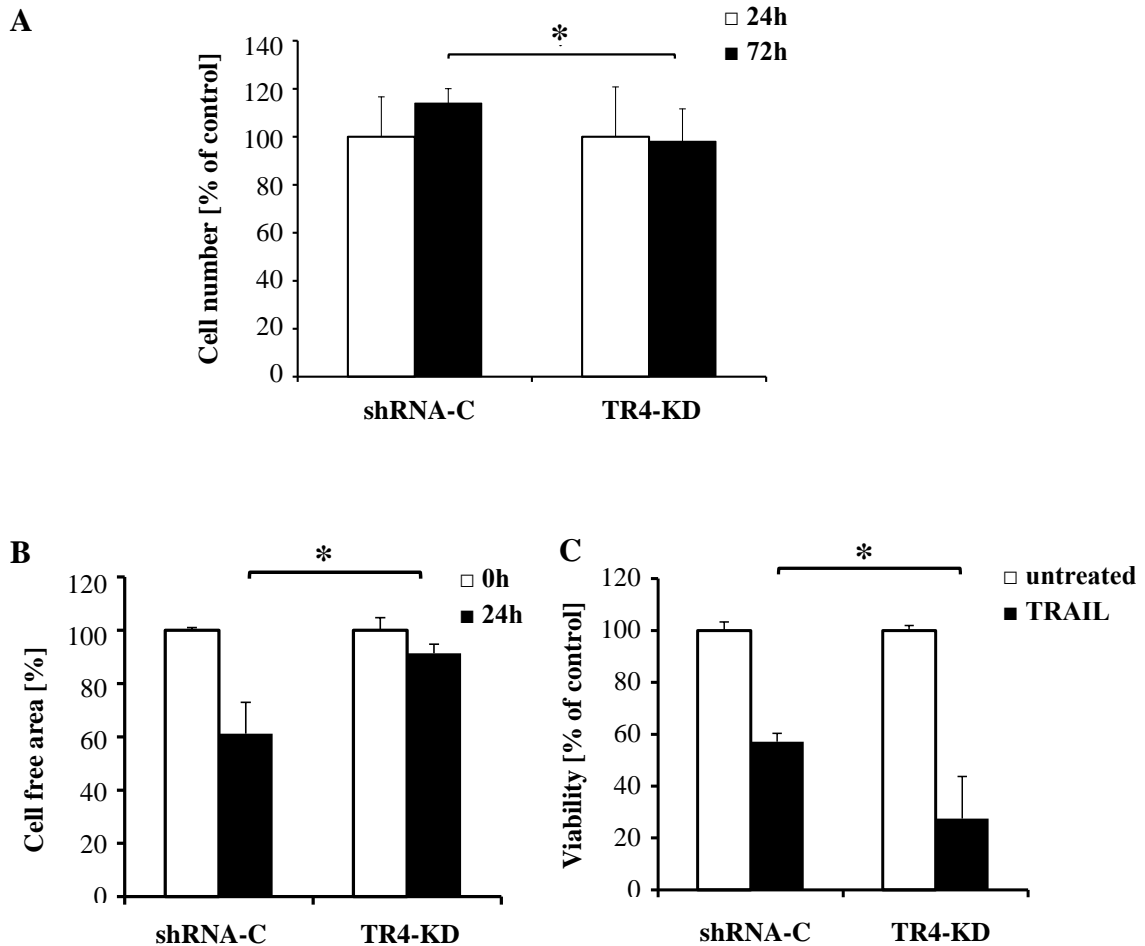


Figure 6.2| *In vitro* functional analyses of Colo357 TRAIL-R4 knockdown cell line (TR4-KD) **A**; proliferation capacity with TR4 knockdown. **B**, migratory potential of TR4-KD. **C**; viability of the TR4-KD under 24 hours TRAIL treatment.

Furthermore, since the main results of the current study was obtained from a single PDAC cell line, namely Colo357, another TRAIL sensitive cell line was also tested as a part of a master study performed in our group (André Seidel unpublished data). This TRAIL-sensitive cell line is a breast cancer cell line named MDA-MB-231. The same proposed TRAIL manipulations were constructed, and thus obtaining another 6-cell line set. As an example, the level of integrins was tested in the MDA-MB-231 cell lines (Figure 6.3). Similar to the Colo357 cell lines, the MDA-MB-231 cell lines exhibited fluctuations

in the protein level of the expressed integrins. TRAIL-R4 up-regulated the levels of the tested integrins however this tendency was lost upon TRAIL-R2 knockdown. Therefore, unlike Colo357, TRAIL-R4 exhibited this effect in collaboration with TRAIL-R1 – as expected– and not with TRAIL-R2. It was previously reported that TRAIL-R2 is more important in MDA-MB-231 TRAIL-mediated signaling unlike Colo357 where TRAIL-R1 is more efficient in eliminating the cells (Kelley et al., 2005; Lemke et al., 2010). In other words, this effect of TRAIL receptors on integrins can be indeed induced by TRAIL. However, since it was shown in the current study that blocking the endogenous TRAIL by means of antibody proved otherwise, therefore this method might be insufficient. Consequently, TRAIL silencing via siRNA might answer the question whether TRAIL is manipulating this process. Nevertheless, these integrin alterations in the MDA-MB-231 cell lines might demonstrate that the possible scenarios elucidated in this work could be reproduced in other cancer entities and are not a matter of chance.

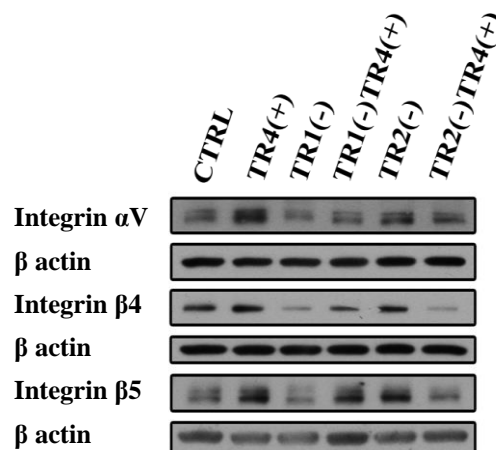


Figure 6.3| Expression levels of some cell-ECM adhesion molecules in MDA-MB-231. The cell lines expressing differential levels of TRAIL-R1, -R2 and -R4 were investigated to measure the levels of integrin α V, β 4 and β 5 via Western blotting. Beta actin served as loading control. Figure modified from the master thesis of André Seidel, Institute for Experimental Cancer Research, CAU Kiel.

In order to further authenticate the results introduced in the current study, a deeper understanding of the pathways involved in the reported and predicted cellular functions of TRAIL receptors is needed. And finally, I recommend the following actions:

- Analyzing TRAIL receptors in a larger patient cohort together with correlating it with the clinical outcome, well-established scoring systems, follow-up and prognosis.

- Further dissecting the TRAIL receptors to determine which form (TRAIL-R4 α or TRAIL-R β) is responsible for each function.
- Precisely evaluate the impact of the intracellular TRAIL receptor form distribution.
- Understanding how to manipulate the sub-cellular localization of the TRAIL receptors.

REFERENCES

- Abdulghani, J., El-Deir, W.S., 2010. TRAIL receptor signaling and therapeutics. *Expert Opin. Ther. Targets* 14, 1091–1108. doi:DOI: 10.1517/14728222.2010.519701
- Arabzadeh, A., Chan, C., Nouvion, A.-L., Breton, V., Benlolo, S., DeMarte, L., Turbide, C., Brodt, P., Ferri, L., Beauchemin, N., 2013. Host-related carcinoembryonic antigen cell adhesion molecule 1 promotes metastasis of colorectal cancer. *Oncogene* 32, 849–60. doi:10.1038/onc.2012.112
- Ashkenazi, A., Pai, R.C., Fong, S., Leung, S., Lawrence, D.A., Marsters, S.A., Blackie, C., Chang, L., McMurtrey, A.E., Hebert, A., DeForge, L., Koumenis, I.L., Lewis, D., Harris, L., Bussiere, J., Koeppen, H., Shahrokh, Z., Schwall, R.H., 1999. Safety and antitumor activity of recombinant soluble Apo2 ligand. *J. Clin. Invest.* 104, 155–62. doi:10.1172/JCI6926
- Azijli, K., Weyhenmeyer, B., Peters, G.J., de Jong, S., Kruyt, F.A.E., 2013. Non-canonical kinase signaling by the death ligand TRAIL in cancer cells: discord in the death receptor family. *Cell Death Differ.* 20, 858–68. doi:10.1038/cdd.2013.28
- Bailey, J.M., Mohr, A.M., Hollingsworth, M.A., 2009. Sonic hedgehog paracrine signaling regulates metastasis and lymphangiogenesis in pancreatic cancer. *Oncogene* 28, 3513–3525. doi:10.1038/onc.2009.220
- Bailey, J.M., Swanson, B.J., Hamada, T., Eggers, J.P., Singh, P.K., Caffery, T., Ouellette, M.M., Hollingsworth, M.A., 2008. Sonic Hedgehog Promotes Desmoplasia in Pancreatic Cancer. *Clin. Cancer Res.* 14, 5995–6004. doi:10.1158/1078-0432.CCR-08-0291
- Bao, X., Song, H., Chen, Z., Tang, X., 2012. Wnt3a promotes epithelial-mesenchymal transition, migration, and proliferation of lens epithelial cells. *Mol. Vis.* 18, 1983–90.
- Bassagañas, S., Allende, H., Cobler, L., Ortiz, M.R., Llop, E., de Bolós, C., Peracaula, R., 2015. Inflammatory cytokines regulate the expression of glycosyltransferases involved in the biosynthesis of tumor-associated sialylated glycans in pancreatic cancer cell lines. *Cytokine* 75, 197–206. doi:10.1016/j.cyto.2015.04.006
- Basturk, O., Hong, S.-M., Wood, L.D., Adsay, N.V., Albores-Saavedra, J., Biankin, A. V., Brosens, L.A.A., Fukushima, N., Goggins, M., Hruban, R.H., Kato, Y., Klimstra, D.S., Klöppel, G., Krasinskas, A., Longnecker, D.S., Matthaei, H., Offerhaus, G.J.A., Shimizu, M., Takaori, K., Terris, B., Yachida, S., Esposito, I., Furukawa, T., 2015. A Revised Classification System and Recommendations From the Baltimore Consensus Meeting for Neoplastic Precursor Lesions in the Pancreas. *Am. J. Surg. Pathol.* 39, 1730–1741. doi:10.1097/PAS.0000000000000533
- Bates, R.C., Bellovin, D.I., Brown, C., Maynard, E., Wu, B., Kawakatsu, H., Sheppard, D., Oettgen, P., Mercurio, A.M., 2005. Transcriptional activation of integrin $\beta 6$ during the epithelial-mesenchymal transition defines a novel prognostic indicator of

- aggressive colon carcinoma. *J. Clin. Invest.* 115, 339–347. doi:10.1172/JCI23183
- Batty, G.D., Kivimaki, M., Morrison, D., Huxley, R., Smith, G.D., Clarke, R., Marmot, M.G., Shipley, M.J., 2009. Risk factors for pancreatic cancer mortality: extended follow-up of the original Whitehall Study. *Cancer Epidemiol. Biomarkers Prev.* 18, 673–5. doi:10.1158/1055-9965.EPI-08-1032
- Beauchemin, N., Arabzadeh, A., 2013. Carcinoembryonic antigen-related cell adhesion molecules (CEACAMs) in cancer progression and metastasis. *Cancer Metastasis Rev.* 32, 643–71. doi:10.1007/s10555-013-9444-6
- Becker, A.E., Hernandez, Y.G., Frucht, H., Lucas, A.L., 2014. Pancreatic ductal adenocarcinoma: risk factors, screening, and early detection. *World J. Gastroenterol.* 20, 11182–98. doi:10.3748/wjg.v20.i32.11182
- Bell, D.W., 2010. Our changing view of the genomic landscape of cancer. *J. Pathol.* 220, 231–43. doi:10.1002/path.2645
- Bentzinger, C.F., Wang, Y.X., von Maltzahn, J., Soleimani, V.D., Yin, H., Rudnicki, M.A., 2013. Fibronectin regulates Wnt7a signaling and satellite cell expansion. *Cell Stem Cell* 12, 75–87. doi:10.1016/j.stem.2012.09.015
- Bergmann, A., Steller, H., 2010. Apoptosis, stem cells, and tissue regeneration. *Sci. Signal.* 3, re8. doi:10.1126/scisignal.3145re8
- Bertsch, U., Röder, C., Kalthoff, H., Trauzold, A., 2014. Compartmentalization of TNF-related apoptosis-inducing ligand (TRAIL) death receptor functions: emerging role of nuclear TRAIL-R2. *Cell Death Dis.* 5, e1390. doi:10.1038/cddis.2014.351
- Bisgin, A., Terzioglu, E., Aydin, C., Yoldas, B., Yazisiz, V., Balci, N., Bagci, H., Gorczynski, R.M., Akdis, C.A., Sanlioglu, S., 2010. TRAIL death receptor-4, decoy receptor-1 and decoy receptor-2 expression on CD8+ T cells correlate with the disease severity in patients with rheumatoid arthritis. *BMC Musculoskelet. Disord.* 11, 192. doi:10.1186/1471-2474-11-192
- Bonazzi, V.F., Nancarrow, D.J., Stark, M.S., Moser, R.J., Boyle, G.M., Aoude, L.G., Schmidt, C., Hayward, N.K., 2011. Cross-platform array screening identifies COL1A2, THBS1, TNFRSF10D and UCHL1 as genes frequently silenced by methylation in melanoma. *PLoS One* 6, e26121. doi:10.1371/journal.pone.0026121
- Brandi, J., Dando, I., Pozza, E.D., Biondani, G., Jenkins, R., Elliott, V., Park, K., Fanelli, G., Zolla, L., Costello, E., Scarpa, A., Cecconi, D., Palmieri, M., 2017. Proteomic analysis of pancreatic cancer stem cells: Functional role of fatty acid synthesis and mevalonate pathways. *J. Proteomics* 150, 310–322. doi:10.1016/j.jprot.2016.10.002
- Brellier, F., Martina, E., Degen, M., Heuzé-Vourc'h, N., Petit, A., Kryza, T., Courty, Y., Terracciano, L., Ruiz, C., Chiquet-Ehrismann, R., 2012. Tenascin-W is a better cancer biomarker than tenascin-C for most human solid tumors. *BMC Clin. Pathol.* 12, 14.

doi:10.1186/1472-6890-12-14

- Brost, S., Koschny, R., Sykora, J., Stremmel, W., Lasitschka, F., Walczak, H., Ganten, T.M., 2010. Differential expression of the TRAIL/TRAIL-receptor system in patients with inflammatory bowel disease. *Pathol. Res. Pract.* 206, 43–50. doi:10.1016/j.prp.2009.09.005
- Brost, S., Zimmermann, A., Koschny, R., Sykora, J., Stremmel, W., Schirmacher, P., Walczak, H., Ganten, T.M., 2014. Hepatocyte expression of TRAIL pathway regulators correlates with histopathological and clinical parameters in chronic HCV infection. *Pathol. Res. Pract.* 210, 83–91. doi:10.1016/j.prp.2013.10.005
- Büneker, C., Mohr, A., Zwacka, R.M., 2009. The TRAIL-receptor-1: TRAIL-receptor-3 and -4 ratio is a predictor for TRAIL sensitivity of cancer cells. *Oncol. Rep.* 21, 1289–1295.
- Campisi, J., Andersen, J.K., Kapahi, P., Melov, S., 2011. Cellular senescence: a link between cancer and age-related degenerative disease? *Semin. Cancer Biol.* 21, 354–9. doi:10.1016/j.semcancer.2011.09.001
- Celik, O., Kutlu, O., Tekcan, M., Celik-Ozenci, C., Koksall, I.T., 2013. Role of TNF-related apoptosis-inducing ligand (TRAIL) in the pathogenesis of varicocele-induced testicular dysfunction. *Asian J. Androl.* 15, 269–74. doi:10.1038/aja.2012.112
- Chen, L., Liu, X., Zhu, Y., Cao, Y., Sun, L., Jin, B., 2004. Localization and variation of TRAIL and its receptors in human placenta during gestation. *Life Sci.* 74, 1479–86.
- Chen, Y., Shi, M., Yu, G.-Z., Qin, X.-R., Jin, G., Chen, P., Zhu, M.-H., 2012. Interleukin-8, a promising predictor for prognosis of pancreatic cancer. *World J. Gastroenterol.* 18, 1123. doi:10.3748/wjg.v18.i10.1123
- Chera, S., Ghila, L., Dobretz, K., Wenger, Y., Bauer, C., Buzgariu, W., Martinou, J.-C., Galliot, B., 2009. Apoptotic cells provide an unexpected source of Wnt3 signaling to drive hydra head regeneration. *Dev. Cell* 17, 279–289. doi:10.1016/j.devcel.2009.07.014
- Chu, D., Kohlmann, W., Adler, D.G., 2010. Identification and screening of individuals at increased risk for pancreatic cancer with emphasis on known environmental and genetic factors and hereditary syndromes. *JOP* 11, 203–12.
- Clancy, L., Mruk, K., Archer, K., Woelfel, M., Mongkolsapaya, J., Screaton, G., Lenardo, M.J., Chan, F.K.-M., 2005. Preligand assembly domain-mediated ligand-independent association between TRAIL receptor 4 (TR4) and TR2 regulates TRAIL-induced apoptosis. *Proc. Natl. Acad. Sci. U. S. A.* 102, 18099–104. doi:10.1073/pnas.0507329102
- Collado, M., Gil, J., Efeyan, A., Guerra, C., Schuhmacher, A.J., Barradas, M., Benguría, A., Zaballos, A., Flores, J.M., Barbacid, M., Beach, D., Serrano, M., 2005. Tumour

- biology: Senescence in premalignant tumours. *Nature* 436, 642–642. doi:10.1038/436642a
- Collado, M., Serrano, M., 2010. Senescence in tumours: evidence from mice and humans. *Nat. Rev. Cancer* 10, 51–57. doi:10.1038/nrc2772
- Dai, X., Zhang, J., Arfuso, F., Chinnathambi, A., Zayed, M.E., Alharbi, S.A., Kumar, A.P., Ahn, K.S., Sethi, G., 2015. Targeting TNF-related apoptosis-inducing ligand (TRAIL) receptor by natural products as a potential therapeutic approach for cancer therapy. *Exp. Biol. Med.* 240, 760–773. doi:10.1177/1535370215579167
- de Miguel, D., Lemke, J., Anel, A., Walczak, H., Martinez-Lostao, L., 2016. Onto better TRAILs for cancer treatment. *Cell Death Differ.* 23, 733–747. doi:10.1038/cdd.2015.174
- Degli-Esposti, M.A., Dougall, W.C., Smolak, P.J., Waugh, J.Y., Smith, C.A., Goodwin, R.G., 1997. The Novel Receptor TRAIL-R4 Induces NF- κ B and Protects against TRAIL-Mediated Apoptosis, yet Retains an Incomplete Death Domain. *Immunity* 7, 813–820. doi:10.1016/S1074-7613(00)80399-4
- Degli-Esposti, M.A., Smolak, P.J., Walczak, H., Waugh, J., Huang, C.P., DuBose, R.F., Goodwin, R.G., Smith, C.A., 1997. Cloning and characterization of TRAIL-R3, a novel member of the emerging TRAIL receptor family. *J. Exp. Med.* 186, 1165–70.
- Delbridge, A.R.D., Strasser, A., 2015. The BCL-2 protein family, BH3-mimetics and cancer therapy. *Cell Death Differ.* 22, 1071–80. doi:10.1038/cdd.2015.50
- Dhar, P., Kalghatgi, S., Saraf, V., 2015. Pancreatic cancer in chronic pancreatitis. *Indian J. Surg. Oncol.* 6, 57–62. doi:10.1007/s13193-014-0373-9
- Dijk, M. van, Halpin-McCormick, A., Sessler, T., Samali, A., Szegezdi, E., 2013. Resistance to TRAIL in non-transformed cells is due to multiple redundant pathways. *Cell Death Dis.* 4, e702. doi:10.1038/cddis.2013.214
- Dimberg, L.Y., Anderson, C.K., Camidge, R., Behbakht, K., Thorburn, A., Ford, H.L., 2013. On the TRAIL to successful cancer therapy? Predicting and counteracting resistance against TRAIL-based therapeutics. *Oncogene* 32, 1341–50. doi:10.1038/onc.2012.164
- Duxbury, M.S., Ito, H., Zinner, M.J., Ashley, S.W., Whang, E.E., 2004. CEACAM6 gene silencing impairs anoikis resistance and in vivo metastatic ability of pancreatic adenocarcinoma cells. *Oncogene* 23, 465–473. doi:10.1038/sj.onc.1207036
- Ebrahimi, B., Tucker, S.L., Li, D., Abbruzzese, J.L., Kurzrock, R., 2004. Cytokines in pancreatic carcinoma. *Cancer* 101, 2727–2736. doi:10.1002/cncr.20672
- Eckelman, B.P., Salvesen, G.S., Scott, F.L., 2006. Human inhibitor of apoptosis proteins: why XIAP is the black sheep of the family. *EMBO Rep.* 7, 988–994.

doi:10.1038/sj.embor.7400795

- Egberts, J.-H., Cloosters, V., Noack, A., Schniewind, B., Thon, L., Klose, S., Kettler, B., von Forstner, C., Kneitz, C., Tepel, J., Adam, D., Wajant, H., Kalthoff, H., Trauzold, A., 2008. Anti-Tumor Necrosis Factor Therapy Inhibits Pancreatic Tumor Growth and Metastasis. *Cancer Res.* 68, 1443–1450. doi:10.1158/0008-5472.CAN-07-5704
- Eggert, T., Wolter, K., Ji, J., Ma, C., Yevsa, T., Klotz, S., Medina-Echeverz, J., Longerich, T., Forgues, M., Reisinger, F., Heikenwalder, M., Wang, X.W., Zender, L., Greten, T.F., 2016. Distinct Functions of Senescence-Associated Immune Responses in Liver Tumor Surveillance and Tumor Progression. *Cancer Cell* 30, 533–547. doi:10.1016/j.ccell.2016.09.003
- Ehrhardt, H., Fulda, S., Schmid, I., Hiscott, J., Debatin, K.-M., Jeremias, I., 2003. TRAIL induced survival and proliferation in cancer cells resistant towards TRAIL-induced apoptosis mediated by NF- κ B. *Oncogene* 22, 3842–3852. doi:10.1038/sj.onc.1206520
- Emery, J.G., McDonnell, P., Burke, M.B., Deen, K.C., Lyn, S., Silverman, C., Dul, E., Appelbaum, E.R., Eichman, C., DiPrinzio, R., Dodds, R.A., James, I.E., Rosenberg, M., Lee, J.C., Young, P.R., 1998. Osteoprotegerin Is a Receptor for the Cytotoxic Ligand TRAIL. *J. Biol. Chem.* 273, 14363–14367. doi:10.1074/jbc.273.23.14363
- Esposito, I., Penzel, R., Chaib-Harrireche, M., Barcena, U., Bergmann, F., Riedl, S., Kayed, H., Giese, N., Kleeff, J., Friess, H., Schirmacher, P., 2006. Tenascin C and annexin II expression in the process of pancreatic carcinogenesis. *J. Pathol.* 208, 673–685. doi:10.1002/path.1935
- Faissner, A., Roll, L., Theocharidis, U., 2016. Tenascin-C in the matrisome of neural stem and progenitor cells. *Mol. Cell. Neurosci.* doi:10.1016/j.mcn.2016.11.003
- Fan, Y., Bergmann, A., 2008. Apoptosis-induced compensatory proliferation. The Cell is dead. Long live the Cell! *Trends Cell Biol.* 18, 467–473. doi:10.1016/j.tcb.2008.08.001
- Feig, C., Gopinathan, A., Nesses, A., Chan, D.S., Cook, N., Tuveson, D.A., 2012. The pancreas cancer microenvironment. *Clin. Cancer Res.* 18, 4266–76. doi:10.1158/1078-0432.CCR-11-3114
- Fuller, K., Wong, B., Fox, S., Choi, Y., Chambers, T.J., 1998. TRANCE is necessary and sufficient for osteoblast-mediated activation of bone resorption in osteoclasts. *J. Exp. Med.* 188, 997–1001.
- Gallmeier, E., Bader, D.C., Kriegl, L., Berezowska, S., Seeliger, H., Göke, B., Kirchner, T., Bruns, C., De Toni, E.N., 2013. Loss of TRAIL-receptors is a recurrent feature in pancreatic cancer and determines the prognosis of patients with no nodal metastasis after surgery. *PLoS One* 8, e56760. doi:10.1371/journal.pone.0056760
- Galluzzi, L., Vitale, I., Abrams, J.M., Alnemri, E.S., Baehrecke, E.H., Blagosklonny, M.

- V, Dawson, T.M., Dawson, V.L., El-Deiry, W.S., Fulda, S., Gottlieb, E., Green, D.R., Hengartner, M.O., Kepp, O., Knight, R.A., Kumar, S., Lipton, S.A., Lu, X., Madeo, F., Malorni, W., Mehlen, P., Nuñez, G., Peter, M.E., Piacentini, M., Rubinsztein, D.C., Shi, Y., Simon, H.-U., Vandenabeele, P., White, E., Yuan, J., Zhivotovskiy, B., Melino, G., Kroemer, G., 2012. Molecular definitions of cell death subroutines: recommendations of the Nomenclature Committee on Cell Death 2012. *Cell Death Differ.* 19, 107–120. doi:10.1038/cdd.2011.96
- Ganten, T.M., Sykora, J., Koschny, R., Batke, E., Aulmann, S., Mansmann, U., Stremmel, W., Sinn, H.-P., Walczak, H., 2009. Prognostic significance of tumour necrosis factor-related apoptosis-inducing ligand (TRAIL) receptor expression in patients with breast cancer. *J. Mol. Med. (Berl)*. 87, 995–1007. doi:10.1007/s00109-009-0510-z
- Garg, A.D., Nowis, D., Golab, J., Vandenabeele, P., Krysko, D. V., Agostinis, P., 2010. Immunogenic cell death, DAMPs and anticancer therapeutics: An emerging amalgamation. *Biochim. Biophys. Acta - Rev. Cancer* 1805, 53–71. doi:10.1016/j.bbcan.2009.08.003
- Gebauer, F., Wicklein, D., Horst, J., Sundermann, P., Maar, H., Streichert, T., Tachezy, M., Izbicki, J.R., Bockhorn, M., Schumacher, U., 2014. Carcinoembryonic Antigen-Related Cell Adhesion Molecules (CEACAM) 1, 5 and 6 as Biomarkers in Pancreatic Cancer. *PLoS One* 9, e113023. doi:10.1371/journal.pone.0113023
- Genkinger, J.M., Spiegelman, D., Anderson, K.E., Bergkvist, L., Bernstein, L., van den Brandt, P.A., English, D.R., Freudenheim, J.L., Fuchs, C.S., Giles, G.G., Giovannucci, E., Hankinson, S.E., Horn-Ross, P.L., Leitzmann, M., Männistö, S., Marshall, J.R., McCullough, M.L., Miller, A.B., Reding, D.J., Robien, K., Rohan, T.E., Schatzkin, A., Stevens, V.L., Stolzenberg-Solomon, R.Z., Verhage, B.A.J., Wolk, A., Ziegler, R.G., Smith-Warner, S.A., 2009. Alcohol intake and pancreatic cancer risk: a pooled analysis of fourteen cohort studies. *Cancer Epidemiol. Biomarkers Prev.* 18, 765–776. doi:10.1158/1055-9965.EPI-08-0880
- Gold, P., Freedman, S.O., 1965. Specific carcinoembryonic antigens of the human digestive system. *J. Exp. Med.* 122, 467–81.
- Griffith, T.S., Wiley, S.R., Kubin, M.Z., Sedger, L.M., Maliszewski, C.R., Fanger, N.A., 1999. Monocyte-mediated tumoricidal activity via the tumor necrosis factor-related cytokine, TRAIL. *J. Exp. Med.* 189, 1343–54.
- Gu, X., Lu, C., He, D., Lu, Y., Jin, J., Liu, D., Ma, X., 2016. Notch3 negatively regulates chemoresistance in breast cancers. *Tumor Biol.* doi:10.1007/s13277-016-5412-4
- Guo, J., Xie, K., Zheng, S., 2016. Molecular Biomarkers of Pancreatic Intraepithelial Neoplasia and Their Implications in Early Diagnosis and Therapeutic Intervention of Pancreatic Cancer. *Int. J. Biol. Sci.* 12, 292–301. doi:10.7150/ijbs.14995
- Gurtner, G.C., Werner, S., Barrandon, Y., Longaker, M.T., 2008. Wound repair and regeneration. *Nature* 453, 314–321. doi:10.1038/nature07039

- Gysin, S., Rickert, P., Kastury, K., McMahon, M., 2005. Analysis of genomic DNA alterations and mRNA expression patterns in a panel of human pancreatic cancer cell lines. *Genes, Chromosom. Cancer* 44, 37–51. doi:10.1002/gcc.20216
- Hamada, S., Masamune, A., Shimosegawa, T., 2013. Novel therapeutic strategies targeting tumor-stromal interactions in pancreatic cancer. *Front. Physiol.* 4, 331. doi:10.3389/fphys.2013.00331
- Hanahan, D., Weinberg, R.A., 2011. Hallmarks of cancer: the next generation. *Cell* 144, 646–74. doi:10.1016/j.cell.2011.02.013
- Hasel, C., Dürr, S., Rau, B., Sträter, J., Schmid, R.M., Walczak, H., Bachem, M.G., Möller, P., 2003. In Chronic Pancreatitis, Widespread Emergence of TRAIL Receptors in Epithelia Coincides with Neoeexpression of TRAIL by Pancreatic Stellate Cells of Early Fibrotic Areas. *Lab. Investig.* 83, 825–836. doi:10.1097/01.LAB.0000073126.56932.46
- Haselmann, V., Kurz, A., Bertsch, U., Hübner, S., Olempska-Müller, M., Fritsch, J., Häslér, R., Pickl, A., Fritsche, H., Annewanter, F., Engler, C., Fleig, B., Bernt, A., Röder, C., Schmidt, H., Gelhaus, C., Hauser, C., Egberts, J.-H., Heneweer, C., Rohde, A.M., Böger, C., Knippschild, U., Röcken, C., Adam, D., Walczak, H., Schütze, S., Janssen, O., Wulczyn, F.G., Wajant, H., Kalthoff, H., Trauzold, A., 2014. Nuclear death receptor TRAIL-R2 inhibits maturation of let-7 and promotes proliferation of pancreatic and other tumor cells. *Gastroenterology* 146, 278–90. doi:10.1053/j.gastro.2013.10.009
- He, S., Lu, Y., Liu, X., Huang, X., Keller, E.T., Qian, C.-N., Zhang, J., 2015. Wnt3a: functions and implications in cancer. *Chin. J. Cancer* 34, 554–62. doi:10.1186/s40880-015-0052-4
- Heiblig, M., Sobh, M., Nicolini, F.E., 2014. Subcutaneous omacetaxine mepesuccinate in patients with chronic myeloid leukemia in tyrosine kinase inhibitor-resistant patients: Review and perspectives. *Leuk. Res.* 38, 1145–1153. doi:10.1016/j.leukres.2014.05.007
- Hidalgo, M., Cascinu, S., Kleeff, J., Labianca, R., Löhner, J.-M., Neoptolemos, J., Real, F.X., Van Laethem, J.-L., Heinemann, V., 2015. Addressing the challenges of pancreatic cancer: future directions for improving outcomes. *Pancreatology* 15, 8–18. doi:10.1016/j.pan.2014.10.001
- Hinz, S., Trauzold, A., Boenicke, L., Sandberg, C., Beckmann, S., Bayer, E., Walczak, H., Kalthoff, H., Ungefroren, H., 2000. Bcl-X L protects pancreatic adenocarcinoma cells against CD95- and TRAIL-receptor-mediated apoptosis. *Oncogene* 19, 5477–5486.
- Hinz, S., Trauzold, A., Boenicke, L., Sandberg, C., Beckmann, S., Bayer, E., Walczak, H., Kalthoff, H., Ungefroren, H., 2000. Bcl-XL protects pancreatic adenocarcinoma cells against CD95- and TRAIL-receptor-mediated apoptosis. *Oncogene* 19, 5477–86. doi:10.1038/sj.onc.1203936

- Hollingsworth, M.A., Swanson, B.J., 2004. Mucins in cancer: protection and control of the cell surface. *Nat. Rev. Cancer* 4, 45–60. doi:10.1038/nrc1251
- Holmer, R., Goumas, F.A., Waetzig, G.H., Rose-John, S., Kalthoff, H., 2014. Interleukin-6: a villain in the drama of pancreatic cancer development and progression. *Hepatobiliary Pancreat. Dis. Int.* 13, 371–380. doi:10.1016/S1499-3872(14)60259-9
- Hong, K.P., Shin, M.H., Yoon, S., Ji, G.Y., Moon, Y.R., Lee, O.-J., Choi, S.-Y., Lee, Y.-M., Koo, J.H., Lee, H.-C., Lee, G.K., Kim, S.R., Lee, K.H., Han, H.-S., Choe, K.H., Lee, K.M., Hong, J.-M., Kim, S.-W., Yi, J.H., Ji, H.-J., Kim, Y.-B., Song, H.G., 2015. Therapeutic effect of anti CEACAM6 monoclonal antibody against lung adenocarcinoma by enhancing anoikis sensitivity. *Biomaterials* 67, 32–41. doi:10.1016/j.biomaterials.2015.07.012
- Horinouchi, M., Nagata, K., Nakamura, A., Goto, M., Takao, S., Sakamoto, M., Fukushima, N., Miwa, A., Irimura, T., Imai, K., Sato, E., Yonezawa, S., 2003. Expression of Different Glycoforms of Membrane Mucin(MUC1) and Secretory Mucin (MUC2, MUC5AC and MUC6) in Pancreatic Neoplasms. *ACTA Histochem. Cytochem.* 36, 443–453. doi:10.1267/ahc.36.443
- Iliopoulos, D., Hirsch, H.A., Struhl, K., 2009. An epigenetic switch involving NF-kappaB, Lin28, Let-7 MicroRNA, and IL6 links inflammation to cell transformation. *Cell* 139, 693–706. doi:10.1016/j.cell.2009.10.014
- Ito, T., Kudoh, S., Ichimura, T., Fujino, K., Hassan, W.A.M.A., Udaka, N., 2016. Small cell lung cancer, an epithelial to mesenchymal transition (EMT)-like cancer: significance of inactive Notch signaling and expression of achaete-scute complex homologue 1. *Hum. Cell.* doi:10.1007/s13577-016-0149-3
- Jablonska, E., Kiersnowska-Rogowska, B., Aleksandrowicz-Bukin, M., Rogowski, F., Sawicka-Powierza, J., 2008. TRAIL receptors in the serum of patients with B-cell chronic lymphocytic leukemia. *Neoplasma* 55, 51–4.
- Jin, Z., El-Deiry, W.S., 2005. Overview of cell death signaling pathways. *Cancer Biol. Ther.* 4, 139–63.
- Jonckheere, N., Lahdaoui, F., Van Seuning, I., 2015. Targeting MUC4 in pancreatic cancer: miRNAs. *Oncoscience* 2, 799–800.
- Jones, S., Zhang, X., Parsons, D.W., Lin, J.C.-H., Leary, R.J., Angenendt, P., Mankoo, P., Carter, H., Kamiyama, H., Jimeno, A., Hong, S.-M., Fu, B., Lin, M.-T., Calhoun, E.S., Kamiyama, M., Walter, K., Nikolskaya, T., Nikolsky, Y., Hartigan, J., Smith, D.R., Hidalgo, M., Leach, S.D., Klein, A.P., Jaffee, E.M., Goggins, M., Maitra, A., Iacobuzio-Donahue, C., Eshleman, J.R., Kern, S.E., Hruban, R.H., Karchin, R., Papadopoulos, N., Parmigiani, G., Vogelstein, B., Velculescu, V.E., Kinzler, K.W., 2008. Core signaling pathways in human pancreatic cancers revealed by global genomic analyses. *Science* (80-.). 321, 1801–1806. doi:10.1126/science.1164368

-
- Kaczmarek, A., Vandenabeele, P., Krysko, D.V., 2013. Necroptosis: The Release of Damage-Associated Molecular Patterns and Its Physiological Relevance. *Immunity* 38, 209–223. doi:10.1016/j.immuni.2013.02.003
- Kaimal, V., Bardes, E.E., Tabar, S.C., Jegga, A.G., Aronow, B.J., 2010. ToppCluster: a multiple gene list feature analyzer for comparative enrichment clustering and network-based dissection of biological systems. *Nucleic Acids Res.* 38, W96-102. doi:10.1093/nar/gkq418
- Katoh, M., 2001. Differential regulation of WNT2 and WNT2B expression in human cancer. *Int. J. Mol. Med.* 8, 657–60.
- Keller, E.T., Brown, J., 2004. Prostate cancer bone metastases promote both osteolytic and osteoblastic activity. *J. Cell. Biochem.* 91, 718–29. doi:10.1002/jcb.10662
- Kelley, R.F., Totpal, K., Lindstrom, S.H., Mathieu, M., Billeci, K., Deforge, L., Pai, R., Hymowitz, S.G., Ashkenazi, A., 2005. Receptor-selective mutants of apoptosis-inducing ligand 2/tumor necrosis factor-related apoptosis-inducing ligand reveal a greater contribution of death receptor (DR) 5 than DR4 to apoptosis signaling. *J. Biol. Chem.* 280, 2205–12. doi:10.1074/jbc.M410660200
- Kiss, N.B., Muth, A., Andreasson, A., Juhlin, C.C., Geli, J., Bäckdahl, M., Höög, A., Wängberg, B., Nilsson, O., Ahlman, H., Larsson, C., 2013. Acquired hypermethylation of the P16INK4A promoter in abdominal paraganglioma: relation to adverse tumor phenotype and predisposing mutation. *Endocr. Relat. Cancer* 20, 65–78. doi:10.1530/ERC-12-0267
- Kojima, Y., Nakayama, M., Nishina, T., Nakano, H., Koyanagi, M., Takeda, K., Okumura, K., Yagita, H., 2011. Importin β 1 protein-mediated nuclear localization of death receptor 5 (DR5) limits DR5/tumor necrosis factor (TNF)-related apoptosis-inducing ligand (TRAIL)-induced cell death of human tumor cells. *J. Biol. Chem.* 286, 43383–93. doi:10.1074/jbc.M111.309377
- Kondo, S., Senoo-Matsuda, N., Hiromi, Y., Miura, M., 2006. DRONC coordinates cell death and compensatory proliferation. *Mol. Cell. Biol.* 26, 7258–68. doi:10.1128/MCB.00183-06
- Koopman Van Aarsen, L.A., Leone, D.R., Ho, S., Dolinski, B.M., McCoon, P.E., LePage, D.J., Kelly, R., Heaney, G., Rayhorn, P., Reid, C., Simon, K.J., Horan, G.S., Tao, N., Gardner, H.A., Skelly, M.M., Gown, A.M., Thomas, G.J., Weinreb, P.H., Fawell, S.E., Violette, S.M., 2008. Antibody-Mediated Blockade of Integrin α 6 Inhibits Tumor Progression In vivo by a Transforming Growth Factor- β -Regulated Mechanism. *Cancer Res.* 68, 561–570. doi:10.1158/0008-5472.CAN-07-2307
- Koschny, R., Krupp, W., Xu, L.-X., Mueller, W.C., Bauer, M., Sinn, P., Keller, M., Koschny, T., Walczak, H., Bruckner, T., Ganten, T.M., Holland, H., 2015. WHO grade related expression of TRAIL-receptors and apoptosis regulators in meningioma. *Pathol. Res. Pract.* 211, 109–16. doi:10.1016/j.prp.2014.11.002
-

- Kren, A., Baeriswyl, V., Lehembre, F., Wunderlin, C., Strittmatter, K., Antoniadis, H., Fässler, R., Cavallaro, U., Christofori, G., 2007. Increased tumor cell dissemination and cellular senescence in the absence of beta1-integrin function. *EMBO J.* 26, 2832–42. doi:10.1038/sj.emboj.7601738
- Krieg, A., Schulte am Esch, J., Ramp, U., Hosch, S.B., Knoefel, W.T., Gabbert, H.E., Mahotka, C., 2006. TRAIL-R4-beta: a new splice variant of TRAIL-receptor 4 lacking the cysteine rich domain 1. *Biochem. Biophys. Res. Commun.* 349, 115–21. doi:10.1016/j.bbrc.2006.08.031
- Kriegel, L., Jung, A., Engel, J., Jackstadt, R., Gerbes, A.L., Gallmeier, E., Reiche, J.A., Hermeking, H., Rizzani, A., Bruns, C.J., Kolligs, F.T., Kirchner, T., Göke, B., De Toni, E.N., 2010. Expression, cellular distribution, and prognostic relevance of TRAIL receptors in hepatocellular carcinoma. *Clin. Cancer Res.* 16, 5529–38. doi:10.1158/1078-0432.CCR-09-3403
- Krtolica, A., Parrinello, S., Lockett, S., Desprez, P.Y., Campisi, J., 2001. Senescent fibroblasts promote epithelial cell growth and tumorigenesis: a link between cancer and aging. *Proc. Natl. Acad. Sci. U. S. A.* 98, 12072–7. doi:10.1073/pnas.211053698
- Kufe, D.W., 2009. Mucins in cancer: function, prognosis and therapy. *Nat. Rev. Cancer* 9, 874–85. doi:10.1038/nrc2761
- Kuhlmann, L., Nadler, W.M., Kerner, A., Hanke, S.A., Noll, E.M., Eisen, C., Espinet, E., Vogel, V., Trumpp, A., Sprick, M.R., Roesli, C.P., 2016. Identification and Validation of Novel Subtype-Specific Protein Biomarkers in Pancreatic Ductal Adenocarcinoma. *Pancreas* 1. doi:10.1097/MPA.0000000000000743
- Labovsky, V., Martinez, L.M., Calcagno, M. de L., Davies, K.M., García-Rivello, H., Wernicke, A., Feldman, L., Giorello, M.B., Matas, A., Borzone, F.R., Howard, S.C., Chasseing, N.A., 2016. Interleukin-6 receptor in spindle-shaped stromal cells, a prognostic determinant of early breast cancer. *Tumor Biol.* 37, 13377–13384. doi:10.1007/s13277-016-5268-7
- Lacey, D., Timms, E., Tan, H.-L., Kelley, M., Dunstan, C., Burgess, T., Elliott, R., Colombero, A., Elliott, G., Scully, S., Hsu, H., Sullivan, J., Hawkins, N., Davy, E., Capparelli, C., Eli, A., Qian, Y.-X., Kaufman, S., Sarosi, I., Shalhoub, V., Senaldi, G., Guo, J., Delaney, J., Boyle, W., 1998. Osteoprotegerin Ligand Is a Cytokine that Regulates Osteoclast Differentiation and Activation. *Cell* 93, 165–176. doi:10.1016/S0092-8674(00)81569-X
- Lalaoui, N., Morlé, A., Mérino, D., Jacquemin, G., Iessi, E., Morizot, A., Shirley, S., Robert, B., Solary, E., Garrido, C., Micheau, O., 2011. TRAIL-R4 promotes tumor growth and resistance to apoptosis in cervical carcinoma HeLa cells through AKT. *PLoS One* 6, e19679. doi:10.1371/journal.pone.0019679
- Lau, D.T., Hesson, L.B., Norris, M.D., Marshall, G.M., Haber, M., Ashton, L.J., 2012. Prognostic Significance of Promoter DNA Methylation in Patients with Childhood

- Neuroblastoma. *Clin. Cancer Res.* 18.
- LeBlanc, H.N., Ashkenazi, A., 2003. Apo2L/TRAIL and its death and decoy receptors. *Cell Death Differ.* 10, 66–75. doi:10.1038/sj.cdd.4401187
- Legate, K.R., Wickstrom, S.A., Fassler, R., 2009. Genetic and cell biological analysis of integrin outside-in signaling. *Genes Dev.* 23, 397–418. doi:10.1101/gad.1758709
- Lemke, J., Noack, A., Adam, D., Tchikov, V., Bertsch, U., Röder, C., Schütze, S., Wajant, H., Kalthoff, H., Trauzold, A., 2010. TRAIL signaling is mediated by DR4 in pancreatic tumor cells despite the expression of functional DR5. *J. Mol. Med.* 88, 729–740. doi:10.1007/s00109-010-0619-0
- Lemke, J., von Karstedt, S., Zinngrebe, J., Walczak, H., 2014. Getting TRAIL back on track for cancer therapy. *Cell Death Differ.* 21, 1350–64. doi:10.1038/cdd.2014.81
- Li, F., Huang, Q., Chen, J., Peng, Y., Roop, D.R., Bedford, J.S., Li, C.-Y., 2010. Apoptotic cells activate the “phoenix rising” pathway to promote wound healing and tissue regeneration. *Sci. Signal.* 3, ra13. doi:10.1126/scisignal.2000634
- Li, X., Ma, Q., Xu, Q., Duan, W., Lei, J., Wu, E., 2012. Targeting the cancer-stroma interaction: a potential approach for pancreatic cancer treatment. *Curr. Pharm. Des.* 18, 2404–15.
- Li, Z., Hu, D.-Y., Chu, Q., Wu, J.-H., Gao, C., Zhang, Y.-Q., Huang, Y.-R., 2004. Cell apoptosis and regeneration of hepatocellular carcinoma after transarterial chemoembolization. *World J. Gastroenterol.* 10, 1876–80. doi:10.3748/wjg.v10.i13.1876
- Liao, Q., Friess, H., Kleeff, J., Büchler, M.W., 2001. Differential expression of TRAIL-R3 and TRAIL-R4 in human pancreatic cancer. *Anticancer Res.* 21, 3153–9.
- Livak, K.J., Schmittgen, T.D., 2001. Analysis of Relative Gene Expression Data Using Real-Time Quantitative PCR and the $2^{-\Delta\Delta C_T}$ Method. *METHODS* 25, 402–408. doi:10.1006
- López-Gómez, C., Oliver-Martos, B., Pinto-Medel, M.-J., Suardiaz, M., Reyes-Garrido, V., Urbaneja, P., Fernández, Ó., Leyva, L., 2016. TRAIL and TRAIL receptors splice variants during long-term interferon β treatment of patients with multiple sclerosis: evaluation as biomarkers for therapeutic response. *J. Neurol. Neurosurg. Psychiatry* 87, 130–7. doi:10.1136/jnnp-2014-309932
- Lu, M., Marsters, S., Ye, X., Luis, E., Gonzalez, L., Ashkenazi, A., 2014. E-Cadherin Couples Death Receptors to the Cytoskeleton to Regulate Apoptosis. *Mol. Cell* 54, 987–998. doi:10.1016/j.molcel.2014.04.029
- Lüttges, J., Feyerabend, B., Buchelt, T., Pacena, M., Klöppel, G., 2002. The mucin profile of noninvasive and invasive mucinous cystic neoplasms of the pancreas. *Am. J. Surg.*

- Pathol. 26, 466–71.
- Mace, T.A., Shakya, R., Pitarresi, J.R., Swanson, B., McQuinn, C.W., Loftus, S., Nordquist, E., Cruz-Monserrate, Z., Yu, L., Young, G., Zhong, X., Zimmers, T.A., Ostrowski, M.C., Ludwig, T., Bloomston, M., Bekaii-Saab, T., Lesinski, G.B., 2016. IL-6 and PD-L1 antibody blockade combination therapy reduces tumour progression in murine models of pancreatic cancer. *Gut* *gutjnl-2016-311585*. doi:10.1136/gutjnl-2016-311585
- Mackie, E.J., Chiquet-Ehrismann, R., Pearson, C.A., Inaguma, Y., Taya, K., Kawarada, Y., Sakakura, T., 1987. Tenascin is a stromal marker for epithelial malignancy in the mammary gland. *Proc. Natl. Acad. Sci. U. S. A.* 84, 4621–5.
- Mahajan, S., Dammai, V., Hsu, T., Kraft, A.S., 2008. Hypoxia-inducible factor-2alpha regulates the expression of TRAIL receptor DR5 in renal cancer cells. *Carcinogenesis* 29, 1734–41. doi:10.1093/carcin/bgn132
- Malvezzi, M., Carioli, G., Bertuccio, P., Boffetta, P., Levi, F., La Vecchia, C., Negri, E., 2017. European cancer mortality predictions for the year 2017, with focus on lung cancer. *Ann. Oncol.* doi:10.1093/annonc/mdx033
- Marechal, R., Bachet, J.-B., Calomme, A., Demetter, P., Delpero, J.R., Svrcek, M., Cros, J., Bardier-Dupas, A., Puleo, F., Monges, G., Hammel, P., Louvet, C., Paye, F., Bachelier, P., Le Treut, Y.P., Vaillant, J.-C., Sauvanet, A., Andre, T., Salmon, I., Deviere, J., Emile, J.-F., Van Laethem, J.-L., 2015. Sonic Hedgehog and Gli1 Expression Predict Outcome in Resected Pancreatic Adenocarcinoma. *Clin. Cancer Res.* 21, 1215–1224. doi:10.1158/1078-0432.CCR-14-0667
- Marsters, S.A., Sheridan, J.P., Pitti, R.M., Huang, A., Skubatch, M., Baldwin, D., Yuan, J., Gurney, A., Goddard, A.D., Godowski, P., Ashkenazi, A., 1997. A novel receptor for Apo2L/TRAIL contains a truncated death domain. *Curr. Biol.* 7, 1003–1006. doi:10.1016/S0960-9822(06)00422-2
- Maslov, A.Y., Vijg, J., 2009. Genome instability, cancer and aging. *Biochim. Biophys. Acta* 1790, 963–9. doi:10.1016/j.bbagen.2009.03.020
- McCabe, N.P., De, S., Vasanji, A., Brainard, J., Byzova, T. V, 2007. Prostate cancer specific integrin alphavbeta3 modulates bone metastatic growth and tissue remodeling. *Oncogene* 26, 6238–43. doi:10.1038/sj.onc.1210429
- McConkey, D.J., Choi, W., Marquis, L., Martin, F., Williams, M.B., Shah, J., Svatek, R., Das, A., Adam, L., Kamat, A., Siefker-Radtke, A., Dinney, C., 2009. Role of epithelial-to-mesenchymal transition (EMT) in drug sensitivity and metastasis in bladder cancer. *Cancer Metastasis Rev.* 28, 335–344. doi:10.1007/s10555-009-9194-7
- Mego, M., Cierna, Z., Janega, P., Karaba, M., Minarik, G., Benca, J., Sedláčková, T., Sieberova, G., Gronesova, P., Manasova, D., Pindak, D., Sufliarsky, J., Danihel, L., Reuben, J., Mardiak, J., 2015. Relationship between circulating tumor cells and

- epithelial to mesenchymal transition in early breast cancer. *BMC Cancer* 15, 533. doi:10.1186/s12885-015-1548-7
- Meng, R.D., McDonald, E.R., Sheikh, M.S., Fornace, A.J., El-Deiry, W.S., 2000. The TRAIL decoy receptor TRUNDD (DcR2, TRAIL-R4) is induced by adenovirus-p53 overexpression and can delay TRAIL-, p53-, and KILLER/DR5-dependent colon cancer apoptosis. *Mol. Ther.* 1, 130–44. doi:10.1006/mthe.2000.0025
- Mérino, D., Lalaoui, N., Morizot, A., Schneider, P., Solary, E., Micheau, O., 2006. Differential inhibition of TRAIL-mediated DR5-DISC formation by decoy receptors 1 and 2. *Mol. Cell. Biol.* 26, 7046–7055. doi:10.1128/MCB.00520-06
- Mérino, D., Lalaoui, N., Morizot, A., Solary, E., Micheau, O., 2007. TRAIL in cancer therapy: present and future challenges. *Expert Opin. Ther. Targets* 11, 1299–1314. doi:10.1517/14728222.11.10.1299
- Mert, U., Sanlioglu, A.D., 2016. Intracellular localization of DR5 and related regulatory pathways as a mechanism of resistance to TRAIL in cancer. *Cell. Mol. Life Sci.* doi:10.1007/s00018-016-2321-z
- Micheau, O., Shirley, S., Dufour, F., 2013. Death receptors as targets in cancer. *Br. J. Pharmacol.* 169, 1723–44. doi:10.1111/bph.12238
- Mielczarek-Palacz, A., Sikora, J., Kondera-Anasz, Z., 2015. Assessment of the concentration of sTRAIL ligand and its sTRAIL-R1 and sTRAIL-R2 receptors – markers monitoring the course of the extrinsic pathway of apoptosis induction - the potential involvement in ovarian cancer diagnostics. *Arch. Med. Sci.* doi:10.5114/aoms.2015.53144
- Mitsunaga, S., Ikeda, M., Shimizu, S., Ohno, I., Furuse, J., Inagaki, M., Higashi, S., Kato, H., Terao, K., Ochiai, A., 2013. Serum levels of IL-6 and IL-1 β can predict the efficacy of gemcitabine in patients with advanced pancreatic cancer. *Br. J. Cancer* 108, 2063–2069. doi:10.1038/bjc.2013.174
- Miura, T., Mitsunaga, S., Ikeda, M., Shimizu, S., Ohno, I., Takahashi, H., Furuse, J., Inagaki, M., Higashi, S., Kato, H., Terao, K., Ochiai, A., 2015. Characterization of Patients With Advanced Pancreatic Cancer and High Serum Interleukin-6 Levels. *Pancreas* 44, 756–763. doi:10.1097/MPA.0000000000000335
- Mocarski, E.S., Upton, J.W., Kaiser, W.J., 2011. Viral infection and the evolution of caspase 8-regulated apoptotic and necrotic death pathways. *Nat. Rev. Immunol.* doi:10.1038/nri3131
- Moore, P.S., Sipos, B., Orlandini, S., Sorio, C., Real, F.X., Lemoine, N.R., Gress, T., Bassi, C., Klöppel, G., Kalthoff, H., Ungefroren, H., Löhr, M., Scarpa, A., 2001. Genetic profile of 22 pancreatic carcinoma cell lines. Analysis of K-ras, p53, p16 and DPC4/Smad4. *Virchows Arch.* 439, 798–802.

- Morgan, R.T., Woods, L.K., Moore, G.E., Quinn, L.A., McGavran, L., Gordon, S.G., 1980. Human cell line (COLO 357) of metastatic pancreatic adenocarcinoma. *Int. J. Cancer* 25, 591–8.
- Morizot, A., Mérino, D., Lalaoui, N., Jacquemin, G., Granci, V., Iessi, E., Lanneau, D., Bouyer, F., Solary, E., Chauffert, B., Saas, P., Garrido, C., Micheau, O., 2011. Chemotherapy overcomes TRAIL-R4-mediated TRAIL resistance at the DISC level. *Cell Death Differ.* 18, 700–11. doi:10.1038/cdd.2010.144
- Mroczo, B., Groblewska, M., Gryko, M., Kędra, B., Szmitkowski, M., 2010. Diagnostic usefulness of serum interleukin 6 (IL-6) and C-reactive protein (CRP) in the differentiation between pancreatic cancer and chronic pancreatitis. *J. Clin. Lab. Anal.* 24, 256–261. doi:10.1002/jcla.20395
- Murphy, J.M., Czabotar, P.E., Hildebrand, J.M., Lucet, I.S., Zhang, J.-G., Alvarez-Diaz, S., Lewis, R., Lalaoui, N., Metcalf, D., Webb, A.I., Young, S.N., Varghese, L.N., Tannahill, G.M., Hatchell, E.C., Majewski, I.J., Okamoto, T., Dobson, R.C.J., Hilton, D.J., Babon, J.J., Nicola, N.A., Strasser, A., Silke, J., Alexander, W.S., 2013. The pseudokinase MLKL mediates necroptosis via a molecular switch mechanism. *Immunity* 39, 443–453. doi:10.1016/j.immuni.2013.06.018
- Narayanan, V., Weekes, C.D., 2016. Molecular therapeutics in pancreas cancer. *World J. Gastrointest. Oncol.* 8, 366–379. doi:10.4251/wjgo.v8.i4.366
- Neumann, S., Bidon, T., Branschädel, M., Krippner-Heidenreich, A., Scheurich, P., Doszczak, M., 2012. The transmembrane domains of TNF-related apoptosis-inducing ligand (TRAIL) receptors 1 and 2 co-regulate apoptotic signaling capacity. *PLoS One* 7, e42526. doi:10.1371/journal.pone.0042526
- Neumann, S., Hasenauer, J., Pollak, N., Scheurich, P., 2014. Dominant negative effects of tumor necrosis factor (TNF)-related apoptosis-inducing ligand (TRAIL) receptor 4 on TRAIL receptor 1 signaling by formation of heteromeric complexes. *J. Biol. Chem.* 289, 16576–87. doi:10.1074/jbc.M114.559468
- Nolan-Stevaux, O., Lau, J., Truitt, M.L., Chu, G.C., Hebrok, M., Fernández-Zapico, M.E., Hanahan, D., 2009. GLI1 is regulated through Smoothed-independent mechanisms in neoplastic pancreatic ducts and mediates PDAC cell survival and transformation. *Genes Dev.* 23, 24–36. doi:10.1101/gad.1753809
- Oberstein, P.E., Olive, K.P., 2013. Pancreatic cancer: why is it so hard to treat? *Therap. Adv. Gastroenterol.* 6, 321–337. doi:10.1177/1756283X13478680
- Okada, S., Okusaka, T., Ishii, H., Kyogoku, A., Yoshimori, M., Kajimura, N., Yamaguchi, K., Kakizoe, T., 1998. Elevated serum interleukin-6 levels in patients with pancreatic cancer. *Jpn. J. Clin. Oncol.* 28, 12–15. doi:10.1093/JJCO/28.1.12
- Ordoñez, C., Screatton, R.A., Ilantzis, C., Stanners, C.P., 2000. Human carcinoembryonic antigen functions as a general inhibitor of anoikis. *Cancer Res.* 60, 3419–24.

- Ordonez, C., Zhai, A.B., Camacho-Leal, P., Demarte, L., Fan, M.M.Y., Stanners, C.P., 2007. GPI-anchored CEA family glycoproteins CEA and CEACAM6 mediate their biological effects through enhanced integrin $\alpha 5\beta 1$ -fibronectin interaction. *J. Cell. Physiol.* 210, 757–765. doi:10.1002/jcp.20887
- Orend, G., Chiquet-Ehrismann, R., 2006. Tenascin-C induced signaling in cancer. *Cancer Lett.* 244, 143–163. doi:10.1016/j.canlet.2006.02.017
- Orzechowska, M., Jędroszka, D., Bednarek, A.K., 2016. Common profiles of Notch signaling differentiate disease-free survival in luminal type A and triple negative breast cancer. *Oncotarget.* doi:10.18632/oncotarget.13451
- Oztas, E., Ozler, S., Ersoy, A.O., Ersoy, E., Caglar, A.T., Uygur, D., Yucel, A., Ergin, M., Danisman, N., 2016. Decreased placental and maternal serum TRAIL-R2 levels are associated with placenta accreta. *Placenta* 39, 1–6. doi:10.1016/j.placenta.2016.01.004
- Pan, G., 1997. An Antagonist Decoy Receptor and a Death Domain-Containing Receptor for TRAIL. *Science (80-.).* 277, 815–818. doi:10.1126/science.277.5327.815
- Pan, G., Ni, J., Yu, G., Wei, Y.-F., Dixit, V.M., 1998. TRUND, a new member of the TRAIL receptor family that antagonizes TRAIL signalling. *FEBS Lett.* 424, 41–45. doi:10.1016/S0014-5793(98)00135-5
- Pan, G., O'Rourke, K., Chinnaiyan, A.M., Gentz, R., Ebner, R., Ni, J., Dixit, V.M., 1997. The Receptor for the Cytotoxic Ligand TRAIL. *Science (80-.).* 276.
- Pare, R., Yang, T., Shin, J.-S., Lee, C.S., 2013. The significance of the senescence pathway in breast cancer progression. *J. Clin. Pathol.* 66, 491–495. doi:10.1136/jclinpath-2012-201081
- Park, J., Schwarzbauer, J.E., 2014. Mammary epithelial cell interactions with fibronectin stimulate epithelial-mesenchymal transition. *Oncogene* 33, 1649–1657. doi:10.1038/onc.2013.118
- Paron, I., Berchtold, S., Vörös, J., Shamarla, M., Erkan, M., Höfler, H., Esposito, I., 2011. Tenascin-C enhances pancreatic cancer cell growth and motility and affects cell adhesion through activation of the integrin pathway. *PLoS One* 6, e21684. doi:10.1371/journal.pone.0021684
- Pei, G.-T., Wu, C.-W., Lin, W.-W., 2010. Hypoxia-induced decoy receptor 2 gene expression is regulated via a hypoxia-inducible factor 1 α -mediated mechanism. *Biochem. Biophys. Res. Commun.* 391, 1274–9. doi:10.1016/j.bbrc.2009.12.058
- Pellettieri, J., Alvarado, A.S., 2007. Cell Turnover and Adult Tissue Homeostasis: From Humans to Planarians. *Annu. Rev. Genet.* 41, 83–105. doi:10.1146/annurev.genet.41.110306.130244

- Philipp, S., Sosna, J., Adam, D., 2016. Cancer and necroptosis: friend or foe? *Cell. Mol. Life Sci.* 73, 2183–2193. doi:10.1007/s00018-016-2193-2
- Philipp, S., Sosna, J., Plenge, J., Kalthoff, H., Adam, D., 2015. Homoharringtonine, a clinically approved anti-leukemia drug, sensitizes tumor cells for TRAIL-induced necroptosis. *Cell Commun. Signal.* 13, 25. doi:10.1186/s12964-015-0103-0
- Pickup, M.W., Mouw, J.K., Weaver, V.M., 2014. The extracellular matrix modulates the hallmarks of cancer. *EMBO Rep.* 15, 1243–53. doi:10.15252/embr.201439246
- Pinto, J.P., Kalathur, R.K., Oliveira, D. V, Barata, T., Machado, R.S.R., Machado, S., Pacheco-Leyva, I., Duarte, I., Futschik, M.E., 2015. StemChecker: a web-based tool to discover and explore stemness signatures in gene sets. *Nucleic Acids Res.* 43, W72-7. doi:10.1093/nar/gkv529
- Pitti, R.M., Marsters, S.A., Ruppert, S., Donahue, C.J., Moore, A., Ashkenazi, A., 1996. Induction of apoptosis by Apo-2 ligand, a new member of the tumor necrosis factor cytokine family. *J. Biol. Chem.* 271, 12687–90. doi:10.1074/JBC.271.22.12687
- Provenzano, P.P., Cuevas, C., Chang, A.E., Goel, V.K., Von Hoff, D.D., Hingorani, S.R., 2012. Enzymatic targeting of the stroma ablates physical barriers to treatment of pancreatic ductal adenocarcinoma. *Cancer Cell* 21, 418–429. doi:10.1016/j.ccr.2012.01.007
- Qi, L., Song, W., Liu, Z., Zhao, X., Cao, W., Sun, B., 2015. Wnt3a Promotes the Vasculogenic Mimicry Formation of Colon Cancer via Wnt/ β -Catenin Signaling. *Int. J. Mol. Sci.* 16, 18564–18579. doi:10.3390/ijms160818564
- Qi, L., Sun, B., Liu, Z., Cheng, R., Li, Y., Zhao, X., 2014. Wnt3a expression is associated with epithelial-mesenchymal transition and promotes colon cancer progression. *J. Exp. Clin. Cancer Res.* 33, 107. doi:10.1186/s13046-014-0107-4
- Qin, S., Li, Y., Cao, X., Du, J., Huang, X., 2016. NANOG regulates epithelial mesenchymal transition and chemoresistance in ovarian cancer. *Biosci. Rep.*
- Rahib, L., Smith, B.D., Aizenberg, R., Rosenzweig, A.B., Fleshman, J.M., Matrisian, L.M., 2014. Projecting cancer incidence and deaths to 2030: the unexpected burden of thyroid, liver, and pancreas cancers in the United States. *Cancer Res.* 74, 2913–21. doi:10.1158/0008-5472.CAN-14-0155
- Ratzinger, G., Mitteregger, S., Wolf, B., Berger, R., Zelger, B., Weinlich, G., Fritsch, P., Goebel, G., Fiegl, H., 2014. Association of TNFRSF10D DNA-methylation with the survival of melanoma patients. *Int. J. Mol. Sci.* 15, 11984–11995. doi:10.3390/ijms150711984
- Recio-Boiles, A., Ilmer, M., Rhea, P.R., Kettlun, C., Heinemann, M.L., Ruetering, J., Vykoukal, J., Alt, E., Recio-Boiles, A., Ilmer, M., Rhea, P.R., Kettlun, C., Heinemann, M.L., Ruetering, J., Vykoukal, J., Alt, E., 2016. JNK pathway inhibition

- selectively primes pancreatic cancer stem cells to TRAIL-induced apoptosis without affecting the physiology of normal tissue resident stem cells. *Oncotarget* 7, 9890–9906. doi:10.18632/oncotarget.7066
- Riccioni, R., Pasquini, L., Mariani, G., Saulle, E., Rossini, A., Diverio, D., Pelosi, E., Vitale, A., Chierichini, A., Cedrone, M., Foa, R., Lo Coco, F., Peschle, C., Testa, U., 2005. TRAIL decoy receptors mediate resistance of acute myeloid leukemia cells to TRAIL. *Haematologica* 90, 612–624.
- Rucki, A.A., Foley, K., Zhang, P., Xiao, Q., Kleponis, J., Wu, A.A., Sharma, R., Mo, G., Liu, A., Eyk, J. Van, Jaffee, E.M., Zheng, L., 2016. Heterogeneous stromal signaling within the tumor microenvironment controls the metastasis of pancreatic cancer. *Cancer Res.* doi:DOI: 10.1158/0008-5472.CAN-16-1383
- Ryoo, H.D., Gorenc, T., Steller, H., 2004. Apoptotic Cells Can Induce Compensatory Cell Proliferation through the JNK and the Wingless Signaling Pathways. *Dev. Cell* 7, 491–501. doi:10.1016/j.devcel.2004.08.019
- Sahin, I.H., Iacobuzio-Donahue, C.A., O'Reilly, E.M., 2016. Molecular signature of pancreatic adenocarcinoma: an insight from genotype to phenotype and challenges for targeted therapy. *Expert Opin. Ther. Targets* 20, 341–359. doi:10.1517/14728222.2016.1094057
- Salvesen, G.S., Duckett, C.S., 2002. Apoptosis: IAP proteins: blocking the road to death's door. *Nat. Rev. Mol. Cell Biol.* 3, 401–410. doi:10.1038/nrm830
- Sánchez-Lázaro, I.J., Almenar-Bonet, L., Romero-Pelechano, A., Portoles-Sanz, M., Martínez-Dolz, L., Roselló-Lleti, E., Ramón González-Juanatey, J., Rivera-Otero, M., Salvador-Sanz, A., 2012. Serum markers of apoptosis in the early period of heart transplantation. *Biomarkers* 17, 254–60. doi:10.3109/1354750X.2012.664168
- Sanlioglu, A.D., Dirice, E., Aydin, C., Erin, N., Koksoy, S., Sanlioglu, S., 2005. Surface TRAIL decoy receptor-4 expression is correlated with TRAIL resistance in MCF7 breast cancer cells. *BMC Cancer* 5, 54. doi:10.1186/1471-2407-5-54
- Sanlioglu, A.D., Dirice, E., Elpek, O., Korcum, A.F., Ozdogan, M., Suleymanlar, I., Balci, M.K., Griffith, T.S., Sanlioglu, S., 2009. High TRAIL death receptor 4 and decoy receptor 2 expression correlates with significant cell death in pancreatic ductal adenocarcinoma patients. *Pancreas* 38, 154–60. doi:10.1097/MPA.0b013e31818db9e3
- Sanlioglu, A.D., Karacay, B., Koksall, I.T., Griffith, T.S., Sanlioglu, S., 2007. DcR2 (TRAIL-R4) siRNA and adenovirus delivery of TRAIL (Ad5hTRAIL) break down in vitro tumorigenic potential of prostate carcinoma cells. *Cancer Gene Ther.* 14, 976–984. doi:10.1038/sj.cgt.7701087
- Sanlioglu, A.D., Korcum, A.F., Pestereli, E., Erdogan, G., Karaveli, S., Savas, B., Griffith, T.S., Sanlioglu, S., 2007. TRAIL Death Receptor–4 Expression Positively Correlates With the Tumor Grade in Breast Cancer Patients With Invasive Ductal Carcinoma.

- Int. J. Radiat. Oncol. 69, 716–723. doi:10.1016/j.ijrobp.2007.03.057
- Schliemann, C., Wiedmer, A., Pedretti, M., Szczepanowski, M., Klapper, W., Neri, D., 2009. Three clinical-stage tumor targeting antibodies reveal differential expression of oncofetal fibronectin and tenascin-C isoforms in human lymphoma. *Leuk. Res.* 33, 1718–22. doi:10.1016/j.leukres.2009.06.025
- Schölzel, S., Zimmermann, W., Schwarzkopf, G., Grunert, F., Rogaczewski, B., Thompson, J., 2000. Carcinoembryonic antigen family members CEACAM6 and CEACAM7 are differentially expressed in normal tissues and oppositely deregulated in hyperplastic colorectal polyps and early adenomas. *Am. J. Pathol.* 156, 595–605. doi:10.1016/S0002-9440(10)64764-5
- Screaton, G.R., Mongkolsapaya, J., Xu, X.-N., Cowper, A.E., McMichael, A.J., Bell, J.I., 1997. TRICK2, a new alternatively spliced receptor that transduces the cytotoxic signal from TRAIL. *Curr. Biol.* 7, 693–696. doi:10.1016/S0960-9822(06)00297-1
- Shall, S., de Murcia, G., 2000. Poly(ADP-ribose) polymerase-1: what have we learned from the deficient mouse model? *Mutat. Res.* 460, 1–15.
- Shen, R., Wang, Q., Cheng, S., Liu, T., Jiang, H., Zhu, J., Wu, Y., Wang, L., 2013. The biological features of PanIN initiated from oncogenic Kras mutation in genetically engineered mouse models. *Cancer Lett.* 339, 135–143. doi:10.1016/j.canlet.2013.07.010
- Sheridan, J.P., Marsters, S.A., Pitti, R.M., Gurney, A., Skubatch, M., Baldwin, D., Ramakrishnan, L., Gray, C.L., Baker, K., Wood, W.I., Goddard, A.D., Godowski, P., Ashkenazi, A., 1997. Control of TRAIL-Induced Apoptosis by a Family of Signaling and Decoy Receptors. *Science* (80-). 277.
- Shibue, T., Weinberg, R.A., 2009. Integrin beta1-focal adhesion kinase signaling directs the proliferation of metastatic cancer cells disseminated in the lungs. *Proc. Natl. Acad. Sci. U. S. A.* 106, 10290–5. doi:10.1073/pnas.0904227106
- Shivapurkar, N., Toyooka, S., Toyooka, K.O., Reddy, J., Miyajima, K., Suzuki, M., Shigematsu, H., Takahashi, T., Parikh, G., Pass, H.I., Chaudhary, P.M., Gazdar, A.F., 2004. Aberrant methylation of trail decoy receptor genes is frequent in multiple tumor types. *Int. J. Cancer* 109, 786–92. doi:10.1002/ijc.20041
- Siegel, R.L., Miller, K.D., Jemal, A., 2017. Cancer statistics, 2017. *CA. Cancer J. Clin.* 67, 7–30. doi:10.3322/caac.21387
- Siegmund, D., Lang, I., Wajant, H., 2016. Cell death-independent activities of the death receptors CD95, TRAILR1 and TRAILR2. *FEBS J.* doi:10.1111/febs.13968
- Singer, B.B., Scheffrahn, I., Kammerer, R., Suttorp, N., Ergun, S., Slevogt, H., 2010. Deregulation of the CEACAM Expression Pattern Causes Undifferentiated Cell Growth in Human Lung Adenocarcinoma Cells. *PLoS One* 5, e8747.

doi:10.1371/journal.pone.0008747

- Soldani, C., Scovassi, A.I., 2002. Poly(ADP-ribose) polymerase-1 cleavage during apoptosis: an update. *Apoptosis* 7, 321–8.
- Sosna, J., Philipp, S., Fuchslocher Chico, J., Saggau, C., Fritsch, J., Föll, A., Plenge, J., Arenz, C., Pinkert, T., Kalthoff, H., Trauzold, A., Schmitz, I., Schütze, S., Adam, D., 2016. Differences and Similarities in TRAIL- and Tumor Necrosis Factor-Mediated Necroptotic Signaling in Cancer Cells. *Mol. Cell. Biol.* 36, 2626–2644. doi:10.1128/MCB.00941-15
- Srivastava, R.K., 2001. TRAIL/Apo-2L: mechanisms and clinical applications in cancer. *Neoplasia* 3, 535–46. doi:10.1038/sj/neo/7900203
- Stamenkovic, V., Stamenkovic, S., Jaworski, T., Gawlak, M., Jovanovic, M., Jakovcevski, I., Wilczynski, G.M., Kaczmarek, L., Schachner, M., Radenovic, L., Andjus, P.R., 2016. The extracellular matrix glycoprotein tenascin-C and matrix metalloproteinases modify cerebellar structural plasticity by exposure to an enriched environment. *Brain Struct. Funct.* 1–23. doi:10.1007/s00429-016-1224-y
- Sun, L., Wang, H., Wang, Z., He, S., Chen, S., Liao, D., Wang, L., Yan, J., Liu, W., Lei, X., Wang, X., 2012. Mixed lineage kinase domain-like protein mediates necrosis signaling downstream of RIP3 kinase. *Cell* 148, 213–27. doi:10.1016/j.cell.2011.11.031
- Sun, X.-J., Jiang, T.-H., Zhang, X.-P., Mao, A.-W., 2016. Role of the tumor microenvironment in pancreatic adenocarcinoma. *Front. Biosci. (Landmark Ed.)* 21, 31–41.
- Suyama, K., Shapiro, I., Guttman, M., Hazan, R.B., 2002. A signaling pathway leading to metastasis is controlled by N-cadherin and the FGF receptor. *Cancer Cell* 2, 301–14.
- Tacutu, R., Craig, T., Budovsky, A., Wuttke, D., Lehmann, G., Taranukha, D., Costa, J., Fraifeld, V.E., de Magalhães, J.P., 2013. Human Ageing Genomic Resources: integrated databases and tools for the biology and genetics of ageing. *Nucleic Acids Res.* 41, D1027-33. doi:10.1093/nar/gks1155
- Takeda K, Hayakawa Y, Smyth MJ, Kayagaki N, Yamaguchi N, Kakuta S, Iwakura Y, Yagita H, Okumura K, 2001. Involvement of tumor necrosis factor-related apoptosis-inducing ligand in surveillance of tumor metastasis by liver natural killer cells. *Nat. Med.* 7, 94–100.
- Tanase, C.P., Neagu, A.I., Necula, L.G., Mambet, C., Enciu, A.-M., Calenic, B., Cruceru, M.L., Albulescu, R., 2014. Cancer stem cells: involvement in pancreatic cancer pathogenesis and perspectives on cancer therapeutics. *World J. Gastroenterol.* 20, 10790–801. doi:10.3748/wjg.v20.i31.10790
- Tchoupa, A., Schuhmacher, T., Hauck, C.R., 2014. Signaling by epithelial members of the

- CEACAM family – mucosal docking sites for pathogenic bacteria. *Cell Commun. Signal.* 12, 27. doi:10.1186/1478-811X-12-27
- Tian, H., Callahan, C.A., DuPree, K.J., Darbonne, W.C., Ahn, C.P., Scales, S.J., de Sauvage, F.J., 2009. Hedgehog signaling is restricted to the stromal compartment during pancreatic carcinogenesis. *Proc. Natl. Acad. Sci. U. S. A.* 106, 4254–4259. doi:10.1073/pnas.0813203106
- Todorova, T., Bock, F.J., Chang, P., 2014. PARP13 regulates cellular mRNA post-transcriptionally and functions as a pro-apoptotic factor by destabilizing TRAILR4 transcript. *Nat. Commun.* 5, 5362. doi:10.1038/ncomms6362
- Torre, L.A., Bray, F., Siegel, R.L., Ferlay, J., Lortet-Tieulent, J., Jemal, A., 2015. Global cancer statistics, 2012. *CA. Cancer J. Clin.* 65, 87–108. doi:10.3322/caac.21262
- Tozluoğlu, M., Tournier, A.L., Jenkins, R.P., Hooper, S., Bates, P.A., Sahai, E., 2013. Matrix geometry determines optimal cancer cell migration strategy and modulates response to interventions. *Nat. Cell Biol.* 15, 751–62. doi:10.1038/ncb2775
- Trauzold, A., Schmiedel, S., Röder, C., Tams, C., Christgen, M., Oestern, S., Arlt, A., Westphal, S., Kapischke, M., Ungefroren, H., Kalthoff, H., 2003. Multiple and synergistic deregulations of apoptosis-controlling genes in pancreatic carcinoma cells. *Br. J. Cancer* 89, 1714–21. doi:10.1038/sj.bjc.6601330
- Trauzold, A., Siegmund, D., Schniewind, B., Sipos, B., Egberts, J., Zorenkov, D., Emme, D., Röder, C., Kalthoff, H., Wajant, H., 2006. TRAIL promotes metastasis of human pancreatic ductal adenocarcinoma. *Oncogene* 25, 7434–9. doi:10.1038/sj.onc.1209719
- Trauzold, A., Wermann, H., Arlt, A., Schütze, S., Schäfer, H., Oestern, S., Röder, C., Ungefroren, H., Lampe, E., Heinrich, M., Walczak, H., Kalthoff, H., 2001. CD95 and TRAIL receptor-mediated activation of protein kinase C and NF-kappaB contributes to apoptosis resistance in ductal pancreatic adenocarcinoma cells. *Oncogene* 20, 4258–69. doi:10.1038/sj.onc.1204559
- Turner, C.E., 2000. Paxillin and focal adhesion signalling 2, E231–E236. doi:10.1038/35046659
- van Noesel, M.M., van Bezouw, S., Salomons, G.S., Voute, P.A., Pieters, R., Baylin, S.B., Herman, J.G., Versteeg, R., 2002. Tumor-specific Down-Regulation of the Tumor Necrosis Factor-related Apoptosis-inducing Ligand Decoy Receptors DcR1 and DcR2 Is Associated with Dense Promoter Hypermethylation. *Cancer Res.* 62, 2157–2161.
- Vaz, J., Ansari, D., Sasor, A., Andersson, R., 2015. SPARC: A Potential Prognostic and Therapeutic Target in Pancreatic Cancer. *Pancreas* 44, 1024–1035. doi:10.1097/MPA.0000000000000409
- Vogler, M., Dur, K., Jovanovic, M., Debatin, K.-M., Fulda, S., 2007. Regulation of TRAIL-induced apoptosis by XIAP in pancreatic carcinoma cells. *Oncogene* 26, 248–

257. doi:10.1038/sj.onc.1209776

- Voigt, S., Philipp, S., Davarnia, P., Winoto-Morbach, S., Röder, C., Arenz, C., Trauzold, A., Kabelitz, D., Schütze, S., Kalthoff, H., Adam, D., 2014. TRAIL-induced programmed necrosis as a novel approach to eliminate tumor cells. *BMC Cancer* 14, 74. doi:10.1186/1471-2407-14-74
- Waddell, N.N., Pajic, M., Patch, A.-M., Chang, D.K., Kassahn, K.S., Bailey, P., Johns, A.L., Miller, D.K., Nones, K., Quek, K., Quinn, M.C.J., Robertson, A.J., Fadlullah, M.Z.H., Bruxner, T.J.C., Christ, A.N., Harliwong, I., Idrisoglu, S., Manning, S., Nourse, C., Nourbakhsh, E., Wani, S., Wilson, P.J., Markham, E., Cloonan, N., Anderson, M.J., Fink, J.L., Holmes, O., Kazakoff, S.H., Leonard, C., Newell, F., Poudel, B., Song, S., Taylor, D., Waddell, N.N., Wood, S., Xu, Q., Wu, J., Pinese, M., Cowley, M.J., Lee, H.C., Jones, M.D., Nagrial, A.M., Humphris, J.L., Chantrill, L.A., Chin, V.T., Steinmann, A.M., Mawson, A., Humphrey, E.S., Colvin, E.K., Chou, A., Scarlett, C.J., Pinho, A. V., Giry-Laterriere, M., Rooman, I., Samra, J.S., Kench, J.G., Pettitt, J.A., Merrett, N.D., Toon, C., Epari, K.P., Nguyen, N.Q.N.Q., Barbour, A.P., Zeps, N., Jamieson, N.B., Graham, J.S., Niclou, S.P., Bjerkgvig, R., Grützmann, R., Aust, D., Hruban, R.H., Maitra, A., Iacobuzio-Donahue, C.A., Wolfgang, C.L., Morgan, R.A., Lawlor, R.T., Corbo, V., Bassi, C., Falconi, M., Zamboni, G., Tortora, G., Tempero, M.A., Australian Pancreatic Cancer Genome Initiative, A.P.C.G., Gill, A.J., Eshleman, J.R., Pilarsky, C., Scarpa, A., Musgrove, E.A., Pearson, J. V., Biankin, A. V., Grimmond, S.M., Johns, A.L., Mawson, A., Chang, D.K., Scarlett, C.J., Brancato, M.-A.L., Rowe, S.J., Simpson, S.H., Martyn-Smith, M., Thomas, M.T., Chantrill, L.A., Chin, V.T., Chou, A., Cowley, M.J., Humphris, J.L., Jones, M.D., Scott Mead, R., Nagrial, A.M., Pajic, M., Pettit, J., Pinese, M., Rooman, I., Wu, J., Tao, J., DiPietro, R., Watson, C., Steinmann, A.M., Ching Lee, H., Wong, R., Pinho, A. V., Giry-Laterriere, M., Daly, R.J., Musgrove, E.A., Sutherland, R.L., Grimmond, S.M., Waddell, N.N., Kassahn, K.S., Miller, D.K., Wilson, P.J., Patch, A.-M., Song, S., Harliwong, I., Idrisoglu, S., Nourse, C., Nourbakhsh, E., Manning, S., Wani, S., Gongora, M., Anderson, M.J., Holmes, O., Leonard, C., Taylor, D., Wood, S., Xu, C., Nones, K., Lynn Fink, J., Christ, A.N., Bruxner, T.J.C., Cloonan, N., Newell, F., Pearson, J. V., Bailey, P., Quinn, M.C.J., Nagaraj, S., Kazakoff, S.H., Waddell, N.N., Krisnan, K., Quek, K., Wood, D., Fadlullah, M.Z.H., Samra, J.S., Gill, A.J., Pavlakis, N., Guminski, A., Toon, C., Asghari, R., Merrett, N.D., Pavey, D., Das, A., Cosman, P.H., Ismail, K., O'Connor, C., Lam Duncan McLeod, V.W., Pleass, H.C., Richardson, A., James, V., Kench, J.G., Cooper, C.L., Joseph, D., Sandroussi, C., Crawford, M., Gallagher, J., Texler, M., Forest, C., Laycock, A., Epari, K.P., Ballal, M., Fletcher, D.R., Mukhedkar, S., Spry, N.A., DeBoer, B., Chai, M., Zeps, N., Beilin, M., Feeney, K., Nguyen, N.Q.N.Q., Ruzkiewicz, A.R., Worthley, C., Tan, C.P., Debrecini, T., Chen, J., Brooke-Smith, M.E., Papangelis, V., Tang, H., Barbour, A.P., Clouston, A.D., Martin, P., O'Rourke, T.J., Chiang, A., Fawcett, J.W., Slater, K., Yeung, S., Hatzifotis, M., Hodgkinson, P., Christophi, C., Nikfarjam, M., Mountain, A., Eshleman, J.R., Hruban, R.H., Maitra, A., Iacobuzio-Donahue, C.A., Schulick, R.D., Wolfgang, C.L., Morgan, R.A., Hodgin, M., Scarpa, A., Lawlor, R.T., Beghelli, S., Corbo, V., Scardoni, M., Bassi, C., Tempero, M.A., Biankin, A. V., Grimmond, S.M., Chang, D.K., Musgrove, E.A., Jones, M.D., Nourse, C., Jamieson, N.B., Graham, J.S., Biankin, A. V., Chang, D.K., Jamieson, N.B., Graham, J.S., Oien, K., Hair, J., Gill, A.J., Eshleman, J.R., Pilarsky, C., Scarpa, A.,

- Musgrove, E.A., Pearson, J. V., Biankin, A. V., Grimmond, S.M., 2015. Whole genomes redefine the mutational landscape of pancreatic cancer. *Nature* 518, 495–501. doi:10.1038/nature14169
- Wajant, H., 2015. Principles of antibody-mediated TNF receptor activation. *Cell Death Differ.* 22, 1727–41. doi:10.1038/cdd.2015.109
- Walczak, H., Degli-Esposti, M.A., Johnson, R.S., Smolak, P.J., Waugh, J.Y., Boiani, N., Timour, M.S., Gerhart, M.J., Schooley, K.A., Smith, C.A., Goodwin, R.G., Rauch, C.T., 1997. TRAIL-R2: a novel apoptosis-mediating receptor for TRAIL. *EMBO J.* 16, 5386–5397. doi:10.1093/emboj/16.17.5386
- Walsh, C.M., 2014. Grand challenges in cell death and survival: apoptosis vs. necroptosis. *Front. cell Dev. Biol.* 2, 3. doi:10.3389/fcell.2014.00003
- Wang, H., Xu, C., Kong, X., Li, X., Kong, X., Wang, Y., Ding, X., Yang, Q., 2014. Trail resistance induces epithelial-mesenchymal transition and enhances invasiveness by suppressing PTEN via miR-221 in breast cancer. *PLoS One* 9, e99067. doi:10.1371/journal.pone.0099067
- Wang, J., Duncan, D., Shi, Z., Zhang, B., 2013. WEB-based GENE SeT AnaLysis Toolkit (WebGestalt): update 2013. *Nucleic Acids Res.* 41, W77-83. doi:10.1093/nar/gkt439
- Waugh, D.J.J., Wilson, C., 2008. The Interleukin-8 Pathway in Cancer. *Clin. Cancer Res.* 14. doi:10.1158/1078-0432.CCR-07-4843
- Whatcott, C.J., Diep, C.H., Jiang, P., Watanabe, A., LoBello, J., Sima, C., Hostetter, G., Shepard, H.M., Von Hoff, D.D., Han, H., 2015. Desmoplasia in Primary Tumors and Metastatic Lesions of Pancreatic Cancer. *Clin. Cancer Res.* 21, 3561–3568. doi:10.1158/1078-0432.CCR-14-1051
- Wicovsky, A., Siegmund, D., Wajant, H., 2005. Interferons induce proteolytic degradation of TRAILR4. *Biochem. Biophys. Res. Commun.* 337, 184–90. doi:10.1016/j.bbrc.2005.09.039
- Wiezorek, J., Holland, P., Graves, J., 2010. Death receptor agonists as a targeted therapy for cancer. *Clin. Cancer Res.* 16, 1701–8. doi:10.1158/1078-0432.CCR-09-1692
- Wiley, S.R., Schooley, K., Smolak, P.J., Din, W.S., Huang, C.-P.P., Nicholl, J.K., Sutherland, G.R., Smith, T.D., Rauch, C., Smith, C.A., Goodwin, R.G., 1995. Identification and characterization of a new member of the TNF family that induces apoptosis. *Immunity* 3. doi:10.1016/1074-7613(95)90057-8
- Witkiewicz, A.K., McMillan, E.A., Balaji, U., Baek, G., Lin, W.-C., Mansour, J., Mollaei, M., Wagner, K.-U., Koduru, P., Yopp, A., Choti, M.A., Yeo, C.J., McCue, P., White, M.A., Knudsen, E.S., 2015. Whole-exome sequencing of pancreatic cancer defines genetic diversity and therapeutic targets. *Nat. Commun.* 6, 6744. doi:10.1038/ncomms7744

- Wong, C.-H., Li, Y.-J., Chen, Y.-C., 2016. Therapeutic potential of targeting acinar cell reprogramming in pancreatic cancer. *World J. Gastroenterol.* 22, 7046. doi:10.3748/wjg.v22.i31.7046
- Wu, G.S., Burns, T.F., McDonald, E.R., Jiang, W., Meng, R., Krantz, I.D., Kao, G., Gan, D.D., Zhou, J.Y., Muschel, R., Hamilton, S.R., Spinner, N.B., Markowitz, S., Wu, G., el-Deiry, W.S., 1997. KILLER/DR5 is a DNA damage-inducible p53-regulated death receptor gene. *Nat. Genet.* 17, 141–3. doi:10.1038/ng1097-141
- Wu, Y.S., Chung, I., Wong, W.F., Masamune, A., Sim, M.S., Looi, C.Y., 2017. Paracrine IL-6 signaling mediates the effects of pancreatic stellate cells on epithelial-mesenchymal transition via Stat3/Nrf2 pathway in pancreatic cancer cells. *Biochim. Biophys. Acta - Gen. Subj.* 1861, 296–306. doi:10.1016/j.bbagen.2016.10.006
- Xie, D., Xie, K., 2015. Pancreatic cancer stromal biology and therapy. *Genes Dis.* 2, 133–143. doi:10.1016/j.gendis.2015.01.002
- Yagita, H., Takeda, K., Hayakawa, Y., Smyth, M.J., Okumura, K., 2004. TRAIL and its receptors as targets for cancer therapy. *Cancer Sci.* 95, 777–83.
- Yagyu, S., Gotoh, T., Iehara, T., Miyachi, M., Katsumi, Y., Tsubai-Shimizu, S., Kikuchi, K., Tamura, S., Tsuchiya, K., Imamura, T., Misawa-Furihata, A., Sugimoto, T., Sawada, T., Hosoi, H., 2008. Circulating methylated-DCR2 gene in serum as an indicator of prognosis and therapeutic efficacy in patients with MYCN nonamplified neuroblastoma. *Clin. Cancer Res.* 14, 7011–9. doi:10.1158/1078-0432.CCR-08-1249
- Yamada, N., Sugai, T., Eizuka, M., Tsuchida, K., Sugimoto, R., Mue, Y., Suzuki, M., Osakabe, M., Uesugi, N., Ishida, K., Otsuka, K., Matsumoto, T., 2016. Tumor budding at the invasive front of colorectal cancer may not be associated with the epithelial mesenchymal transition. *Hum. Pathol.* doi:10.1016/j.humpath.2016.10.007
- Yang, J., Li, G., Zhang, K., 2016. Pro-survival effects by NF- κ B, Akt and ERK(1/2) and anti-apoptosis actions by Six1 disrupt apoptotic functions of TRAIL-Dr4/5 pathway in ovarian cancer. *Biomed. Pharmacother.* 84, 1078–1087. doi:10.1016/j.biopha.2016.10.028
- Yang, Q., Kiernan, C.M., Tian, Y., Salwen, H.R., Chlenski, A., Brumback, B.A., London, W.B., Cohn, S.L., 2007. Methylation of CASP8, DCR2, and HIN-1 in neuroblastoma is associated with poor outcome. *Clin. Cancer Res.* 13, 3191–7. doi:10.1158/1078-0432.CCR-06-2846
- Yauch, R.L., Gould, S.E., Scales, S.J., Tang, T., Tian, H., Ahn, C.P., Marshall, D., Fu, L., Januario, T., Kallop, D., Nannini-Pepe, M., Kotkow, K., Marsters, J.C., Rubin, L.L., de Sauvage, F.J., 2008. A paracrine requirement for hedgehog signalling in cancer. *Nature* 455, 406–410. doi:10.1038/nature07275
- Yeo, T.P., 2015. Demographics, epidemiology, and inheritance of pancreatic ductal adenocarcinoma. *Semin. Oncol.* 42, 8–18. doi:10.1053/j.seminoncol.2014.12.002

- Yildiz, R., Benekli, M., Buyukberber, S., Kaya, A.O., Ozturk, B., Yaman, E., Berk, V., Coskun, U., Yamac, D., Sancak, B., Uner, A., 2010. The effect of bevacizumab on serum soluble FAS/FASL and TRAIL and its receptors (DR4 and DR5) in metastatic colorectal cancer. *J. Cancer Res. Clin. Oncol.* 136, 1471–6. doi:10.1007/s00432-010-0803-1
- Yokoyama, S., Higashi, M., Kitamoto, S., Oeldorf, M., Knippschild, U., Kornmann, M., Maemura, K., Kurahara, H., Wiest, E., Hamada, T., Kitazono, I., Goto, Y., Tasaki, T., Hiraki, T., Hatanaka, K., Mataka, Y., Taguchi, H., Hashimoto, S., Batra, S.K., Tanimoto, A., Yonezawa, S., Hollingsworth, M.A., Yokoyama, S., Higashi, M., Kitamoto, S., Oeldorf, M., Knippschild, U., Kornmann, M., Maemura, K., Kurahara, H., Wiest, E., Hamada, T., Kitazono, I., Goto, Y., Tasaki, T., Hiraki, T., Hatanaka, K., Mataka, Y., Taguchi, H., Hashimoto, S., Batra, S.K., Tanimoto, A., Yonezawa, S., Hollingsworth, M.A., 2016. Aberrant methylation of MUC1 and MUC4 promoters are potential prognostic biomarkers for pancreatic ductal adenocarcinomas. *Oncotarget* 7, 42553–42565. doi:10.18632/oncotarget.9924
- Yonezawa, S., Higashi, M., Yamada, N., Goto, M., 2008. Precursor lesions of pancreatic cancer. *Gut Liver* 2, 137–54. doi:10.5009/gnl.2008.2.3.137
- Zhai, D., He, J., Li, X., Gong, L., Ouyang, Y., 2016. Bisphenol A regulates Snail-mediated epithelial-mesenchymal transition in hemangioma cells. *Cell Biochem. Funct.* 34, 441–448. doi:10.1002/cbf.3206
- Zhang, B., Kirov, S., Snoddy, J., 2005. WebGestalt: an integrated system for exploring gene sets in various biological contexts. *Nucleic Acids Res.* 33, W741-8. doi:10.1093/nar/gki475
- Zhang, X.D., Franco, A. V, Nguyen, T., Gray, C.P., Hersey, P., 2000. Differential localization and regulation of death and decoy receptors for TNF-related apoptosis-inducing ligand (TRAIL) in human melanoma cells. *J. Immunol.* 164, 3961–3970. doi:10.4049/JIMMUNOL.164.8.3961
- Zhang, Y., Yan, W., Collins, M.A., Bednar, F., Rakshit, S., Zetter, B.R., Stanger, B.Z., Chung, I., Rhim, A.D., di Magliano, M.P., 2013. Interleukin-6 is required for pancreatic cancer progression by promoting MAPK signaling activation and oxidative stress resistance. *Cancer Res.* 73, 6359–6374. doi:10.1158/0008-5472.CAN-13-1558-T
- Zhao, X., Guan, J.-L., 2011. Focal adhesion kinase and its signaling pathways in cell migration and angiogenesis. *Adv. Drug Deliv. Rev.* 63, 610–615. doi:10.1016/j.addr.2010.11.001

ACKNOWLEDGEMENT

I would like to express my deepest thankfulness and gratitude to the ***Deutscher Akademischer Austauschdienst (DAAD)*** for supporting me and giving me this invaluable experience, cherished memories and unforgettable journey.

I am greatly thankful to ***Prof. Dr. rer. nat. Anna Trauzold*** for her meticulous supervision, help and thorough guidance throughout this work.

I also want to demonstrate my profound thanks and gratitude to ***Prof. Dr. rer. nat. Holger Kalthoff*** for giving me the opportunity to prove myself and for his continuous support, valuable guidance and great advice throughout my journey in Germany.

Also, I would like to convey my appreciation to our skillful and dedicated technical assistant ***Herr Gökhan Alp*** for his help during the difficult times.

Furthermore, I would like to express my gratitude and thanks to ***Dr. med. Jan-Paul Gundlach, Dr. med. Charlotte Hauser, Prof. Dr.med. Jan Egberts, Karen Legler, and Prof. Dr. rer. nat. Susanne Sebens*** for their help in performing the animal experiments.

I would also like to express my sincere appreciation to my colleague ***Angela Zaccagnino*** for her help, support and friendliness that made my quest much easier and more enjoyable.

I also want to thank all my colleagues in the Institute for Experimental Cancer Research, UKSH, for their support and help during this work especially ***Dr rer.nat. Ole Helm*** for his help in the ELISA testing. Moreover, I would like to extend my gratitude to ***Prof. Dr. med. Wolfram Klapper*** and ***Dr. med. Monika Szczepanowski*** for their help in the Nanostring experiment.

Last but definitely not least, I want to convey my utmost thanks and greatest appreciation to ***my Family*** as they stood by me during the good and difficult times, and supported my decisions and for their unconditional help, support and encouragement.

DECLARATION

I – HEREBY – DECLARE THAT APART FROM THE SUPERVISOR’S GUIDANCE, THE CONTENT AND DESIGN OF THIS ESSAY IS ALL MY OWN WORK. THIS THESIS WAS NOT SUBMITTED EITHER PARTIALLY OR WHOLLY AS PART OF A DOCTORAL DEGREE TO ANOTHER EXAMINING BODY AND IT WAS NEITHER PUBLISHED NOR SUBMITTED FOR PUBLICATION. FURTHERMORE, THIS THESIS HAS BEEN PREPARED IN ACCORDANCE WITH THE RULES OF GOOD SCIENTIFIC PRACTICE OF THE GERMAN RESEARCH FOUNDATION.

KIEL, APRIL 2017

DOAA TAWFIK EL-SHEIKH